Insulin-Mediated Capillary Recruitment:

Regulatory and Anatomical Aspects

By

Lei Zhang, BSc

A thesis submitted in fulfilment of the requirements for the degree of
Doctor of Philosophy

Division of Biochemistry
University of Tasmania

September 2005

TABLE OF CONTENTS

STATEMENT

The work in this thesis has been undertaken exclusively for the use of Ph.D in the area of Biochemistry, and has not been used for any other higher degree or graduate diploma in any university. All written and experimental work is my own, except that which has been referenced accordingly.

Zhang Lei

Lei Zhang

AUTHORITY OF ACCESS

This thesis may be available for loan and limited copying in accordance with the Copyright Act 1968.

Zhang Lei

Lei Zhang

ABSTRACT

Insulin-mediated increase in total blood flow has been proposed to be an important factor in determining insulin-mediated glucose uptake in skeletal muscle. However, not all researchers have seen an effect of insulin on limb blood flow in humans when the concentration of insulin and the time of exposure to hyperinsulinemia are physiologically meaningful. Recently, it has been revealed that insulin has a second hemodynamic action in skeletal muscle to recruitment microvascular perfusion, an effect that is dissociable from increases in total blood flow. This microvascular action of insulin has been demonstrated to occur at a physiological dose of insulin and precede insulin-mediated increase in bulk blood flow. In conjunction with our observations in the constant-flow pump-perfused rat hindlimb that flow redistribution between nutritive and non-nutritive routes is able to control muscle metabolism, we proposed that a capillary recruitment resulting from flow redistribution by insulin rather than increase in total flow has physiological significance in determining insulin-mediated glucose uptake in muscle.

The aims of the thesis were twofold. The first was to investigate the regulatory aspects of insulin-mediated capillary recruitment in relation to insulin-mediated increase in total blood flow and glucose uptake. To this end, hyperinsulinemia euglycemic clamps were performed in anaesthetized rats. Femoral blood flow was measure by Transonic flow probe. Capillary recruitment was determined by 1-MX metabolism and contrast-enhanced ultrasound (CEU). Hindleg glucose uptake and muscle glucose uptake were also determined. In response to various doses of insulin, capillary recruitment showed a higher sensitivity to plasma insulin than total blood flow and muscle glucose uptake. In response to a termination of a physiological hyperinsulinemia, the reversal of insulin-mediated capillary recruitment had a similar time-course with that of total blood flow but slower than the reversal of insulin-mediate glucose uptake. In response to TNFα, insulin-mediated capillary recruitment and glucose uptake showed a close coupling; both were opposed at low but not high insulin concentrations. The second aspect of the thesis was to seek anatomical evidence that insulin-mediated capillary recruitment may result from a redistribution of flow from non-nutritive vessels to nutritive capillaries. In the constant-flow pump-perfused rat hindlimb, flow routes were mapped using either perfusion fixation with glutaraldehyde or fluorescent dextran under basal, predominantly nutritive or non-nutritive conditions created by vasoconstrictors. The results suggest that non-nutritive vessels are on average of greater diameter than capillaries and found in connective tissue between the fibres.

Overall, these findings support a physiological contribution of insulin-mediated capillary recruitment to insulin-stimulated glucose uptake and suggest that total flow and capillary recruitment are regulated by insulin via different mechanisms. Insulin-mediated capillary recruitment may result from flow redistribution from non-nutritive connective vessels to nutritive capillaries.

ACKNOWLEDGEMENTS

First and foremost, I would like to thank my supervisor Professor Michael Clark for his advice, mentorship, guidance and continual encouragement during my candidature. I would also like to thank my co-supervisors A/Prof Steve Rattigan and Dr. Stephen Richards for all their help, support and astute advice on experimental and theoretical matters. Thank you also to our colleagues at the University of Virginia Charlottesville for their help with the ultrasound studies and for their warm welcome during my stay in the US. Importantly, I would like to acknowledge the contribution made by Dr. Michelle Vincent and Dr. Lucy Clerk in Chapter 3. In addition, I am very appreciative of the assistance and professional advice given by Ms Teresa Clark, A/Prof MI Chuan, Rob Gasperini, Rob Tennent and Steve Weston regarding the tissue section studies in Chapter 6.

Many thanks to Dr. Michelle Wallis who introduced me to the insulin clamp technique with amazing patience and understanding and Dr. John Newman to whom I always turned with statistical problems. A special thank you goes to Geoffrey Appleby and the animal house staff for their technical support. My gratitude and thanks go to all the members of the Biochemistry Department, who made it such an enjoyable place to work; Cate Wheatley, Eloise Bradley, Sara Jackson, Georgina Vollus, Renee Ross, Cathryn Kolka, Maree Smith, Julie Harris, Gemma O'Farrell, Katy O'May, Hema Mahajan, Kathleen Downey, Rachel Carins and Amanda Genders.

A special mention also goes to my friends and BayWest church members for their never ending support.

Last but not the least, I thank my family; in particular my mum for her loving support and encouragement during my many, many years as student; and Lin for being my source of love and strength. This thesis is dedicated to them.

ABBREVIATIONS

Ach	acetylcholine
AII	angiotensin II
ANOVA	analysis of variance
APS	3-aminopropyltriethoxysilane
ATP	adenine triphosphate
BSA	bovine serum albumin
cGMP	cyclic guanosine monophosphate
CEU	contrast-enhanced ultrasound
2-DG	2-deoxyglucose
EDHF	endothelium-dependent hyperpolarization factor
EDL	extensor digitorum longus
ELISA	enzyme-linked immunosorbent assay
EM	electron microscopy
ET-1	endothelin-1
eNOS	endothelial nitric oxide synthase
FFA	free fatty acid (unesterified)
GA	glutaraldehyde
GIR	glucose infusion rate
GLUT4	glucose transporter 4
GSL-1	*Griffonia (Bandeiraea) Simplicifolia* lectin 1
HUVEC	human umbilical vein endothelial cells
5-HT	serotonin
α-met5-HT	α-methyl serotonin
IDDM	insulin dependent diabetes mellitus
IGF	insulin like growth factor
Ins	insulin
InsR	insulin reversal
IRS-1	insulin receptor substrate 1
K_{ATP}	ATP dependent K^+ channel
K_{Ca}	Ca^{2+} dependent K^+ channel
LDF	laser Doppler flowmetry

LDNE	low dose norepinephrine
L-NAME	Nω-nitro-L-arginine-methyl ester
L-NMMA	N^G-monomethly-L-arginine
L-NNA	N^G-nitro-L-arginine
Mch	methacholine
MRS	magnetic resonance spectroscopy
MSNA	muscle sympathetic nervous activity
1-MU	1-methyl urate
1-MX	1-methyl xanthine
NE	norepinephrine
nNOS	neuronal nitric oxide synthase
NO	nitric oxide
NOS	nitric oxide synthase
NIDDM	non-insulin dependent diabetes mellitus
PDK1	3-phosphoinositide protein kinase 1
PET	positron emission tomography
PI3-kinase	phosphatidyl inositol-3 kinase
PKB/Akt	protein kinase B
PI	pulsing interval
Plan	plantaris
PO_2	partial pressure of oxygen
RBC	red blood cell
RG	red gastrocnemius
R'g	glucose uptake
R.U.	resistance units
SNP	sodium nitroprusside
Sol	soleus
SE	standard error
TB	Tris buffer
TBS	Tris buffer with 0.9% sodium chloride
TEA	tetraethylammonium chloride
Tib	tibialis
TNFα	tumor necrosis factor α

VENIRKO	vascular endothelial cell insulin receptor knock-out
VO_2	oxygen consumption
VSMC	vascular smooth muscle cell
WG	white gastrocnemius
XO	xanthine oxidase

PREFACE

Some of the data presented in this thesis has been published or presented at scientific meetings and has been listed below.

LIST OF PUBLICATIONS DIRECTLY ARISING FROM THIS THESIS

Zhang L, Wheatley CM, Richards SM, Barrett EJ, Clark MG, and Rattigan S. TNFα acutely inhibits vascular effects of physiological but not high insulin or contraction. Am. J. Physiol. (2003) **285**: E654 – E660.

Zhang L, Vincent MA, Richards SM, Clerk LH, Rattigan S, Clark MG, and Barrett EJ. Insulin sensitivity of muscle capillary recruitment *in vivo*. Diabetes (2004) **53**: 447 – 453.

Zhang L, Newman JMB, Richards SM, Rattigan S and Clark MG. Microvascular flow routes in muscle controlled by vasoconstrictors. Microvas. Res (2005), Jul 1; [Epub ahead of print]

Wallis MG, Smith ME, Kolka CM, **Zhang L**, Richards SM, Rattigan S, Clark MG. Acute glucosamine-induced insulin resistance in muscle in vivo is associated with impaired capillary recruitment. Diabetologia (2005 Jul 30; [Epub ahead of print]

Rattigan S, **Zhang L**, Mahajan H, Kolka CM, Richards CM and Clark MG. Factors influencing the hemodynamic and metabolic effects of insulin in muscle. 2005, Current Diabetes Reviews (Invited Review), submitted

PRESENTATIONS AT SCIENTIFIC MEETINGS

1. **Zhang L,** Richards SM, Rattigan S, Barrett EJ & Clark MG. Capillary recruitment in muscle is a highly sensitive event in insulin action in vivo. Diabetes 52, Suppl 1: A48, 2003 (Abstract # 206-OR).

2. **Zhang L,** Rattigan S, Richards SM & Clark MG. TNFα inhibits low physiologic but not high insulin-mediated muscle capillary recruitment and glucose uptake in vivo. Diabetes 51, Suppl. 2: A565, 2002. (Abstract # 2335-PO)

3. Bradley EA, **Zhang L**, Newman JMB, Richards SM, Clark MG & Rattigan S. Acute and divergent effect of AICAR on insulin action in vivo. **Diabetes** 52, Suppl. 1: A344, 2003. (Abstract # 1490-PO)

4. Richards SM, Wheatley CM, **Zhang L,** Rattigan S, Barrett EJ & Clark MG. Contraction-mediated muscle capillary recruitment and metabolic responses in vivo are resistant to TNFα. Diabetologia 46 [Suppl 2]: Abstract 161, A58, 2003.

5. Clark MG, **Zhang L,** Wheatley CM, Febbraio MA & Rattigan S. TNFα and IL-6 differently affect insulin action in vivo. Diabetologia 46 [Suppl 2]: Abstract 162, A58, 2003.

6. Freycinet Conference On: Diabetes and Exercise: Impact of Muscle Blood Flow. Hobart, Australia. August 2004. **Zhang L,** Clark MG, Rattigan S. Attempt to map nutritive and non-nutritive routes in rat perfused hindlimb. (Poster).

CHAPTER 1
INTRODUCTION

Insulin, apart from its effects on promoting glucose metabolism in skeletal muscle, also has effects on vasculature in this tissue. Its vascular actions in muscle have been demonstrated so far to have two aspects. One is to increase total limb blood flow. The other is to enhance microvascular blood volume (capillary recruitment). It has long been recognized that perfusion of muscle tissue is important for adequate delivery of hormones and nutrients. Thus, the hemodynamic actions of insulin lead to the notion that insulin may improve the access for glucose and itself to skeletal muscle and in turn to facilitate muscle glucose uptake. However, recent studies suggest that insulin-mediated increase in bulk blood flow require relatively high insulin concentrations and long exposure to this hormone (325, 347). Thus, questions arose as to whether stimulation of bulk blood flow is a physiological action of insulin and whether it contributes to insulin-mediated muscle glucose uptake at physiological conditions. On the other hand, insulin-mediated capillary recruitment appears to be an independent vascular phenomenon and dissociable from insulin-stimulated total blood flow (273, 333). Thus the possibility remains that improving insulin and glucose delivery through microvascular rather than macrovascular action of insulin may facilitate insulin-mediated glucose uptake at physiological conditions. In deed, capillary recruitment has been considered as a particularly important regulator of nutrient exchange between vasculature and muscle tissue (279). Furthermore, this dissociation of capillary recruitment from increase in total blood flow indicates that insulin may induce flow redistribution within skeletal muscle and possibly increase nutritive flow at the expense of non-nutritive flow.

1.1 INSULIN-MEDIATED CAPILLARY RECRUITMENT

1.1.1 Insulin-Mediated Increase in Total Blood Flow to Skeletal Muscle

The vascular actions of insulin were first described shortly after the introduction of insulin into clinical practice. In 1939, Abramson and colleagues (3) reported that massive doses (40-280 Units) of insulin increased blood flow in human forearm, hand and leg. Similar effects of insulin to induce an increase in human forearm blood flow were also demonstrated in other clinical reports (4, 5, 83, 84). However, because these studies were associated with hypoglycemia, the effect of insulin could not be distinguished from that produced by hypoglycemia-elicited counter-regulatory hormone release. Much later in 1982, by a combination of the hyperinsulinemic euglycemic clamp and radiolabled techniques on normal conscious dogs, Liang and co-workers (186) observed a significant increase in blood flow in response to insulin in the absence of hypoglycemia. Although this study used pharmacological insulin doses (4 and 8 $mU.min^{-1}.kg^{-1}$), it clearly demonstrated that insulin-mediated vasodilation in muscle is due to a direct action of insulin rather than a consequence of changes in glycemia.

More recent literature relating to insulin-mediated vasodilation shows certain parallels to the older reports. Thus, a number of *in vivo* studies have documented an effect of insulin to increase blood flow to skeletal muscle in both human (6, 76, 269, 314, 321, 325, 335) and experimental animals (186, 278). However, there are considerable variations in the magnitude of insulin-stimulated vasodilation in the limb muscle among those reports and additionally some researchers failed to observe an increase in muscle blood flow by insulin (34, 86, 151, 164, 348). The location of the flow measurement, *i.e.* forearm or leg, seems unlikely to contribute the discrepant results, as blood flow rates measured in the same subject using the same technique, namely venous occlusion plethysmography in forearm and calf did not significantly differ under basal conditions or at any hyperinsulinemic level (325). This may be not unexpected when considering muscles of the leg and forearm have remarkable similarity in muscle fibre composition (87, 348) and rates of insulin-stimulated glucose uptake (232). Furthermore, methodological factors also do not appear to explain the contradictory data because significant flow changes have been reported in human subjects using plethysmography (6, 321, 325, 335), dye dilution (111), thermodilution (76, 171) and positron emission tomography (PET) combined with $[^{15}O]$ H_2O (269). Doppler ultrasound appears to be clearly less sensitive. Thus, 6h of sequential hyperinsulinemia with a supra-physiological end dose of insulin increased

blood flow on average by 113% when measured by venous occlusion plethysmography but only by 27% when measured with Doppler ultrasound (325). This may explain why Buchanan *et al.* (39) did not observe any flow response to maximal hyperinsulinemia (~5000mU.L^{-1}) even after 4h insulin infusion in normal subjects.

Based on existing data in the literature, Yki-Jarvinen and Utriainen (347) plotted the percent increase in flow against an insulin exposure index which was defined as the product of insulin dose (mU.min^{-1}.kg^{-1}) times the duration of the infusion (h). The analysis revealed a significant correlation between these two variables, suggesting that the dose or/and duration of insulin infusion may contribute considerably to the discrepancies regarding to the stimulation of blood flow by insulin in muscle. In fact, insulin has been reported to increase limb blood flow in a time- and concentration-dependent fashion (171, 325). For instance, during a 1.7mU.$kg^{-1}min^{-1}$ hyperinsulinemia, calf blood flow increased 39% at 2h and 91% at 6h (195). When limb blood flow was measured during a similar duration of insulin infusion (90-100min), a 50% increase was detected at an insulin concentration of 92mU.L^{-1} (552pM) in one study (314), whereas a 35% increase was recorded in another study with insulin level of 376pM (335). Therefore, measuring flow at different insulin dose and/or at different stage during insulin infusion is likely to have different blood flow response. An increase in blood flow is more apparent when insulin is administrated for a longer time and at higher doses.

Nevertheless, for flow to increase to skeletal muscle there must have been an increase in cardiac output or redistribution of flow between organs. Insulin has been reported to cause an increase in cardiac output in lean subjects at circulating levels of 468pM and 12870pM but not 212pM (19). Mean arterial pressure during hyperinsulinemia was shown to either not change (171, 225, 335) or slightly decrease (19, 325). Therefore, peripheral vascular resistance which is calculated from mean arterial pressure divided by cardiac output may decline with insulin. Moreover, there is evidence that different vascular beds appear to respond differentially to insulin. In experimental animals, hindquarter and renal vascular beds dilated whereas the superior mesenteric vascular bed constricted in response to insulin at a range of concentrations (955-22850pM) (110, 259). Baron and Brechtel (19) examined limb

and systemic vascular resistance during hyperinsulinemia (468pM and 12870pM) and observed a greater fall in vascular resistance in human leg. These researchers (19) further concluded that insulin differentially regulates vascular resistance and preferentially dilates in skeletal muscle where 80% of the insulin-mediated glucose uptake occurs (20, 73).

1.1.2 Capillary Recruitment in Skeletal Muscle

Using various methods and techniques such as microsphere deposition (245, 255, 256), autoradiography (306), positron emission tomography (PET) combined with inhalation of [^{15}O] H_2O (326, 330), intravital microscopy (190), it was convincingly demonstrated in both human (326, 329, 330) and animals (149, 190, 245, 255, 256, 306) that microcirculatory perfusion in resting skeletal muscle is neither continuous nor uniform, but rather intermittent and heterogeneous in its distribution. Thus capillaries in skeletal muscle are not always equally perfused but rather display "on-off' or alternating perfusion. In fact, there are reports that two thirds of the total capillaries are actually reserved in skeletal muscle under resting conditions (139) and stimuli such as exercise is able to recruit capillaries resulting in a more homogenous perfusion. This capillary recruitment would allow a greater exchange surface area for substances and better oxygen and nutrient delivery, thus has been considered as a particularly important regulator of nutrient exchange between vasculature and muscle tissue (279). Given that exercise also increases the total muscle blood flow rate, it appears tempting to conclude capillary recruitment and increase in bulk blood flow are necessarily associated. However, a study by Honig *et al.* (139) revealed that this is not the case. These researchers performed a careful, quantitative histomorphometric analysis of the responses of the muscle microvascular perfusion to graded electrical stimulation. The results showed that the recruitment of reserved capillaries occurred at lower levels of electrical stimulation and were essentially completed prior to the effect of muscle stimulation to enhance bulk flow, suggesting muscle capillary recruitment does not require the occurrence of an increase in bulk flow. Furthermore in the same study (139), denervation increased flow by three fold in autoperfused muscle but did not affect the capillary flow distribution, indicating an increase in total flow does not necessarily result in capillary recruitment. The dissociated responses of capillary flow and bulk flow also occurred in other experimental conditions including anaesthetics (91), O_2 tension changing (190), vasodilation using vasoactive agents (106) and

exercise (114). Therefore, it appears that microvascular and macrovascular perfusion in muscle are differentially regulated and it is possible that different stimuli have different mechanisms to exert their vascular control. One general mechanism considered is that capillary flow and bulk flow are regulated at different vascular segments. Thus, whereas resistance vessels control total flow to muscle, the terminal arterioles regulate microvascular perfusion and determine the flow redistribution within muscle tissue (218). Nevertheless, the dissociated stimulation of capillary recruitment and increase in bulk flow leads to the key question of whether insulin has a microvascular action in skeletal muscle in addition to its effect to enhance bulk flow.

1.1.3 Evidence for Capillary Recruitment by Insulin in Muscle

Raitakari and colleagues (267) used positron emission tomography (PET) with inhalation of [^{15}O] carbon monoxide ([^{15}O] CO) to determine human skeletal muscle blood volume in the basal state and during hyperinsulinemia. PET allows localization and quantitation of radioactive tracer concentration in different tissues. By determining the steady-state muscle tissue [^{15}O] CO radioactivity concentration and the [^{15}O] CO activity concentration in blood, they were able to quantify skeletal muscle blood volume. These authors estimated that in healthy subjects the average muscle blood volume at basal to be approximately 3ml.100^{-1}g muscle. During pharmacological hyperinsulinemia (3200pM), muscle blood volume increased by 9%. Furthermore, insulin-stimulated muscle blood volume was strongly correlated with insulin-mediated whole body glucose disposal (267). Using PET to measure muscle tissue microvascular blood volume has the advantage of being non-invasive. However the application of the hematocrit ratio between total body tissues and great veins into the calculation instead of human skeletal muscle hematocrit may have limited the accuracy of the evaluation (267). Moreover, the radiation exposure and high expense also creates difficulties for a wider utilization of this method. Most importantly, PET scanning measures total vascular blood volume thus has the potential disadvantage of being strongly influenced by blood in larger vessels, thereby may not show the same responses as the microvasculature to vasoactive agents. Nevertheless, this method provided valuable insight into the vascular action of insulin and indicates insulin may have a vasodilator effect in the muscle microvasculature *in vivo*.

Subsequently, Bonadonna *et al.* (35) examined the wash-out curves of a non-metabolizable extracellular marker (1-[^{3}H]-L-glucose) in the deep forearm vein after a pulse injection of this maker into the brachial artery. Based on classic kinetic theory (178), they reasoned that the kinetics of a non-metabolizable extracellular marker such as L-glucose can be used to measure the accessible extracellular volume and therefore provides an index of the amount of the tissue available for metabolic exchange with the blood stream (35). Thus, during a supra-physiological hyperinsulinemia (5600pM), these researchers observed a 39% increase in muscle tissue drained by the deep forearm vein. Based on this observation it was concluded supra-physiological hyperinsulinemia increased limb blood flow which was associated with tissue recruitment. However, because vascular volume only constitutes approximately 10% of the extracellular space, capillary recruitment is not assessed directly with this method.

A direct measurable effect of insulin to increase capillary recruitment in muscle, both in animals (273) and in humans (62) has been recently reported by us. This new observation relies on the development of specific techniques for the assessment of changes in flow distribution within muscle tissue. One of these techniques is based on the metabolism of 1-methylxanthine (1-MX), an exogenous substrate for xanthine oxidase (XO). In skeletal muscle, XO is expressed primarily in the endothelial cells of capillaries and small arterioles but not large vessels or muscle itself (132, 156). Thus an increase in capillary exchange surface area (capillary recruitment) will increase the exposure of its substrate to this enzyme. This in turn will result in an increase in the metabolism of the substrate provided the concentration of the substrate is saturating. 1-MX was chosen as substrate because it met a number of prerequisites. Firstly, it is converted by XO solely to 1-methylurate (1-MU) (67, 273). 1-MU is not further metabolized by any tissue nearby; hence the recoveries are quantitative (67). Secondly, 1-MX is non-vasoactive on its own over the concentration range at which its metabolism could be readily studied (273). Thirdly, 1-MX and 1-MU can be readily separated from each other as well as from physiological purine- and pyrimidine-based compounds by current separation technologies (273). Most importantly, changes in 1-MX metabolism correlated positively with changes in the proportion of nutritive capillary flow in perfused muscle under a number of conditions (52, 271, 349). Therefore, we believe the changes in 1-MX metabolism are indicative of capillary

recruitment. With this background, we found during a high physiological hyperinsulinemia ($10mU.min^{-1}.kg^{-1}$), insulin *in vivo* increased 1-MX metabolism by 50% in experimental animals in association with stimulated glucose uptake in muscle (273). This finding firmly established that insulin *in vivo* has a microvascular action to induce capillary recruitment that may play a role in determining insulin-mediated glucose uptake. Insulin at this dose also increased femoral blood flow significantly (273). However, an increase in femoral blood flow of similar magnitude induced by epinephrine changed neither the capillary recruitment measured by 1-MX metabolism nor the muscle glucose uptake in anesthetized animals (273), suggesting that an increase in total blood flow does not necessarily result in capillary recruitment and enhanced glucose uptake.

Another technique that we have adapted to quantify capillary perfusion in skeletal muscle is contrast-enhanced ultrasound (CEU) imaging, a method that has been used extensively in the past to measure microvascular flow in the myocardium (191, 244, 337). This method involves a vascular administration of perfluorocarbon gas-filled albumin-coated bubbles as contrast enhancing agent. When exposed to a high-energy ultrasound pulse, these microbubbles are destroyed and simultaneously generate an acoustic signal which is proportional to microbubble concentration within the vasculature under the ultrasound beam. Essentially, all the microbubbles in the ultrasound probe field are destroyed by an initial pulse of high-energy ultrasound. By step-wise prolonging the time between two successive ultrasound pulses, the vasculature is progressively replenished with microbubbles. At the end, all the microvessels will be refilled with microbubbles and a further increase in pulsing interval will not further increase the acoustic signal. Thus, the plateau acoustic signal (measured as video-intensity) is indicative of capillary blood volume. Because the microvascular rheology of microbubbles is similar to that of red blood cells (157), the reappearance rate of microbubbles provides a measure of cell velocity in the capillaries. Furthermore, in contrast to PET scanning used by Raitakari *et al.* (267), CEU allows background subtraction of the tissue image to eliminate signal from large vessels which fill very rapidly, providing a more precise measurement of capillary flow. By this approach, we assessed changes in capillary blood volume in skeletal muscle in response to insulin in both human forearm (62) and the rat hindlimb *in vivo* (66, 333). In both cases, compared with the baseline values, insulin administration

increased microvascular perfusion and capillary blood volume was increased more than two-fold in response to physiologic insulin ($3mU.min^{-1}.kg^{-1}$) in anesthetized rats (66). Moreover, capillary recruitment in response to insulin or exercise measured by CEU correlated well with values obtained using 1-MX metabolism (50).

Laser Doppler flowmetry (LDF) is the third approach that we have employed to investigate the effects of insulin on skeletal muscle tissue perfusion. For LDF measurements it is generally thought that movement of the blood cells causes a frequency shift with some of the photons also scattered or absorbed by the tissue. Doppler frequency shift carries information about the movement and concentration of the cells. LDF probes are thus considered to provide a measure of tissue perfusion and have recently been used as a method for the continuous measurement of blood flow in small, discrete areas of various tissues (49, 158, 194, 236). We applied this technique to rats under the euglycemic hyperinsulinemic clamp ($10mU.min^{-1}.kg^{-1}$) and observed an increased laser Doppler signal coincident with insulin-mediated glucose disposal in hindlimb muscle (48). This would lend support to the findings with 1-MX metabolism and CEU. In addition, there is evidence that LDF is indicative of microvascular flow rather than bulk flow as LDF signal was unaffected when femoral blood flow increased by 49% during adrenaline infusion (48). This is in accordance with the 1-MX metabolism data where bulk flow increases in response to adrenaline administration were not accompanied by capillary recruitment (273).

1-MX metabolism, CEU and LDF each depends on a different principle to provide information on skeletal muscle microvascular perfusion. Euglycemic hyperinsulinemia induced a positive response of all the three measurements, indicating that insulin stimulates capillary recruitment and improves perfusion in muscle tissue. An increase in femoral flow in anesthetized rats during adrenaline infusion affected neither 1-MX metabolism nor LDF signal, consistent with the concept that total blood flow and capillary recruitment are two separate vascular events in muscle.

1.2 INSULIN-MEDIATED CAPILLARY RECRUITMENT AND INSULIN-MEDIATED GLUCOSE UPTAKE IN SKELETAL MUSCLE

1.2.1 Insulin's Hemodynamic Actions and Insulin-Mediated Glucose Uptake in Skeletal Muscle

Based on their observations (23, 171, 172), Baron and his colleagues pioneered the concept that insulin acts as a vasodilator and can thereby control the access of itself, glucose and other nutrients to skeletal muscle. They demonstrated that insulin increased total muscle blood flow in lean healthy subjects in a time- and dose-dependent manner. In addition, an impaired insulin-mediated whole body glucose disposal in obese and diabetic subjects was paralleled by a decreased effect of insulin to stimulate skeletal muscle blood flow (23, 171, 172). The magnitude of insulin-mediated leg flow blood flow response during systemic hyperinsulinemia was significantly correlated with insulin-mediated whole body glucose disposal in populations with varying insulin sensitivity (26, 171, 172, 201). Using Positron emission tomography (PET), Yki-Jarvinen and colleagues were able to measure total limb blood flow as well as muscle flow. In accord with Baron's reports, their results demonstrated that skeletal muscle explained 70% of the increase in leg blood flow with insulin (268) and there was a co-localization of insulin-stimulated muscle blood flow with regional glucose uptake in normal subjects during a hyperinsulinemia clamp (326). Moreover, vasodilation induced by the local intra-arterial infusion of insulin/glucose was also demonstrated to be functionally linked to whole-body insulin-mediated glucose uptake in lean healthy subjects (57). However, despite the compelling correlation, other investigators have questioned the physiological relevance of insulin-mediated increase in bulk blood flow as a determinant of muscle glucose uptake (347). Thus in human forearm, Utriainen *et al.* (325) demonstrated maximal glucose arteriovenous difference was achieved at the high physiological insulin concentration (61mU.L^{-1}, ~366pM) that only minimally stimulated forearm flow. With further increasing insulin to supra-physiological level (462mU.L^{-1}, ~2776pM), glucose extraction did not increase further but forearm blood flow increased progressively resulting in a further increased forearm glucose uptake. Based on these observations, these researchers concluded that blood flow becomes an important determinant for glucose uptake only at a supra-physiological insulin concentration (325). Although Laakso *et al.* (171, 172) reported the half-maximal insulin concentrations for blood flow stimulation to be physiological and similar to that for glucose uptake in human leg (266pM and 420pM respectively), most of the studies reporting an increase in total flow with insulin used supra-physiological dose

insulin (22, 35, 269), in keeping with Utriainen's conclusion (325). Fugmann *et al.* (108) conducted a time course study to examine the relative importance of blood flow and glucose extraction as determinants of insulin-mediated glucose uptake during a hyperinsulinemic clamp that raised plasma insulin to 92mU.L^{-1}. These researchers demonstrated the increase in forearm blood flow was preceded by glucose extraction and blood flow kept increasing during prolonged insulin infusion while glucose extraction remained constant. These findings are in accordance with studies of Laakso *et al.* (171) and Utriainen *et al.* (325). Thus it was concluded that glucose extraction is the principal determinant of forearm glucose uptake early after induction of hyperinsulinemia and that only during prolonged elevation of plasma insulin was the insulin-mediated increase in blood flow deemed to play an important role (108, 325). Since insulin is secreted in a phasic manner in response to food and its level rises and falls rapidly, whether the slow increase in bulk blood flow plays a role in determining insulin-mediated glucose disposal is questionable.

Even so, there remains considerable interest in the possibility that insulin-mediated hemodynamic actions are somehow linked to improving access for insulin and perhaps glucose and more particularly, that a defect in this process might be responsible for part of the insulin resistance in muscle of type 2 diabetics. As discussed in section 1.1.3, we (62, 273) and others (35, 267) have reported insulin to have a second hemodynamic action of increasing microvascular volume (capillary recruitment) that is independent and thus dissociable from insulin's effect on total blood flow (273). By using a number of interventions in rats (58, 272, 331, 336, 350) we showed a tight link between insulin-mediated capillary recruitment and glucose uptake in muscle and further suggested that about 50% of the glucose uptake *in vivo* may be accounted for by capillary recruitment. However, since a major concern as to the relationship of insulin-mediated increase in bulk blood flow and metabolic actions is related to the dose and time characteristic of insulin action, detailed studies to lineate the dose and time-course response of insulin-mediated capillary recruitment may be critical to further establish a relation between insulin's microvascular action and metabolic effect in skeletal muscle. Thus, we performed a time course study in rats and revealed that insulin at physiological dose recruited microvasculature within 5-10min, and this preceded both activation of insulin signalling pathways and increases in muscle glucose disposal as well as changes in total limb blood flow (332,

333). The quick onset of insulin-mediated capillary recruitment suggests capillary recruitment is a primary action of insulin and likely to play an important role in facilitating insulin action to enhance muscle glucose uptake. However, to consolidate this view and to obviate the other concern that is related to insulin-mediated total blood flow, a dose-response of insulin-mediated capillary recruitment and its relation to glucose uptake still needs to be determined.

1.2.2 Influence of Vasoactive Agents on Insulin-Mediated Muscle Glucose Uptake

As discussed above, the role of insulin-stimulated increase in total blood flow as a determinant of glucose uptake remains controversial. Investigators reasoned that if blood flow is important for insulin-mediated glucose uptake, augmenting or restricting total blood flow during insulin exposure using vasoactive agents should modulate insulin-mediated glucose uptake accordingly. However, studies aimed at testing the role of total blood flow as a determinant of insulin-stimulated glucose uptake by decreasing or increasing total flow using vasoactive agents yielded inconsistent results. Thus sodium nitroprusside (SNP) (224, 258, 285) adenosine (223) and bradykinin (174, 233) when infused locally in human markedly increased limb blood flow, but did not increase muscle glucose uptake. Methacholine (Mch) on the other hand, has been reported in both human (25, 27, 285) and experimental animals (197) to significantly augment limb blood flow as well as glucose uptake into muscle. Decreasing flow using L-NMMA (26, 308) was associated with a 50% reduction in insulin-mediated muscle glucose uptake but had no effect on whole body glucose disposal. Interpretation of these studies was confounded by a possible direct metabolic action of the vasoactive agents as vasoactive actions of some compounds such as SNP, Mch and L-NMMA involve nitric oxide (NO) and NO itself has been demonstrated to stimulate glucose uptake in incubated muscle (13, 89, 160). However, discrepancies among studies do not appear to relate to the possible metabolic action of NO because both increased (25, 27, 197) and unaffected (224, 258) insulin-mediated glucose uptake have been observed during a NO-dependent vasodilation. Alternatively, varying glucose extractions across the skeletal muscle among studies may play a role in causing inconsistent results. Based on Renkin's arguments (279), increases in blood flow would not be expected to significantly impact the uptake of substrates with a low

extraction fraction across a vascular bed. Thus in the context of muscle glucose uptake, one would expect a change in blood flow rate only to have a greater modulating effect on glucose uptake with relatively higher glucose extraction across skeletal muscle. However there is more than circumstantial evidence suggesting this is not the case when it comes to comparing effects of various vasoactive agents on muscle glucose uptake. Thus, in post-absorptive states where the arterial-venous glucose gradient across skeletal muscle is only 0.1-0.2mM, significant increases in blood flow with bradykinin (233) or SNP (285) had no effect on glucose uptake. When glucose extraction across skeletal muscle was increased to 20-49% using a physiological or high physiological hyperinsulinemia clamp, superimposed infusion of bradykinin (174, 233) or SNP (224, 258) increased limb flow remarkably but again did not affect insulin-stimulated glucose uptake. In contrast, vasodilation induced by Mch was accompanied by an increase in muscle glucose uptake across a wide range of glucose-extraction from 2% in post-absorptive state (285) to ~70% during a hyperinsulinemic clamp (27). Overall, a positive relation between changes in total blood flow and insulin-mediated muscle glucose uptake are not compelling. Rather, this would be consistent with studies on perfused hindlimb where two types of vasoconstrictors had opposite effects on muscle metabolism through controlling flow redistribution (51) within in muscle without altering total blood flow (will be discussed in section 1.5). Indeed, Mahajan *et al.* (197) have recently reported in experimental animals that local Mch with systemic physiological hyperinsulinemia which enhanced total limb blood flow as reported in human studies, increased insulin-mediated capillary recruitment in association with a potentiation of insulin-mediated glucose uptake. In the same experimental setting, bradykinin which increased flow to a similar extent as Mch, had no effect on either insulin-mediated glucose uptake or capillary recruitment. In keeping with this, in a human study using PET to measure muscle flow heterogeneity, Pitkanen *et al.* (258) reported that SNP which increased total flow neither increased insulin-mediated muscle glucose uptake nor changed flow distribution within muscle tissue. Therefore, although similarly altering total blood flow, vasoactive agents appear to differently control microvascular perfusion or influence insulin-mediated capillary recruitment *in vivo*. These microvascular changes seem to play the key role in modulating insulin-mediated glucose uptake in skeletal muscle.

1.3 INSULIN RESISTANCE

Insulin resistance, defined as a smaller than expected biological response to a given dose of insulin, is a fundamental component of the pathogenesis of many glucose disorder conditions including non-insulin-dependent diabetes mellitus (NIDDM) (71), obesity (171), hypertension (94, 261) etc. Incubated muscle preparations from insulin resistant obese and NIDDM patients had markedly lower rates of insulin-mediated glucose transport (80) and subsequent glucose metabolism (102), even at the maximal insulin concentration ($10000mU.L^{-1}$) (7), indicating a significant defect in insulin action at the level of the myocytes. However, given the recent evidence that insulin has hemodynamic actions which may contribute to insulin-mediated glucose uptake in muscle *in vivo*, it is possible that insulin resistance also has a hemodynamic component and impairment in the hemodynamic mechanisms or vascular reactivity may contribute to the pathology of insulin resistance *in vivo*.

1.3.1 Impaired Insulin-Mediated Capillary Recruitment

Recently, we have generated three states of acute insulin resistance in anesthestized rats and demonstrated that insulin-mediated capillary recruitment determined by 1-MX metabolism was indeed impaired in these animals. Firstly, insulin resistance was induced by systemic administration of a vasoconstrictor (α-methylserotonin, α-met5-HT) indicated by a 56% reduction in insulin-mediated glucose uptake across rat hindlimb (272). This treatment of α-met5-HT infusion commenced before insulin infusion prevented insulin-mediated increase in total blood flow and inhibited insulin-stimulated capillary recruitment indicated by 1-MX metabolism by 71%. Furthermore, α-met5-HT infusion alone had no effect on glucose metabolism, suggesting no direct receptor-mediated metabolic action occurred on skeletal muscle. This is supported by previously studies demonstrating no effects of serotonin on glucose uptake in the isolated incubated muscles where a functional vascular delivery is absent (275). Therefore, α-met5-HT-mediated inhibition of insulin-stimulated glucose uptake *in vivo* appears to be due to its vascular actions. Moreover, hindleg glucose uptake was significantly correlated to 1-MX metabolism but not total blood flow (272), suggesting a defect in insulin-mediated capillary recruitment due to α-met5-HT may be a determinant contributor to α-met5-HT-induced insulin resistance in these animals.

The second state of insulin resistance was generated by TNFα infusion (350). Elevated serum TNFα levels are associated with number of insulin resistant conditions in rodents and humans such as obesity and diabetes (179, 211, 229) and have been implicated as the cause of insulin resistance observed in septic shock and infection (192, 235). Consistently lowering the active level of TNFα *in vivo* by infusion of a TNFα receptor IgG fusion protein (142), a soluble TNFα-binding protein (143), or polyclonal anti-TNFα (38) in insulin-resistant animal models improves insulin action. Thus, it is not unexpected to observe in our study a 50% reduction in insulin-mediated muscle glucose uptake in anesthetized rats treated by acute TNFα infusion started 1h before and 2h during euglycemic hyperinsulinemia clamp ($10mU.min^{-1}.kg^{-1}$) (350). Notably, this marked insulin resistance was associated with a complete loss of insulin-mediated changes in blood flow and capillary recruitment, indicating a significant hemodynamic component in TNFα-induced acute insulin resistance (350). In keeping with this, TNFα treatment up to 8h and 24h had no effect on insulin-mediated glucose uptake in incubated muscle preparations devoid of vascular involvement (109, 231). Furthermore, TNFα has been shown to interfere with insulin signalling pathway in bovine aortic endothelial cells (165) and vascular smooth muscle cells (113) where insulin may act to stimulate capillary recruitment.

Elevation of plasma free fatty acid (FFA) levels by a combined infusion of intralipid and heparin was the third mean we used to induce insulin resistance in experimental animals (58). By this approach, we showed that 6h elevation of plasma FFA levels during a hyperinsulinemic-euglycemic clamp at physiologic insulin ($3mU.min^{-1}kg^{-1}$) led to insulin resistance evidenced by 45% reduction in insulin-mediated glucose uptake by the rat hindleg and impaired insulin-mediated capillary recruitment determined as 1-MX metabolism. Furthermore, a positive correlation between hindleg glucose uptake and 1-MX metabolism was observed which contrasted with hindleg glucose uptake and femoral blood flow where there was no significant correlation. The mechanisms by which raising FFA concentrations results in insulin resistance are not fully understood although it is generally agreed that a direct inhibitory effect on skeletal muscle glucose metabolism is likely involved (92, 93). However, based on the recent findings that FFA elevation impairs endothelial function in humans (187,

310) together with our current observation, it is reasonable to propose that FFA elevation-induced insulin resistance in muscle may be partly due to an impairment in insulin's microvascular actions resulting in reduced access for insulin and glucose to myocytes. This may provide a novel mechanism for insulin resistance associated with obesity. In support of this, obese Zucker rats that have elevated plasma levels of FFA (29) showed marked muscle insulin resistance in association with equally markedly impaired insulin-mediated capillary recruitment (336).

Some researchers investigated skin microvascular perfusion and capillary recruitment as microvasculature in this tissue is readily accessible particularly in the human. Skin capillary density was measured using capillary microscopy and the increase in this parameter after arterial occlusion is regarded as capillary recruitment. By this approach, Serne *et al.* reported that recruitment of capillaries in human skin was induced during systemic hyperinsulinemia (409pM) (291) and positively correlated to insulin's metabolic actions (292). Furthermore, by simultaneously measuring intramuscular microvascular perfusion by implanted laser Doppler fluxmetry, the same group of researchers reported an augmented intramuscular reactive hyperaemia, indicating an association between skeletal muscle microvascular recruitment and skin capillary recruitment during physiological systemic hyperinsulinemia (68). There are some inconsistent results as to whether insulin increases basal capillary density since enhanced pre-arterial occlusion capillary density by insulin was reported in one occasion (291) but not the other (70) despite a similar circulating insulin concentration. Nevertheless, capillary recruitment after arterial occlusion is impaired in essential hypertensive (290) and obese (70) individuals with insulin resistance and in lean subjects during plasma FFA elevation (69). Given the demonstrated association between skin and intramuscular microvascular perfusion (68), it is likely that insulin-mediated capillary recruitment in skeletal muscle is also impaired in these insulin resistant humans.

1.3.2 Impaired Insulin-Mediated Increase in Total Blood Flow to Skeletal Muscle

There is evidence of impaired insulin-mediated increase in bulk blood flow in insulin resistant states. Baron and colleagues (171, 172) examined insulin action across a range of insulin sensitivity in lean insulin-sensitive subjects, obese and type 2 diabetic subjects. They demonstrated that there was a right shift in the dose-response curves

for both glucose uptake and insulin-mediated increase in leg blood flow in both the obese and diabetic subjects. The obese had similar maximal flow response to insulin compared to lean subjects but the insulin concentration for half maximal stimulation of leg blood flow was 3 fold higher than lean control whereas the maximal flow response in type 2 diabetes was much lower than lean and obese subjects. However, the association between impaired insulin-mediated flow response and insulin resistance has not been universally observed and appears more prominent when high insulin dose was applied. During supra-physiological systemic hyperinsulinemia (>2000pM), insulin-dependent diabetic patients (IDDM) characterized by insulin resistance in peripheral tissue (72, 75, 243) had markedly reduced insulin-stimulated blood flow compared to nondiabetic control individuals (23, 268). However, at physiological insulin concentration (~350pM), blood flow wasn't changed in either IDDM or control subjects (199, 346), indicating no impairment in flow response to insulin in IDDM at this physiological condition. Similarly, Baron *et al* (22) and Laine *et al.* (173) deployed supra-physiological hyperinsulinemia (2100 - 2700pM) and reported that impaired insulin stimulation of blood flow in skeletal muscle characterizes insulin resistance in essential hypertension, yet Natali *et al* (225) and Capaldo *et al.* (40) reported the opposite in studies where insulin level was raised either locally in forearm to $120mU.L^{-1}$ (720pM) or systemically to 360pM. A reduction in total skeletal blood flow response was also observed in type 2 diabetic (172) and obese (171) subjects at a high circulating insulin concentration, but not during a physiological hyperinsulinemia (500 – 600pM) (34, 71). The lack of a relationship between insulin resistance and defective flow response at physiological insulin concentrations in these human studies is mainly due to an inability to demonstrate an insulin-stimulated increase in total blood flow in healthy control subjects (34, 40, 71, 199, 225, 346). This is in accordance with the discussion in Section 1.2.1 that the occurrence of insulin's stimulation of muscle blood flow appears to require high insulin concentration and prolonged exposure period. Therefore, some researchers have concluded that defects in glucose extraction predominate when insulin-resistant and sensitive individuals are compared using physiological insulin concentrations and defects in total blood flow distinguish between the groups in studies using supra-physiological insulin concentrations. It is important to note that defects in glucose extraction do not necessarily solely result from the metabolic impairment at myocytes but impaired microvascular exchange or

capillary delivery of insulin and glucose to muscle cells may also play a role. Furthermore, the relationship between impaired insulin-mediated increase in total blood flow and metabolic insulin resistance during supra-physiological hyperinsulinemia does not always hold, as some studies reported intact flow responses to supra-phyiological insulin in NIDDM (76, 326), obesity (240) and hypertension (145, 147). Overall the inability of insulin to enhance glucose uptake in skeletal muscle at supra-physiological concentration may be associated with a defect in insulin stimulation of total blood flow. However, at physiological insulin doses, an association between impairment in insulin's metabolic effects on glucose uptake and vascular action to stimulate total blood flow is not compelling.

1.3.3 Endothelial Dysfunction

Since a number of studies favour the involvement of endothelial cells and nitric oxide (NO) production in insulin-mediated vasodilation (will be discussed in section 1.6.2, (56, 288, 308, 331)), it has been proposed that the impaired insulin-mediated hemodynamic effects in insulin resistance states may reflect an endothelial dysfunction. Put in another words, insulin resistance may be linked to endothelial dysfunction either as a cause or as a consequence. However, studies evaluating vascular function by examining vasodilator response to endothelium-dependent stimuli such as acetylcholine (Ach) and methacholine (Mch) in relation to insulin sensitivity have produced inconsistent results. In diabetics and obese patients with insulin resistance, impaired vasodilator response to Ach or Mch was reported in some (202, 206, 309) but not all studies (11, 315). In essential hypertensive subjects who had impaired insulin-mediated glucose uptake, Taddei *et al.* (316) reported a diminished increase in Ach-induced vasodilation, yet Natali *et al.* (226) saw no correlation between insulin sensitivity and Ach-induced vasodilation. Furthermore, young adults with low birth weight had reduced glucose disposal by insulin but had normal forearm blood flow response to Ach (134). The limb vasoconstrictor response to a NOS inhibitor is also used as an index of endothelial response but seems unaltered in insulin resistant conditions such as obesity (315) and hypertension (56). Collectively, an impaired flow response to endothelium-dependent stimuli is not consistently observed with insulin resistance. Moreover, in healthy individuals with varying insulin sensitivity, Petrie *et al.* (252) and Utriainen *et al.* (323) each reported no correlation between insulin sensitivity and Ach-mediated vasolidation whereas

Petrie *et al.* (252) found a correlation between insulin sensitivity and vasoconstrictor response to L-NMMA. Thus, whether insulin sensitivity and endothelial function are positively related, remains unclear.

As defects in insulin's hemodynamic actions especially capillary recruitment appear to firmly associate with insulin resistance, the unclear relation between insulin resistance and endothelial dysfunction may indicate that insulin-mediated vascular action and endothelial function assessed by flow response to Ach/Mch or L-NMMA are not necessarily related. Indeed, Utriainen *et al.* (324) examined forearm blood flow response to Ach, L-NMMA and supra-physiologic hyperinsulinemia ($5mU.min^{-1}kg^{-1}$) in normal subjects and found no correlation between insulin-mediated increase in blood flow and Ach-induced vasodilation although they did observe a correlation between flow response to insulin and L-NMMA. Indirect evidence in support of the Utriainen *et al.* observation (324) comes from findings suggesting that the mechanisms underlying the vasodilation induced by Ach and insulin appear to differ. Compared to Ach, the vasodilatory effect of insulin is slow. While Ach increases blood flow several-fold within minutes in normal subjects (46), doubling of blood flow with high insulin concentration takes hours (325). Furthermore, Taddei *et al.* (316) observed blunted endothelium-dependent responses (by Ach) in hypertensive as compared to normotensive subjects, but normal potentiation of Ach-induced vasodilation by insulin. There is also evidence that vascular reactivity assessed by flow response to L-NMMA may not reflect the vascular response to insulin. Vasoconstrictor response to L-NMMA in human leg was blunted by 2h of FFA elevation while insulin-mediated blood flow was not affected till after 4h exposure to elevated circulating FFA levels (310). Taken together, vasodilation by insulin seems to differ from that induced by some other endothelium-dependent vascular stimuli. As a consequence, endothelial function assessed by determining vascular response to endothelium-dependent vasoactive agents dose not necessarily reflect the response of the vasculature to insulin which is associated with insulin resistance. This may partly explain the lack of clear relationship between insulin resistance and endothelial dysfunction. In keeping with this, insulin resistance was coincident with endothelial dysfunction during TNFα infusion (270) and FFA elevation (310), each of which was demonstrated to impair insulin-mediated capillary recruitment and increase in total

blood flow (58, 350). Additionally, Rosiglitazone, an insulin-sensitizing agent, improved insulin sensitivity and endothelium-dependent vasodilation (by Ach) in NIDDM and was accompanied by decrements in circulating levels of FFA and TNFα (222).

1.4 RATE-LIMITING STEPS IN INSULIN-MEDIATED MUSCLE GLUCOSE UPTAKE IN THE CONTEXT OF CAPILLARY RECRUITMENT

It is well documented that insulin acts slower *in vivo* to enhance glucose utilization than *in vitro*. During a euglycemia hyperinsulinemic clamp, despite a rapid increment of plasma insulin, the rate to reach the half maximal activation of insulin-mediated whole body glucose disposal (209, 264, 265, 344) or limb muscle glucose uptake (214, 230, 320) in lean healthy man has been reported to be 20-60min depending on the dose of insulin. In contrast, in incubated 3T3-L1 adipocytes, glucose uptake in response to insulin (100nM) reached maximum within 15min (98). In recent years, the cause of this slowness of insulin action *in vivo* has been suggested to be due to an endothelial barrier for the transcapillary transport of insulin. This view is evidenced by number of studies showing that steady state insulin concentrations in the interstitium of skeletal muscle (133, 137, 299) and abdominal subcutaneous tissue (155) or the hindlimb lymph (307) are lower than that in plasma. As a consequence of this barrier, insulin in the interstitium and lymph is slower reaching equilibrium than in plasma (264, 344). Thus, there is both an attenuation and a retardation of the insulin signal as it crosses from the blood to the interstitium. From studies using cultured endothelial cells, the transendothelial transport of insulin appears to be both saturable and receptor-mediated (166). Evidence from *in vivo* studies remains controversial. In skeletal muscle of lean rats (137) and in human subcutaneous tissue (155), the plasma/interstitial concentration ratio of insulin increases in higher physiological concentration ranges then appears to be compatible with a saturable transport system. However, this was not evident in human muscle (299). In fact in the dog limb, Steil *et al.* (307) observed an increase in interstitial fluid-to-plasma insulin concentration ratio when the insulin dose was increased to pharmacological level. Based on this observation, these researchers further suggested a possible role of an increase in diffusion area due to capillary recruitment to account for this increase in transport

with pharmacologic plasma insulin (307). Nevertheless, whatever constitutes the barrier, there is evidence that movement of insulin from the interstitium seems further restricted in type 2 diabetic patients when compared to healthy controls. Thus, despite an increase in capillary filtration of albumin, there was a decrease in labelled insulin transfer in the same type 2 diabetic patients (327).

Within the context of regulation, the dynamics of glucose uptake by muscle follow closely the time rate of change of interstitial insulin rather than plasma insulin (264, 344). Calibrated microdialysis technique in human muscle has also shown that the interstitial muscle glucose concentration is less than that in arterial plasma after overnight fasting, again supporting the view that free diffusion of glucose across the capillary endothelium limits glucose uptake (215). However, in insulin resistant muscle when steady state values are assessed, blood flow appears not to be limiting and vasodilatation due to insulin under clamp conditions leads to increased interstitial glucose levels without increasing the glucose transport rate (138). Indeed, neither the interstitial glucose concentration, nor the arterial-interstitial glucose differences differed between normal and type 2 diabetic subjects (300). From one point of view, if insulin resistance in muscle were to be the result of impaired capillary recruitment, then a larger gradient in steady state arterial-interstitial glucose concentration might be expected relative to normally responsive individuals not only before, but also following, insulin. However from another point of view and in the context of a temporal relationship, the time rate of delivery of insulin to the interstitium may be the key process in determining the relative insulin response in terms of muscle glucose uptake. Three recent studies from Peter Lonnroth's group have shown that in insulin resistant subjects there is a delayed rise in the interstitial concentration of insulin when compared to normal insulin responsive individuals (119, 297, 298). This finding is in harmony with earlier studies that showed a kinetic defect in the insulin-mediated activation of glucose uptake in insulin resistant subjects such as obesity (265, 320), hypertension (33) and type 2 diabetes (230, 320). Furthermore in these same studies from Peter Lonnroth's group, inulin (a polysaccharide of similar molecular size as insulin) delivery was similarly delayed in the insulin resistant subjects (297). Thus, such data would imply that a receptor-mediated transendothelial delivery of insulin, if present, plays only a minor role in normal insulin action and is not responsible for the delayed delivery evident in insulin resistant patients. Rather, these

findings are consistent with impaired capillary recruitment (54) that would lead to a delayed delivery evident in insulin resistant patients.

Consistent with the view that endothelial barrier is rate-limiting for insulin-mediated glucose disposal *in vivo*, Wasserman's group using labelled glucose analogues and markers for the extra-cellular space, found a rate-limiting step for muscle glucose uptake during insulin stimulation to be glucose delivery from plasma to interstitium (123, 234), particularly in white fiber type muscle of the rat (121) In addition, this rate limiting step of glucose delivery became a greater barrier in high fat fed rats, which show insulin resistance (107, 122). Thus a rate-limiting step for glucose delivery into the interstitium of muscle exists at the endothelium, and it appears that this step is further limiting in diabetes as it is for insulin delivery. Yet another approach using magnetic resonance spectroscopy (MRS) (295), which has the advantage of being non-invasive, has shown that fatty acid-induced insulin resistance in humans resulted from a significant reduction in the intramyocellular glucose concentration, suggestive of glucose transport as the affected rate-limiting step. However, since MRS only identified a gradient from extracellular to intracellular glucose (295), it remains to be proven that the gradient did not occur between the plasma and interstitial glucose and thus reflect a rate-limiting step of glucose delivery induced by fatty acids. This would be consistent with the data of Halseth *et al.* (122) and our own findings that fatty acids prevented insulin-mediated capillary recruitment in rats *in vivo* (58).

Overall, increasing evidence suggests the existence of an endothelial barrier that is rate-limiting for insulin-mediated glucose disposal in skeletal muscle. Considering the transfer of insulin from the plasma compartment to the interstitium in a kinetic sense, an insulin-mediated decrease in an endothelial barrier, an increase in delivery, or capillary recruitment are indistinguishable. Since insulin mediates capillary recruitment *in vivo* and this process is defective in a number of other models of insulin resistance (54), a defect in insulin signalling perhaps in the endothelial cells that are responsible for capillary recruitment may be a key issue.

1.5 TWO VASCULAR ROUTES IN SKELETAL MUSCLE

1.5.1 Early Evidence for the Existence of Two Vascular Routes in Skeletal Muscle

Evidence for the existence of two vascular routes in skeletal muscle can be traced back to over 30 years ago (17, 115, 144, 242). These early studies documented a mismatch between total blood flow into muscle and either metabolic and heat transfer responses (242), or the clearance of intramuscular injected or infused radioactive substances (16, 17). For example, using the isolated, constant-pressure perfused hindlimb or gastrocnemius muscle of the dog, Pappenheimer *et al.* (242) showed that when blood flow was reduced to the same degree either by stimulation of vasoconstrictor nerves or by the action of a low dose of epinephrine, the A-V difference in both O_2 content and temperature decreased, or increased respectively. On another occasion, Barlow *et al.* (17) simultaneously recorded clearance of ^{24}Na and venous outflow, and observed the capillary bed before, during and after intravenous infusions of adrenaline. These researchers found that the clearance of ^{24}Na injected into sites of semi-isolated biceps preparation known to consist mainly of muscle fibers was quicker than the clearance rate of ^{24}Na injected into the intramuscular septa or tendons. Furthermore, intravenous infusion of epinephrine (~100nM) increased the ^{24}Na clearance rate in the former tissue but slowed down or unaffected the rate in the latter. Based on these observations, it was proposed there are two separate circulatory systems within muscle, namely "nutritive" and "non-nutritive". Vessels in the nutritive route are considered to be those that have extensive contact with the skeletal muscle cells (144) and thus promote nutrient exchange. The "non-nutritive" route (17), which is considered to serve as a functional vascular shunt thus minimizes the opportunity for nutrient exchange to occur between the muscle cells and the constituents of the blood, has been difficult to identify. There was a vigorous search for the existence of arteriovenous shunts which could serve as the non-nutritive route in skeletal muscle. However, the absence of large shunts in skeletal muscle was demonstrated by the failure to pass injected wax microspheres of 20, 30 or 40μm either under basal conditions or during stimulation of vasodilator nerves (257). Furthermore, intravital microscopy studies by Hammersen *et al.* (125) failed to find any evidence of arteriovenous shunts in skeletal muscles from dog, monkey and rabbit. Using a double injection technique which succeeded in detecting arteriovenous anastomoses in rabbit's ear and cat's stomach (15), Barlow *et al.* (17)

failed to find evidence for arteriovenous anastomoses of a similar kind in skeletal muscle. In fact, these researchers indicated that the connective tissue vessels of the septa and tendon were likely the candidates for the non-nutritive route. In support of Barlow's conclusion and providing an anatomical basis, Grant and Wright (115) observed numerous arteriovenous channels wider than capillaries in the tibial tendon of the biceps femoris muscle in the rat.

A direct demonstration that skeletal muscle has two vascular routes and the non-nutritive routes may be those of connective tissue comes from studies on tenuissimus muscle which is accessible and transparent. Using intravital microscopy, it was revealed that the vasculature of this muscle preparation comprised transverse arterioles supplying both capillaries in muscle tissue proper and adjacent connective tissue. The two networks, muscle capillaries and adjacent connective tissue capillaries were found to be operating in parallel. By measuring the microvascular flow rates in both vascular networks in the tenuissimus muscle of anaesthetized rabbits, Lindbom and Arfors (188, 189) found flow to connective tissue to be 50% higher at higher environmental oxygen tension. Furthermore, using the same preparation, Borgstrom *et al.* (37) revealed that topically applied isoproterenol caused a marked redistribution of microvascular blood flow from muscle to connective tissue, indicating blood flow between the two vascular routes was controlled by vasoactive agents. However, despite these convincing observations in rabbit tenuissimus muscle, it is unknown whether this muscle preparation, which has special properties including high proportion of connective tissue vessels, is representative of the general anatomy of the bulk load-bearing cylindrical muscles. Although Myrhage and Eriksson (220) have argued that the vascular arrangement of the tenuissimus muscles existed as a basic unit in hind leg musculature, direct anatomical demonstration of non-nutritive routes in bulk muscle remains absent.

1.5.2 Recent Evidence for Two Vascular Routes in Rat Hindlimb

Work done in our laboratory has lent support to the notion of dual vascular routes in skeletal muscle. Using the constant-flow pump-perfused rat hindlimb, we have shown that skeletal muscle metabolism including oxygen uptake and lactate release as well as aerobic contractile performance is controlled by vasoconstrictors (51). One group of vasoconstrictors, typified by angiotensin II (AII) or low-dose norepinephrine

(LDNE) acts to increase oxygen uptake (64) and lactate release (136) as well as contractile performance (276). A second group of vasoconstrictors, typified by serotonin (5-HT), has the opposite effect and although causing the same changes in perfusion pressure, acts to decrease oxygen uptake (82), lactate release (136) and contractile activity (81). These metabolic effects of vasoconstrictors in the perfused hindlimb appear to be due to their vascular actions and not due to direct actions on the skeletal muscle as all of these effects could be reversed by vasodilators (63, 345). Also the vasoconstrictors had no effect upon contractility or insulin-mediated glucose uptake in isolated incubated muscles where supply of nutrients is by diffusion and not dependent upon the vasculature (81, 274, 275). The vascular actions of these vasoconstrictors in the perfused hindlimb appear to involve flow redistribution as total flow into this preparation was held constant. This view is supported by some indirect evidence from vascular casts (228), surface fluorometry and dye entrapment (228) and changes in the pattern of red blood cell washout (227). Furthermore, studies with fluorescent microspheres to measure flow rates in individual tissues showed that flow had not been redistributed between muscle and non-muscle tissues, or between muscles, as a result of LDNE- or 5-HT-induced vasoconstriction (52). Thus it appears likely that distribution of flow either away from the nutritive to the non-nutritive route or *vice a versa* occurred within individual muscles (52).

There is evidence that the non-nutritive route of the muscle of rat hindlimb lies in connective tissue. When pulses of fluorescein isothiocyanate dextran were infused into the hindlimb, the appearance of this substance in the tibial tendon vessels of the biceps femoris muscle of the perfused leg increased during 5-HT infusion which enhances non-nutritive flow in comparison to control (228). Consistently, when India ink was infused during perfusion, photomicroscopy of the India ink-filled vessels confirmed that the tendon vessels had generally increased in diameter in response to 5-HT (228). Moreover, studies investigating the effects of flow redistribution induced by vasoconstrictors on the clearance rate of chylomicron emulsion showed a much higher capacity of non-nutritive routes to clear triglyceride, indicating that lipoprotein lipase was likely to be more concentrated in the non-nutritive than the nutritive route (59). Since adipose tissue contains more activity of lipoprotein lipase than muscle, the higher clearance of triglyceride during non-nutritive flow would suggest an active presence of adipocytes on this route. Indeed, adipocytes have been reported to be

present on connective tissue vessels in muscle, particularly on the vessels that pass through the perimysium and epimysium (220). Thus, it would appear likely that non-nutritive vessels interpose within muscle but nourish fat cells and connective tissue rather than myocytes.

Although the identity of the non-nutritive route has not been fully clarified, there is evidence that altering flow redistribution between nutritive and non-nutritive pathways is able to control the access of nutrients and hormones to the muscle fibres and thereby to influence muscle metabolism. For example, in the constant flow pump-perfused muscle preparation the action of insulin to increase glucose uptake is markedly reduced when a vasoconstrictor is present that induces predominantly non-nutritive flow (275).

1.5.3 Evidence for Flow Redistribution Involvement in Insulin-Mediated Capillary Recruitment within Skeletal Muscle

Muscle microvascular blood volume measured by CEU increased maximally within 30min upon the commencement of insulin infusion ($3mU.min^{-1}.kg^{-1}$) in anesthetized rats which contrasted with total blood flow that remained unaffected (333). In addition, insulin administration at 3 or $40mU.min^{-1}.kg^{-1}$ significantly increased human femoral blood flow to a similar degree by the end of 2h infusion, but increased microvascular blood volume in a dose-dependent manner with greater capillary recruitment seen at the higher dose (66). These observations demonstrated the ability of insulin to recruit microvascular perfusion in the absence of a change in bulk blood flow. For this to occur, insulin may have caused a sharing of existing flow, which would consequently result in a slowing down in cell velocity in the capillaries. However, direct measurement of cell velocity in muscle capillaries by CEU shows that cell velocity remained unchanged during the capillary recruitment process that occurred during the first 30min insulin infusion at $3mU.min^{-1}.kg^{-1}$ (333) or during increasing insulin dose from 3 to $40mU.min^{-1}.kg^{-1}$ (66). This finding favours an alternative explanation that insulin may have induced a redistribution of blood flow from "non-nutritive" to "nutritive" vascular pathways within muscle. This "non-nutritive" pathway may have a rapidly-filled characteristic so that blood in these vessels is subtracted from the background and thus not included in microvascular blood volume measurement. Also since the non-nutritive route is unlikely to have high levels of xanthine oxidase, 1-MX metabolism in this route would be relatively low. The probability of flow

redistribution within the muscle by insulin is further supported by the greater increase in insulin-mediated microvascular blood flow calculated from capillary blood volume and capillary cell velocity (337) in comparison to changes in total blood flow in experimental animals during physiological and supra-physiological hyperinsulinemia (66).

1.6 POSSIBLE MECHANISMS FOR INSULIN-MEDIATED MUSCLE CAPILLARY RECRUITMENT

As discussed above, the two hemodynamic effects of insulin of bulk blood flow increase and capillary recruitment now appear to be independent of each other and capillary recruitment may involve an alteration in the proportion of nutritive to non-nutritive flow within muscle tissue. Thus, whereas an increase in total blood flow is generally considered to result from a vasodilation presumably at the resistant vessels, capillary recruitment may result from a constriction at sites that control entry to non-nutritive routes or relaxation of terminal arterioles controlling nutritive capillary bed or mostly likely the combination of both.

1.6.1 Possible Vasoconstriction Mechanisms

It is now generally recognized that in both animals and humans, acute insulin infusion (31, 181, 217, 248, 283) and carbohydrate ingestion (30) stimulate sympathetic nerve activity. In humans, acute physiological and pharmacological eulgycemia hyperinsulinemia is associated with an elevation of plasma circulating levels of catecholamine concentration (31, 283, 334) and norepinephrine spillover (181). Specifically, with the use of direct microelectrode recordings, it has been demonstrated that in humans, insulin stimulates marked sympathetic outflow to skeletal muscle (6, 31, 304, 335). The insulin-induced sympathetic activation is considered to cause vasoconstriction that which would be consistent with the marked fall in blood pressure following insulin injection absent in normal individuals, but revealed in patients with autonomic failure where there is no sympathetic pressor effect (203). Accordingly, the sympathetic outflow into muscle in response to insulin infusion would be expected to cause skeletal muscle vasoconstriction. In fact, this muscle sympathetic nerve activation (MSNA) has been suggested to be able to partly mask insulin-meditated vasodilation in human innervated limb (286). Thus, it is possible that MSNA induced by insulin selectively constricts non-nutritive vessels

and in turn redirects non-nutritive flow into nutritive routes. Although this hypothesis has not been experimentally explored, there is some evidence suggesting this possibility from current literature. MSNA appears to be a quick action of insulin. In non-diabetic Pima Indian men, systemic hyperinsulinemia ($80mU.m^{-2}.min^{-1}$) increased MSNA approximately 15min after the onset of insulin infusion and the time required to reach the half maximal effect was approximately 25min while calf blood flow showed significantly rise only after 45 min of insulin infusion (304). Similar early rise in MSNA in response to insulin infusion was also reported in other studies (6, 31). Such a time frame of MSNA would match our studies in rats where during physiological hyperinsulinemia ($3mU.min^{-1}.kg^{-1}$), capillary recruitment which preceded the increase in femoral blood flow, was activated within 10min and reached maximal activation within 30min after the onset of insulin infusion (332, 333). The blood pressure was unchanged from baseline despite a marked increase in MSNA in those non-diabetic Pima Indian men during hyperinsulinemia (304), indicating that increase in MSNA after insulin infusion has no presser effect although there was a lack of insulin-mediated vasodilation. It is possible that sympathetic nervous system response may be variable in different vascular beds (213) thus constriction in leg skeletal muscle may be cancelled by vasodilation in some other tissue or organ vasculature. However, it is equally possible that insulin constricts non-nutritive vessels via MSNA and simultaneously dilates terminal arterioles via other mechanisms. In this way, capillary recruitment occurs while vascular resistance in skeletal muscle remains constant. Furthermore, there is evidence that MSNA has a high sensitivity to insulin. Using a low-dose hyperinsulinemic clamp to raise plasma insulin to a modest level ($25\mu U.ml^{-1}$), Hausberg *et al.* (131) reported MSNA rose from 16 $bursts.min^{-1}$ (basal) to 25 $bursts.min^{-1}$ which is similar to those reported by others using a much higher dose of insulin ($>50uU.ml^{-1}$) (6, 334, 335). More importantly, forearm blood flow did not change at this very low dose of insulin (131). These observations suggest that MSNA is more sensitive to insulin than total blood flow and can be maximally activated at a relatively low dose of insulin. This would be in support of the hypothesis supporting the involvement of MSNA in insulin-mediated capillary recruitment. It is worth noting that Anderson *et al.* (6) reported in human limb that MSNA persists 1h after insulin had been stopped. This slow reversal of MSNA would be in accordance with Berne's finding that MSNA had not returned to

the basal level at 90 min after carbohydrate ingestion (30). Thus if MSNA had involved in insulin-mediated capillary recruitment, it would be expected that the reversal of capillary recruitment after the removal of insulin from circulation would also be a slow process. Nevertheless, the mechanism for insulin sympathoexcitatory effects is not clear although it has been suggested to be mediated at least in part by a central neural action (216). The ability of insulin to cross the blood-brain barrier (200) and the presence of insulin receptors in several distinct regions of the central nervous system such as the median hypothalamus (287) appear to support this concept. In the context of possible involvement of MSNA in insulin-mediated capillary recruitment, it may imply that capillary recruitment activation has a central neural component. In experimental animals, the observation that systemic hyperinsulinemia stimulated capillary recruitment would be consistent with this notion (273). The effect of local insulin infusion has not been examined in these animals. However, in human forearm, the observation that an intra-brachial artery insulin infusion activated capillary recruitment assessed by CEU (62) argues against a central neural involvement. Overall, although the mechanism(s) of insulin-associated MSNA remains elusive, the remarkable similarity in the time frame and dose responses to insulin between MSNA and capillary recruitment support the possibility of MSNA involvement in insulin-mediated capillary recruitment possibly via constricting vessels preceding non-nutritive route and directing flow into nutritive capillary bed while keeping a constant total blood flow and vascular resistance in skeletal muscle.

Alternatively, vasoconstriction that could take part in insulin-mediated capillary recruitment may be caused by a vasoconstrictor released in response to insulin. One agent likely to fulfil this role is endothelin-1 (ET-1). ET-1 is produced and secreted by the endothelial cells and is the most potent and enduring vasoconstrictor among the natural products tested so far both *in vivo* and *in vitro* (112, 260, 303, 341, 342). Thus, it is not surprising that ET-1 has been demonstrated to be involved in the maintenance of resting vascular tone (42, 204) and that endothelial dysfunction occurs in various vascular diseases including obesity and type 2 diabetes (41, 202, 280). More importantly, insulin is known to stimulate the release of ET-1. Studies performed in cell cultures have demonstrated an increased ET-1 gene expression in endothelial cells (237) and enhanced ET-1 release in both human endothelial and vascular smooth muscle cells (VSMCs) (8, 97). In whole body studies, after administration of insulin,

increased plasma levels of ET-1 have been observed in most (97, 254, 339) although not all (207) studies. Therefore, it is tempting to hypothesize ET-1 released in response to insulin may serve as a candidate to constrict non-nutritive vessels and redirect flow into nutritive capillaries leading to capillary recruitment and thereby facilitating insulin action. Unexpectedly, some whole body studies have established a relationship between ET-1 and insulin resistance. Elevated levels of ET-1 have been reported in a number of clinical disorders associated with insulin resistance, including type 2 diabetes (41, 96), obesity (95, 202) and hypertension (42, 184). A negative correlation between total glucose uptake and plasma ET-1 levels has been reported in NIDDM patients (96). Furthermore, intravenous infusion of ET-1 has been reported to be associated with decreased insulin-stimulated glucose uptake in humans (241) and animals (159) *in vivo*. Interestingly, *in vitro* studies investigating a possible direct metabolic action of ET-1 have produced conflicting results, *e.g.*, evidence of stimulatory (340) and inhibitory (45, 180) effects of ET-1 on insulin-mediated glucose uptake in isolated adipocytes. Idris *et al.* (148) further reported that acute exposure to ET-1 (30min) attenuated insulin-stimulated glucose uptake transiently in fat cells while acute or prolonged (24h) exposure of skeletal muscle derived L6 cells to ET-1 had no effect on insulin-mediated glucose uptake. Idris *et al.* (148) have therefore suggested that insulin resistance associated with hyperendothelinaemia *in vivo* is likely to be an indirect effect due to vasoconstriction with ET-1 and reduced perfusion of skeletal muscle, leading to decreased insulin and glucose delivery to insulin-sensitive tissues. In humans, lowered insulin-mediated leg glucose uptake during ET-1 infusion was associated an increase in mean arterial pressure, decreases in splanchnic and renal blood flow, but no change in total blood flow in the leg (241). Although the authors acknowledge that any possible redistribution of flow nutritive to non-nutritive or *vice versa* was not measured (241), it appears that ET-1 contrary to the proposed action of blocking non-nutritive route and mediating capillary recruitment, acts to block nutritive flow. Interestingly, in the constant-flow pump-perfused rat hindlimb, whereas ET-1 caused a dose-dependent increase in perfusion pressure, the effects on hindlimb oxygen consumption were biphasic with low doses increasing and higher doses leading to a net inhibition (168). Moreover in accordance with Idris's conclusion (148), studies with the addition of SNP to block ET-1-induced vasoconstriction suggest that the vascular effects of ET-1 account for the observed metabolic effects (168). Therefore, it appears that ET-1 has a biphasic dose-dependent

vasoconstrictor effect on hindlimb blood vessels. ET-1 at low dose may be able to constrict sites controlling entry to non-nutritive vessels to recruit capillaries leading to increased nutrient delivery and thus potentially assist insulin action, but at higher doses to redistribute flow to restrict muscle perfusion presumably via a more global vasoconstriction across the muscle vascular bed, thereby becoming potentially antagonistic of insulin action. Such findings would explain why elevated ET-1 is associated with insulin resistance rather than potentiating insulin action *in vivo*.

1.6.2 Possible Vasodilation Mechanisms

At present, studies on the mechanisms of insulin-mediated vasodilation mainly focus on total blood flow rather than flow redistribution. For the former, NO involvement is convincing. Locally infused L-NMMA was found to block insulin-mediated increase in leg blood flow and partially (~25%) inhibit glucose uptake (21, 308). A number of other groups also reported that the vasodilator action of insulin was blocked by inhibitors of NOS (56, 288). Furthermore, locally infused Mch, a cogener of acetylcholine and producer of NO, increased insulin-mediated leg glucose uptake and blood flow (25). Such data lend strong support to the probability that the limb blood flow action of insulin is mediated by NO.

The control of capillary recruitment by insulin, although confirmed in human forearm studies (62), has not been assessed with regard to NO-dependency by infusing NOS inhibitors locally. In rats we have deployed systemic inhibitors of NOS (331, 332) and in each of these studies L-NAME raised blood pressure, completely inhibited insulin-mediated increases in limb blood flow, capillary recruitment and partly the uptake of glucose by the hindlimb. However, whole body glucose requirement, indicated by the glucose infusion rate to maintain euglycaemia was not inhibited (331, 332). Thus a complex picture emerges, where it seems likely that systemic L-NAME alters hepatic glucose production to match the partially inhibited insulin-mediated glucose uptake by the hindlimb. Until this is resolved conclusions that both limb blood flow and capillary recruitment are mediated by insulin through NO-dependent mechanisms may be premature. An alternate view, based again on data from experimental animals, suggests that NOS inhibitors when applied systemically may act via neural effects. For example, Shankar *et al.* (293) showed in rats that stereotactically infused L-NAME into the lateral ventricle created the same hypertension-associated insulin

resistance as did systemically applied L-NAME. These effects occurred without any detectable presence of L-NAME in peripheral blood. More recently, using a technique for studying the effects of locally infused agents in the rat hind leg, Mahajan *et al.* (196) have found that tetraethylammonium chloride (TEA), an inhibitor of Ca^{2+} dependent K^+ channels, but not L-NAME, blocked systemic insulin-mediated capillary recruitment and glucose uptake in muscle *in vivo*. Furthermore, locally infused Mch, but not bradykinin, enhanced insulin-mediated capillary recruitment and glucose uptake, when both strongly vasodilated the hindlimb (197). Taken together, these findings imply that insulin mediates vasodilation leading to capillary recruitment in muscle by a central neural effect that is NO-dependent and which manifests in the muscle microvasculature through an EDHF-dependent process controlling capillary recruitment that can be potentiated by local Mch in an NO-dependent mechanism. In human studies Mch has been reported to potentiate insulin's action in muscle in normally responsive individuals (25) and to enhance insulin action in hypertensive insulin resistant patients (285). Indirect evidence for neural involvement in the microvascular actions of insulin also comes from a recent study of normally responsive subjects where impaled laser Doppler probes detected an insulin-mediated increase in low frequency vasomotion (68).

The fragmentary evidence implicating a neural involvement in insulin-mediated capillary recruitment where insulin primarily interacts with central receptors is in contrast to the direct actions of insulin to dilate isolated segments of large and medium size blood vessels of 50-100microns (44, 289), as well as to stimulate NO production in isolated endothelial cells (352). However, these large resistance vessels which are considered to control bulk blood flow may act differently in response to insulin from smaller arterioles (e.g. third- or fourth-order arterioles) that are more likely to regulate microvascular perfusion and flow redistribution within tissue. Although dilation of third (~20μm diameter) and fourth-order (~10μm diameter) arterioles has been observed in response to insulin either systemically or topically applied to the muscle (150, 205, 262, 278), the inaccessibility of these small arterioles to isolation means that direct actions of insulin have not been studied. Therefore, whereas studies using isolated blood vessels (44, 289) and local infusion of NO inhibitors (21, 308) have provided compelling evidence for a direct

vasodilator action of insulin to regulate bulk flow, whether the vasodilation of small arterioles involved in insulin-mediated capillary recruitment through a similar direct vascular mechanism remains elusive.

Nevertheless, the possibility exits that insulin acts directly on the microvasculature to control capillary recruitment. In this regard, there are at least two possible mechanisms. First, insulin may act at insulin receptors on endothelial cells (352) to activate the insulin signalling cascade leading to the release of a vasodilator which causes VSMCs relaxation. Recent studies in primary cultures of endothelial cells have elucidated a complete insulin signalling cascade from the insulin receptor to activation of endothelial NO synthase (eNOS) and NO production via insulin receptor substrate (IRS)-1, PI 3-kinase, PDK-1 and PKB/Akt (212, 351, 352). NO in turn permeates adjacent VSMCs to activate soluble guanylyl cyclase and lower the vascular tone of pre-capillary sphincters resulting in vasorelaxation. This mechanism is consistent with recent findings that insulin-mediated capillary recruitment and leg glucose uptake was blocked by systemically infused L-NAME (331, 332), but inconsistent with the findings that local infusion L-NAME did not block systemic physiological hyperinsulinemia-mediated capillary recruitment in rat hindlimb and the findings that insulin vascular endothelial receptor knock out mice (VENIRKO) are not insulin resistant (328). The second possibility by-passes an endothelial insulin receptor-dependent mechanism and instead involves insulin interacting at insulin receptors on the VSMCs. This mechanism would also be NO-dependent as suggested by studies in human VSMCs where the NOS inhibitor L-NAME blocked insulin-induced increases in cGMP level (318, 319), and attractive since TNFα which blocks insulin-mediated capillary recruitment (350) is known to inhibit insulin signaling in VSMCs, although to date this has been restricted to the ERK1/2 activation step (113).

Another possibility is that the signal may derive from the stimulation of muscle metabolism via insulin receptors on skeletal muscle cells. For instance adenosine, a potent dilator released as metabolic by-product in response to an increased tissue metabolism, has been suggested to play a role in topically applied insulin-mediated vasodilation in cremaster muscle of anesthetized hamsters (205). Furthermore, NO

derived from skeletal muscle may also play a role as skeletal muscles express the neuronal type NO synthase (nNOS) (162, 167, 296). However, the quicker response of insulin-mediated capillary recruitment than glucose uptake *in vivo* appears to argue against a metabolic vasodilation mechanism for capillary recruitment (332, 333). Rather, this mechanism is consistent with insulin-mediated increase in bulk blood flow which lags behind insulin-mediated muscle glucose disposal (332, 333).

Taken together, it seems that insulin may have both vasodilator and vasoconstrictor actions in skeletal muscle vascular bed and capillary recruitment are likely the net result of the combination of the both effects. When *in vivo* studies are considered where insulin recruits capillaries without altering total flow and capillary flow velocity, the vasoconstriction is likely at the sites controlling the entry to non-nutritive routes resulting in a recruitment of flow into nutritive network. Furthermore, both central neural and local mechanisms with an involvement of different cell types appear to contribute to the overall action of insulin to enhance skeletal muscle microvascular perfusion.

1.7 AIMS OF THIS STUDY

Whereas there are on-going debates regarding the physiological relevance of the increase in bulk blood flow in insulin action (325, 347), there is growing evidence that insulin's microvasclar action to recruit new capillaries may be more important in influencing muscle glucose uptake (272, 273, 332, 333). This concept was further explored in the first aspect of the thesis by looking at the regulatory aspects of insulin-mediated capillary recruitment in relation to insulin-mediated increase in total blood flow and glucose uptake. Thus, insulin's effects on total blood flow, capillary recruitment and glucose metabolism were investigated at a range of insulin concentrations in anaesthetized rats using euglycemic hyperinsulinemic clamp. Then a physiologic insulin dose was chosen to activate hemodynamic and metabolic responses in these animals and the time course effects of these responses were examined after the termination of insulin infusion. Furthermore, TNFα which was reported previously to be able to influence insulin's metabolic and vascular actions (350) was used against serial doses of insulin to further explore the relationship between insulin-mediated capillary recruitment and muscle glucose uptake.

There is evidence suggesting insulin-mediated capillary recruitment may involve enhanced nutritive flow at the expense of non-nutritive flow (66, 333). Using the constant flow pump-perfused rat hindlimb preparation, we have provided indirect evidence of flow redistribution between the two vascular routes within hindlimb muscle using two types of vasoconstrictors (51), yet direct evidence, in particular regarding to the identity of non-nutritive routes, remains absent. Thus, the second aspect of the thesis attempted to identify the vascular routes perfused by basal flow, predominantly nutritive (created by AII) or non-nutritive (created by 5-HT) flow in the muscle sections with the aim of providing anatomical insights into insulin-mediated capillary recruitment.

CHAPTER 2
MATERIALS AND METHODS

2.1 ANIMAL CARE

Male Hooded Wistar rats were cared for in accordance with the principles of the Australian Code of Practice of the Care and Use of Animals for Scientific Purposes (1990, Australian Government Printing Service, Canberra). Experimental procedures were approved by the committee on the Ethical Aspects of Research Involving Animals of the University of Tasmania. Rats were housed (5-8 rats per cage) at 22°C in a 12h light/12h dark cycle with free access to water and a commercial rat chow (Gibsons, Hobart) containing 21.4% protein, 4.6% lipid, 68% carbohydrate and 6% crude fibre with added vitamins and minerals.

For studies using contrast-enhanced ultrasound (CEU) in Chapter 3, male Sprague-Dawley rats weighing 250 – 350 grams were obtained from Hilltop Laboratory Animals (Scottdale, PA). Animals were housed at 22 ± 2 °C and maintained with a 12h light/12h dark cycle. The animals were provided with food and water ad libitum until food was removed at 5:00 P.M. on the evening before the experiment. The University of Virginia Animal Care and Use Committee approved these experimental protocols.

2.2 *IN VIVO* EXPERIMENTS

2.2.1 Surgery for *In Vivo* Experiments

Rats were anaesthetized using pentobarbital sodium (50 $mg.kg^{-1}$ body weight) and had polyethylene cannulae (PE-50, Intramedic®) surgically implanted into the carotid artery, for arterial sampling and measurement of blood pressure (pressure transducer Transpac IV, Abbott Critical Systems) and into both jugular veins for continuous infusion of anesthetic and other intravenous infusions. A tracheotomy tube was inserted, and the animal was allowed to spontaneously breathe room air throughout

the course of the experiment. Small incisions (1.5 cm) were made in the skin overlaying the femoral vessels of each leg, and the femoral artery was separated from the femoral vein and saphenous nerve. The epigastric vessels were then ligated, and an ultrasonic flow probe (Transonic Systems, VB series 0.5 mm) was positioned around the femoral artery of the right leg just distal to the rectus abdominus muscle. The cavity in the leg surrounding the probe was filled with lubrication jelly (H-R, Mohawk Medical Supply, Utica, NY) to provide acoustic coupling to the probe. The probe was then connected to the flow meter (Model T106 ultrasonic volume flow meter; Transonic Systems). This was in turn interfaced with an IBM compatible PC computer which acquired the data (at sampling frequency of 100Hz) for femoral blood flow, heart rate and blood pressure using WINDAQ data acquisition software (DATAQ Instruments). The surgical procedure generally lasted approximately 30min and then the animals were maintained under anesthesia for the duration of the experiment using a continual infusion of pentobarbital sodium ($0.6 mg.min^{-1}.kg^{-1}$). The femoral vein of the left leg was used for venous sampling, using an insulin syringe with an attached 29G needle (Becton Dickinson). The body temperature was maintained at 37°C using a water-jacketed platform and a heating lamp positioned above the rat.

2.2.2 *In Vivo* Experimental Procedures

Once the surgery was completed, a 60min equilibration period was allowed so that leg blood flow and blood pressure could become stable and constant. Detailed experimental protocols are given in each of the experimental chapters. Generally, an arterial sample was taken at the end of equilibration and multiple arterial samples were taken at regular intervals during the experiment. During euglycemia hyperinsulinemic clamps when insulin (Humulin R, Eli Lilly, Indianapolis, IN) was infused alone or co-infused with the inflammatory cytokine, glucose (30% w/v solution) was administrated to maintain blood glucose levels at or above basal level. In control groups, saline or the inflammatory cytokine infusions were matched to the volumes of insulin, glucose and/or inflammatory cytokine infused during the clamp. A duplicate venous sample (V) was taken only on completion of the experiment to prevent alteration of the blood flow from the hindlimb due to sampling, and to

minimize the effects of blood loss. The total blood volume withdrawn from the animals before the final arterial and venous samples did not exceed 1.5ml. Provided that the total blood volume in a rat of 250g is about 16ml (79), the blood lost during the experiment was easily compensated by the volume of fluid infused. Arterial samples for biochemical assays were centrifuged immediately and kept in a -20°C freezer. Lower leg muscles were dissected individually after taking all blood samples and stored in -20°C until assayed for 2-DG uptake.

As described above, these in vivo experiments were performed in pentobarbital-anesthetized animals to minimize the surgery-associated stress, eliminate the influence of environmental factors and allow the flow probe positioning and blood flow measurement. Whereas the aesthetic status were well controlled in these animals, it is worth to note that pentobarbital has established effects on lowering sympathetic nervous system activity and pentobarbital-induced anaesthesia has been reported to associate with reduced insulin sensitivity in muscle (153) and liver (55). Therefore, insulin actions observed in the current studies using anethetized animals may be found to differ and likely to be more profound when studies were performed in conscious unstrained animals.

2.2.3 Glucose Assay

A glucose analyser (Yellow Springs Instruments, Model 2300 Stat plus) was used to determine whole blood glucose and plasma glucose (by the glucose oxidase method) during and at the conclusion of the *in vivo* experiments. A sample volume of 25 μl was required for each determination.

2.2.4 Hindleg Glucose Uptake

To measure the glucose uptake across the lower hindlimb, both arterial sample (A) and venous sample (V) from the femoral vein which drains blood from lower leg were taken and glucose levels were determined. Hindleg glucose uptake was calculated from A-V glucose difference, multiplied by femoral blood flow and expressed as μmol.min^{-1}. Since hindleg glucose uptake is a single-point measurement and these

samples were taken at the conclusion of each experiment, end-point femoral blood flow was used for this calculation.

2.2.5 2-Deoxyglucose Uptake

To measure glucose uptake in individual muscles, a 50μCi bolus of 2-deoxy-D-[2,6-^{3}H]glucose (2DG; specific activity = 44.0 Ci/mmol, Amersham Life Science) in saline was administrated at 45min prior to the completion of the experiment. Plasma samples (25μl) were collected at 5, 10, 15, 30 and 45min after the 2-DG injection to determine plasma clearance of the radioactivity. At the conclusion of the experiment, the soleus, plantaris, red gastrocnemius (RG), white gastrocnemius (WG), extensor digitorum longus (EDL) and tibialis muscle were removed, clamp-frozen in liquid nitrogen and stored at –20°C until assayed for 2DG uptake.

The frozen muscles were ground under liquid nitrogen and homogenised using an Ultra Turrax™. Free and phosphorylated 2-DG were separated by ion exchange chromatography using an anion exchange resin (AG1-X8) (154, 169). Scintillant (16ml; Biodegradable Counting Scintillant-BCA, Amersham USA) was added to each radioactive sample and radioactive counts (disintegrations per minute, dpm) were determined using a scintillation counter (Beckman LS3810, USA). From this measurement and knowledge of plasma glucose and the time course of plasma 2DG disappearance, R'g, which reflects glucose uptake into the muscle, was calculated as previously described in detail by others (154, 169) and expressed as $\mu g.g^{-1}.min^{-1}$. R'g for the combined muscle was calculated from the sum of R'g of each individual muscle times the wet weight of the individual muscle and divided by the sum of each individual muscle wet weight.

2.2.6 1-MX Metabolism

To assess the perfused capillary area, a method utilizing the metabolism of exogenously added 1-methylxanthine (1-MX, Sigma Aldrich Inc) has been established in our laboratory (273). 1-MX is the exogenous substrate of xanthine oxidase (XO) which converts 1-MX to a single product 1-methylurine (1-MU) (67, 273). Both 1-MX and 1-MU are non-vasoactivce (67, 273) and can be fully recovered

and measured by high-performance liquid chromatography (HPLC) (273). In skeletal muscle, XO is expressed primarily in the endothelial cells of the capillaries and small arterioles and not large vessels (132, 156). Thus 1-MX uptake/metabolism across hindleg corresponds to hindleg capillary surface area which increases when capillary recruitment occurs.

To determine hindleg 1-MX metabolism, 1-MX ($0.4mg.min^{-1}.kg^{-1}$, dissolved in saline) was infused systemically through one of the cannulated jugular veins at 60min prior to the end of the experiment. Since 1-MX clearance was very rapid, it was necessary to partially inhibit the xanthine oxidase activity (273) to obtain a constant arterial 1-MX concentration. To do this, an injection of a specific xanthine oxidase inhibitor, allopurinol (88) ($10\mu mole.kg^{-1}$) was administered as a bolus dose 5min prior to commencing the 1-MX infusion. Our previous report has shown that after the bolus of injection, allopurinal was only detectable in plasma for 15min as it was rapidaly converted to oxypurinol which could be detected throughout the rest of the experiment (273). Importantly, a constant arterial 1-MX concentration was achieved at 15min after the commencement of 1-MX infusion and maintained throughout the experiment (273).

At the end of the experiment duplicate arterial (A) and venous (V) samples ($100\mu l$) were taken and placed on ice. These blood samples were immediately centrifuged and $20\mu l$ of plasma mixed with $80\mu l$ of 0.42M PCA. The PCA treated samples were then stored at -20°C until assayed for 1-MX. When required, samples were thawed on ice, centrifuged for 10min and the supernatant used to determine 1-MX, allopurinol and oxypurinol concentrations by reverse-phase HPLC as described previously (272, 273). The 1-MX metabolism in $nmoles.min^{-1}$ was calculated from the following equation:

$$1\text{-}MX\ metabolism = ([1\text{-}MX]a - [1\text{-}MX]v) \times 0.871 \times FBF$$

Where [1-MX]a and [1-MX]v are the plasma 1-MX concentrations ($\mu mol.L^{-1}$) obtained from arterial and venous blood samples respectively; 0.871 is the factor to convert the 1-MX concentration measured in plasma to that in whole blood; FBF is the femoral blood flow rate ($ml.min^{-1}$) measured at the same time when venous blood samples were withdrawn.

2.2.7 Contrast-Enhanced Ultrasound (CEU)

CEU has been used extensively in the past to measure microvascular flow in the myocardium (191, 244, 337). Modification of this technique for its use for rats has been described previously (333). Thus, a linear-array transducer interfaced with an ultrasound system (HDI-5000; Philips Ultrasound, Santa Ana, CA) was positioned over the right hindlimb of the rat to image the proximal adductor muscle group (adductor magnus and semimembranosus), which comprises ~5% slow-twitch oxidative, 30% fast-twitch oxidative-glycolytic, and 65% fast-twitch glycolytic fibers (9), and secured for the duration of the experiments. Pulse inversion imaging was performed at a transmission frequency of 3.3 MHz. The mechanical index ([peak negative acoustic pressure] x [frequency]$^{-1/2}$), a measure of acoustic power, was set at 0.8. The acoustic focus was set at the mid-portion of the muscles. Gain settings were optimized and held constant, and data were recorded on 1.25cm videotape using a S-VHS recorder (Panasonic MD830; Matsushita Electric). Perfluorocarbon gas-filled, albumin-coated microbubbles (Optison; Mallinckrodt Medical) were infused intravenously as the contrast-enhancement agent. A microbubble infusion rate of 120μl.min^{-1} was chosen because this rate resulted in video intensity measurements that were well within the linear rage of the microbubble concentration and video intensity (333). The acoustic signal that is generated from the microbubbles when exposed to ultrasound is proportional to the concentration of microbubbles within the volume of tissue being imaged. Essentially, all microbubbles within the ultrasound beam are destroyed in response to a single pulse of high-energy ultrasound, and as the time between each pulsing is prolonged, the beam becomes progressively replenished with microbubbles. Eventually, the beam will be fully replenished and further increases in the time between each pulsing will not produce a change in tissue opacification (Fig 2.1) (333). The rate of microbubbles reappearance within the ultrasound beam provides an indication of microvascular flow velocity (β), and the plateau video intensity reached at a long pulsing interval provides a measurement of microvascular volume.

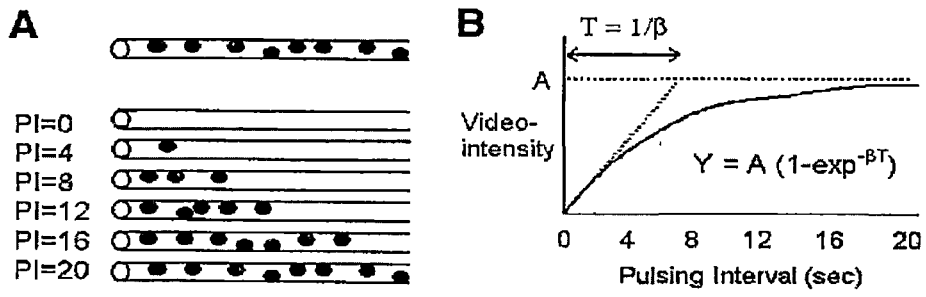

Figure 2.1 A: Schematic depiction of the replenishment of microbubbles in capillaries after a pulse of high-energy ultrasound. As the time between each ultrasound pulse is prolonged, more microbubbles reappear. PI, pulsing interval. B: A typical relation between pulsing interval and acoustic signal, measured as video intensity. As the pulsing interval is prolonged, the number of microbubbles within the capillaries increases, resulting in a higher video intensity. Eventually a plateau is reached where an increase in the time interval between each pulsing interval dose not cause a further increase in video intensity due to complete replenishment of the vessels in the beam. The asymptote that intercepts the y-axis is the maximal video intensity signal and a measurement of microvascular volume (capillary recruitment). The x-intercept of the y-axis asymptote and the tangent to the upward sloping hyperbolic function is a measure of the rate constant of video intensity rise (β), an indicator of microvascular flow velocity. Reproduced from Vincent (333).

Images were acquired at pulsing intervals from 1 to 20sec. Image analysis was performed off-line. Frames were aligned by cross-correlating several frames at each pulsing interval, and these were separately averaged and digitally subtracted from images obtained during continuous imaging, which served as background. Using images acquired with delays of 0.5sec as background allowed for the elimination of larger vessels (velocity > $0.1 cm.s^{-1}$) that fill promptly. The background-subtracted video intensity at each pulsing interval was measured from the muscle, and pulsing interval versus video intensity data were fitted to the function, $y=A\ (1 - e^{-\beta t})$, where y is video intensity, t is the pulsing interval, A is plateau video intensity (an index of microvascular volume), and β is the rate constant, which provides a measure of flow velocity in the microvasculature (Fig 2.1) (333).

2.2.8 Biochemical Assays

Insulin levels at the beginning and the end of experiments were determined from arterial plasma samples by ELISA assay (Mercodia AB, Sweden). A Murine TNFα ELISA Kit (Pierce Endogen USA) was used to determine plasma TNFα levels in experiments involving TNFα infusion.

2.2.9 Hemodynamic Data Analysis

Mean femoral blood flow, mean heart rate and mean arterial blood pressure were calculated from 5sec sub-samples of the data, representing approximately 500 flow and pressure measurements every 15min. Vascular resistance in the hindleg was calculated as mean arterial blood pressure in millimetres of mercury divided by femoral blood flow and expressed as resistance units (R.U.).

2.2.10 Statistical Analysis

Repeated measures two-way analysis of variance was used to test the hypothesis that there was no difference among treatment groups for femoral blood flow, blood pressure, heart rate and vascular resistance throughout the time course. When a significant difference ($P<0.05$) was found, pair wise comparisons by the Student-

Newman-Keuls test were used to determine at which individual times the differences were significant. Statistical difference among treatments for arterial glucose and 1-MX, hind leg glucose uptake, and hindleg 1-MX metabolism was determined by unpaired *t*-test. These tests were performed using the SigmaStat statistical program (Jandel Software).

2.3 RAT HINDLIMB PERFUSION EXPERIMENTS

This technique was first described by Ruderman *et al* (284) and has been proved to be a useful tool for studying muscle metabolism under physiological conditions at the isolated organ level (36).

2.3.1 Hindlimb Surgery

Hindlimb surgery was essentially as described by Ruderman *et al.* (284) with additional details as given previously (64).

Rats were anaesthetized with an intraperitoneal injection of pentobarbital sodium (60mg.kg^{-1} body weight). Surgery was then performed with reference to Fig 2.2 (for anatomical nomenclature see Greene (117)). After a midline abdominal incision, the abdominal wall was reflected and the superior epigastric vessels were ligated. The abdominal wall was then incised from the pubic symphysis to the xiphoid process. The superficial epigastric artery and vein of the right leg were ligated for single hindlimb perfusion. The internal spermatic vessels and other vessels supplying the testes, the neck of the bladder and the seminal vesicles were ligated. The testes and seminal vesicles were removed. The colon was excised between two ligatures placed around the colon, proximal to the inferior mesenteric artery. The colon and large intestine were separated from the connective tissue to the level of the renal vessels. A ligature was placed around the duodenum and the gastro-intestinal tract excised below the level of the ligature. A ligature was placed around the iliolumbar vessels, the internal spermatic vessels and the ureter on both sides. Ligatures were placed around the tail near the anus and around the tarsus of the right foot. The left common iliac artery and vein were ligated to prevent the flow from reaching the left leg. Two pairs

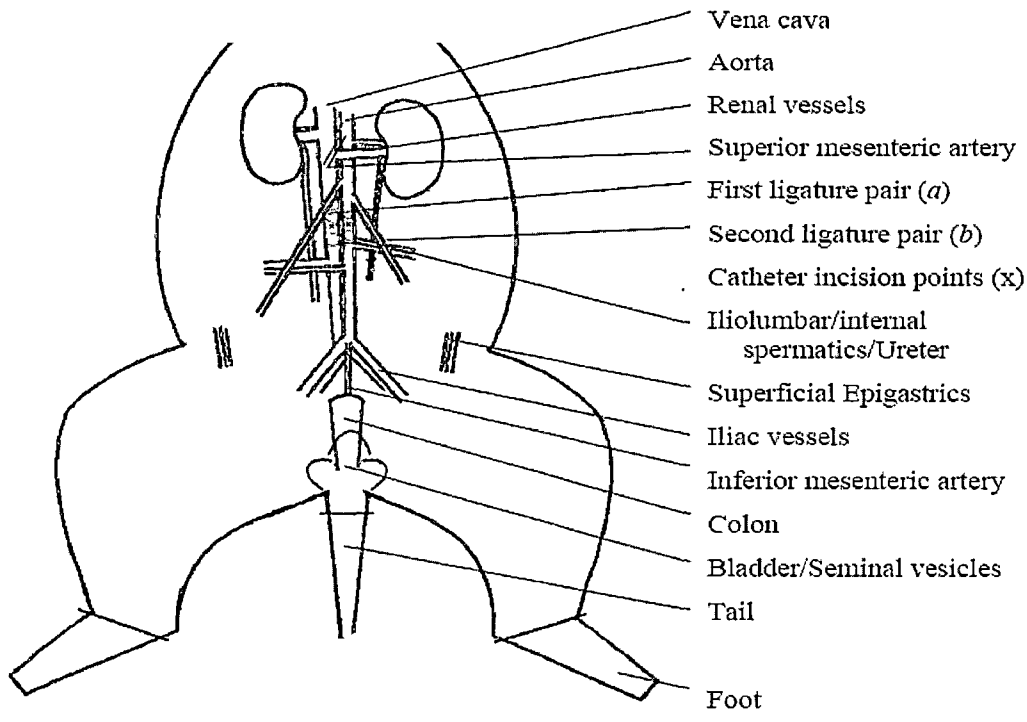

Figure 2.2 Surgery for perfused rat hindlimb

Surgery details are given in section 2.3.1. The surgical procedure was a modification of that of Ruderman (284). Nomenclature was from Greene (117).

of loose ligatures were placed around the vena cava and descending aorta between the renal vessels and the iliolumbar vessels. Heparin was injected (1000 IU.100g^{-1} body weight) into the vena cava above the renal vessels and allowed to circulate for 1min. The vena cava ligature (a) was tightened and the vena cava cannulated by using a Terumo 18G needle with a 16G catheter. The catheter tip was positioned ~5mm above the aortic bifurcation and the catheter was secured within the vena cava by tying both ligatures (a and b) around it. Then the aortic ligature was tightened (a) and a small cut in the aorta was made to allow the insertion of a 20G catheter attached to a 1ml syringe filled with saline (0.9% NaCl). The catheter was pushed gently until the tip was at the same level as the venous catheter, then secured by tying both ligatures (a and b). The preparation was transferred to the perfusion apparatus and the arterial catheter was connected to the oxygenated perfusion medium flow line. The venous catheter was connected to the outflow line. Approximately 2min elapsed from the time the vena cava was ligated and the circulation was re-established. The rat was sacrificed with an overdose of pentobarbital sodium (12mg) injected into the heart. A final ligature was placed around the torso at the level of the L3-L4 vertebrae to prevent flow reaching the upper torso. The entire procedure required 20~25min.

2.3.2 Perfusion Medium

A modified Krebs-Henseleit bicarbonate buffer (118mM NaCl, 4.7mM KCl, 1.2mM KH_2PO_4, 1.2mM $MgSO_4$, 25mM $NaHCO_3$ and 8.3mM Glucose) was used containing 4% bovine serum albumin (BSA, fraction V: Boehringer Mannheim, Australia). The perfusion buffer was filtered (0.45μm filter) and stored in the -20°C freezer until use.

2.3.3 Perfusion Procedure

Perfusions were conducted in a thermostatically-controlled cabinet (32°C) and the set up of this cabinet is shown in Fig 2.3. Perfusion medium reservoir was gassed with carbogen (95% O_2-5% CO_2) to enable full oxygenation and attainment of pH 7.4. After gassing for 30 minutes, $CaCl_2$ was added to give a final concentration of 2.54mM. The perfusion medium was pumped by a peristaltic pump (Masterflex, Cole-Palmer, USA) at a constant rate of 8ml.min^{-1}. The medium passed through a Silastic

lung which consisted of a glass jar containing 7 metres of Silastic tubing (ID 1.47mm/OD 1.91 mm, Dow Corning, USA) and was gassed with carbogen as well. This ensured constant arterial PO_2 levels. The perfusion medium then passed through a heat exchanger coil to raise the temperature to 32°C. An infusion port (for addition of drugs) and bubble trap proximal to the arterial inflow line was also included. A peristaltic pump (LKB Microperpex 2132, USA) was used for the infusion of drugs and other compounds. A pressure transducer proximal to the aorta continuously monitored arterial perfusion pressure. Venous oxygen tension was also continuously monitored using a temperature controlled (32°C) in-line Clark-type oxygen electrode (0.5ml capacity). Venous partial pressure of oxygen and arterial perfusion pressure were recorded on a computer via a Windaq Data acquisition system. Before any perturbations were made, the hindlimb preparation was allowed to equilibrate for 40 minutes.

2.3.4 Oxygen Consumption Calculation

At the beginning and end of each experiment, the oxygen electrode was calibrated with 100% oxygen and air (21% oxygen). Any drift in the electrode was assumed to be linear over the course of the experiment. At the end of the experiment, the arterial oxygen pressure was determined by bypassing the preparation and joining the arterial and venous lines. The oxygen consumption in $\mu mol.h^{-1}.g^{-1}$ was calculated according to the following equation:

$$VO_2 = \frac{60\ \beta\ (PaO_2 - PvO_2)\ Q}{1000\ M}$$

where β is the Bunsen coefficient for the solubility of oxygen in plasma (1.351 $\mu mol.L^{-1}.mmHg^{-1}$ at 32°C, (47)), PaO_2 and PvO_2 are the arterial and venous partial pressure of oxygen (mmHg) respectively, Q is the perfusion flow rate ($ml.min^{-1}$), M is the perfused muscle mass which has been previously determined to be $1/12^{th}$ of the body weight of a 180-200g rat (281), 60 and 1000 are conversion factors ($min.h^{-1}$ and $ml.L^{-1}$ respectively).

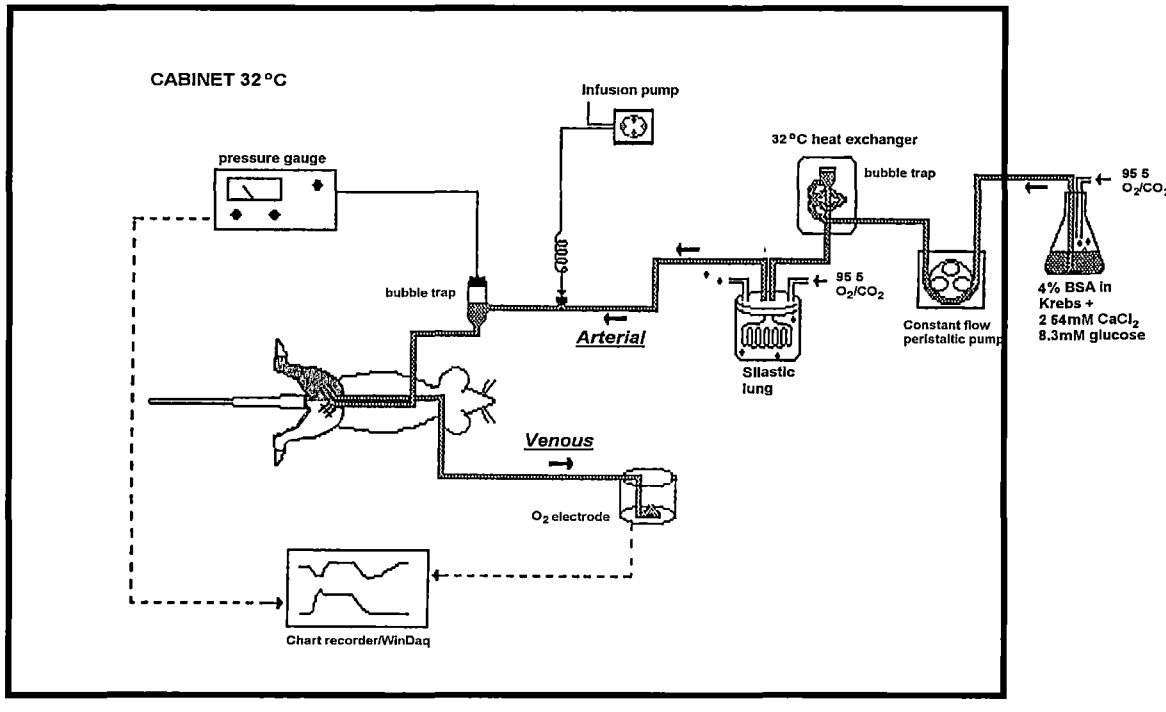

Figure 2.3 Hindlimb perfusion apparatus

Details of this apparatus and perfusion procedure are given in section 2.3.2 and 2.3.3.

2.3.5 Perfusion Fixation

When the perfusion pressure and oxygen consumption reached steady state after the various treatments, perfusion fixation was performed in study 1 and 2 in Chapter 6. Prior to fixation, BSA was washed out of hindlimb vascular bed by perfusing for 2min with carbogen-gassed Krebs buffer containing 1.27mM Ca^{2+}. Perfusion fixation followed using 2.5% glutaraldehyde (Sigma, EM grade) in 0.1M phosphate buffer with a pH of 7.4. In study 1 of Chapter 6, the hindlimb was perfused with glutaraldehyde for 3min. In study 2 of Chapter 6, a total amount of 40ml of glutaraldehyde was pumped through hindlimb. In both cases, perfusion flow rate was varied to maintain a constant pressure at the value attained during the steady-state BSA perfusion.

2.3.6 Statistical Analysis

Statistical difference between groups was assessed by one-way measure analysis of variance (ANOVA). Paired *t*-test was used to assess whether a treatment has a significant effect on the same experimental animals. These tests were performed using the SigmaStat statistical program (Jandel Software). All data is presented as means ± SE with significant difference recognised at $P<0.05$ level.

2.4 MUSCLE PERFUSION PATTERN EXAMINATION

2.4.1 Tissue Preparation

The extensor digitorum longus (EDL) muscle was chosen to analyse since the fibre composition of the EDL is representative of the average hindlimb composition (10). The EDL muscle of the perfused leg was excised and cut transversely into four blocks of approximately equal size. Each block was mounted onto a cork disk with transverse orientation and snap-frozen in isopentane cooled by liquid nitrogen. For study 3 of Chapter 6, an additional overnight cryo-protection in 30% sucrose at 4°C was performed prior to tissue freezing. Frozen tissue was cut into 7μm sections on a cryostat (Leica, Jung Frigocut 2800E) at -20°C. Five sections were cut from each

tissue block and sections from the same experiment were mounted onto one slide. For study 3 of Chapter 6, where rhodamine-dextran70 (Lysine fixable, Molecular Probes) was infused to mark perfused vasculature, sections were mounted in the aqueous mounting medium (Permafluor, Immunotech) and subjected to fluorescence microscopy. For study 1 and 2 of Chapter 6 where glutaraldehyde was perfused to fix perfused tissue, sections were air-dried and subjected to immunohistochemistry staining and subsequent bright-field microscopy.

2.4.2 Immunohistochemistry

Griffonia (Bandeiraea) Simplicifolia lectin 1 (GSL-1) (Vector, Burlingame, CA, USA), a lectin exhibiting binding specificity for α-D-galactopyranosyl groups (218) and specifically binding to endothelial cells and basement membrane (127, 175, 251) was used to identify capillary endothelial cells and outline the muscle fibers in transverse frozen sections. Air-dried sections on 3-aminopropyltriethoxysilane (APS, Sigma) coated slides were rinsed twice in 50mM Tris buffer (TB) pH 7.6, and then treated with peroxidase blocking reagent (Dako) for 15min, rinsed twice in TB with 0.9% sodium chloride (TBS). Sections were then immersed for 45min in GSL-1 at $4\mu g.ml^{-1}$ in modified TBS containing $1mM.L^{-1}$ each of calcium chloride, manganese chloride, magnesium chloride and 0.01% Igepal (Sigma). Sections were rinsed in modified TBS and subsequent procedures were performed as described previously (246). The goat anti-GSL-1 (Vector) antibody was used at $1.5mg.ml^{-1}$ and the biotinylated secondary antibody and peroxidase binding were performed using a (goat) Vectastain® ABC kit (Vector).

2.4.3 Image Analysis

Sections stained with GSL-1 were examined under bright-field microscope (Olympus BX50). The area that had wide-open capillaries and invisible muscle fibers resulting from the exposure to glutaraldehyde was identified as a perfused region. The area where the capillaries remained closed and surrounding muscle fibers had dark GSL-1 staining resulting from the denied access of glutaraldehyde was identified as an unperfused area. Total section area and the unperfused area were measured using the

Image-Pro-Plus software. The ratio of unperfused to total area was calculated. An average of 10 and 15 sections were analyzed for each experiment for study 1 and 2 of Chapter 6, respectively.

In study 3 of Chapter 6, Rhodamine-dextran70 (lysine fixable, Molecular Probes, 50$\mu g.ml^{-1}$ final concentration) was infused during perfusion to mark perfused vessels. Sections from these experiments were examined using an Olympus BX50 microscope equipped with an Olympus U-RFL-T lamp. Images of the perfused capillaries marked by fluorescence were captured using an Olympus DP50 digital camera. Approximately 2-4 images (400X) were required to cover each fluorescent capillary-containing area in a section. The number of perfused capillaries was counted in each section. An average of 8 sections was analyzed for each experiment.

2.4.4 Statistical Analysis

A mean value was generated for each experiment from a number of sections and the coefficient variance was also calculated to indicate the variation among sections. The mean values from each experiment were used to compute the mean and SE for each treatment group. Data are expressed as means ± SE. Difference between groups was determined by one way analysis of variance. When a significant difference ($P<0.05$) was found, the Student-Newman-Keuls test was used to determine which two groups had the significant difference. These tests were performed using the SigmaStat statistical program (Jandel Software).

CHAPTER 3
DOSE EFEECTS OF INSULIN ON CAPILLARY RECRUITMENT IN MUSCLE

3.1 INTRODUCTION

Insulin, apart from its classic metabolic action to increase glucose disposal, exerts a hemodynamic role *in vivo* to regulate vascular tone (18, 186, 313). In skeletal muscle vascular bed, insulin's hemodynamic actions have been suggested to have two aspects. One is considered to dilate resistance arterioles resulting in increased total blood flow (18, 22, 171, 325). The other is considered to relax terminal arterioles to recruit muscle capillaries (48, 62, 273, 332, 333). More importantly, there is a close association between insulin's hemodynamic actions and insulin-mediated glucose uptake. Thus, in normal experimental animals (273) and lean human subjects (26), insulin-induced hemodynamic responses are positively correlated to insulin-mediated glucose disposal. Consistently, typical insulin resistance states, such as obesity (24, 171, 336) and NIDDM (172), manifest both cellular and vascular resistance to insulin action.

Based on the above observations, it was proposed that insulin's metabolic actions depend in part on a hemodynamic component that increases glucose disposal by enhancing delivery of glucose, insulin itself and other nutrients to the myocytes (26, 54). Based on this hypothesis, it was reasoned that if glucose uptake has a significant flow-dependent component, then altering blood flow during the exposure of insulin should modulate insulin-mediated glucose uptake accordingly. However, studies aimed at testing the role of total blood flow as a determinant of insulin-stimulated glucose uptake by decreasing or increasing total flow using vasoactive agents yielded inconsistent results. Whereas some reports support the contribution of total flow in regulating insulin-mediated glucose uptake (25, 26, 39, 99, 317), others oppose it (174, 223, 224, 233). However, it's important to note that there are data indicating capillary recruitment is independent of total flow (273). Therefore, although vasoactive agents may similarly alter total blood flow, they may have distinct effects on microvascular

perfusion, resulting in different outcomes in terms of modulating insulin's metabolic action. This raised the important aspect that, whereas insulin is able to increase both total blood flow and microvascular perfusion via capillary recruitment, the latter vascular effect may play a more important role in promoting insulin's metabolic action in skeletal muscle.

Indeed, there are studies challenging the physiological relevance of the insulin-mediated increase in total blood flow by showing that enhancement in total flow generally requires supra-physiological dose insulin over prolonged exposure time (221, 325, 347). Therefore, it is necessary to investigate whether this is the case for insulin-mediated capillary recruitment to address the issue of physiological contribution of insulin's hemodynamic actions to its metabolic effects. Thus, in the present study, we characterized insulin-mediated capillary recruitment and the increase in total blood flow by examining their responses to insulin at various doses (1 – 30mU.min^{-1}.kg^{-1}) and compared their relationships with insulin-mediated glucose uptake at each dose.

3.2 MATERIALS AND METHODS

3.2.1 Animal Care

Experiments using 1-MX metabolism were conducted on male Hooded Wistar rats (240 – 260 grams) at the University of Tasmania, Australia. Studies involving contrast-enhanced ultrasound (CEU) technique were carried out on male Sprague-Dawley rats at the University of Virginia Health Sciences Centre, Charlottesville, VA, USA. Animals were raised or obtained as described in section 2.1.

3.2.2 *In vivo* Experiments

In vivo experiments were carried out in anesthetized rats using one of two protocols (Fig 3.1). In protocol A (Fig 3.1 A), microvascular perfusion was investigated using 1-MX metabolism. The experimental procedure was as described in section 2.2. Briefly, in fed Wistar rats, after a 60min stabilization period, basal measurements were made and saline or insulin (1, 3, 10 or 30mU.min^{-1}.kg^{-1}) infusion began and

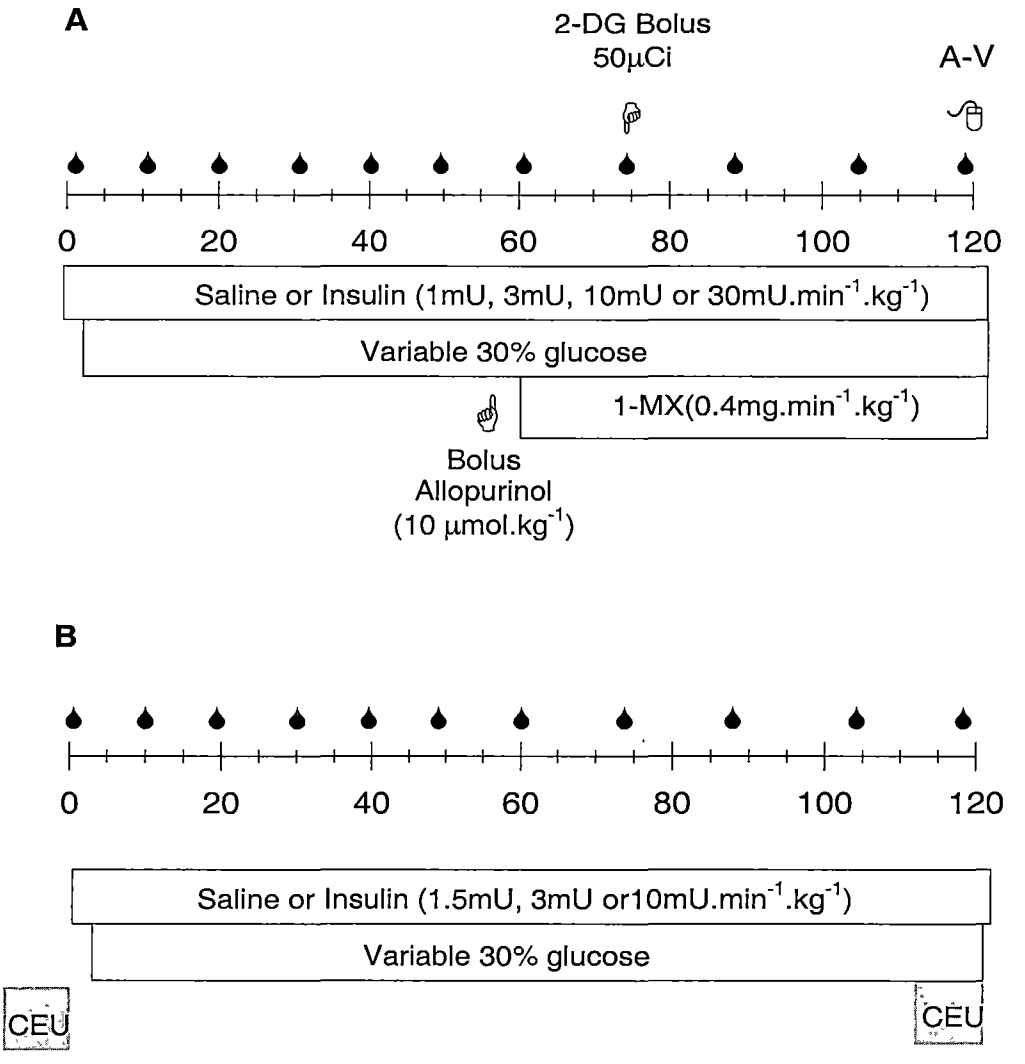

Figure 3.1 Experimental Protocols. Venous infusions are indicated by open bars. Bolus injections are shown by ☝ or ☝. Arterial and venous samples collected for HPLC assay are indicated by ☜. Arterial blood glucose levels were measured at times indicated by ♦. In protocol A, fed male Hooded Wistar rats were infused with either saline or insulin at various doses (1, 3, 10 or 30mU.min^{-1}.kg^{-1}) for 2h. Microvascular perfusion was assessed using 1-MX metabolism. In protocol B, saline infusion or insulin clamps (1.5, 3 or 10mU.min^{-1}.kg^{-1}) were conducted on fasted Sprague-Dawley rats. Contrast-Enhanced Ultrasound (CEU) technique was used to measure microvascular volume. CEU measurements were performed before and at the end of each experiment.

continued for 2h. 1-MX was infused (0.4mg.min^{-1}.kg^{-1}) for the last 60min of the 2h clamp, with a bolus of allopurinol (10μmol.kg^{-1}) at 5min before the infusion commenced. This allowed partial inhibition of the activity of xanthine oxidase and constant arterial concentration of 1-MX to be maintained throughout the experiment. In these animals, 45min before the completion of the experiment, a bolus of [^{3}H]2-DG (50μCi) was administrated. Plasma samples (20μl) were collected at 5, 10, 15, 30 and 45min following the injection to generate the radioactivity decay curve. At the completion of the experiment, blood was withdrawn from carotid artery and femoral vein to determine hindleg glucose uptake and 1-MX metabolism. After taking blood samples, lower leg muscles including soleus, plantaris, gastrocnemius white, gastrocnemius red, extensor digitorum longus, and tibialis muscles were removed and clamp-frozen in liquid nitrogen and stored in -20°C freezer for 2-DG uptake assay as described in section 2.2.5. In protocol B (Fig 3.1 B), microvascular perfusion was assessed using contrast-enhanced ultrasound (CEU) on fasted Sprague-Dawley rats. The surgical procedures were essentially as described in section 2.2. However, because the circulating microbubbles required for CEU measurement interfere with the Transonic™ flow probe signal, femoral blood flow could not be determined and thus both legs of the animals were not operated. Due to the lack of blood flow information, hindleg glucose uptake was not measured in these experiments. Also because the 1-MX method requires a measurement of FBF, 1-MX metabolism could not be determined in animals undergoing CEU measurements. After the completion of the surgery, a 60min equilibration period was followed to allow heart rate, blood pressure and respirations to become stable. Then basal measurements were made and saline or insulin (1.5, 3 or 10mU.min^{-1}.kg^{-1}) was infused for 2h. To measure microvascular volume, perfluorocarbon gas-filled albumin-coated microbubbles were infused intravenously at 120μl.min^{-1} for 2min before and during 3min of ultrasound data acquisition to measure microvascular volume at baseline and after 2h infusion of either saline or insulin. The CEU set-up and methods for data analysis were as described in section 2.2.7. Plasma insulin concentrations were determined after the 2h infusions for both protocols using an ELISA kit (Mercodia AB, Sweden).

3.2.3 Data Analysis

All data are expressed as means ± SE. Hemodynamic data including femoral blood flow, heart rate and mean arterial blood pressure were collected by WINDAQ data acquisition system and data analysis methods were described in section 2.2.9. Statistical differences between treatments throughout the time course were ascertained by two-way repeated analysis of variance. Once a significant difference ($P<0.05$) was found, pair wise comparisons by the Student-Newman-Keuls test were used to determine at which individual time points the differences were significant. Unpaired *t*-test was used to determine statistical differences among treatments at a single time point. These tests were performed using the SigmaStat statistical program (Jandel Software).

3.3 RESULTS

3.3.1 Plasma Insulin Concentrations

After the 2h infusions, plasma insulin concentrations rose progressively with increasing insulin doses from 0 (saline infusion) to 30mU.min^{-1}.kg^{-1} in both fed and fasted animals (Fig 3.2). Thus, there was a small increase in plasma insulin by 2h insulin infusion at 1 or 1.5mU.min^{-1}.kg^{-1} in comparison to that after 2h saline infusion. As insulin dose was increased to 3, 10 and 30mU.min^{-1}.kg^{-1}, plasma insulin concentrations were elevated by ~2- , 6- and 35-fold respectively at the end of 2h infusions (Fig 3.2). The non-linear increase in plasma insulin level as insulin dose rose from 10 to 30mU.min^{-1}.kg^{-1} was not unexpected because insulin clearance mechanisms saturate at the concentrations above 3000 pmol.L^{-1} (282).

3.3.2 Hemodynamic Measurements

Mean arterial pressure and heart rate were similar at basal state and remained stable throughout the experiments (Fig 3.3). None of the treatments had effect on mean arterial pressure or heart rate (Fig 3.3). At very low insulin dose such as 1mU.min^{-1}.kg^{-1}, there was no significant change in femoral blood flow throughout the 2h infusion. As the insulin dose was increased, femoral blood flow rose markedly and the changes were seen sooner after starting the insulin infusion (Fig 3.4A).Thus, with the 3mU.min^{-1}.kg^{-1} insulin infusion, femoral blood flow begun to increase at the end of

the first hour and rose further during the second hour. With 10 and 30mU.min^{-1}.kg^{-1} insulin infusion, significant increases in femoral blood flow were seen after 60 and 30min respectively. Furthermore, the magnitude of the flow increase was higher with higher insulin doses (Fig 3.4A). Since the arterial pressure did not change throughout the experiment, the progressive increases in femoral blood flow with increasing insulin doses resulted in progressive decreases in hindlimb vascular resistance (Fig 3.4B). Similar to the changes in femoral blood flow, the decline of vascular resistance occurred earlier during insulin infusion at higher doses (Fig 3.4B).

3.3.3 Capillary Recruitment Measured By 1-MX Metabolism and CEU

Capillary recruitment (microvascular blood volume) in hindlimb muscles was measured by hindlimb metabolism 1-MX in the fed Wistar rats and by CEU of the proximal adductor muscle group in fasted Sprague-Dawley rats. The two methods gave similar outcomes. In studies where 1-MX metabolism measurement was involved, arterial 1-MX and oxypurinol concentrations were achieved to a similar level in all treatment groups (Fig 3.5). At the lowest dose of insulin (1mU.min^{-1}.kg^{-1}), hindlimb 1-MX metabolism increased significantly (Fig 3.6A). There was a further small rise in 1-MX hindlimb metabolism as the insulin dose increased to 3mU.min^{-1}.kg^{-1}, but no further increase despite much greater increases in total flow in these animals at high insulin doses (Fig 3.4). In studies using CEU to assess microvascular perfusion, video intensity began to rise even with the lowest dose (1.5mU.min^{-1}.kg^{-1}) of insulin infused (Fig 3.6B). However, the dose of 3mU.min^{-1}.kg^{-1} appeared to fully recruit microvascular volume, as higher doses did not result in further increases (Fig 3.6B).

3.3.4 Whole Body Glucose Metabolism

Blood glucose concentrations were similar under basal conditions in all experimental groups and were maintained at or above the basal value during insulin clamps by infusing 30% glucose at variable rates (Fig 3.7). With the insulin clamp at 1mU.min^{-1}.kg^{-1}, a small amount of glucose was needed to maintained euglycemia during the first 90min of insulin infusion. Then the glucose infusion declined to a level that was not significantly different from zero. With insulin clamps at 3, 10 and 30mU.min^{-1}.kg^{-}

^{1}, glucose infusion rate was increased rapidly once insulin infusion began and reached a plateau within 60min that was higher in proportion to the insulin dose (Fig 3.7). The steady-state glucose infusion rates were 2.0 ± 0.3, 11.1 ± 0.6, 21.1 ± 0.8 and 25.5 ± 0.9 $mg.kg^{-1}.min^{-1}$ for insulin clamps at 1, 3, 10 and 30$mU.min^{-1}.kg^{-1}$ respectively.

3.3.5 Hindlimb Glucose Metabolism

Insulin stimulated hindleg glucose uptake in a dose-dependent manner (Fig 3.8A) but this was only evident at dose of insulin equal to or exceeding 3$mU.min^{-1}.kg^{-1}$. Thus, insulin failed to increase hindleg glucose uptake at 1$mU.min^{-1}.kg^{-1}$, started to stimulate hindleg glucose uptake at 3$mU.min^{-1}.kg^{-1}$, significantly enhanced hindleg glucose uptake at 10$mU.min^{-1}.kg^{-1}$ and did not further increase glucose uptake at 30$mU.min^{-1}.kg^{-1}$, suggesting a maximal stimulation on hindleg glucose uptake by insulin was achieved at 10$mU.min^{-1}.kg^{-1}$ (Fig 3.8A). Glucose disposal into skeletal muscle measured by 2-DG uptake showed a similar pattern for individual lower leg muscles (Fig 3.9) as well as combined muscle tissues (Fig 3.8B).

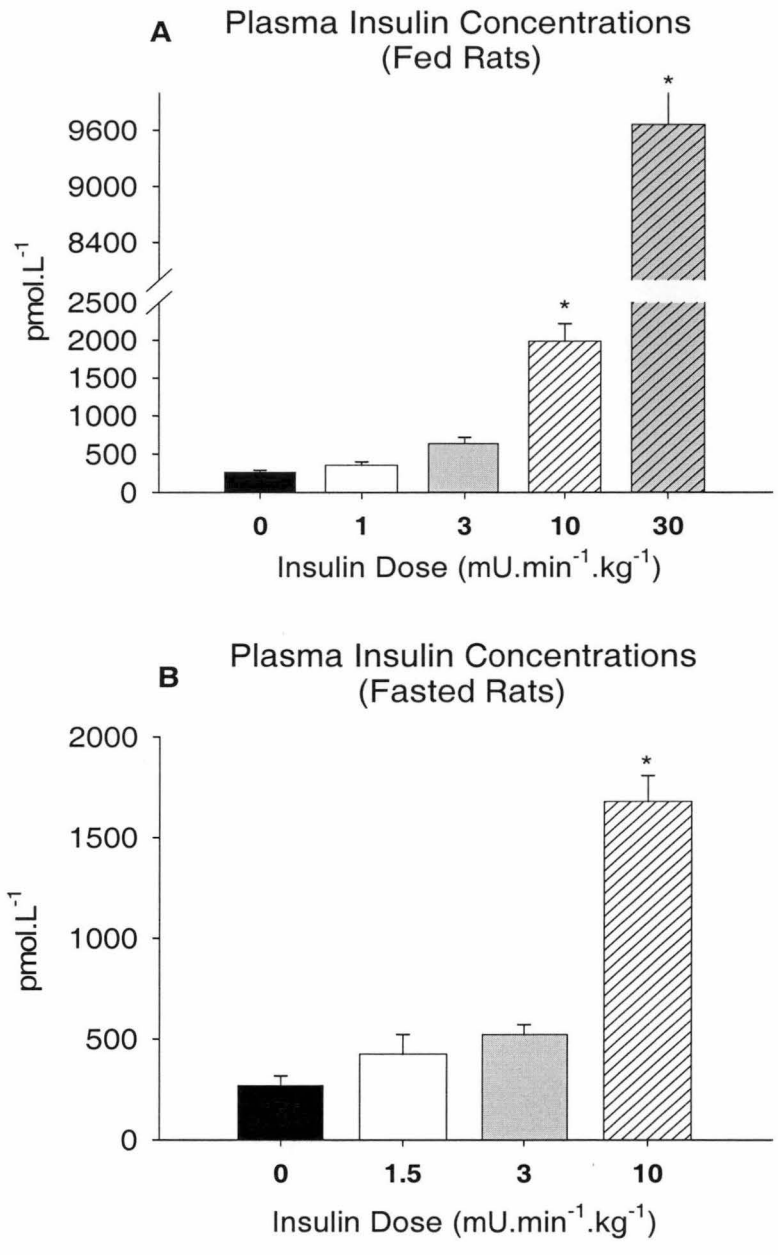

Figure 3.2 Plasma insulin concentrations of fed Hooded Wistar rats (A) or fasted Sprague-Dawley rats after 2h of infusion of either saline [■ in A (n=8) and B (n=7)] or insulin at various doses [1mU.min^{-1}.kg^{-1} (1mU): □ in A (n=9); 1.5mU.min^{-1}.kg^{-1} (1.5mU): □ in B(n=7); 3mU.min^{-1}.kg^{-1} (3mU): ■ in A (n=8) and B (n=7); 10mU.min^{-1}.kg^{-1} (10mU): ▨ in A (n=6) and B (n=7); 30mU.min^{-1}.kg^{-1} (30mU): ▨ in A (n=7)]. Values are means ± SE. *Significantly different (P<0.05) from saline infusion.

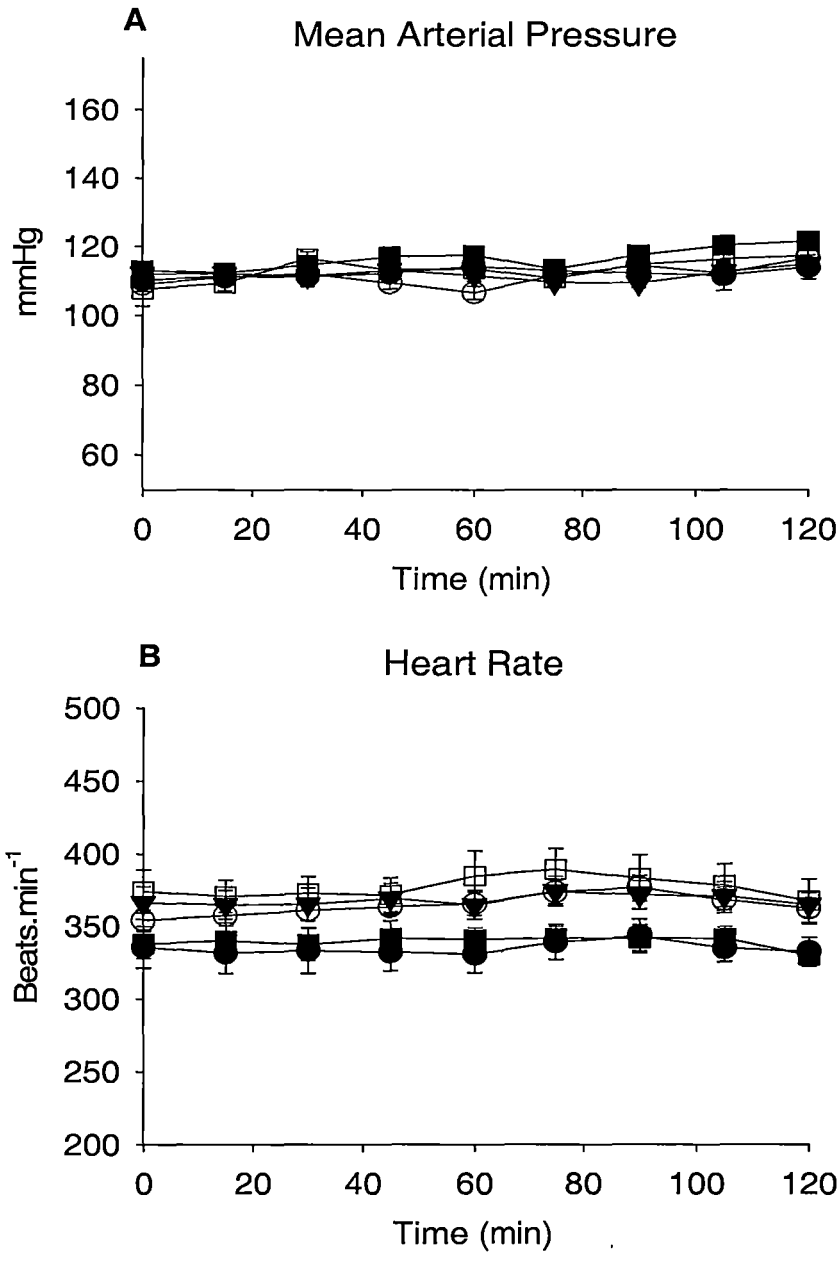

Figure 3.3 Mean arterial pressure (A) and heart rate (B) for saline infusion (▼, n=8) and insulin clamps at 4 doses [○, 1mU (n=9); ●, 3mU (n=8); □ 10mU (n=6); ■, 30mU (n=7)]. Data were collected from fed Hooded Wistar rats. Values are means ± SE.

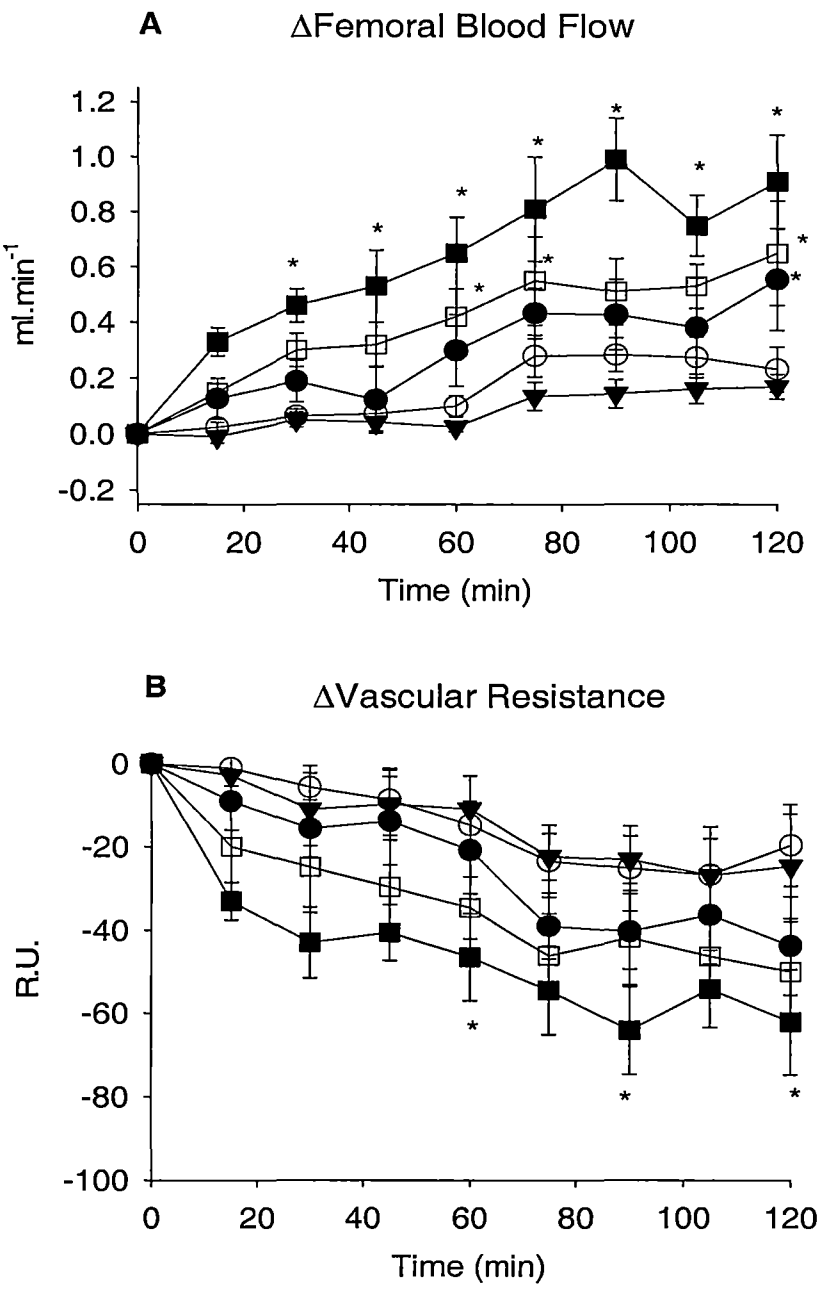

Figure 3.4 Changes in femoral blood flow (A) and vascular resistance (B) for saline infusion (▼, n=8) and insulin clamps at 4 doses [○, 1mU (n=9); ●, 3mU (n=8); □ 10mU (n=6); ■, 30mU (n=7)]. Data were collected from fed Hooded Wistar rats. Values are means ± SE. * Significantly different ($P<0.05$) from saline infusion.

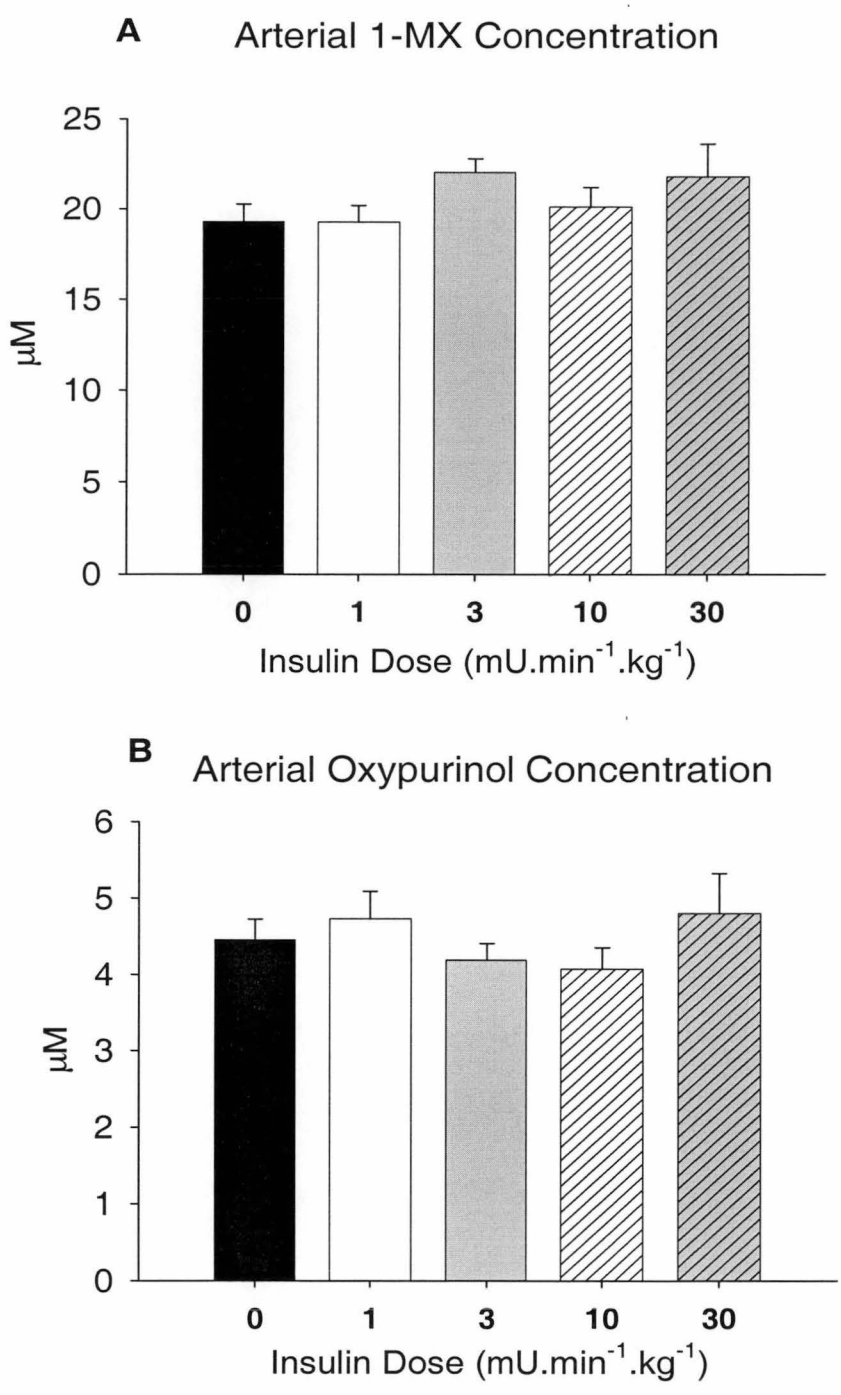

Figure 3.5 Arterial concentrations of 1-MX (A) and oxypurinol (B) for saline infusion (■, n=8) and insulin clamps at 4 doses [□, 1mU (n=9); ■, 3mU (n=8); ▨,10mU (n=6); ▨, 30mU (n=7)]. Data were collected from fed Hooded Wistar rats. Values are means ± SE.

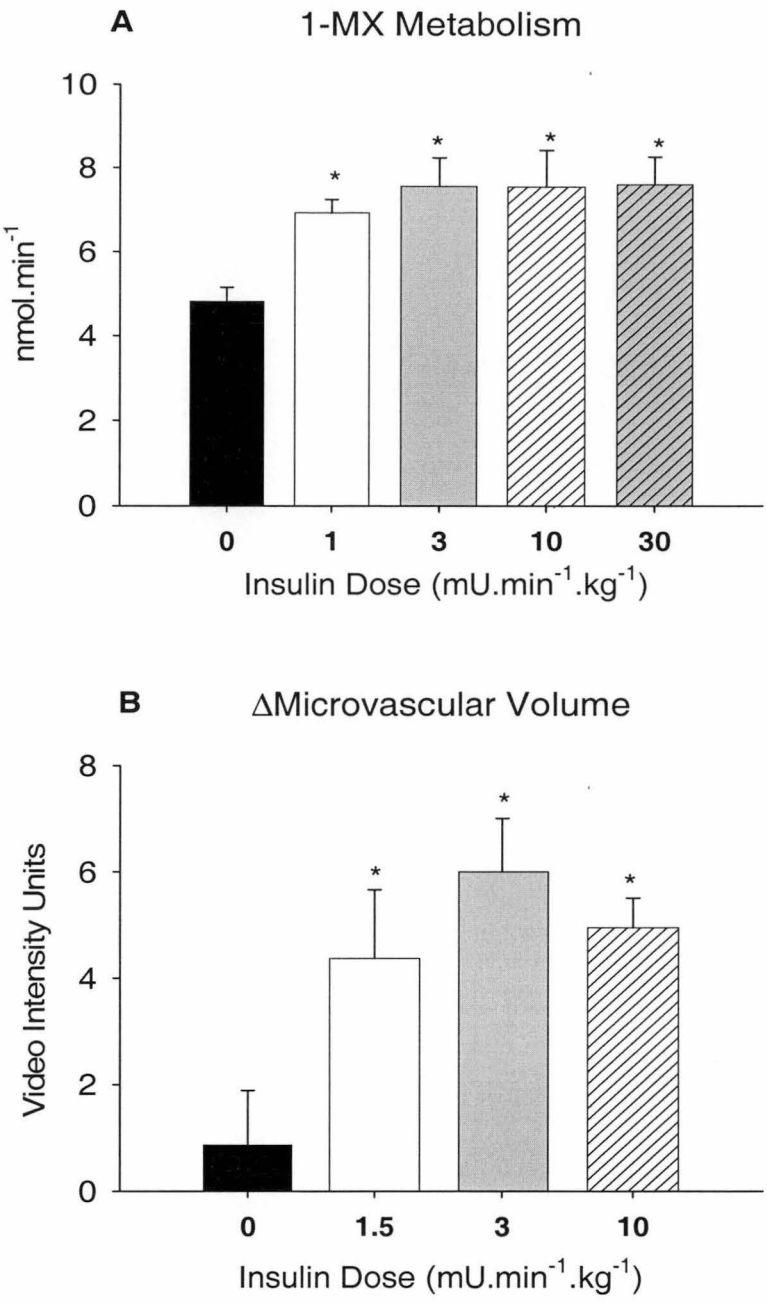

Figure 3.6 Microvascular perfusion determined by 1-MX metabolism (A) or CEU (B). A: The rate of 1-MX disappearance across the rat hindlimb at the end of 2h infusion of saline (■, n=8) or insulin at each dose [□, 1mU (n=9); ■, 3mU (n=8); ▨,10mU (n=6); ▨, 30mU (n=7)] to fed, Hooded Wistar rats. B: The changes in microvascular volume (CEU) seen between baseline and 2h infusion of saline (■, n=7) or insulin at each dose [□, 1.5mU (n=9); ■, 3mU (n=8); ▨,10mU (n=6)] to overnight-fasted Sprague-Dawley rats. Values are means ± SE. * Significantly different ($P<0.05$) from saline infusion.

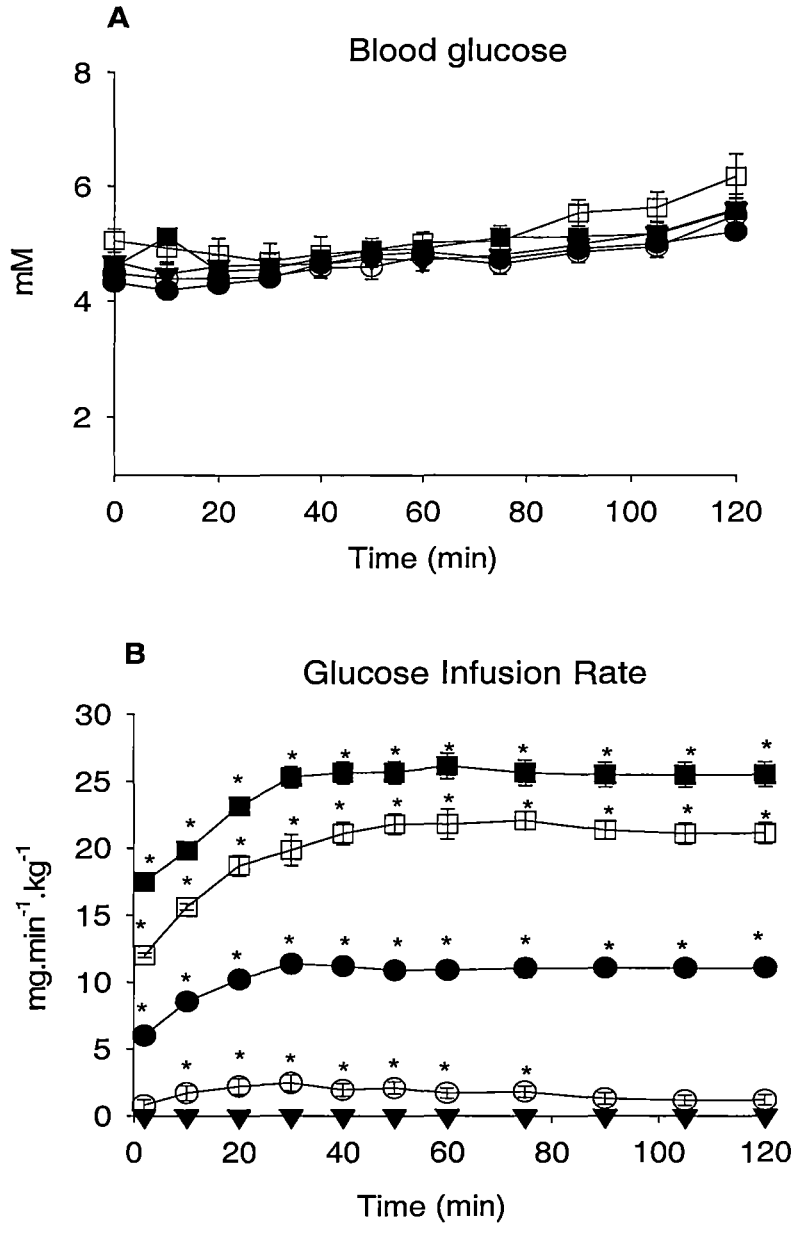

Figure 3.7 Blood glucose levels (A) and glucose infusion rates (B) for saline infusion (▼, n=8) and insulin clamps at 4 doses [○, 1mU (n=9); ●, 3mU (n=8); □ 10mU (n=6); ■, 30mU (n=7)]. Glucose infusion started at the 2min time point. Data were collected from fed Hooded Wistar rats. Values are means ± SE. * Significantly different ($P<0.05$) from zero.

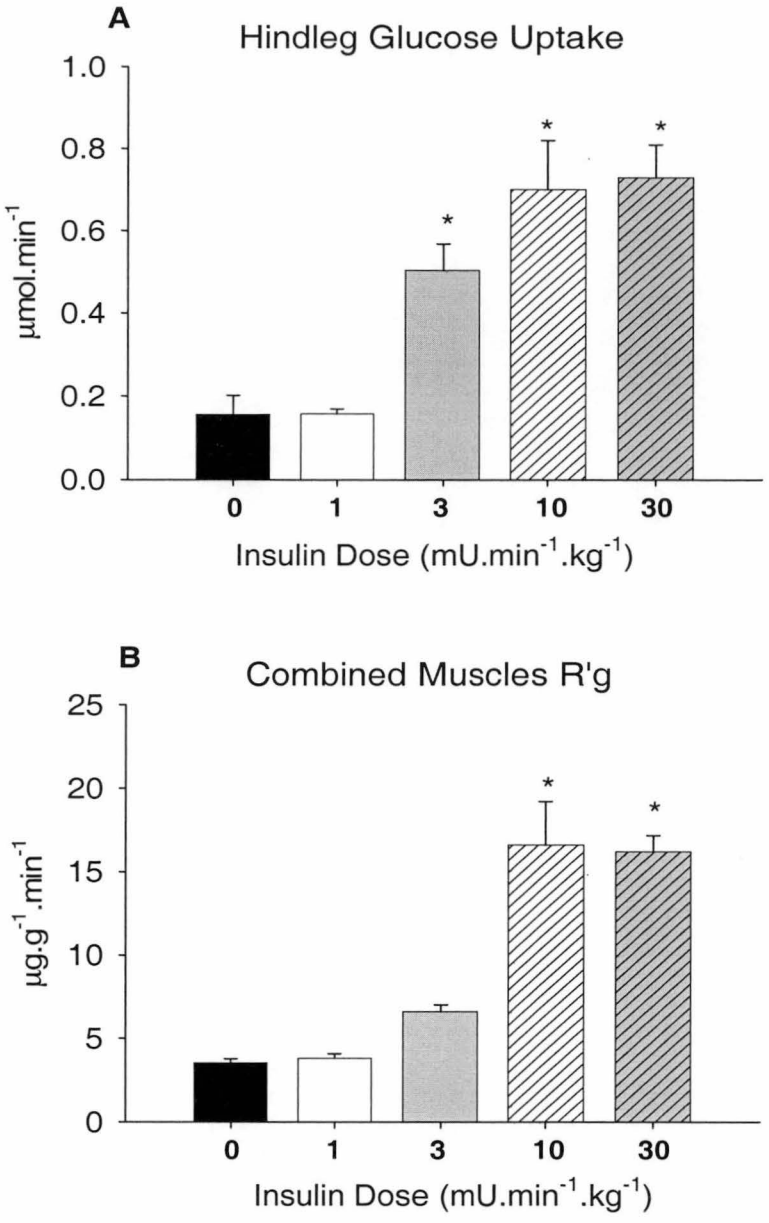

Figure 3.8 Hindleg glucose uptake (A) and R'g of combined lower leg muscles (soleus, plantaris, gastrocnemius, extensor digitorum longus and tibialis anterior muscles) (B) after 2h infusion of saline (■, n=8) or insulin [□, 1mU (n=9); ■, 3mU (n=8); ▨,10mU (n=6); ▨, 30mU (n=7)]. Data were collected from fed Hooded Wistar rats. Values are means ± SE. * Significantly different (P<0.05) from saline infusion.

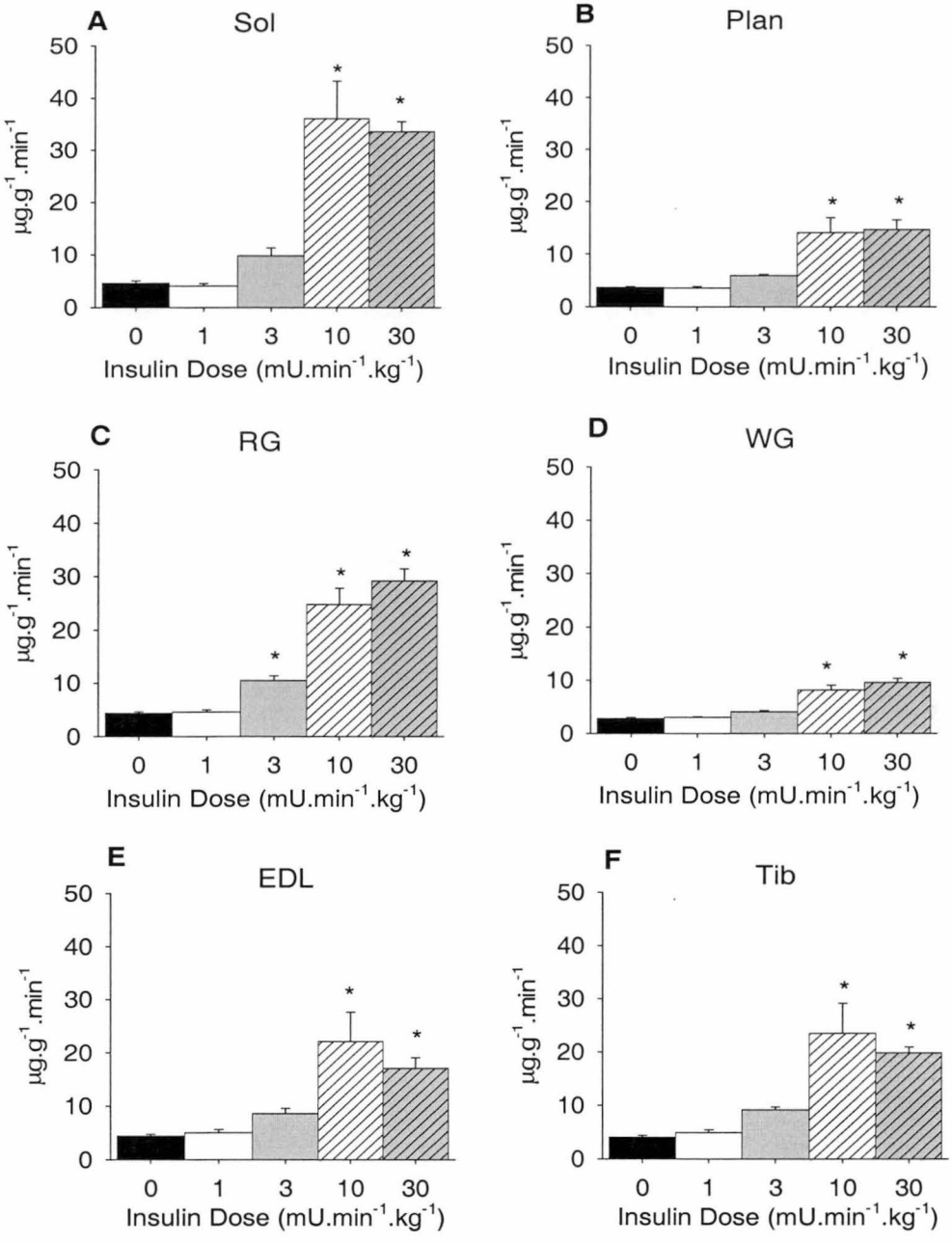

Figure 3.9 2-DG uptake (R'g) in soleus (A), plantaris (B), red gastrocnemius (C), white gastrocnemius (D), extensor digitorum longus (E) and tibialis anterior (F) muscles after 2h infusion of saline (■, n=8) or insulin [□, 1mU (n=9); ■, 3mU (n=8); ▨,10mU (n=6); ▨, 30mU (n=7)]. Data were collected from fed Hooded Wistar rats. Values are means ± SE. * Significantly different (P<0.05) from saline infusion.

3.4 DISCUSSION

The dose effects of insulin on hepatic and peripheral glucose metabolism have been investigated extensively in the past (265, 282, 294, 301). While obtaining consistent results to those previous reports on insulin's dose-dependent action to stimulate glucose disposal, the present study also defined the dose-response characteristics of insulin effects on total limb blood flow and microvascular recruitment and examined their relationships with insulin's metabolic action. To our knowledge, this is the first study comprehensively investigating both hemodynamic and metabolic actions of insulin at various doses in experimental animals.

The present data obtained from experimental animals showed that insulin augmented limb total blood flow in a dose-dependent manner, in agreement with reported human studies (171, 325). Using 1-MX metabolism and ultrasound video intensity as index of the microvascular perfusion, the current study also demonstrated that insulin has a second hemodynamic action of microvascular recruitment, providing further support for our previous reports (62, 273, 332, 333). The observation that the effect of insulin on microvascular recruitment saturates at insulin infusion rate between 1 and 3mU.min^{-1}.kg^{-1}, whereas total flow continues to increase with increments of insulin infusion rates between 3 and 10mU.min^{-1}.kg^{-1} and increases further between 10 and 30mU.min^{-1}.kg^{-1}, suggests these two hemodynamic actions of insulin are discrete and have different insulin sensitivity. This apparent difference in insulin sensitivity can not be attributed to differences in measurement sensitivity for total flow and capillary recruitment. We estimate that we would have >80% power to detect a 30% change in hindlimb blood flow by studying six animals ($\alpha < 0.05$). The corresponding value for a change in microvascular recruitment was ~ 50% at the lowest insulin dose used.

It has been proposed that insulin exerts control of the two distinct hemodynamic effects by acting on different vascular segments (60). Dilation of resistant vessels may result in an increased total blood flow. Relaxing terminal arterioles that are further down the arterial tree would lead to flow redistribution and microvascular recruitment. The currently observed difference in insulin sensitivity between insulin-mediated

increase in total limb flow and capillary recruitment indicates that microvascular insulin sensitivity is considerable higher than that of resistant vessels.

There is evidence from the present study that capillary recruitment is also more sensitive to plasma insulin than glucose uptake in skeletal muscle. Thus, whereas insulin started to enhance microvascular perfusion at the doses of 1- 1.5mU.min^{-1}.kg^{-1}, glucose uptake in skeletal muscle remained inactivated. In addition, insulin at 3mU.min^{-1}.kg^{-1} was saturating for capillary recruitment, but only minimally activated glucose disposal into the hindlimb. Maximal activation of insulin-mediated muscle glucose uptake was reached at 10mU.min^{-1}.kg^{-1} and additional increase in the dose to 30mU.min^{-1}.kg^{-1} did not further enhance muscle glucose disposal. It is relevant to note that the arteriovenous glucose measurement is not a very sensitive measure of glucose metabolism. However, measurement of glucose uptake by 2DG is very sensitive, and flow is not involved in the calculation. We are confident that even small (30-50%) increases in glucose uptake would be detectable with this method. Therefore, the lower insulin sensitivity observed with muscle glucose uptake than capillary recruitment can not be attributed to differing sensitivity of the methods.

A comparison of insulin sensitivity between capillary recruitment and muscle glucose uptake need some caution because terminal arterioles controlling microvascular perfusion and myocytes where glucose is taken up are within different spatial compartments (vascular compartment for the former and interstitial space for the latter) that may have different insulin concentrations. Indeed, there is data indicating that under physiological and pharmacological hyperinsulinemia conditions there is an arterial-interstitial concentration gradient for insulin (137, 155, 299, 300, 343) and the insulin concentration in the interstitium may be only 40 – 50% that of the plasma. Under basal conditions or when plasma insulin is elevated to a low physiological level, interstitial insulin concentrations have been reported on average to be lower than ((133, 264, 343, 344) compared with (137) who reported no difference) plasma insulin concentration. As such, the lower insulin concentration in the interstitium in relation to the plasma insulin level may be responsible for the different dose-effects of insulin on capillary recruitment and muscle glucose uptake in the present study, and thus may not reflect an actual difference in insulin sensitivity. Nevertheless, the important aspect is that capillary recruitment can be activated at very low insulin dose

that is unable to activate muscle glucose uptake, suggesting the effect of insulin on recruiting microvascular volume is primary rather than secondary to the metabolic actions of insulin. In view of the fact that insulin is secreted in a phasic manner in response to food, and its level rises and falls rapidly, the primary characteristic of insulin-induced capillary recruitment may not be regarded as a functional disassociation from insulin-mediated glucose uptake, but an advantage of insulin under the physiological condition to prepare the routes for the nutrients delivery to muscle. This may also be of physiological significance to ensure optimal muscle glucose storage after meals.

As reported in the introduction, whereas there is virtually uniform acknowledgment of insulin's action to increase total blood flow (26, 171, 288), there is considerable divergence of the findings among investigators with regard to the dose relationship between insulin and increases in total blood flow and as result, the physiological importance of this action of insulin to stimulate glucose disposal (172, 221, 325, 347). The observation from this study that capillary recruitment is fully stimulated using insulin infusion of $3mU.min^{-1}.kg^{-1}$ while increasing insulin dosage beyond $3mU.min^{-1}.kg^{-1}$ progressively increases femoral blood flow and muscle glucose uptake supports the hypothesis that steps in insulin action beyond any effect on capillary recruitment are important determinants of muscle glucose uptake. Indeed, at very high insulin concentrations, when the extraction ratio for glucose across a muscle vascular bed approaches 50%, it would be predicted on theoretical grounds (35) and is observed experimentally (308) that total blood flow would be a determinant of glucose uptake. However, as discussed previously, at more physiological insulin concentrations, capillary recruitment is likely a necessary primary response for insulin-mediated glucose uptake.

In summary, the present study demonstrates that insulin recruits microvasculature within skeletal muscle at concentrations lower than those required to enhance total muscle blood flow and lower than those needed to stimulate glucose disposal. These insulin dose-response observations show that microvascular recruitment has the highest sensitivity to plasma insulin and thus support the hypothesis that recruitment of microvasculature is a primary action of insulin and is necessary for muscle to obtain the optimal metabolic response to insulin under physiological conditions.

CHAPTER 4
TIME COURSE OF INSULIN REVERSAL

4.1 INTRODUCTION

Insulin regulates peripheral glucose uptake and utilization. However, when insulin is infused intravenously, whole body glucose disposal (264,.265, 344) and skeletal muscle glucose uptake (214) proceed with much slower kinetics than the rise in the plasma insulin concentration. Among the multiple extracellular (14, 166) and intracellular (163, 305, 338) steps insulin has to overcome to ultimately stimulate glucose phosphorylation, transcapillary insulin movement has been suggested to be the primary step determining the delay in insulin's metabolic action (101, 209, 344). Therefore, the endothelial wall, the first barrier insulin encounters once it enters the circulation, has until recently, been considered to be the rate-limiting barrier for insulin to exert its metabolic control.

The mechanism by which the endothelial barrier might control the transcapillary insulin movement and the rate of insulin appearance in interstitium is unknown. Whereas a number of studies have been carried out to try to solve this issue by examining whether transendothelial insulin transport is via a receptor-mediated and thus saturable process (137, 155, 166) or through a concentration gradient-dependent passive diffusion (124, 307), the additional delay in insulin-mediated glucose disposal in insulin-resistant subjects compared to normal subjects (33, 208, 230, 265, 320) raised an interesting aspect that there may be a factor that facilitates the movement of insulin across the endothelial barrier but is impaired in insulin-resistant state. Indeed, we and others have demonstrated that insulin has hemodynamic actions *in vivo* to increase total blood flow (25, 26, 171, 325) and microvascular perfusion (48, 62, 273, 333). Additionally, these hemodynamic actions are impaired in insulin resistant conditions (24, 171, 336). Since enhancing insulin delivery and capillary exchanging surface area by increasing total blood flow and capillary recruitment can augment the chance for insulin to move across the endothelial wall, it appears likely that insulin's hemodynamic actions take part in the endothelial barrier-associated regulation in the

rate of transcapillary insulin movement. It follows that a defect in insulin's hemodynamic effects may partly contribute to the additional temporal lag in insulin's metabolic action reported in the insulin resistant state (33, 208, 230, 265, 320). It is also important to note that a rate-limiting step at the transendothelial movement of insulin can not readily be distinguished from impaired capillary recruitment by insulin.

However, the possible involvement of total flow increase in the temporal regulation of the onset of insulin's metabolic action is controversial and has been challenged by observations that increase in total blood flow needs prolonged insulin exposure time and thus, lags behind the stimulation of muscle glucose (171, 325). Since insulin's microvascular action to recruit capillaries is independent and thus can be dissociated from enhancement in total blood flow (273), we investigated the time-course relationship between insulin-mediated capillary recruitment, increase in total blood flow and muscle glucose uptake during the physiological hyperinsulinemic clamp in experimental animals (332, 333). These studies revealed that insulin at physiological dose recruited microvasculature within 5-10min, and this preceded both activation of insulin signalling pathways and increases in muscle glucose disposal that occurred at 15-30min, as well as changes in total limb blood flow that happened after 30min of insulin exposure (332, 333). The quick onset of insulin-mediated capillary recruitment supports the hypothesis that enhancement in capillary exchanging surface area by capillary recruitment has a role in regulating the rate of insulin transcapillary movement and consequently the rate of the onset of insulin-mediated glucose uptake.

Whereas the temporal dependence of insulin's metabolic and hemodynamic actions following insulin administration have been clearly elucidated, the time course characteristics after the removal of insulin from the circulation have mainly focused on insulin's metabolic parameters (116, 265, 343). Therefore, the aim of the present study is to define the time course responses of insulin-mediated both metabolic and hemodynamic effects during the insulin deactivation phase with an attempt to gain further insights into the regulatory aspects of and interaction between insulin-meditated muscle glucose uptake, increase in total blood flow and microvascular perfusion.

4.2 MATERIALS AND METHODS

4.2.1 Animal Care

Male Hooded Wistar rats weighing 240 – 260 grams were used for this study. Animals were raised as described in section 2.1.

4.2.2 *In Vivo* Experiments

In vivo experiments were carried out in anaesthetized rats as described in section 2.2. Briefly, after 1h equilibration, rats were allocated into either protocol A (Fig 4.1 A) where insulin at the physiological dose of $3mU.min^{-1}.kg^{-1}$ was infused for 1h (euglycemia was maintained using a variable infusion rate of 30% glucose) and discontinued at the 0 time point (euglycemia continued to be maintained) followed by variable periods of reversal of 15min (Fig 4.1A Ins R15', n=8), 30min (Fig 4.1.A Ins R30', n=7) or 60min (Fig 4.1A Ins R60', n=8), or protocol B (Fig 4.1B) where a euglycemic insulin clamp at $3mU.min^{-1}.kg^{-1}$ was conducted for 2 h (n=8), or protocol C (Fig 4.1C) where saline infusion continued for 2h (n=14). Regardless of the duration of each experiment, 1-MX was infused at $0.4mg.min^{-1}.kg^{-1}$ for the last 60min with a bolus of allopurinol ($10\mu mol.kg^{-1}$) given 5min before the commencement of 1-MX infusion. Mean arterial pressure, heart rate and femoral artery blood flow were measured continuously using WINDAQ data acquisition software (DATAQ Instruments, Akron, OH). Arterial and venous samples from the femoral vein were withdrawn at the end of the experiment to determine 1-MX metabolism and hindleg glucose uptake. Basal and end-point plasma insulin levels were determined by ELISA assay (Mercodia AB, Sweden).

Due to the strict timing to determine the 1-MX metabolism and the blood loss from taking both arterial and venous samples to measure hindleg glucose uptake and 1-MX metabolism, we could not perform these two measurements in one group of animals, but had to have several groups where the experiments were terminated at different time points to examine the time effects during the insulin reversal period (Protocol A).

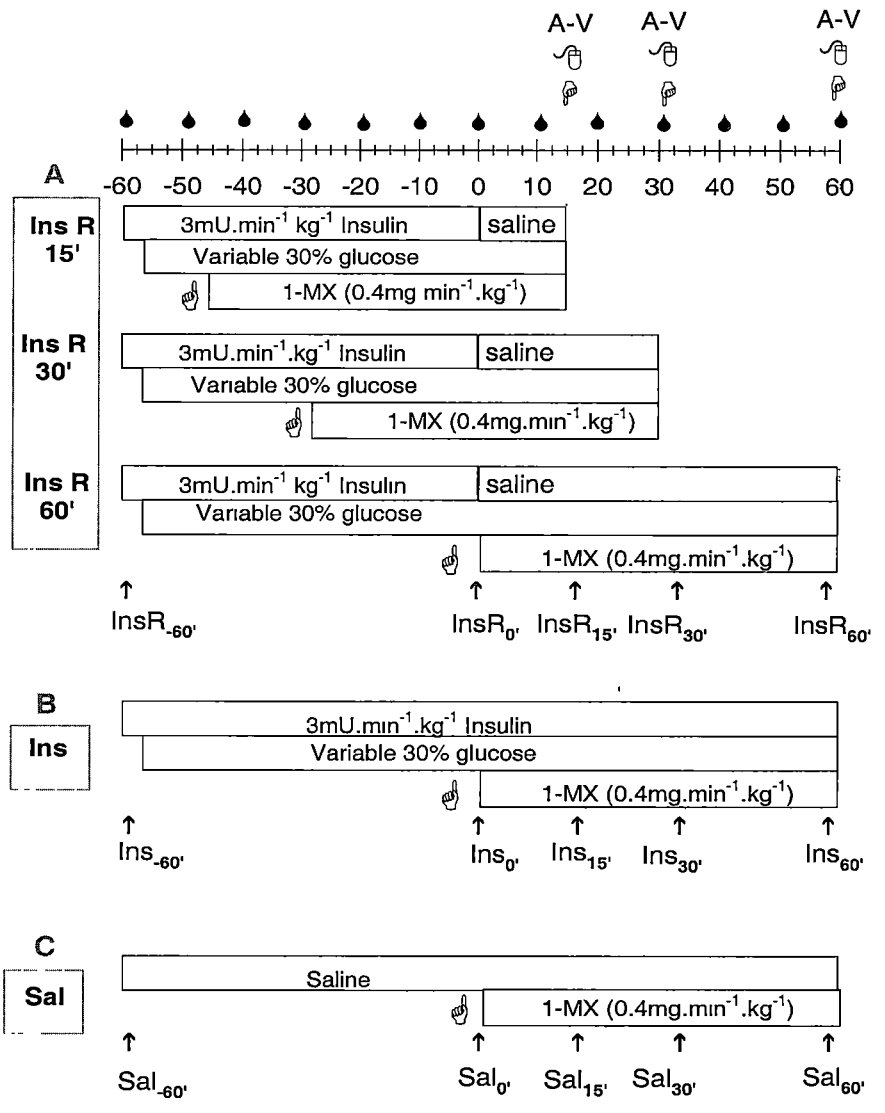

Figure 4.1 Experimental protocols. Venous infusions are indicated by open bars. Arterial and venous samples collected for HPLC assays are indicated by 🖐. Arterial blood glucose levels were measured at times indicated by ♦. Samples taken for the analysis of the hemodynamic parameters (Fig 4.2-4.5), blood glucose levels (Fig 4.7) and glucose infusion rate (Fig 4.8) are indicated by ↑. In protocol A, insulin clamp at 3mU.min^{-1}.kg^{-1} was conducted for 1h. Then insulin infusion was discontinued followed by 15min (InsR 15'), 30min (InsR 30') or 60min (InsR 60') of reversal period. In protocol B and C, either insulin at 3mU.min^{-1}.kg^{-1} (B) or saline (C) was infused for 2h. In all protocols, 1-MX was infused for the last 60min regardless the duration of the experiments with a bolus injection of allopurinol (10μmol.kg^{-1}) indicated by ☝ given 5min before the commencement of 1-MX infusion.

For a clearer presentation, these reversal groups in Protocol A were combined together although the "n" values are variable through the 2h time course.

4.2.3 Data Analysis

All data are expressed as means ± SE. Hemodynamic data including femoral blood flow, heart rate and mean arterial blood pressure were collected by WINDAQ data acquisition system and data analysis methods were described in section 2.2.9. Differences between treatment groups at different time points were determined by one way analysis of variance. When a significant difference ($P<0.05$) was found, the Student-Newman-Keuls test was used to determine which two groups had the significant difference. These tests were performed using the SigmaStat statistical program (Jandel Software).

4.3 RESULTS

4.3.1 Hemodynamic Measurements

Basal mean arterial pressure was similar in all groups (Fig 4.2). By the end of the 1h insulin infusion at 3mU.min^{-1}.kg^{-1}, mean arterial pressure was not different from that after 1h saline infusion. During the rest of the experiment regardless whether the insulin infusion was continued or not, the mean arterial pressure remained stable and did not differ from that of saline infusion. Similarly, heart rate was not affected by different treatments and was in the normal heart rate range of 330 – 380 beats.min^{-1}, although it was slightly lower in the 2h insulin clamp group (Fig 4.3).

Insulin infusion at 3mU.min^{-1}.kg^{-1} for 1h significantly increased femoral blood flow and the increase persisted during the second hour of insulin infusion (Fig 4.4). In contrast, upon the cessation of insulin infusion, the increase in femoral blood flow started to reverse and within 30min came back to a level that was not significantly different from that seen in either saline infusion or insulin infusion (Fig 4.4). The insulin-mediated increase in femoral blood flow was fully reversed after insulin infusion was discontinued for 60min (Fig 4.4). Since mean arterial pressure was constant throughout the experiments, the change in femoral blood flow resulted in a

corresponding change in vascular resistance (Fig 4.5). Thus, 1h insulin infusion at 3mU.min^{-1}.kg^{-1} decreased vascular resistance although this decrease was not significant in the 2h insulin clamp group. Whereas the vascular resistance further decreased as insulin was continuously infused for another 1h, the cessation of insulin administration resulted in a reversal in vascular resistance within 30min (Fig 4.5).

4.3.2 1-MX Metabolism

The arterial plasma concentrations of oxypurinol and 1-MX were not significantly different in all treatment groups (Fig 4.9), indicating the enzyme activity of xanthine oxidase was inhibited to the same extent. Hindlimb 1-MX metabolism was significantly increased by the end of 2h insulin infusion compared to saline infusion (Fig 4.10A). Since it has been reported that capillary recruitment is fully activated by insulin at the dose of 3mU.min^{-1}.kg^{-1} within 30min of insulin administration, and remains fully activated during the following 90min of insulin infusion (333), 1-MX metabolism, an index of capillary recruitment, measured at the end of 2h insulin clamp would be comparable to that determined after the 1h insulin clamp. As shown in Figure 4.10A, upon cessation of the 1h insulin infusion, 1-MX metabolism remained maximally elevated at 15min, then at 30min, dropped to a level that wasn't significantly different from either the basal value or the value for maximal activation. At 60min the 1-MX metabolism had returned to the basal level (Fig 4.10A).

4.3.3 Glucose Metabolism

Basal blood glucose concentration was between 4-5mM in all experimental groups although it was slightly but significantly lower in InsR group (Fig 4.6A, Fig 4.7). Euglycemia was maintained using variable rates of 30% glucose infusion. Glucose infusion rate required to maintain euglycemia increased rapidly and reached a plateau within 1h (Fig 4.6B, Fig 4.8), indicating the steady state of insulin-stimulated glucose metabolism was achieved in these experimental animals. Following cessation of the 1h insulin infusion, the glucose infusion rate dropped quickly, returning within 30min to a value not significantly different from zero (Fig 4.8).

Hindleg glucose uptake was significantly enhanced by the end of 2h insulin clamp (Fig 4.10B). Since the steady-state of glucose metabolism has been reached within the first 1h of insulin infusion indicated by the plateaued glucose infusion rate, and maximal glucose uptake by skeletal muscle which is the major insulin-responsive tissue in the hindlimb has been shown to be achieved within 40 – 55min after the onset of hyperinsulinemia (plasma insulin level of ~130mU.L^{-1} which is similar to 615pM achieved in the present study) (152), the hindleg glucose uptake determined at the end of 2h insulin clamp would be comparable to that assessed at the end of 1h insulin clamp. Upon the cessation of 1h insulin infusion, hindleg glucose uptake decreased rapidly back to basal (saline) within 15min (Fig 4.10B). There was a trend of a further decrease in hindleg glucose uptake during the following 45min reversal period, although this trend was not significant (Fig 4.10B).

4.3.4 Plasma Insulin Concentrations

There was a small but significant increase in plasma insulin level during the saline infusion (Fig 4.11), which may be due to the effect of pentobarbitone anesthesia on insulin clearance (153) or due to the slight increase in blood glucose concentration. Insulin infusion at 3mU.min^{-1}.kg^{-1} for 2h elevated plasma insulin concentration by 5-fold from 136 ± 10pM at basal to 615 ± 69pM. Since the insulin clearance mechanism is saturated at concentrations above 3000pM (282), the currently achieved plasma insulin level of 615pM by 2h insulin infusion suggests that circulating insulin has reached equilibrium within this period. As shown in Chapter 3 increasing the insulin dose from 3 to 10mU.min^{-1}.kg^{-1} will further enhance insulin-mediated glucose disposal whereas glucose metabolism in the present study reached steady state within 1h, plasma insulin may have reached equilibrium within 1h insulin infusion at 3mU.min^{-1}.kg^{-1}. Therefore, plasma insulin concentration measured at the end of 2h insulin administration may be comparable to that measured 1h after the onset of insulin clamp. As shown in Figure 4.11, upon the cessation of insulin infusion, plasma insulin level decreased rapidly to the basal value within 15min. There was a trend of an increase in insulin level at 60min, although this increase wasn't significant.

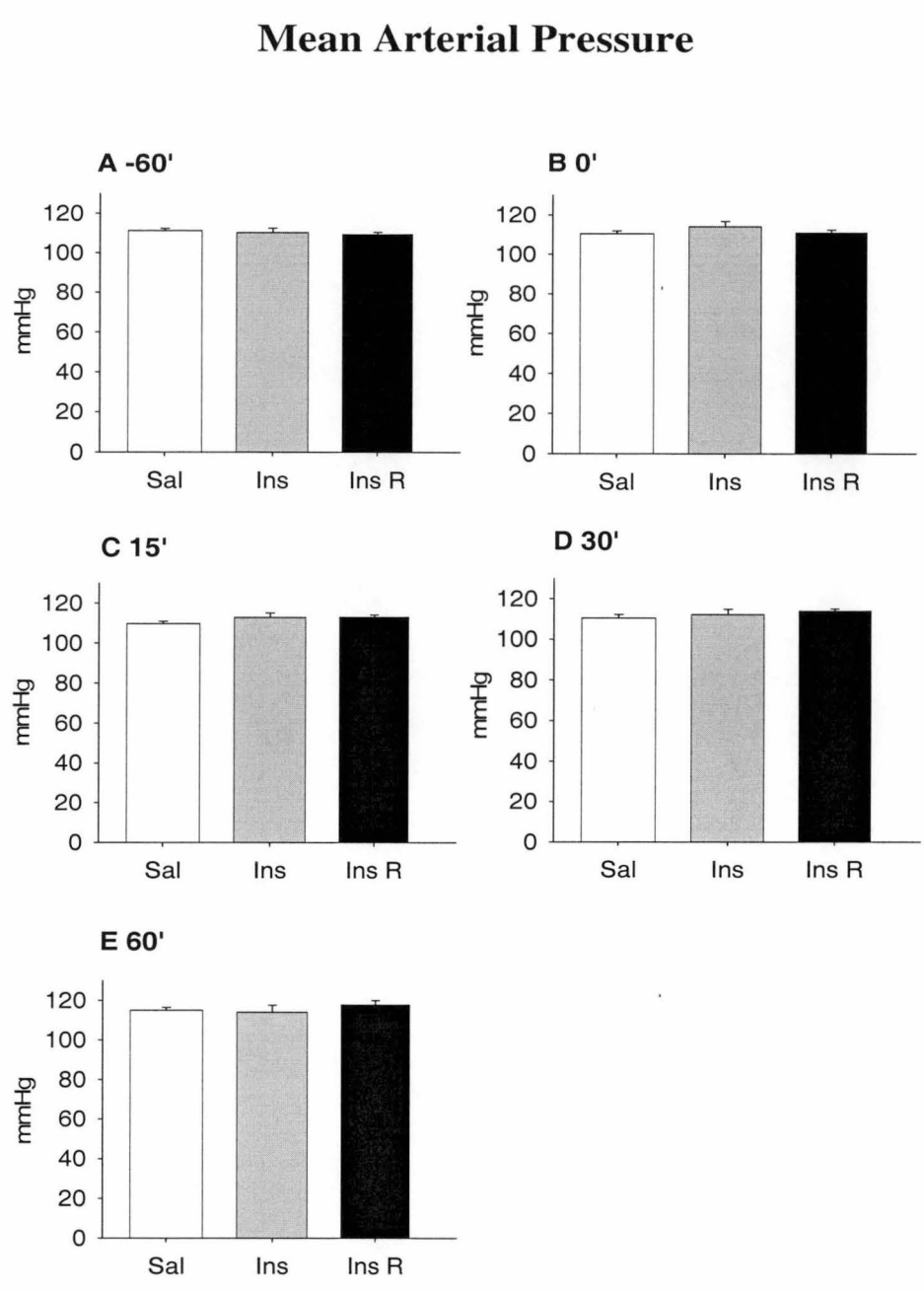

Figure 4.2 Mean arterial pressure for saline group (□, n=14), insulin clamp (3mU.min^{-1}.kg^{-1}) group (▒, n=8) and insulin (3mU.min^{-1}.kg^{-1}) reversal group (■) at the –60 (A), 0 (B), 15 (C), 30 (D) and 60 (E) min time points as indicated by ↑ in Fig 4.1. Insulin reversal group is the combination of 3 sub-groups (InsR 15', InsR 30' and InsR 60') and the "n" values are 23, 23, 23, 14 and 8 for the –60, 0, 15, 30 and 60min time point respectively. Values are means ± SE.

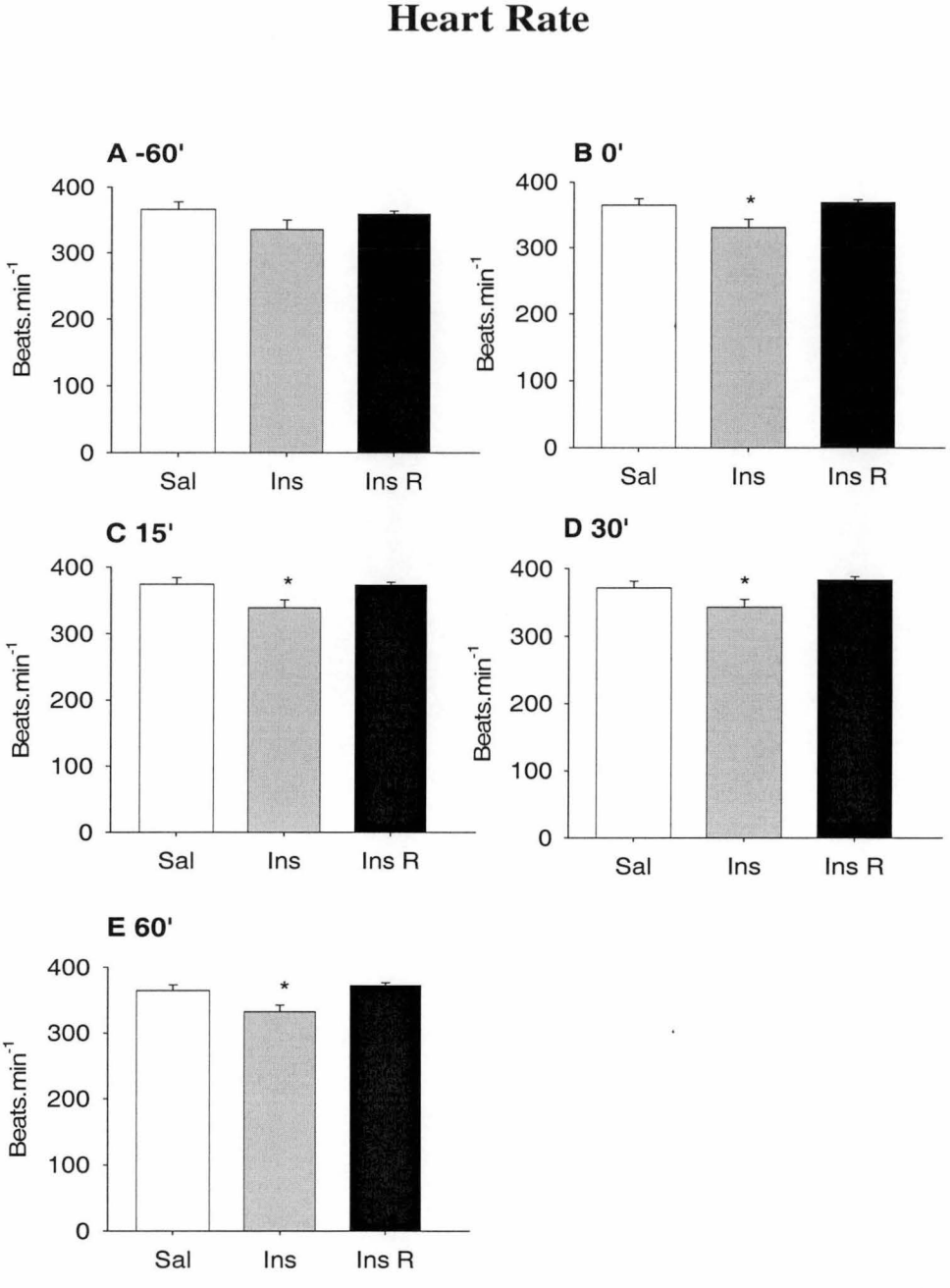

Figure 4.3 Heart rate for saline group (□, n=14), insulin clamp (3mU.min^{-1}.kg^{-1}) group (▨, n=8) and insulin (3mU.min^{-1}.kg^{-1}) reversal group (■) at the –60 (A), 0 (B), 15 (C), 30 (D) and 60 (E) min time points as indicated by ↑ in Fig 4.1. Insulin reversal group is the combination of 3 sub-groups (InsR 15', InsR 30' and InsR 60') and the "n" values are 23, 23, 23, 14 and 8 for the –60, 0, 15, 30 and 60min time point respectively. Values are means ± SE. *Significantly different (P<0.05) from saline group.

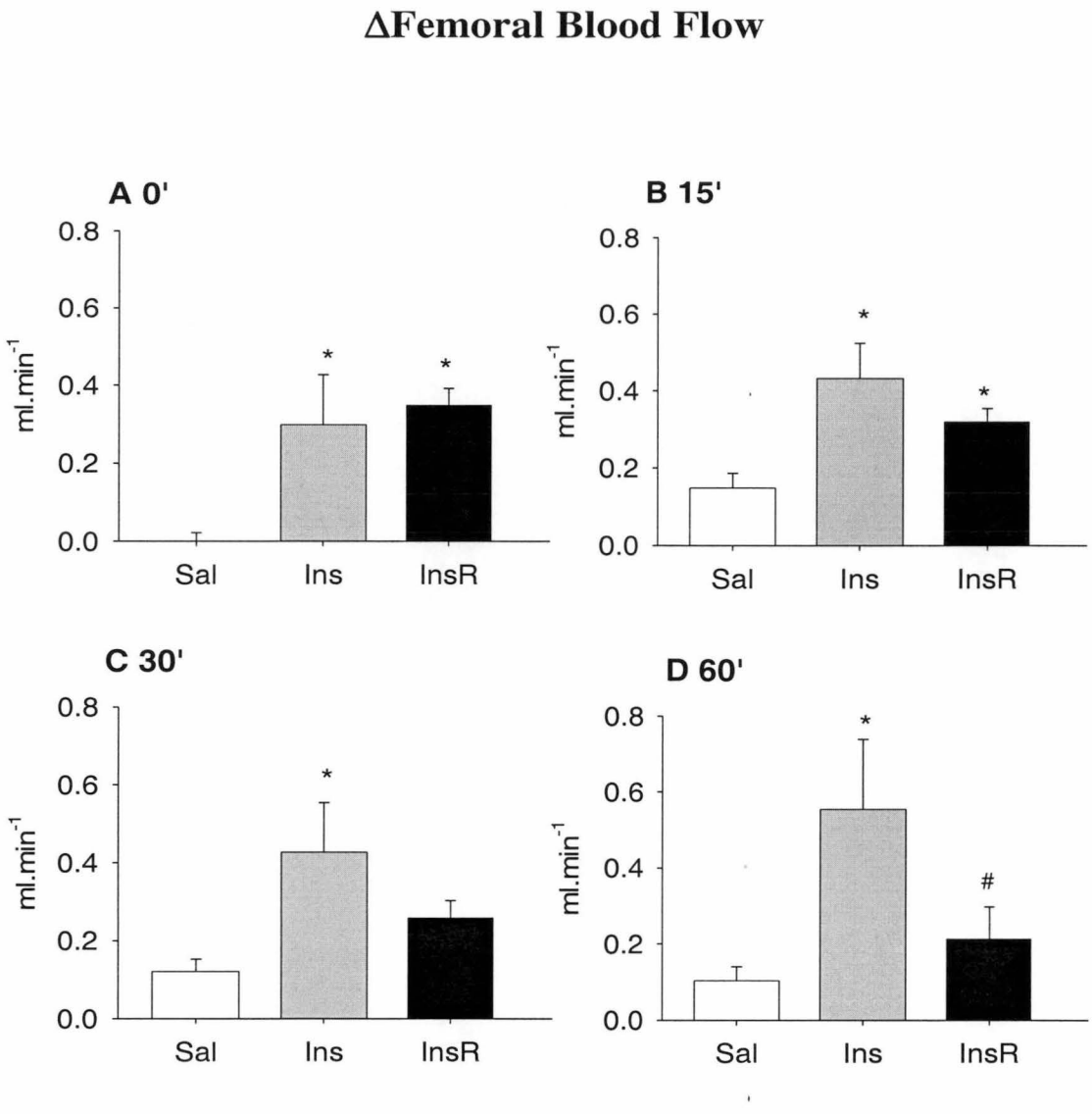

Figure 4.4 Changes in femoral blood flow seen between baseline (-60min) and 0 (A), 15 (B), 30 (C) and 60 (D) min time points as indicated by ↑ in Fig 4.1 for saline group (□, n=14), insulin clamp (3mU.min^{-1}.kg^{-1}) group (▒, n=8) and insulin (3mU.min^{-1}.kg^{-1}) reversal group (■). Insulin reversal group is the combination of 3 sub-groups (InsR 15', InsR 30' and InsR 60') and the "n" values are 23, 23, 14 and 8 for the 0, 15, 30 and 60min time point respectively. Values are means ± SE. *Significantly different (P<0.05) from saline group. #Significantly different (P<0.05) from insulin group.

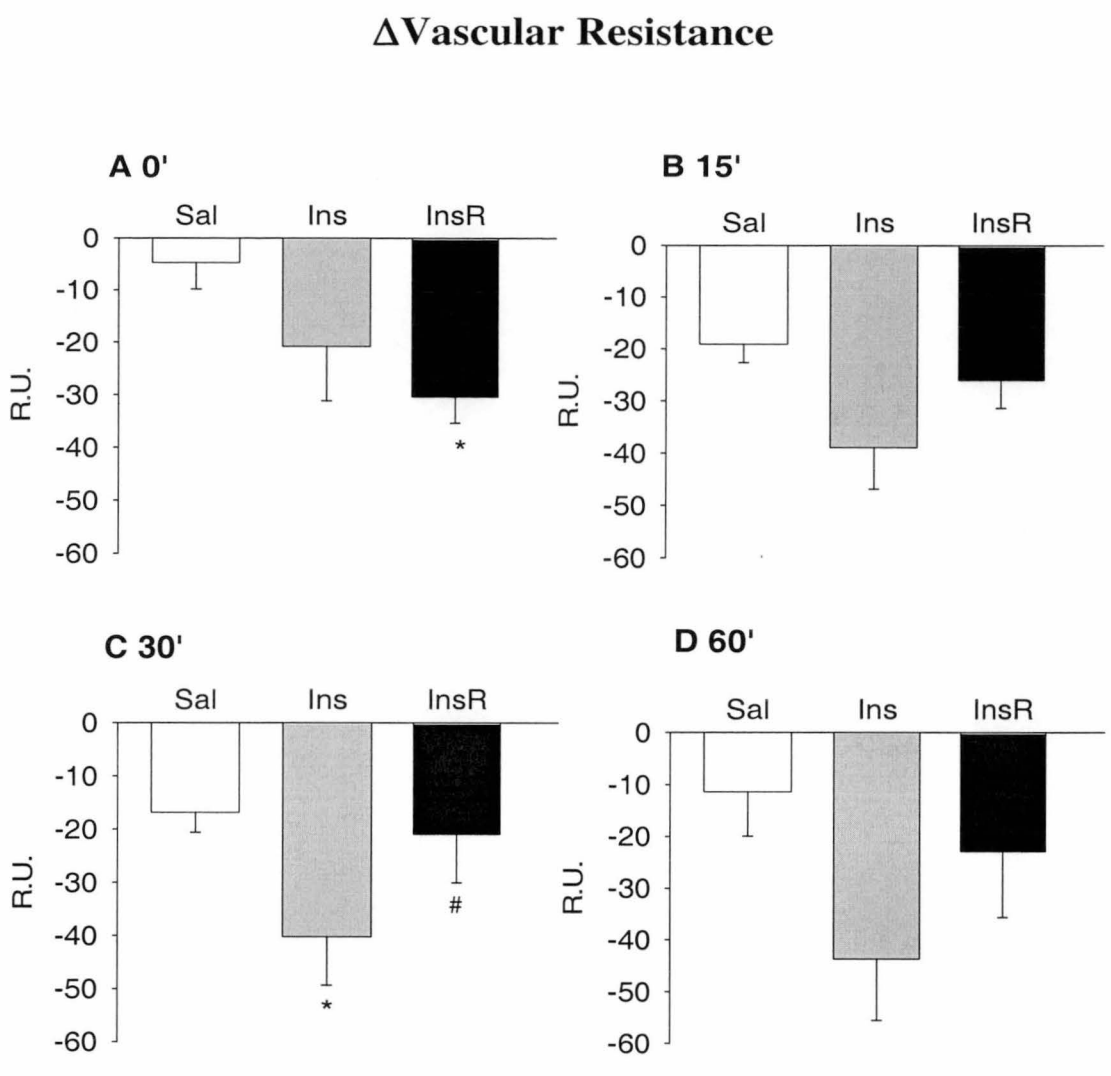

Figure 4.5 Changes in vascular resistance seen between baseline (-60min) and 0 (A), 15 (B), 30 (C) and 60 (D) min time points as indicated by ↑ in Fig 4.1 for saline group (□, n=14), insulin clamp (3mU.min^{-1}.kg^{-1}) group (▒, n=8) and insulin (3mU.min^{-1}.kg^{-1}) reversal group (■). Insulin reversal group is the combination of 3 sub-groups (InsR 15', InsR 30' and InsR 60') and the "n" values are 23, 23, 14 and 8 for the 0, 15, 30 and 60min time point respectively. Values are means ± SE. *Significantly different (P<0.05) from saline group. #Significantly different (P<0.05) from insulin group.

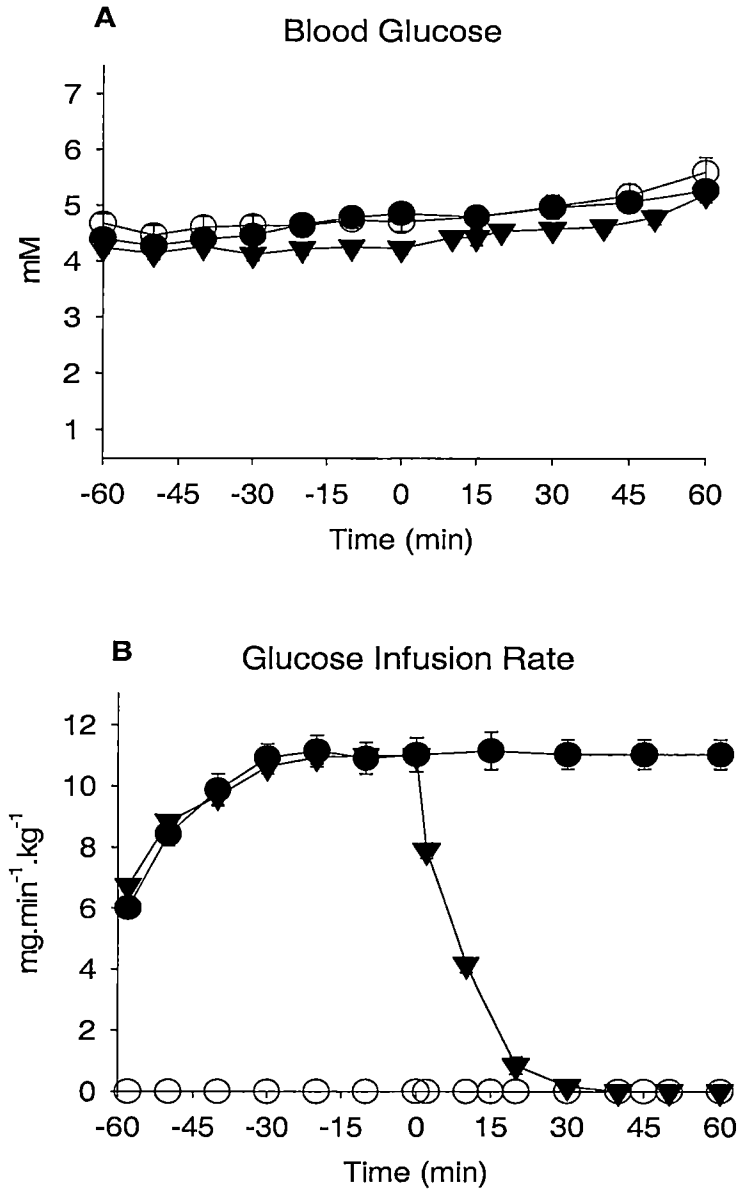

Figure 4.6 Blood glucose concentrations (A) and glucose infusion rates (B) during the 2h infusion of saline (○, n=14) or insulin at 3mU.min^{-1}.kg^{-1} (●, n=8), or 1h insulin infusion at 3mU.min^{-1}.kg^{-1} and the following 1h reversal period (▼). For insulin reversal study, the "n" values are 23, 14 and 8 for time course of –60min – 15min, 15min-30min and 30min-60min respectively. Values are means ± SE.

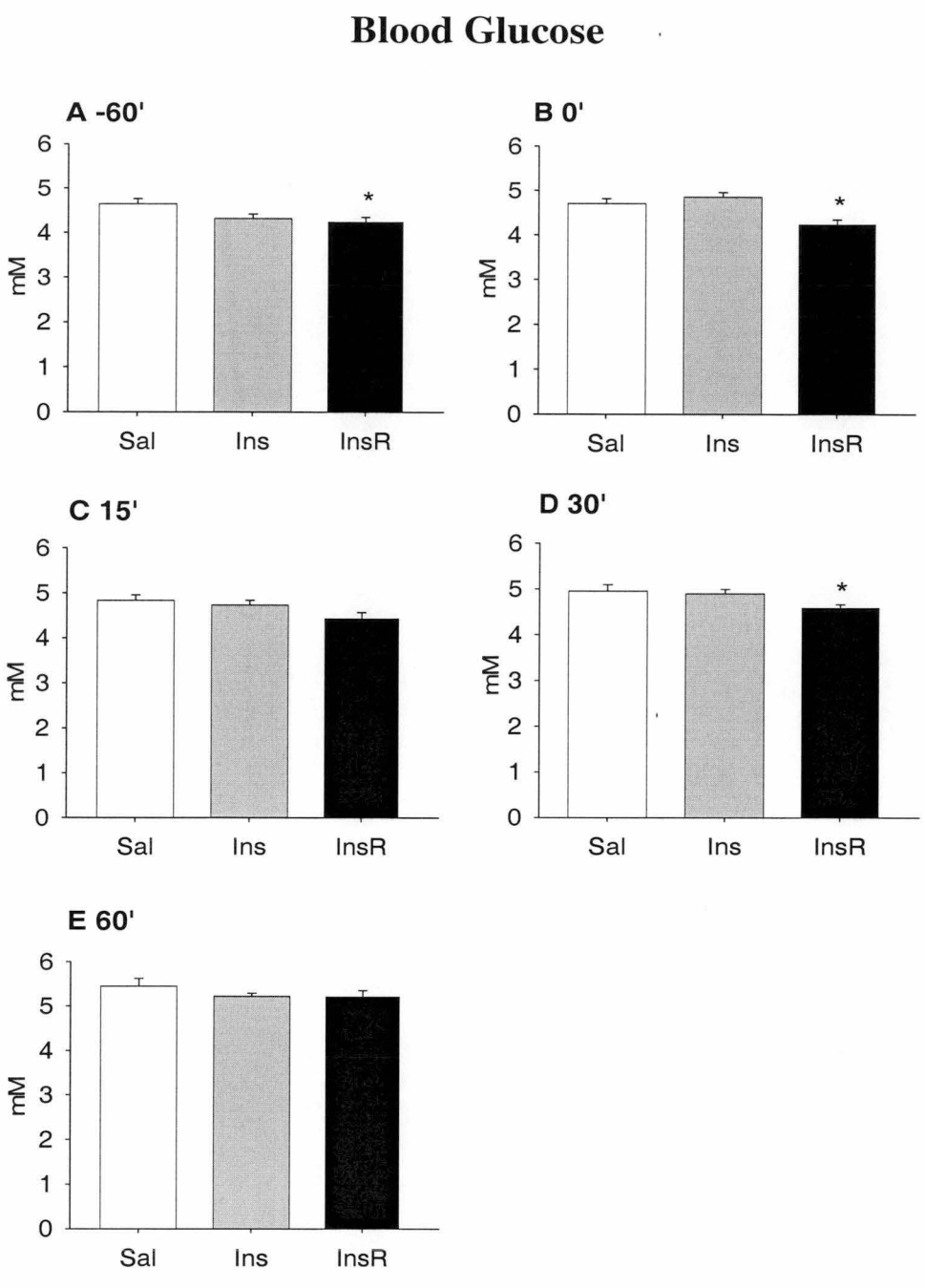

Figure 4.7 Arterial blood glucose levels for saline group (□, n=14), insulin clamp (3mU.min^{-1}.kg^{-1}) group (▨, n=8) and insulin (3mU.min^{-1}.kg^{-1}) reversal group (■) at the –60 (A), 0 (B), 15 (C), 30 (D) and 60 (E) min time points as indicated by ↑ in Fig 4.1. Insulin reversal group is the combination of 3 sub-groups (InsR 15', InsR 30' and InsR 60') and the "n" values are 23, 23, 23, 14 and 8 for the –60, 0, 15, 30 and 60 min time point respectively. Values are means ± SE. *Significantly different (P<0.05) from saline group.

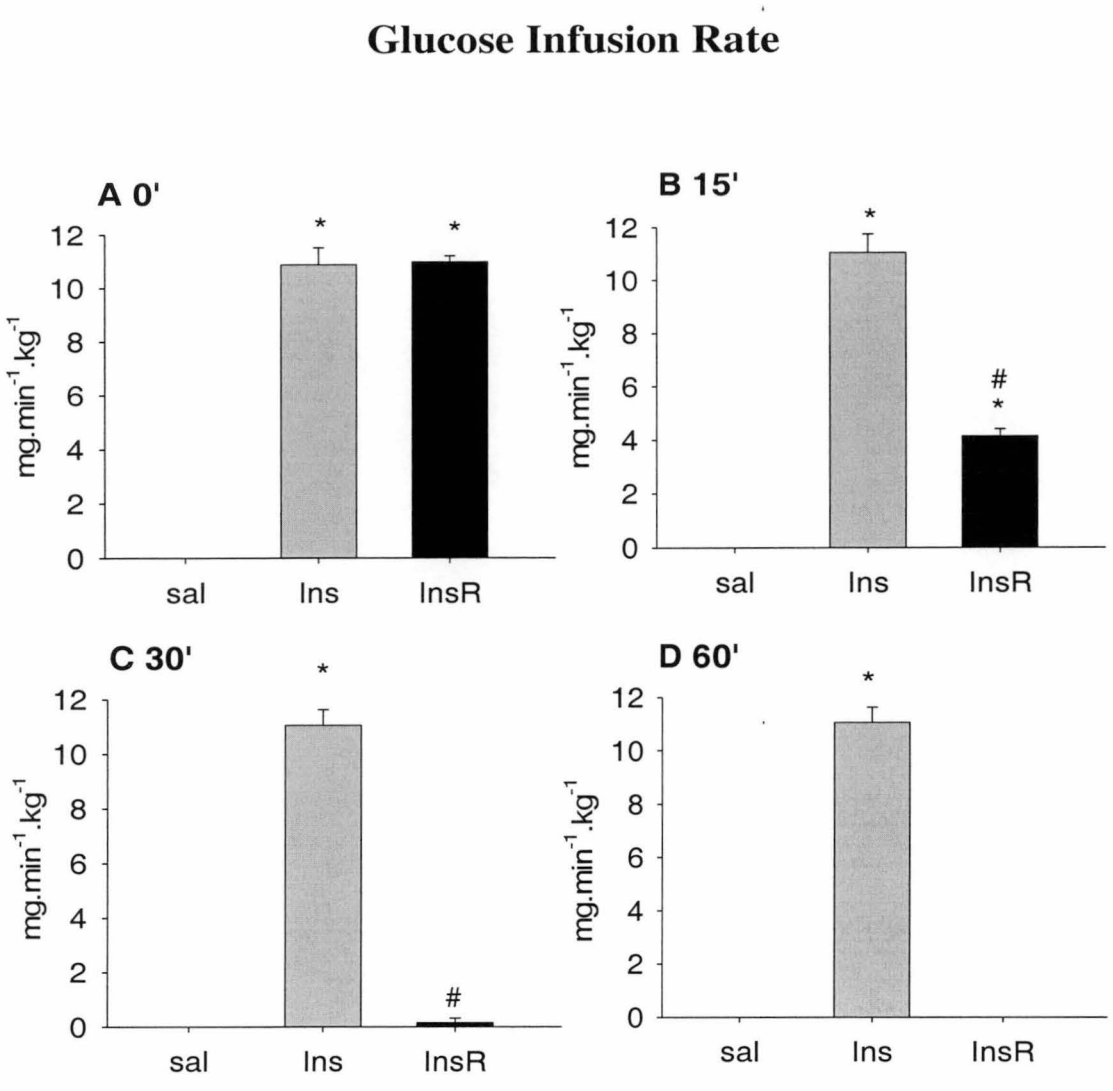

Figure 4.8 Glucose infusion rate for saline group (□, n=14), insulin clamp (3mU.min^{-1}.kg^{-1}) group (▨, n=8) and insulin (3mU.min^{-1}.kg^{-1}) reversal group (■) at the 0 (A), 15 (B), 30 (C) and 60 (D) min time points as indicated by ↑ in Fig 4.1. Insulin reversal group is the combination of 3 sub-groups (InsR 15', InsR 30' and InsR 60') and the n values are 23, 23, 14 and 8 for the 0, 15, 30 and 60 min time point respectively. Values are means ± SE. *Significantly different (P<0.05) from saline group. #Significantly different (P<0.05) from insulin group.

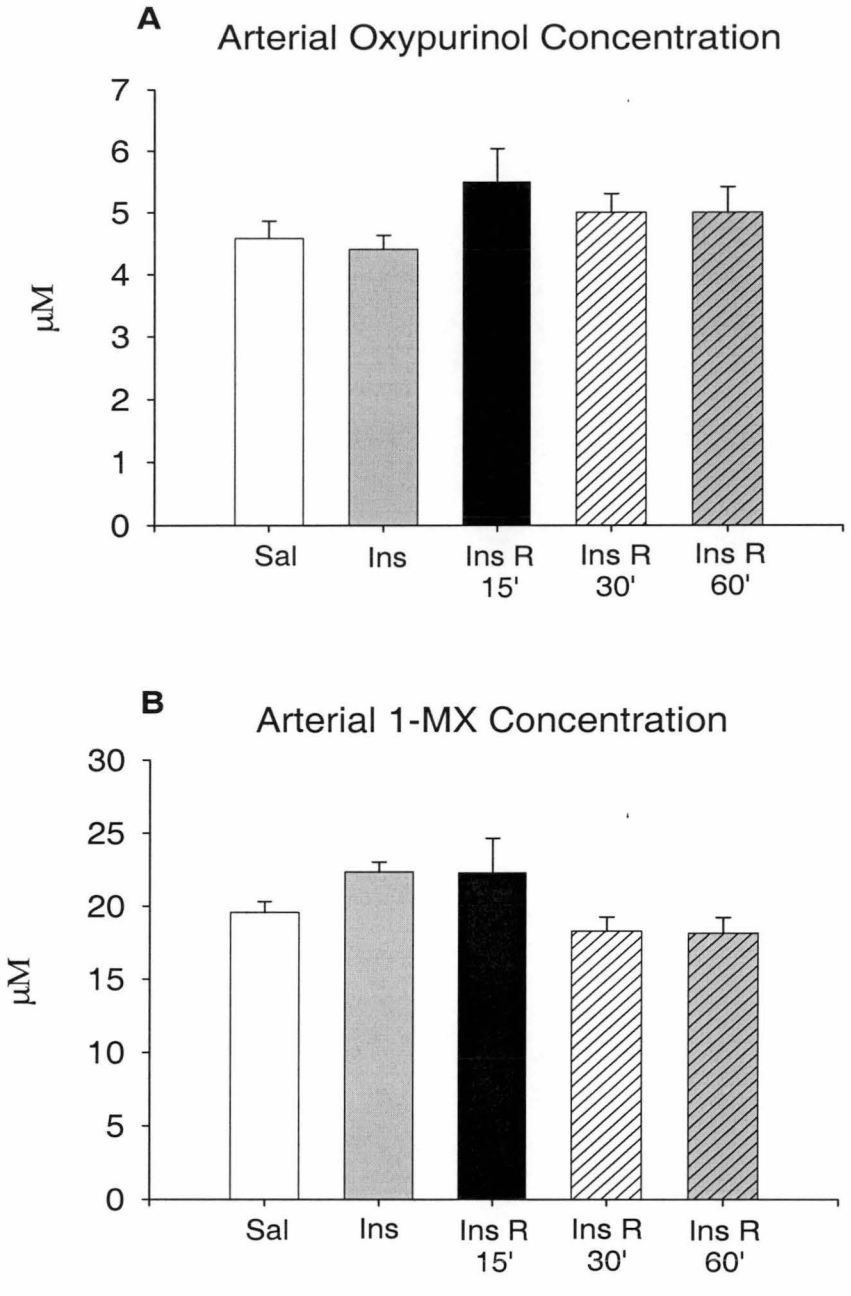

Figure 4.9 Arterial oxypurinol (A) and 1-MX (B) concentrations after 2h infusion of saline (□, n=14) or insulin at 3mU.min^{-1}.kg^{-1} (▒, n=8) or after 1h infusion of insulin at 3mU.min^{-1}.kg^{-1} and the following variable periods of reversal of 15min (■, InsR15', n=8), 30min (▨, InsR 30', n=7) or 60min (▨, InsR 60', n=8). Values are means ± SE.

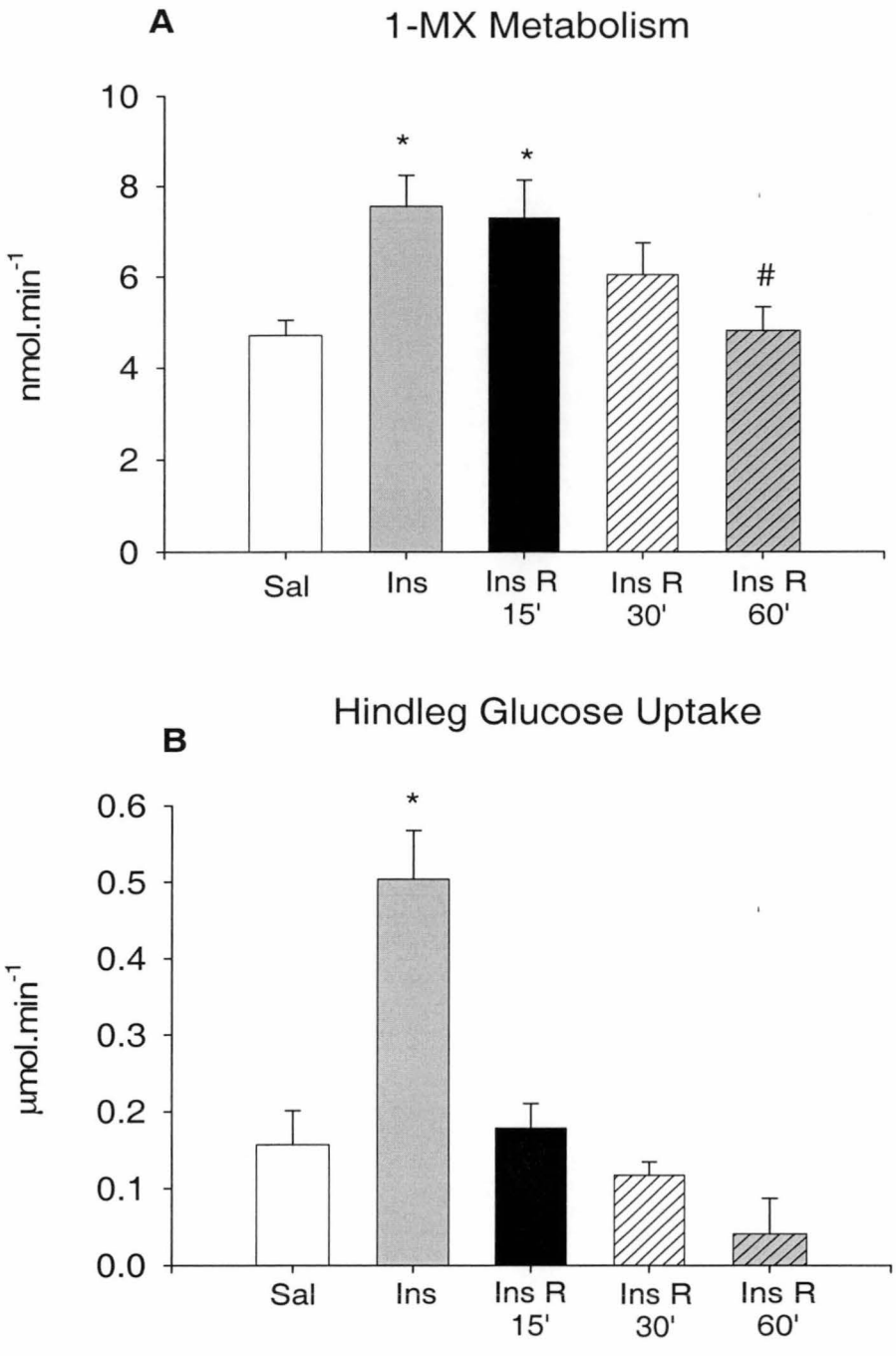

Figure 4.10 1-MX metabolism (A) and hindleg glucose uptake (B) after 2h infusion of saline (□, n=14) or insulin at 3mU.min^{-1}.kg^{-1} (▩, n=8), or after 1h infusion of insulin at 3mU.min^{-1}.kg^{-1} and the following variable periods of reversal of 15min (■, InsR15', n=8), 30min (▨, InsR 30', n=7) or 60min (▨, InsR 60', n=8). Values are means ± SE. *Significantly different (P<0.05) from saline infusion. #Significantly different (P<0.05) from insulin infusion.

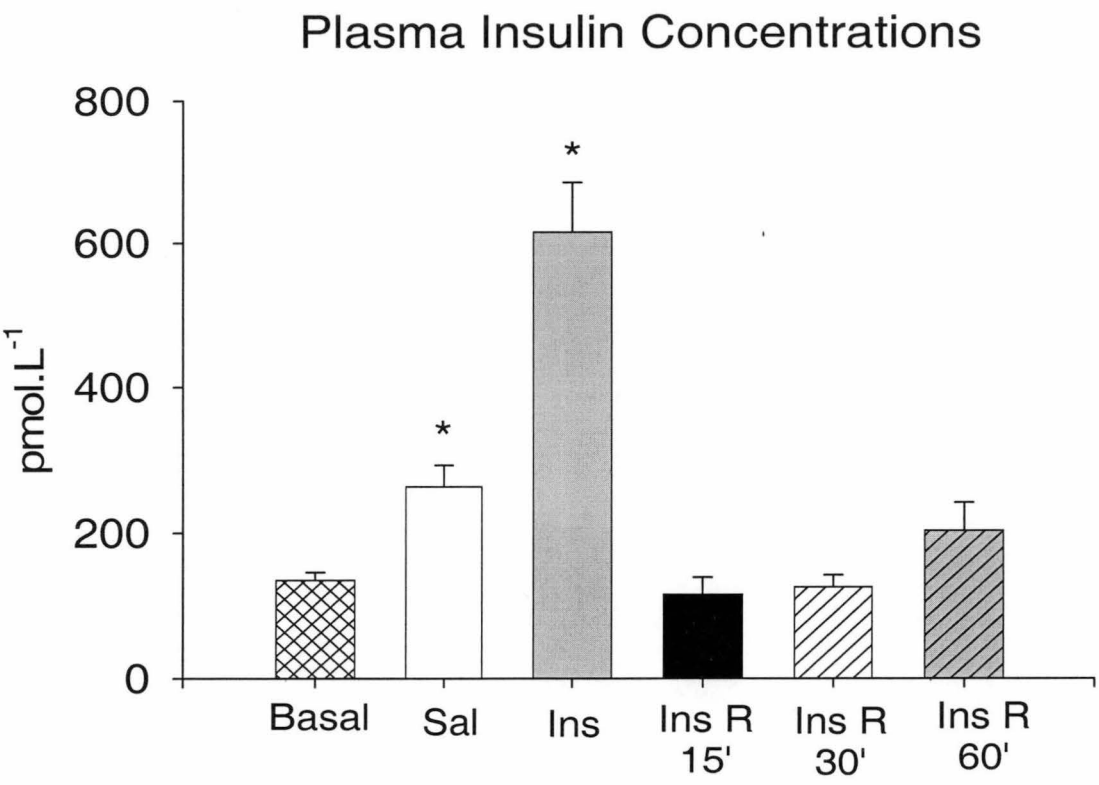

Figure 4.11 Plasma insulin concentrations at baseline (⊠, -60min time point, n= 46), after 2h infusion of saline (□, n=14) or insulin at 3mU.min^{-1}.kg^{-1} (■, n=8) or after 1h infusion of insulin at 3mU.min^{-1}.kg^{-1} and the following variable periods of reversal [15min reversal: InsR15' (■), n=8; 30min reversal: InsR 30' (▨), n=7; 60 min reversal: InsR 60' (▨), n=8]. Values are means ± SE. *Significantly different (P<0.05) from basal value.

4.4 DISCUSSION

The present study investigated the *in vivo* deactivation of insulin action and represents the first report of the temporal relationship of the reversal of insulin's metabolic and hemodynamic effects in rats. To summarize the results, following the cessation of 3mU.min^{-1}.kg^{-1} insulin infusion, both plasma insulin concentration and hindleg glucose uptake returned to their basal levels within 15min. In contrast, insulin-mediated increase in total blood flow and capillary recruitment persisted for another 15min and then gradually returned to basal levels after further 45min.

Although in the current study the plasma insulin and hindleg glucose uptake both returned to basal values at 15min after the cessation of insulin infusion, it is well recognized that in human and larger experimental animals, the activated state of glucose uptake reverses at a slower rate than the fall in plasma insulin level after either the termination of a continuous insulin infusion (116, 209, 264, 266) or a intravenous insulin bolus injection (61). Considering rats metabolize quicker than humans and larger animals, to detect a similar lag in the deactivation of insulin-stimulated glucose uptake may require more frequent sampling after insulin infusion is terminated. Consistent with the reversal of insulin-activated hindleg glucose uptake, glucose infusion rate required further 15min to return to zero. Therefore, this extra amount of glucose may also be required to maintain euglycemia by compensating for a still suppressed hepatic production. This may suggest that insulin's inhibitory effect on liver reverses slower than its stimulatory actions on peripheral tissues in rats. This is consistent with the reports in human that after the discontinuation of insulin infusion, it takes longer for hepatic glucose production to return to half of its basal level than that required for the insulin-mediated glucose disposal to fall to half of its maximal response (116, 265).

Although plasma insulin levels and muscle glucose uptake returned to basal within 15min of stopping insulin infusion, capillary recruitment and increases in total flow required a further 45min to reach their basal levels. The mechanism for the slow deactivation of insulin's hemodynamic actions is unknown. Additionally, a comparison with other *in vivo* (116, 209, 265, 344) or *in vitro* (129, 185) studies on kinetics of insulin actions during the deactivation phase is difficult since those studies

mainly looked at metabolic aspects. However, possible mechanisms suggested for the slow reversal in insulin-mediated glucose uptake might be helpful in shedding some light on the even slower deactivation of insulin-stimulated hemodynamic effects. Firstly, interstitial insulin has been demonstrated to be cleared at a lower rate than plasma insulin after the termination of insulin infusion (209, 264). In the present study, the fully reversed insulin-mediated hindleg glucose uptake indicates that the interstitial insulin has returned to basal level. This might appear to be at odds with the studies of Miles *et al.* (209) and Poulin *et al.* (264). However, since insulin's hemodynamic actions remain activated beyond the deactivation of insulin-mediated glucose uptake, neither plasma nor interstitial insulin clearance appears to contribute to this delay. Secondly, since a decline in the extracellular insulin concentration results in a rapid dissociation of insulin from its receptors in both *in vivo* (253, 302) and *in vitro* (77, 78, 210) conditions, it is conceivable that a persistent intracellular signalling activation is responsible for the slow reversal of insulin-mediated increase in total blood flow and capillary recruitment after the cessation of insulin infusion.

The lag in the deactivation of insulin's hemodynamic actions compared to the reversal of hindleg glucose uptake may reflect a different intracellular control on the two aspects of insulin actions. Indeed, there is evidence that capillary recruitment (331) and total blood flow (308) are each nitric oxide dependent and that nitric oxide production in endothelial cells involves a phosphorylation cascade from the insulin receptor via insulin receptor substrate-1, phosphatidylinositol 3-kinsase, and Akt to endothelial nitric oxide synthase (351). Thus, although sharing some elements of the insulin-signalling cascade with glucose transport (43, 65), lower phosphatase activity at one or more steps in the insulin signalling cascade may be attributable to the slow reversal of total flow increase and capillary recruitment.

Insulin-mediated muscle glucose uptake has been demonstrated to lag behind insulin-stimulated capillary recruitment but precede the increases in total blood flow, suggesting a different control of insulin on the activation of these two vascular events. A number of factors may be considered to account for the different regulation. Thus, since smaller vessels are more sensitive to insulin-mediated vasodilation than larger vessels (205, 238, 262) and capillary recruitment is more sensitive to insulin than bulk blood flow (Chapter 3), insulin may act on larger resistant vessels to regulate total

blood flow and on terminal arterioles to stimulate capillary recruitment. Furthermore, although the involvement of nitric oxide has been suggested for insulin-mediated total flow (308) and capillary recruitment (331), the source of nitric oxide may differ as endothelial cells (212, 351, 352), vascular smooth muscle cells (318, 319) and skeletal muscle cells (160) are each capable of producing nitric oxide. In addition, other factors such as Na^+-K^+-ATPase activation (146, 239) and adenosine release (205) have been suggested to take part in insulin-mediated vasodilation and thus they may have different involvements in insulin-mediated total flow increase and capillary recruitment. Despite there being a number of possibilities that could account for the different control of insulin on total blood flow and capillary recruitment, the present observation of a similar reversal time course of the two vascular events suggests the proposed mechanisms may have a similar deactivation component.

The reason for the slow reversal of insulin's hemodynamic actions is not clear. One explanation could be the slow reversal allows washout of insulin from muscle for clearance by liver and kidney following the decline of the peak of plasma insulin at the end of the absorptive state. In this manner, anabolic processes stimulated by insulin in the myocytes would be more readily reversed. This might limit late hypoglycemia which wouldn't occur under a clamp condition since it has been prevented by infusing variable rates of glucose.

In summary, the current study demonstrated that following the cessation of insulin infusion, the deactivation of insulin-mediated increases in total blood flow and capillary recruitment lags behind the fall in plasma insulin and the reversal of insulin-stimulated hindleg glucose uptake. This suggests the intracellular signalling mechanisms involved in insulin-mediated capillary recruitment and total blood flow increase differ from those involved in glucose uptake. In addition, although the activation of bulk blood flow and microvascular recruitment by insulin is likely to be regulated differently, the current study suggests they may have similar deactivation mechanisms. The persistence of insulin's vascular effects after insulin withdrawal might facilitate the clearance of insulin from muscle to prevent late hypoglycemia.

CHAPTER 5

TNFα AS AN ANTAGONIST OF INSULIN-MEDIATED CAPILLARY RECRUITMENT

5.1 INTRODUCTION

Tumor Necrosis Factor alpha (TNFα) has marked effects on whole body lipid and glucose metabolism (32, 118), and over-expression of TNFα in adipose tissue and muscle of animals and humans may contribute to the development of insulin resistance. Indeed, there are reports that insulin resistance and obesity are associated with elevated levels of TNFα mRNA and protein (142). In addition, lowering the active level of TNFα *in vivo* by infusion of a TNFα receptor IgG fusion protein (142), a soluble TNFα-binding protein (143), or polyclonal anti-TNFα (38) in insulin-resistant animal models improves insulin action. Moreover, in genetically obese mice that are insulin resistant, deletion of either or both of the TNFα receptors improves insulin sensitivity (140), and null mutations of TNFα in obese mice significantly improve insulin receptor signalling capacity and, consequently, insulin sensitivity (141). Acute effects of TNFα *in vivo* have also been reported, Thus TNFα administration to rats under hyperinsulinemic clamp gives rise to insulin resistance, particularly of muscle (192).

A number of studies *in vitro* have provided evidence that TNFα can directly cause loss of insulin sensitivity over both long and short periods. Thus 3-5 days of exposure of 3T3-L1 or 3T3-F442A adipocytes to TNFα causes reductions in insulin receptor and insulin receptor substrate (IRS-1) tyrosine phosphorylation in response to a maximum dose of insulin (120, 143). Others report that 3-4 days of exposure of 3T3-L1 adipocytes to TNFα gives rise to transcriptional changes including decreases in GLUT4, insulin receptor, and IRS-1 mRNA and protein (311, 312). These reported effects from chronic exposure to TNFα in cell culture have downstream consequences consistent with insulin resistance; for example, decreased insulin-stimulated glucose

transport has been noted in L6 myocytes (28). Over a shorter period (1h), C2C12 muscle cells exposed to TNFα exhibited impaired insulin-dependent phosphatidylinositol 3-kinase activation mediated by IRS-1 and -2. This was accompanied by a decrease in 2-deoxyglucose uptake (74). Despite such reports, isolated incubated muscle appears to be completely unaffected by TNFα. Thus incubation of isolated soleus and epitrochlearis muscles with 6nmol.L^{-1} for 45min or 4h, or 2 nmol.L^{-1} for 8 h, had no effect on insulin signalling on glucose uptake (231). In contrast, we have recently shown (350) that TNFα infusion evoked acute insulin resistance [euglycemic hyperinsulinemic clamp (10mU.min^{-1}.kg^{-1}) *in vivo*], and this was accompanied by the loss of insulin-mediated hemodynamic responses, including capillary recruitment and increases in total limb blood flow. Taken together, this raises the interesting possibility that, although muscle cell lines respond acutely to TNFα *in vitro*, the vasculature *in vivo* may be an important target for TNFα. The loss of the hemodynamic responses may limit insulin and/or glucose access and account for inhibition of ~50% of the insulin-stimulated glucose uptake by muscle (350). Such a loss would be apparent only *in vivo* and thus be consistent with the negative outcomes of using TNFα in isolated incubated muscles, as found by Nolte *et al.* (231).

In the present study, the potential role of the vasculature in TNFα-induced insulin resistance was further explored by challenging TNFα's action with a supra-physiological dose of insulin at 30mU.min^{-1}.kg^{-1}. We hypothesize that if the loss of insulin-mediated hemodynamic responses due to TNFα was restored by this high dose of insulin, the metabolic action of insulin would also be restored. The effect of TNFα against a physiological dose of insulin at 3mU.min^{-1}.kg^{-1} was also investigated.

5.2 MATERIALS AND METHODS

5.2.1 Animal Care

Animals were raised as described in section 2.1. Male Hooded Wistar rats weighing 240~260 grams were chosen for this study.

5.2.2 *In vivo* Experiments

In vivo experiments were carried out in anaesthetized rats as described in section 2.2. Briefly, once the surgery was completed, a 45- to 60-min equilibration period was allowed so that blood pressure and femoral blood flow could become stable and constant. Rats then were allocated into either protocol A (Fig 5.1), where animals were infused with either saline or TNFα (mouse recombinant; Sigma-Aldrich, Inc.) at $0.5\mu g.kg^{-1}.h^{-1}$ for 3h, or protocol B (Fig 5.1), where animals were infused with either saline or TNFα for 3h and underwent a euglycemic insulin clamp (3, 10, or $30mU.min^{-1}.kg^{-1}$) for the last 2h. Xanthine oxidase activity was partially inhibited by a bolus injection of oxypurinol ($10\mu mol.kg^{-1}$) injected through the arterial line 5min before the administration of 1-MX. 1-MX infusion ($0.4mg.min^{-1}.kg^{-1}$) was continuous over the final hour to achieve a constant arterial 1-MX concentration. At the completion of each experiment, blood was sampled from the femoral vein and carotid artery. From the arteriovenous difference multiplied by the femoral blood flow, hindleg glucose uptake and 1-MX metabolism were calculated. The latter was used as an indicator of perfused capillary surface area. A bolus dose of [^{3}H]2-DG (50μCi) was given at 45min before the end of the experiment. The radioactivity decay curve was generated from arterial plasma samples collected at 5, 10, 15, 30, and 45min following the injection. Hindleg muscles were excised at the completion of the experiment and freeze clamped in liquid nitrogen to assess the 2-DG uptake as described in section 2.2.5. Insulin levels were determined in arterial plasma samples collected at the beginning and end of each experiment by ELISA assay (Mercodia AB, Sweden). Plasma TNFα levels in experiments involving TNFα infusion were also determined using a Murine TNFα ELISA Kit (Pierce Endogen USA).

5.2.3 Data Analysis

All data are expressed as means ± SE. Time course data were presented from the 0 time point when the insulin clamp started. Analytical methods for hemodynamic data collected by WINDAQ data acquisition system and data calculation were described in section 2.2.9. To ascertain differences between treatments throughout the time course, two-way repeated analysis of variance was used. Once a significant difference ($P<0.05$) was found, pair wise comparisons by the Student-Newman-Keuls test were used to determine at which individual time points the difference was significant. Statistical differences among treatments at a single time point were determined by

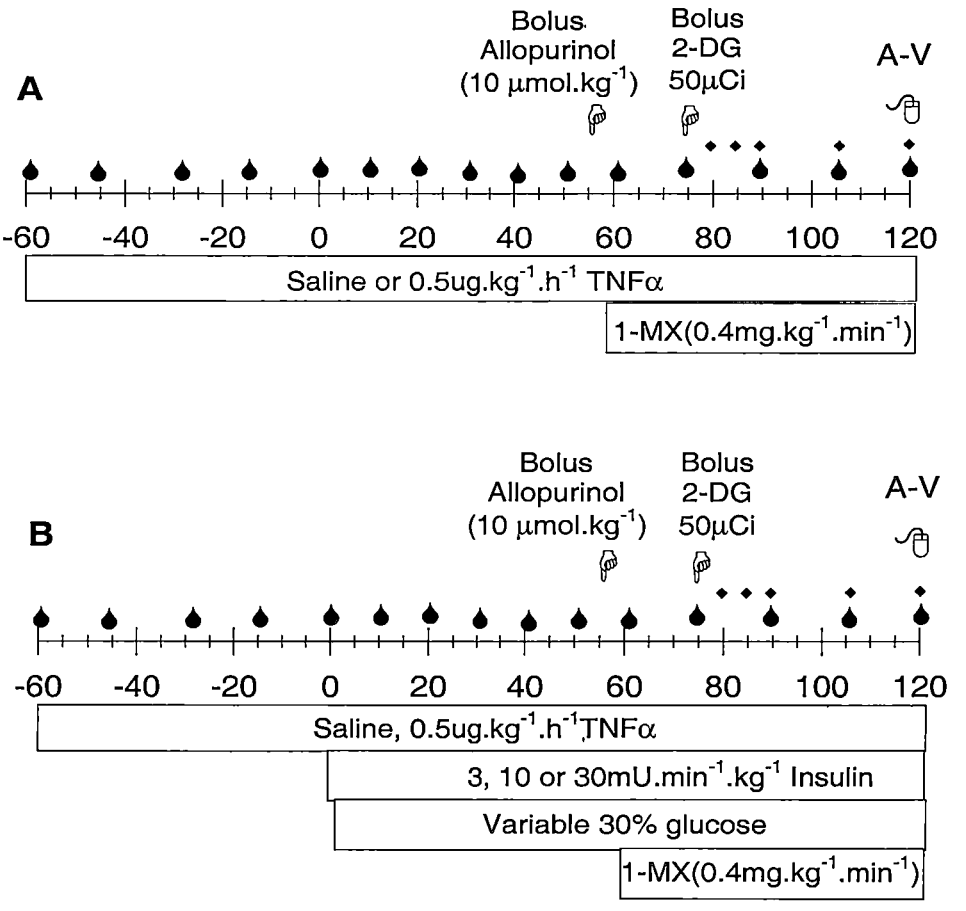

Figure 5.1 Experimental Protocols. Venous infusions are indicated by the bars. Bolus injections are shown by ☞. Arterial blood glucose levels were measured at times indicated by ♦. Arterial samples for determination of radioactivity are shown by ✦. Arterial and venous samples collected for HPLC assay are indicated by ☜. In protocol A, saline or TNFα at 0.5μg.kg^{-1}.h^{-1} was infused for 3h. Protocol B involved a euglycemic hyperinsulinemic clamp and TNFα infusion where the insulin clamp started at 0 time point which was 1h after the commencement of TNFα infusion.

unpaired *t*-test. These tests were performed using the SigmaStat statistical program (Jandel Software).

5.3 RESULTS

5.3.1 Hemodynamic Measurements

Basal mean arterial pressure was similar in all groups (Fig 5.2). TNFα infusion at $0.5\mu g.h^{-1}.kg^{-1}$ and insulin infusion at 3 or $10mU.min^{-1}.kg^{-1}$ had no effect on blood pressure whereas a supra-physiological dose of insulin at $30mU.min^{-1}.kg^{-1}$ slightly but significantly augmented mean arterial pressure after 45min infusion (Fig 5.2). TNFα had no effect on blood pressure during the insulin clamp. Heart rate remained stable at a normal range of 325-375 $beats.min^{-1}$ during the experiment and was not significantly different among groups apart from the $3mU.min^{-1}.kg^{-1}$ insulin clamp group where the heart rate was decreased transiently (Fig 5.3).

Femoral blood flow did not change during the first hour of TNFα infusion (0.86 ± 0.04 and 0.85 ± 0.04 $ml.min^{-1}$at -60min and 0 time point respectively). After another 45-60min infusion of TNFα, there was a significant decrease in femoral blood flow (Fig 5.4). Insulin increased blood flow in a dose-dependent manner with an earlier onset and bigger magnitude of increase at higher doses (Fig 5.4). TNFα infusion for 1h before and during the 2h insulin clamp completely inhibited the increase in femoral blood flow at 3 and $10mU.min^{-1}.kg^{-1}$ of insulin but only partly (50% at the end of experiment) inhibited the increase due to the highest insulin dose of $30mU.min^{-1}.kg^{-1}$ (Fig 5.4).

During the first hour before the 0 time point, TNFα did not change vascular resistance (127 ± 8 R.U. and 131 ± 7 R.U. at -60min and 0 time point). After another 2h of infusion, TNFα significantly increased vascular resistance with an onset at 45min (Fig 5.5). Insulin infusion decreased vascular resistance and the decrease became significant at an earlier time point during higher dose insulin infusions (Fig 5.5). TNFα infusion for 1h before and during 2h insulin infusion completely blocked the decrease in vascular resistance at 3 and $10mU.min^{-1}.kg^{-1}$ of insulin but only partly

(45% at the end of the experiment) blocked the decrease due to 30mU.min^{-1}.kg^{-1} insulin (Fig 5.5).

5.3.2 1-MX Metabolism

No significant difference was found between experimental groups in arterial plasma concentrations of 1-MX (Fig 5.6) or oxypurinol (Fig 5.7). 1-MX metabolism after 3-hour infusion of TNFα was not significantly different from saline infusion (Fig 5.8). However, insulin alone did significantly increase 1-MX metabolism at all three concentrations, and the increase compared with saline control was the same at all three doses of insulin (Fig 5.8). TNFα completely blocked the insulin-mediated increase in 1-MX metabolism at 3 and 10mU.min^{-1}.kg^{-1} of insulin but had no effect at the highest dose of 30mU.min^{-1}.kg^{-1} (Fig 5.8).

5.3.3 Glucose Metabolism

Basal arterial blood glucose levels were similar among all groups (Fig 5.9). There was no significant difference in blood glucose level between saline and TNFα treatment during the first one hour before the 0 time point (4.98 ± 0.3 and 4.65 ± 0.11mM, 4.68 ± 0.10 and 4.48 ± 0.08mM at -60min and the 0 time point for saline and TNFα infusion respectively). During the next 2h after the 0 time point, TNFα infusion decreased the blood glucose level and the decrease became significant at the 40min time point (Fig 5.9). During the euglycemic insulin clamp experiments with or without TNFα, arterial blood glucose was well maintained at or above basal values by infusion of glucose and statistical analysis showed no significant difference in blood glucose between different doses of insulin and saline treatments (Fig 5.9). Glucose infusion rates were shown in Fig 5.10. Steady-state rates were 11.5 ± 0.4, 21.0± 0.8, and 25.5 ± 0.08 mg.kg^{-1}.min^{-1} for 3, 10, and 30mU.min^{-1}.kg^{-1} insulin respectively (Fig 5.10). TNFα infusion inhibited the glucose infusion rates for the two lower insulin doses of 3 and 10mU.min^{-1}.kg^{-1} by ~50 and 29%, respectively. TNFα had no effect on the glucose infusion rate due to 30mU.min^{-1}.kg^{-1} of insulin (Fig 5.10).

TNFα infusion for 3h showed a trend to decrease basal hindleg glucose uptake although it was not significant (Fig 5.11). Insulin stimulated hindleg glucose uptake by 2.5-fold at 3mU.min^{-1}.kg^{-1} and 3.5-fold at 10 and 30mU.min^{-1}.kg^{-1} insulin (Fig 5.11). TNFα completely blocked insulin-mediated hindleg glucose uptake at 3 and 10mU.min^{-1}.kg^{-1} but was without effect at 30mU.min^{-1}.kg^{-1} insulin (Fig 5.11).

5.3.4 2-DG Uptake

A bolus of radioactive 2-DG was administrated for the final 45min of each experiment. Six lower leg muscles were removed at the completion of each experiment. The 2-DG uptake for combined muscles (A) and individual muscles (B) are shown in Fig 6.12 – 6.14 for different experimental groups. The response to insulin varied depending on the muscle, but in general 3mU.min^{-1}.kg^{-1} of insulin led to a twofold increase, and maximal stimulation was reached at 10mU.min^{-1}.kg^{-1}, as reflected by the combined data (A in Fig 5.12 -5.13). The highest dose of insulin (30mU.min^{-1}.kg^{-1}) did not further increase R'g for individual muscles or for the combination (Fig 5.14). There was a trend of basal 2-DG uptake to be inhibited by TNFα alone infusion although this trend only became significant when it was compared among groups with relatively small variation (Fig 5.12). When administrated with insulin, TNFα fully inhibited the stimulation due to 3mU.min^{-1}.kg^{-1} insulin for combined muscles and all individual muscles except for RG in which it was only partly blocked (Fig 5.12). TNFα also partly blocked the stimulation of 2-DG uptake by 10mU.min^{-1}.kg^{-1} for combined muscles and all individual muscles apart from EDL muscle in which the increase in R'g was completely blocked (Fig 5.13). TNFα was without effect on R'g due to 30mU.min^{-1}.kg^{-1} insulin for either combined or individual muscles (Fig 5.14).

5.3.5 Plasma Insulin and TNFα Levels

Basal and end-of-experiment arterial plasma insulin levels were determined. The results were summarized in Table 5.1. Briefly, insulin infusion increased arterial insulin concentration depending on the dose of insulin used in the experiment. TNFα infusion had no effect on elevated insulin level due to insulin infusion. There was a small but significant increase in arterial insulin concentration during saline infusion,

which may be due to the effect of pentobarbitone anaesthesia on insulin clearance (153) or due to the slightly increased blood glucose concentration. The insulin concentration after 3h TNFα infusion was not different from that after 3h saline treatment and not different from the basal value either, suggesting TNFα may have slightly decreased the plasma insulin level.

The TNFα concentration was determined by ELISA assay in experiments where TNFα infusion was involved. End-of-experiment (120min) arterial plasma TNFα concentrations were 354 ± 65 $pg.ml^{-1}$ (n=20). TNFα levels were not detectable before the commencement of TNFα infusion.

Table 5.1 Arterial plasma insulin concentration at the beginning (T = -60min) and the end (T = 120min) of experiments.

	n	[Insulin](pmol.L^{-1}) (T = -60 min)	[Insulin](pmol.L^{-1}) (T = 120 min)
Saline	13	123 ± 12	219 ± 24*
TNFα	10	159 ± 19	160 ± 15
3mU Insulin	11	132 ± 16	512 ± 58*†
3mU Insulin + TNFα	7	159 ± 52	414 ± 34*†
10mU Insulin	6	185 ± 35	1655 ± 192*†
10mU Insulin + TNFα	6	147 ± 18	1475 ± 238*†
30mU Insulin	7	171 ± 36	8055 ± 550*†
30mU Insulin + TNFα	7	149 ± 61	7725 ± 488*†

*Significantly ($P<0.05$) different from basal for each group.

†Significantly ($P<0.05$) different from saline group at corresponding time point.

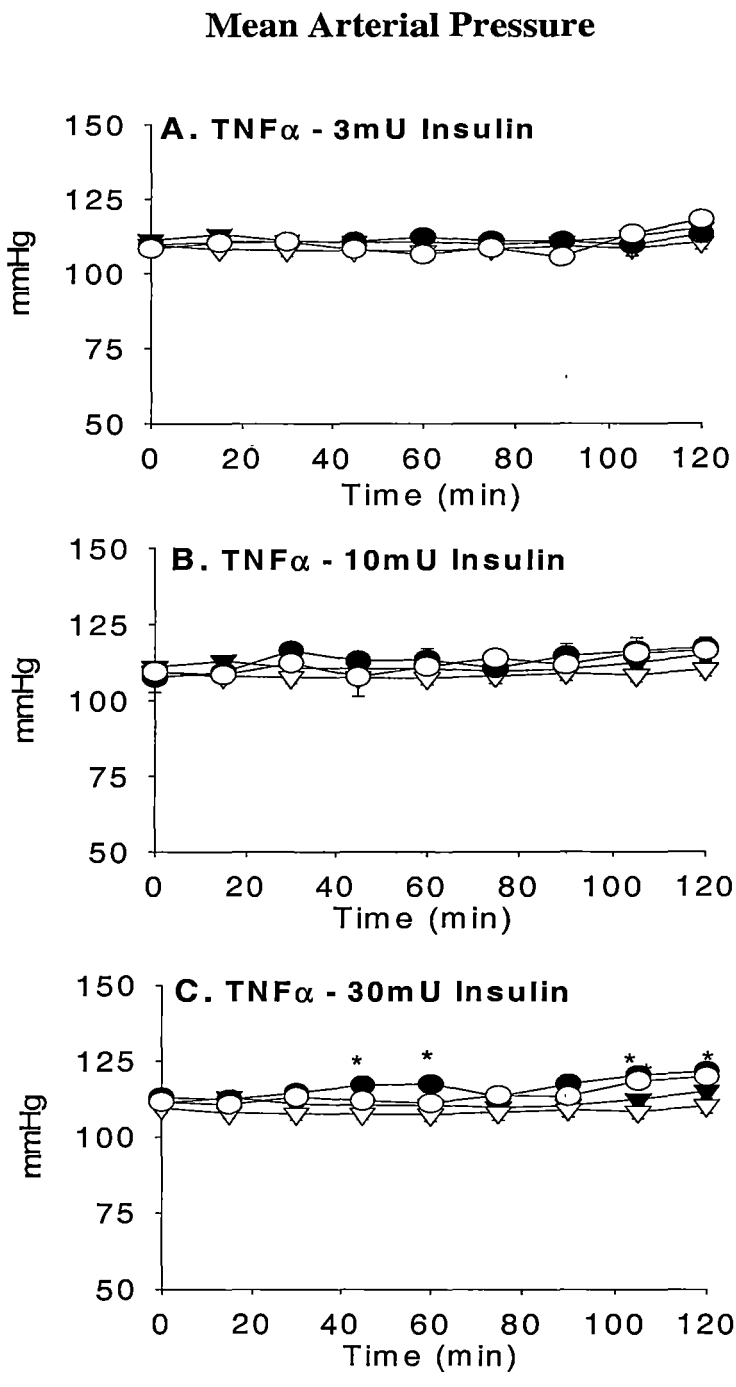

Fig 5.2 Mean arterial pressure for saline infusion (▼ in A, B and C, n=14), TNFα infusion (▽ in A, B, and C, n=5), insulin clamps at 3 doses without TNFα [●, 3mU (A, n=10), 10mU (B, n=6) and 30mU (C, n=7)] or with TNFα (○ in A, B and C, n=7 for each of these three groups)]. Values are means ± SE. * Significantly different (P<0.05) from saline infusion.

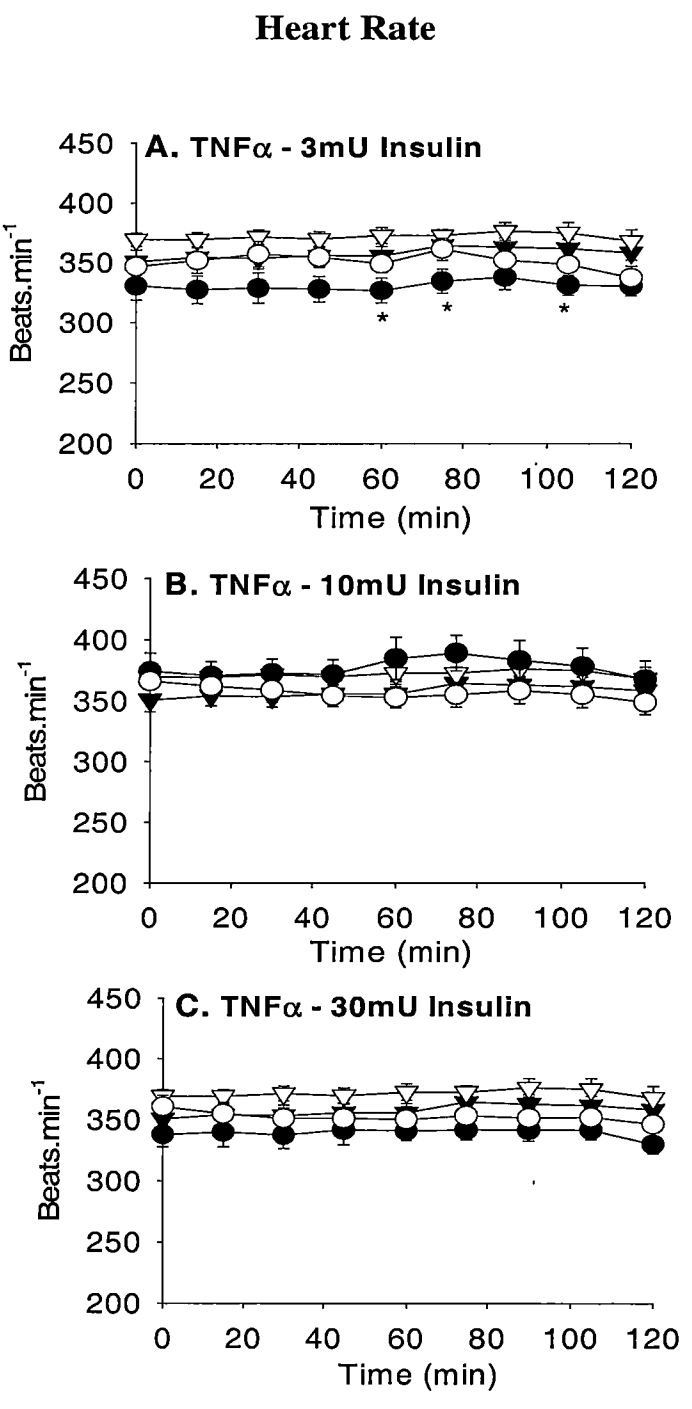

Fig 5.3 Heart rate for saline infusion (▼ in A, B and C, n=14), TNFα infusion (▽ in A, B, and C, n=5), insulin clamps at 3 doses without TNFα [●, 3mU (A, n=10), 10mU (B, n=6) and 30mU (C, n=7)] or with TNFα (○ in A, B and C, n=7 for each of these three groups). Values are means ± SE. * Significantly different ($P<0.05$) from saline infusion.

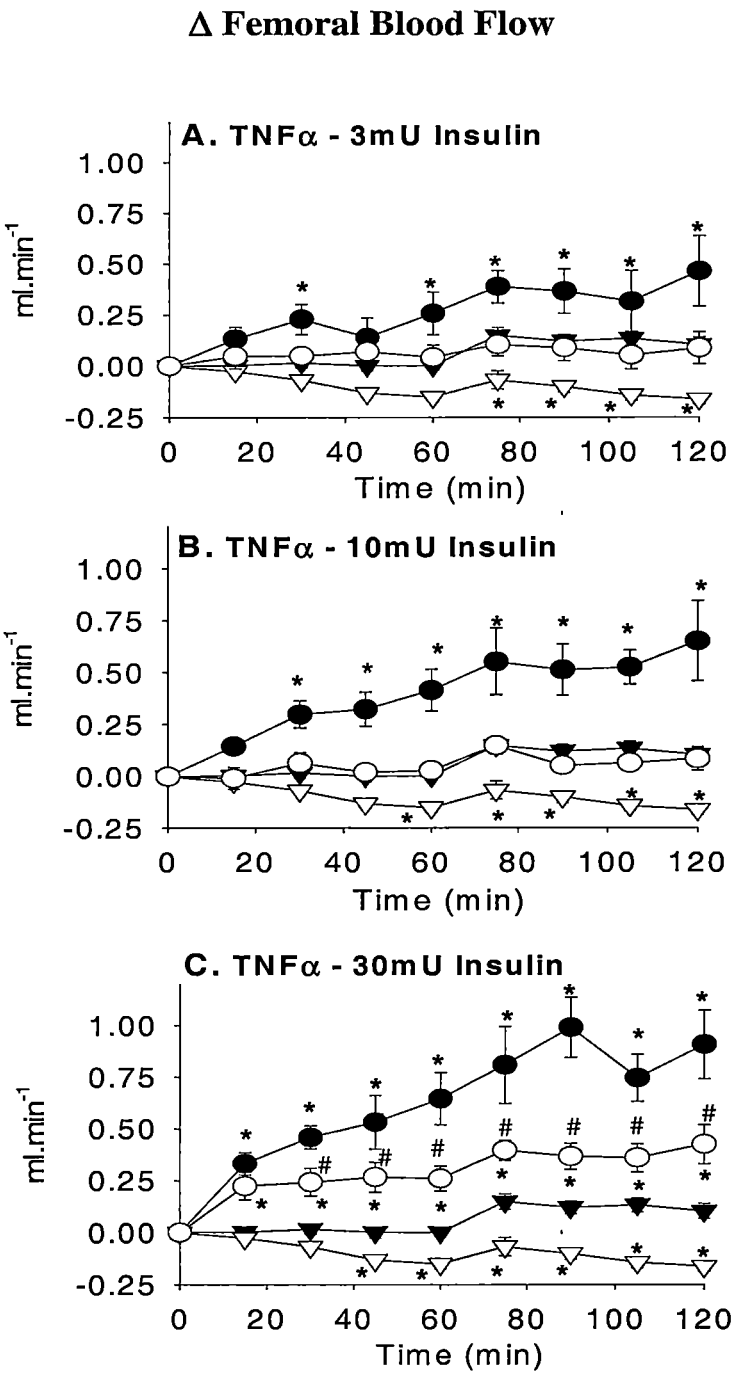

Fig 5.4 Change in femoral blood flow for saline infusion (▼ in A, B and C, n=14), TNFα infusion (▽ in A, B, and C, n=5), insulin clamps at 3 doses without TNFα [●, 3mU (A, n=10), 10mU (B, n=6) and 30mU (C, n=7)] or with TNFα (○ in A, B and C, n=7 for each of these three groups). Values are means ± SE. * Significantly different ($P<0.05$) from saline infusion; #significantly different ($P<0.05$) from clamp group of insulin alone infusion.

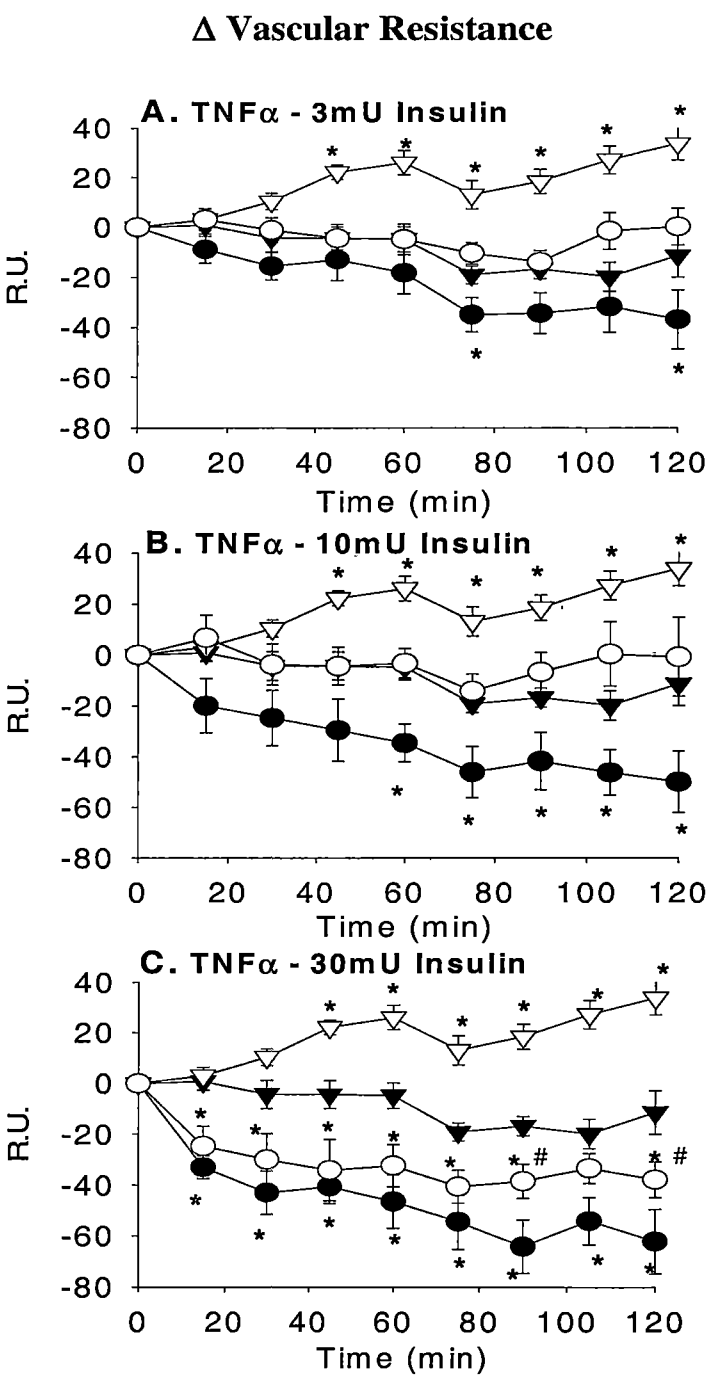

Fig 5.5 Change in vascular resistance for saline infusion (▼ in A, B and C, n=14), TNFα infusion (▽ in A, B, and C, n=5), insulin clamps at 3 doses without TNFα [●, 3mU (A, n=10), 10mU (B, n=6) and 30mU (C, n=7)] or with TNFα (○ in A, B and C, n=7 for each of these three groups). Values are means ± SE. * Significantly different (P<0.05) from saline infusion; #significantly different (P<0.05) from clamp group of insulin alone infusion.

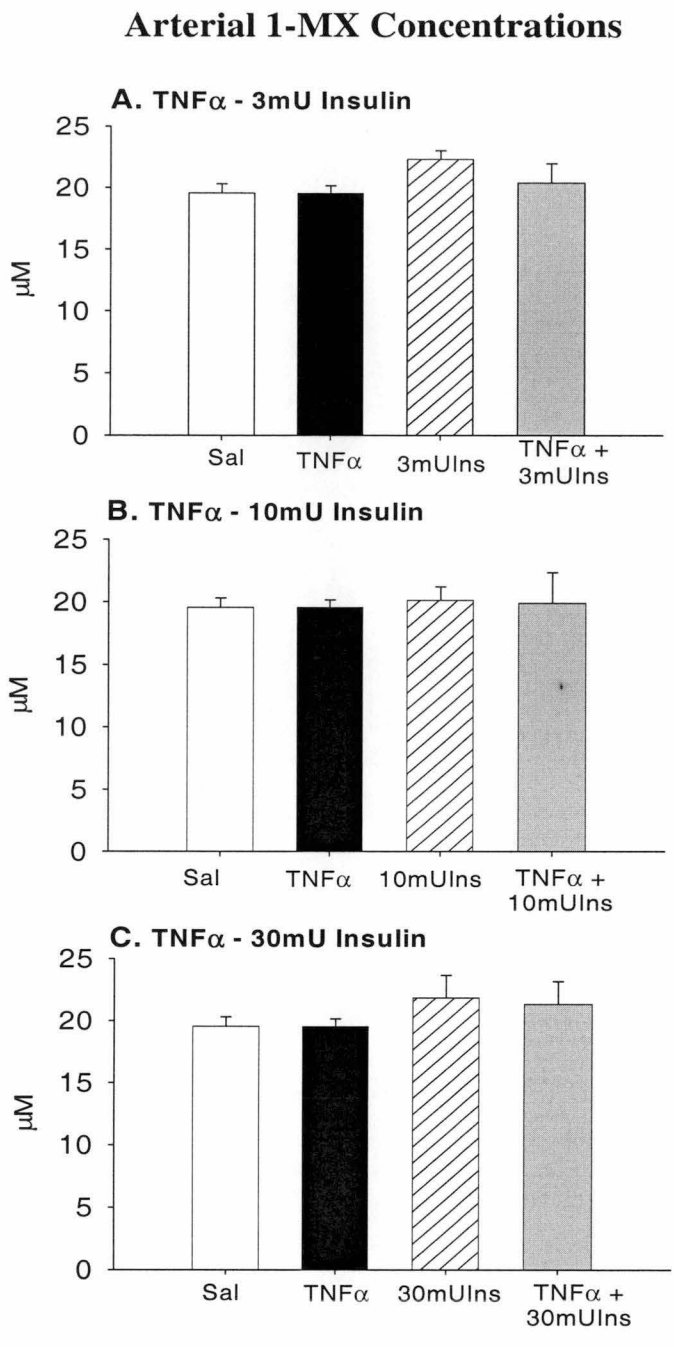

Fig 5.6 Arterial 1-MX concentrations for saline group (□ in A, B and C, n=14), TNFα group (■ in A, B and C, n=5), clamp groups of insulin alone infusion at 3 doses [▨, 3mU (A, n=10), 10mU (B, n=6) and 30mU (C, n=7)] or with TNFα (■, A, B and C, n=7 for all three groups)]. Data were collected at the 120min time point. Values are means ± SE.

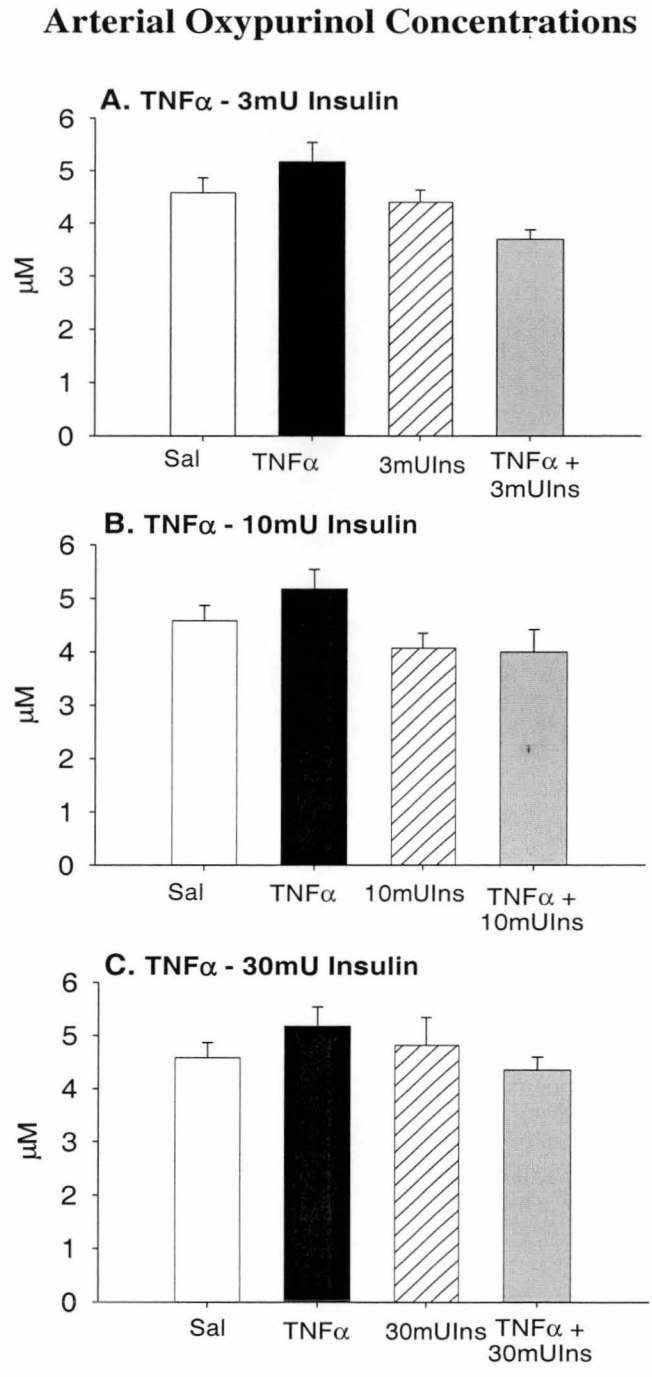

Fig 5.7 Arterial oxypurinol concentrations for saline group (□ in A, B and C, n=14), TNFα group (■ in A, B and C, n=5), clamp groups of insulin alone infusion at 3 doses [▨, 3mU (A, n=10), 10mU (B, n=6) and 30mU (C, n=7)] or with TNFα (■, A, B and C, n=7 for all three groups)]. Data were collected at the 120min time point. Values are means ± SE.

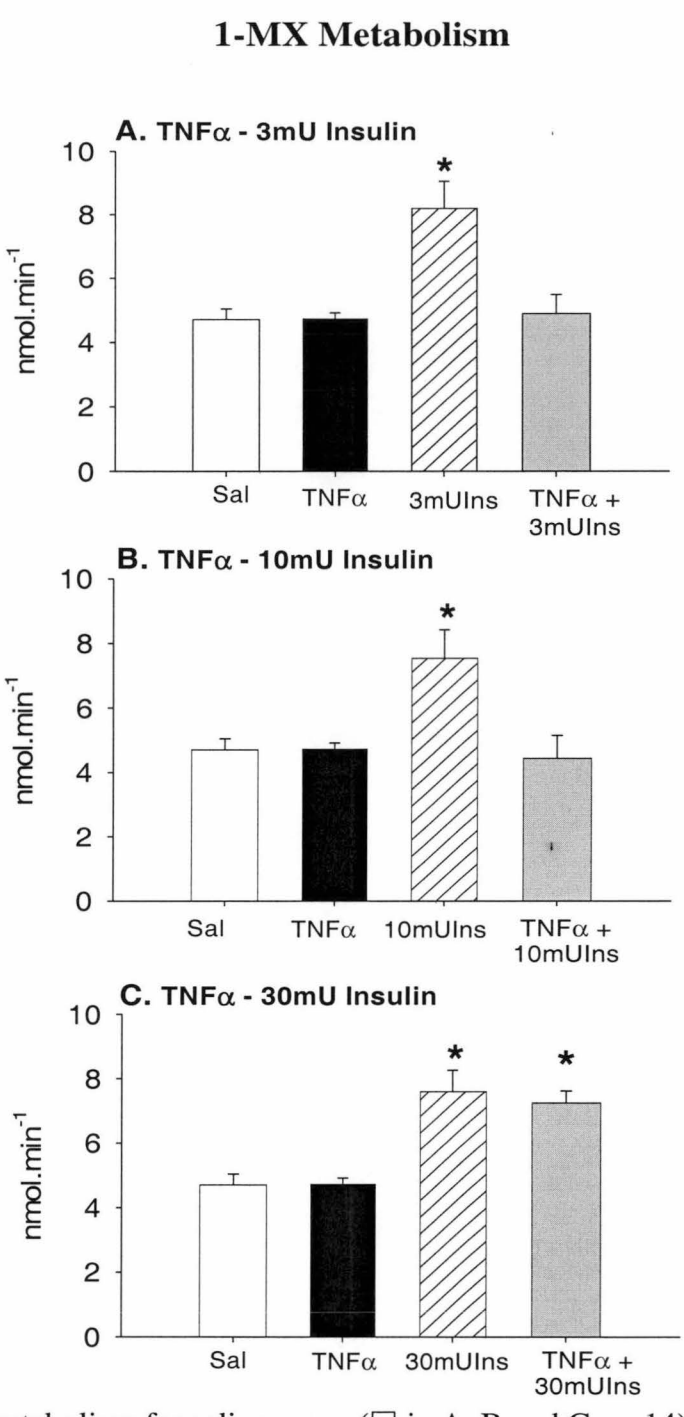

Fig 5.8 1-MX metabolism for saline group (□ in A, B and C, n=14), TNFα group (■ in A, B and C, n=5), clamp groups of insulin alone infusion at 3 doses [▨, 3mU (A, n=10), 10mU (B, n=6) and 30mU (C, n=7)] or with TNFα (■, A, B and C, n=7 for all three groups)]. Data were collected at the 120min time point. Values are means ± SE. *Significantly different ($P<0.05$) from saline infusion.

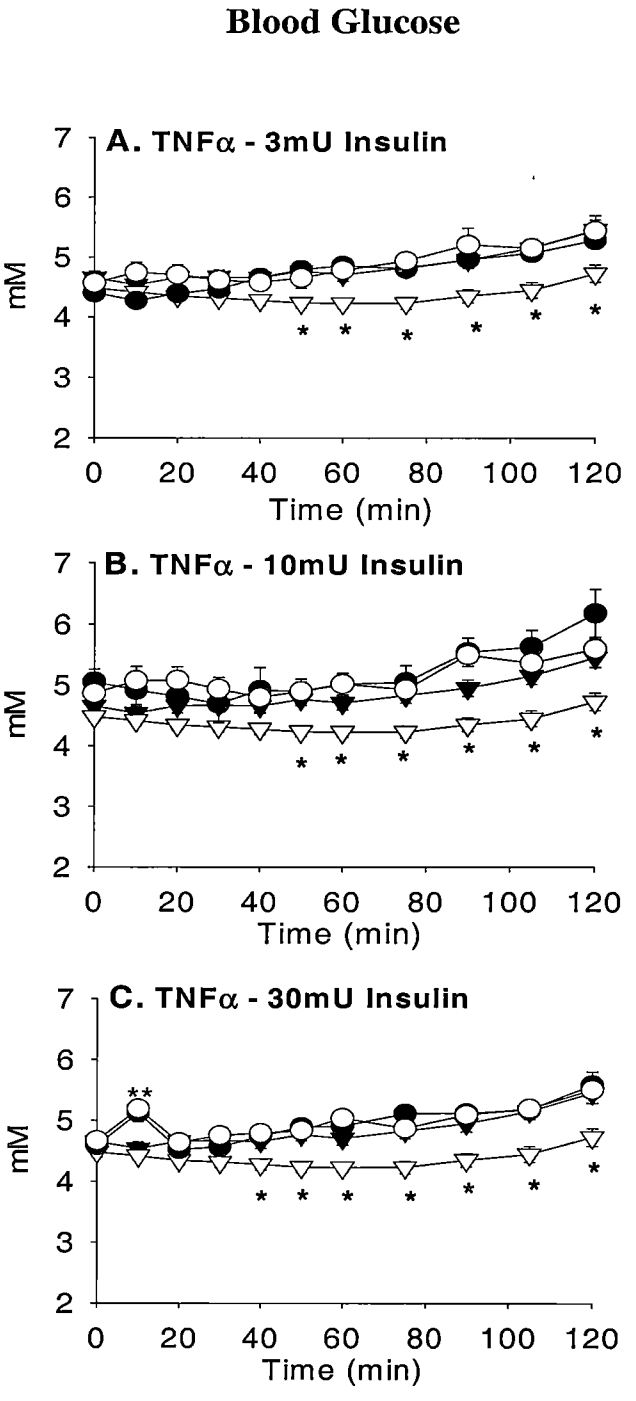

Fig 5.9 Blood glucose concentration for saline infusion (▼ in A, B and C, n=14), TNFα infusion (▽ in A, B, and C, n=5), insulin clamps at 3 doses without TNFα [●, 3mU (A, n=10), 10mU (B, n=6) and 30mU (C, n=7)] or with TNFα (○ in A, B and C, n=7 for each of these three groups). Values are means ± SE. * Significantly different ($P<0.05$) from saline infusion.

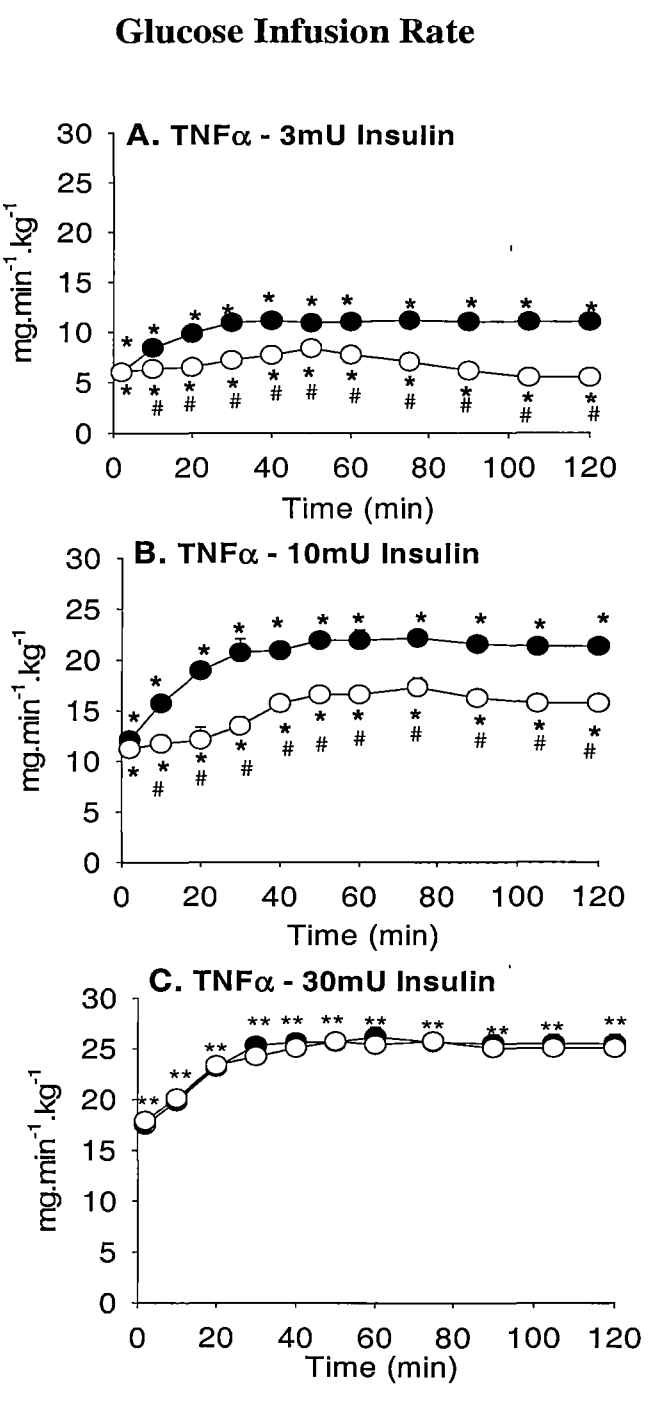

Fig 5.10 Glucose infusion rate for insulin clamps at 3 doses without TNFα [●, 3mU (A, n=10), 10mU (B, n=6) and 30mU (C, n=7)] or with TNFα (○ in A, B and C, n=7 for each of these three groups). Values are means ± SE. * Significantly different ($P<0.05$) from saline infusion; #significantly different ($P<0.05$) from clamp group of insulin alone infusion.

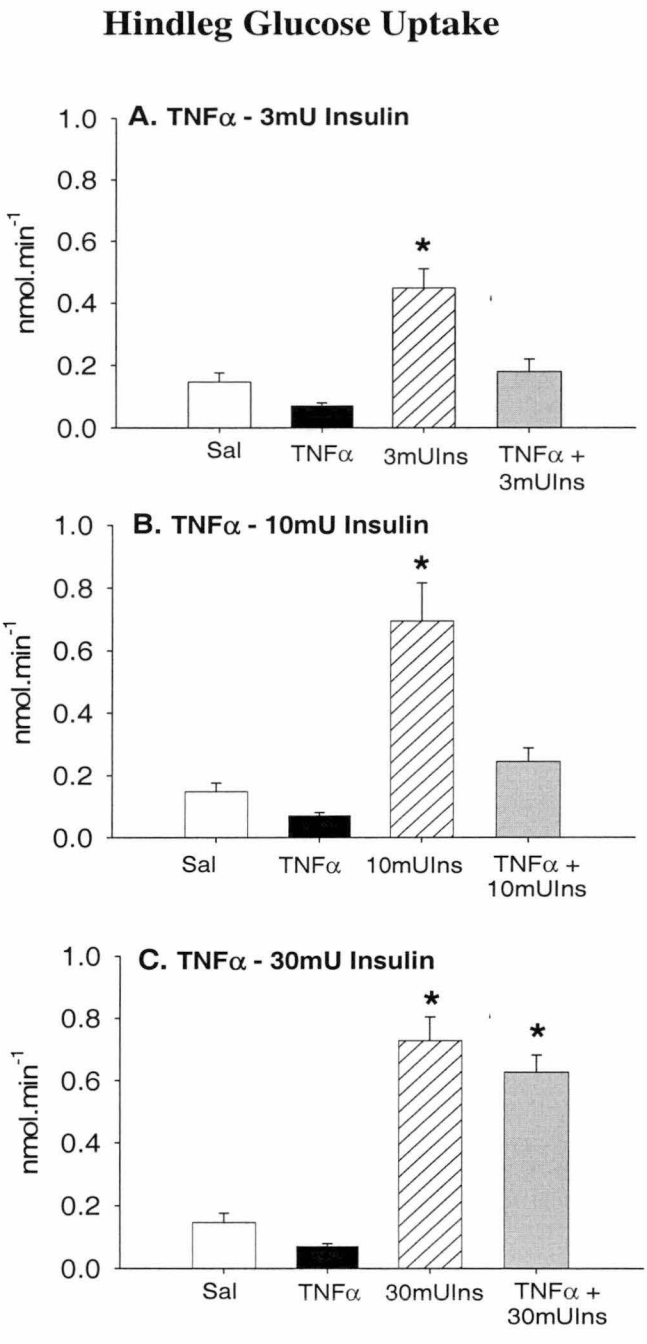

Fig 5.11 Hindleg glucose uptake for saline group (□ in A, B and C, n=14), TNFα group (■ in A, B and C, n=5), clamp groups of insulin alone infusion at 3 doses [▨, 3mU (A, n=10), 10mU (B, n=6) and 30mU (C, n=7)] or with TNFα (■, A, B and C, n=7 for all three groups)]. Data were collected at the 120min time point. Values are means ± SE. *Significantly different (P<0.05) from saline infusion.

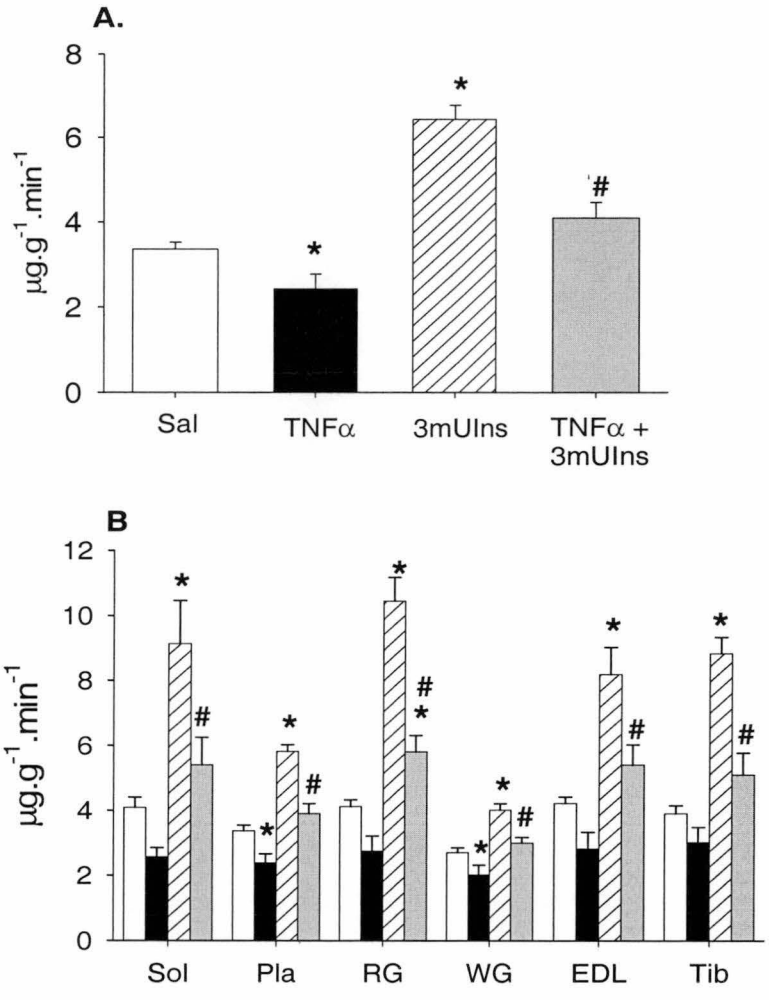

Fig 5.12 R'g of combined muscles (A) and individual muscles (B) for saline infusion (□, n=14), TNFα infusion (■, n=5), insulin clamp at 3mU without (▨, n=10) and with (▩, n=7) TNFα. Muscles were taken at the end of the experiment. Values are means ± SE. *Significantly different ($P<0.05$) from saline infusion; #significantly different ($P<0.05$) from insulin clamp at 3mU.

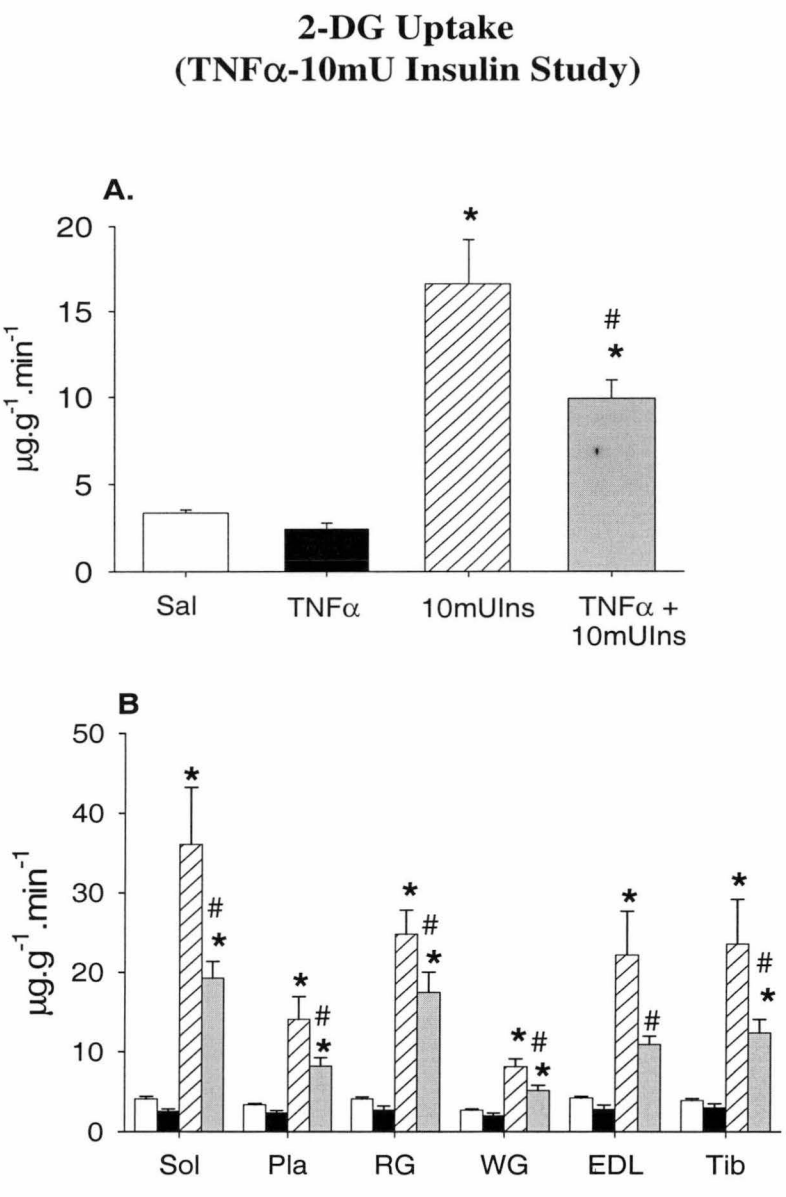

Fig 5.13 R'g of combined muscles (A) and individual muscles (B) for saline infusion (□, n=14), TNFα infusion (■, n=5), insulin clamp at 10mU without (▨, n=7) and with (■, n=6) TNFα. Muscles were taken at the end of the experiment. Values are means ± SE. *Significantly different ($P<0.05$) from saline infusion; #significantly different ($P<0.05$) from insulin clamp at 10mU.

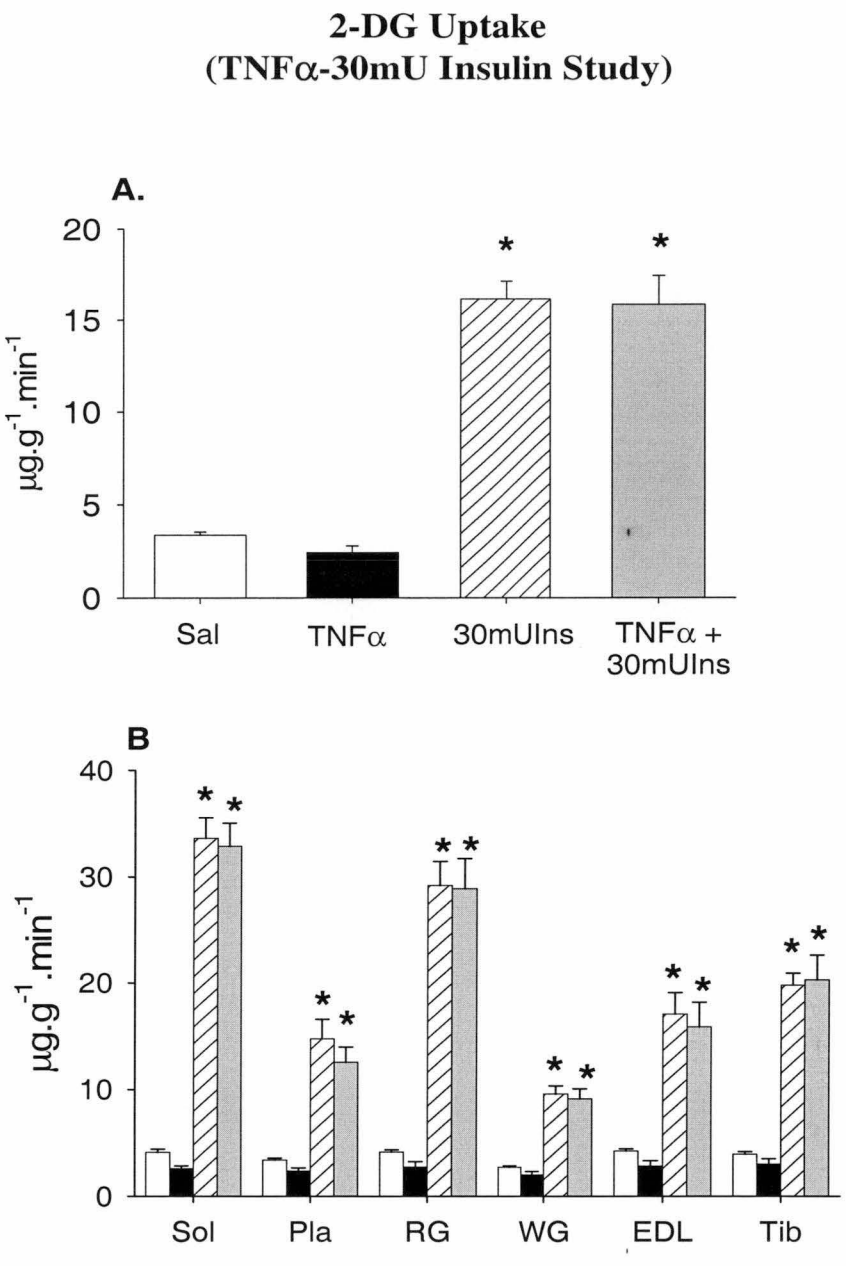

Fig 5.14 R'g of combined muscles (A) and individual muscles (B) for saline infusion (□, n=14), TNFα infusion (■, n=5), insulin clamp at 30mU without (▨, n=7) and with (■, n=7) TNFα. Muscles were taken at the end of the experiment. Values are means ± SE. *Significantly different ($P<0.05$) from saline infusion.

5.4 DISCUSSION

In agreement with other reports (177, 192, 350), TNFα administration *in vivo* is able to cause insulin resistance in experimental animals. In the present study, TNFα at a dose that yielded a final concentration of ~350pg.ml^{-1} after 3h infusion was used against physiological (3mU.min^{-1}.kg^{-1}), pharmacological (10mU.min^{-1}.kg^{-1}) and supra-physiological (30mU.min^{-1}.kg^{-1}) doses of insulin. Whereas most other studies (177, 192) mainly looked at the metabolic aspects, the current study also examined the effect of TNFα on insulin's hemodynamic actions. The results confirmed our previous report (350) that TNFα-induced insulin resistance was manifested on both metabolic and hemodynamic parameters. The novel finding in this study was that insulin at a supra-physiological dose was able to oppose TNFα-induced inhibition on insulin-stimulated glucose metabolism which was associated with fully restored insulin-mediated capillary recruitment. This parallel relationship between insulin-mediated glucose uptake and capillary recruitment supports the notion that insulin-mediated capillary recruitment has physiological relevance and may be a primary contributor to insulin's metabolic action by enhancing delivery of glucose, insulin itself and other nutrient.

When comparing the dose of TNFα with other studies (12, 100, 177, 192), a much lower dose was used in this study. TNFα at this low dose mildly stimulated whole body glucose utilization indicated by a small decrease in blood glucose and may have caused flow redistribution among organs indicated by the decreased total limb blood flow in association with constant mean arterial pressure. However, the magnitude of these changes were much smaller than those reported by others using high dose TNFα (12, 100, 177, 192). Furthermore, TNFα at high dose has been reported to stimulate skeletal muscle glucose uptake although the effect appeared to require longer exposure to this cytokine (12, 90, 177). In contrast, TNFα at low dose as used in this study showed a trend to decrease muscle glucose uptake. This may due to an indirect effects of TNFα such as limiting glucose availability by redirecting flow away from muscle (100) or slightly decreasing circulating insulin level rather than a direct metabolic action on myocytes. In addition, TNFα at this dose did not appear to affect basal skeletal muscle capillary recruitment as indicated by the unchanged 1-MX

metabolism in comparison with saline control. Taken together, TNFα at a dose that does not appear to exert direct metabolic control on skeletal muscle glucose uptake or affect basal capillary recruitment was used to investigate its interaction with 3 doses of insulin on both metabolic and hemodynamic parameters.

At the two lower insulin doses, TNFα inhibited both the metabolic and hemodynamic actions of insulin. Thus, TNFα completely blocked the hemodynamic responses of capillary recruitment and increased femoral blood flow due to physiological ($3mU.min^{-1}.kg^{-1}$) and pharmacological ($10mU.min^{-1}.kg^{-1}$) insulin. In addition, at $3mU.min^{-1}.kg^{-1}$, the whole body glucose infusion rate was inhibited 50% and the R'g of individual muscles 80-90%. At higher doses of insulin, the effects became less such that, at $10mU.min^{-1}.kg^{-1}$, TNFα blocked the whole body glucose infusion rate 25% and R'g of individual lower leg muscles 50%. In contrast to these *in vivo* results, in the incubated muscle preparation neither acute nor prolonged exposure of TNFα was able to elicit insulin resistance (109, 231). The major difference between *in vivo* and isolated muscle system is the functionally responsive vasculature that is intact in *in vivo* but absent in isolated muscle preparation. Therefore, the vasculature appears to be the major target for TNFα-induced insulin resistance *in vivo*. Thus, the TNFα–caused loss in insulin-mediated capillary recruitment and increase in total flow could be a primary contributor to impaired insulin's metabolic action in skeletal muscle due to this cytokine. Moreover, because it is unlikely that the hemodynamic responses account for more than 50% of the insulin-mediated glucose uptake by muscle *in vivo* (331), complete inhibition of hindleg glucose uptake suggests that insulin's action at the myocyte is likely to have also been affected by TNFα. At the highest dose insulin ($30mU.min^{-1}.kg^{-1}$), the inhibition of insulin-mediated capillary recruitment by TNFα was completely prevented and thus insulin-mediated capillary recruitment fully restored. Insulin-mediated increase in total blood flow was only partly restored. This recovery of insulin's hemodynamic parameters was associated with a fully restored glucose metabolic response of insulin. The closely correlated relationship between insulin's hemodynamic effect, particularly capillary recruitment and its metabolic effects gives support to the idea that insulin-mediated hemodynamic responses are of physiological relevance. There is on-going debate as to whether this association is causal and if it is, which one is the cause. The message emerging from this study is

that in TNFα-associated insulin resistance condition, the defects in insulin-mediated hemodynamic responses are primary. Although this can not be applied directly to the insulin sensitive situation, it favours the view that insulin-mediated hemodynamic effects of capillary recruitment and increase in total blood flow are not secondary to insulin's metabolic action.

There is evidence that the insulin-mediated hemodynamic responses of femoral blood flow and capillary recruitment were more vulnerable to the TNFα. Thus with the dose of insulin increasing from 3 to 10mU.min^{-1}.kg^{-1}, the hemodynamic responses remained completely inhibited whilst the metabolic responses partly recovered. Only at the highest dose of insulin used of 30mU.min^{-1}.kg^{-1} were some of the hemodynamic responses to insulin recovered. The mechanism for the dose-dependent ability of insulin to act against TNFα's action at the endothelium and other insulin-responsive tissues is not fully understood. Whereas a number of *in vitro* studies elucidated possible defects in insulin cellular signalling in response to TNFα (142, 165, 247, 311), it is unknown whether these defects are exerted via TNFα itself or via an intermediary that is released *in vivo* by the cytokine. Furthermore, the effects of TNFα against a serial dose curve of insulin have not been investigated. In one *in vivo* study where insulin at a dose capable of maximally stimulating glucose uptake did not completely oppose TNFα-induced inhibition on peripheral glucose uptake (177), the total amount of TNFα administrated into the rats was 20 fold higher than that infused in the present experiments. Thus, the results from these two studies may not be comparable. Nevertheless, in at least one system, there is evidence that TNFα and insulin oppose each other (126), suggesting, as does the present study, that insulin's action is most vulnerable to TNFα-mediated inhibition when insulin levels are low and least vulnerable when levels are high. Interestingly, insulin-like growth factor-1 (IGF-1), a peptide homologous to insulin, has been reported to normalize TNFα-mediated insulin resistance in experimental animals (193). In addition, other insulin resistance models such as sepsis (176) and chronic renal failure (198) animals, where TNFα levels are normally elevated (2, 235), glucose metabolic response to IGF-1 were preserved (176, 198). These studies suggest that the TNFα-induced defect in insulin signalling may not be a step in the IGF-1 pathway. Since insulin receptor and IGF-1 receptor share 60% amino acid identity (183, 322), it is possible that insulin at

a supra-physiological dose such as $30mU.min^{-1}.kg^{-1}$ may cross react with IGF receptor (182) and normalize TNFα-associated insulin resistance via eliciting IGF-1 signalling pathway. However, in these IGF-1-involved *in vivo* studies, hemodynamic measurements were not conducted. Since high dose insulin is able to oppose TNFα's inhibition at both the hemodynamic and metabolic sites as demonstrated in the present study, the possible involvement of IGF-1 signalling in this process can not be concluded without knowledge of the changes in hemodynamic parameters.

To summarise, the present findings suggest the insulin signalling at sites in the vasculature where capillary recruitment and total flow are controlled by insulin is particularly sensitive to inhibition by TNFα. Thus, the TNFα-induced defects in insulin-mediated hemodynamic responses may contribute to the impaired insulin-mediated metabolic action. The close association between insulin's hemodynamic and metabolic actions suggests insulin-mediated capillary recruitment and increase in total flow are of physiological significance and impairment by TNFα may contribute to insulin resistance of muscle when circulating levels of the cytokine are elevated.

CHAPTER 6
MICROVASCULAR FLOW ROUTES IN MUSCLE CONTROLLED BY VASOCONSTRICTORS

6.1 INTRODUCTION

The notion that skeletal muscle microvascular perfusion is not always directly related to the total blood flow of muscle can be traced to studies now over 30 years old (17, 115, 144, 242). Those studies showed a mismatch between total blood flow into muscle and either metabolic and heat transfer responses (242), or the clearance of intramuscular injected or infused radioactive substances (16, 17). These findings together with more recent work (170) are regarded as evidence for two separate circulatory systems within muscle, one of which acts as a shunt that minimizes the opportunity for nutrient exchange to occur between the muscle cells and the constituents of the blood, and the other of which promotes nutrient exchange. Operationally, in the pump-perfused hindlimb these two vascular routes are referred to as "non-nutritive" and "nutritive", respectively. Anatomically, vessels in the nutritive route are considered to be those that have extensive contact with the skeletal muscle cells (144). The "non-nutritive" route (17), that is considered to serve as a functional vascular shunt for muscle has been difficult to identify. There are a few reports showing that some of the vessels for this route are closely associated with connective tissue (17, 37, 115). Evidence from early study (144) and more recent estimate (130) suggests that at least half of the blood flow to muscle is carried by the so-called non-nutritive network in resting muscle under basal conditions.

Studies in this laboratory have focused on the regulation of these two vascular routes of skeletal muscle. Using the constant-flow pump-perfused rat hindlimb it has been shown that skeletal muscle metabolism including oxygen uptake and lactate release as well as aerobic contractile performance is controlled by vasoconstrictors that have been considered to act to alter flow distribution within muscle (51, 53). One group of vasoconstrictors, typified by angiotensin II or low-dose norepinephrine acts to increase oxygen uptake and lactate release (51) as well as contractile performance (51,

276) by redirecting flow from a putative non-nutritive route to nutritive capillaries within muscle (227). A second group of vasoconstrictors, typified by serotonin, has the opposite effect and although causing the same changes in perfusion pressure, acts to decrease oxygen uptake, lactate release and contractile activity (51, 81). These metabolic effects of vasoconstrictors in the perfused hindlimb appear to solely rely on their vascular actions rather than the direct actions on the skeletal muscle as in the incubated muscle preparation devoid of functional vasculature, vasoconstrictors had no effect upon either the contractility or insulin-mediated glucose uptake (81, 274, 275). Furthermore, diminishing nutritive capillary perfusion seems the key effect of thes vasoconstrictors. As total blood flow is constant in this preparation, these vasoconstrictors do not alter total flow to muscles but appear to redirect flow within the hindlimb muscle (227, 276), either away from the nutritive route to the non-nutritive route, or *vice a versa*. Indeed, when fluorescent microspheres (15μm) were introduced during steady state with or without low-dose norepinephrine (predominantly nutritive) or serotonin (predominantly non-nutritive) it was found, by recovery of the microspheres, that flow had not redistributed between muscles or between muscle and non-muscle tissue, even though norepinephrine had produced a marked increase, and serotonin had produced a marked inhibition of oxygen uptake in the same legs that had been analysed for microsphere distribution (52).

The hemodynamic actions of these vasoconstrictors to raise perfusion pressure is critical, thus the metabolic changes (oxygen uptake and lactate release) are blocked if vasodilators are added to block the vasoconstriction (51, 63, 136). Moreover, the access of nutrients and hormones to the muscle fibres appears to be controlled by the relative distribution of flow when total flow remains constant. For example, the action of insulin to increase glucose uptake in a constant flow pump-perfused muscle preparation is markedly influenced by the ratio of nutritive to non-nutritive flow (53) and acute insulin resistance results when a vasoconstrictor is present that induces predominantly non-nutritive flow (53, 275).

Thus, in this Chapter, I have attempted to further test the hypothesis that the differing effects of the vasoconstrictors on perfused muscle metabolism are a result of differing extents of nutritive and non-nutritive flow. I have approached the problem by

perfusing muscle with marker substances with flow maintained at steady state under basal, predominantly nutritive or non-nutritive conditions with an attempt to identify perfused vascular routes in muscle sections.

6.2 MATERIALS AND METHODS

6.2.1 Animal Care

Hooded Wistar rats weighing 180 – 200 grams were used for this study. Animals were raised as section 2.1.

6.2.2 Hindlimb Perfusion

Single hindlimb perfusions were performed at 32°C with a flow rate of 8ml.min^{-1}. The surgical and experimental procedures and perfusion medium were as described in section 2.3 except that hindlimbs were skinned in study 3 (section 6.2.5). The hindlimb was allowed to equilibrate for 40min before commencing the experiment. The experimental protocols are shown in Fig 6.1. At t=0, vehicle, 15nM angiotensin II (AII), or 1μM 5-hydroxytryptamine (serotonin, 5-HT) was infused and maintained throughout until the end of the experiment despite medium changes. Steady state of oxygen consumption and perfusion pressure was achieved within 20min after the commencement of treatment infusions.

6.2.3 Study 1 (GA-3min): Perfusion Fixation with Glutaraldehyde (GA) for 3min and Post-perfusion with *Griffonia Simplicifolia* Lectin 1 (GSL-1)

Prior to fixation, BSA was washed out of the hindlimb vascular bed by perfusing for 2 minutes with carbogen-gassed Krebs buffer containing 1.27mM Ca^{2+}. The intent was to remove the albumin as it prevented successful fixation of the tissue by GA. Perfusion fixation followed for 3min using 2.5% glutaraldehyde (Sigma, EM grade) in 0.1M phosphate buffer pH of 7.4. In preliminary experiments when GA was perfused at a constant rate of 8ml.min^{-1}, perfusion pressure rose followed by red blood cell (RBC) efflux. This is consistent with the report that perfusion fixation caused an

increase in vascular resistance and reduction in resistance vessel radius (128). During the constant flow perfusion, an increase in vascular resistance may force the flow into previously unperfused regions resulting in the washout of RBC in that area and a change in perfusion pattern. Therefore in the present study, the flow rate during GA perfusion was varied in each experiment to keep a constant pressure and prevent the RBC efflux. The final flow rate at the end of perfusion fixation was measured in some experiments. Vasoconstrictor infusion was stopped during GA perfusion since alterations in perfusion flow rate have the potential to alter the agent concentration reaching the hindlimb. Instead, the vasoconstrictor was added into the GA medium at the same concentration as used above in the BSA perfusion. Muscle tissue preparation and vasculature identification by GSL-1 binding were followed as described in Section 6.2.6.

6.2.4 Study 2 (GA-40ml): Perfusion Fixation with 40ml GA and Post-perfusion GSL-1

The procedure to remove BSA from hindlimb vascular bed prior to fixation was the same as Study 1. As in Section 6.2.3 above, the vasoconstrictor infusion was stopped and followed by perfusion fixation using 2.5% GA (in 0.1M phosphate buffer, pH=7.4) containing the same concentration of the vasoconstrictor as used in the BSA perfusion. A total of 40ml of GA medium was pumped through the hindlimb while maintaining the pressure constant at the value attained during the initial 20min BSA perfusion by varying perfusion flow rate. The duration of GA fixation was recorded. Hindleg muscle tissue was prepared and the vasculature was identified by GSL-1 binding as detailed in Section 6.2.6.

6.2.5 Study 3 (Rhod-dex): Perfusion with Rhodamine-dextran70 (lysine fixable) and Post-perfusion Fixation with Formaldehyde

During the steady state achieved after perturbations, Rhodamine-dextran70 (Lysine fixable, Molecular Probe) at a final concentration of 50$\mu g.ml^{-1}$ was infused for the final 4.5min to mark the perfused vasculature. Preliminary experiments showed that the fluorescent intensity in venous flow reached a plateau within 4.5min following the

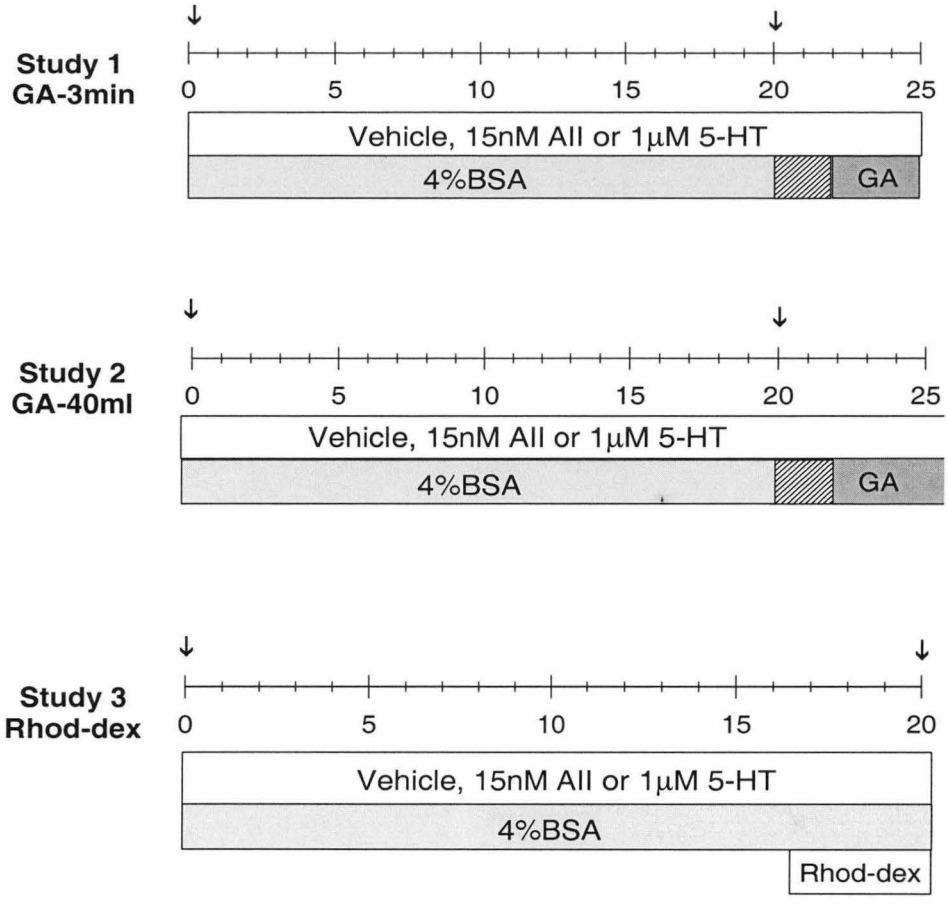

Figure 6.1 Experimental protocols. Treatment of AII (15nM), 5-HT (1μM) or vehicle is indicated by open bars. BSA (4%) perfusion is indicated by □. Carbogen-gassed Krebs buffer perfusion to flush out albumin is indicated by ▨. Glutaraldehyde (GA, 2.5% in 0.1M phosphate buffer, pH=7.4) perfusion is indicated by ■. Samples taken for perfusion pressure and oxygen consumption analysis (Fig 6.2) are indicated by ↓. In Study 1, GA was perfused for 3min (n=6, 6, 7 for vehicle, AII and 5-HT group respectively) at slightly varied rates to keep a constant perfusion pressure. In Study 2, 40ml of GA was perfused through the hindlimb and the duration of GA perfusion varied among experiments due to variable flow rate to maintain a constant perfusion pressure (n=4 for all groups). In Study 3, rhodamine-dextran70 was infused for 4.5min in addition to the treatment infusions (n=3 for all groups). All experiments were conducted using the single hindlimb perfusion at 32°C and the flow rate was 8ml.min^{-1} during BSA perfusion.

commencement of fluorescent dextran infusion, indicating the dextran had reached equilibrium within the hindlimb vascular bed. For these perfusions the apparatus was modified slightly so as to incorporate two 3-way taps immediately before and after the hindlimb so that at the end of the perfusion (20min) they could be closed to contain the rhodamine-dextran70 within the hindlimb vasculature during the fixation period. Thus, at the end of the perfusion the taps were closed, the pump stopped and the rat was bisected above the ligature placed around the torso at the level of the L3-L4 vertebrae and the lower part of the torso was immersed in neutral buffered formaldehyde for 7 days to fix rhodamine-dextran in the vasculature.

6.2.6 Muscle Perfusion Examination

Due to its similarity in muscle fiber composition to the whole hindlimb (10), only the EDL muscle was analysed. Accordingly, the EDL was excised from the perfused hindlimb and prepared for the subsequent examination as described in section 2.4. Briefly, the EDL muscle was cut into four blocks and snap-frozen in isopentane cooled by liquid nitrogen. *Griffonia (Bandeiraea) Simplicifolia* lectin-1 (GSL-1) was used in Study 1 and 2 to identify vasculature and muscle fibres in 7μm frozen sections. The GSL-1 binding was detected by a goat anti-GSL-1 primary antibody which was in turn was detected by a biotinylated secondary antibody and peroxidase binding using a (goat) Vectastain® ABC kit. Typical GSL-1 binding results from frozen sections of fresh muscle tissue are represented by region **a** in Fig 6.6 **A** where both blood vessels and muscle fibers were clearly identified. In addition, blood vessels were stained much heavier than muscle fibres, suggesting a stronger binding affinity of GSL-1 to the vascular endothelial cells. When GA is introduced during perfusion, perfused vessels will be fixed open and surrounding tissues will also be fixed by GA that diffuses out of the vasculature. Tissue fixation by GA destroys GSL-1-binding sites, resulting in a 'blanched' appearance with little or no GSL-1 staining. Thus, the wide-open blood vessels and essentially invisible muscle fibres in region **b** of Fig 6.6 **A** are typical of the results from GA perfusion fixation. As GA follows the vascular routes accessed during BSA perfusion, a well-perfused area would be well fixed by GA like region **b** of Fig 6.6 **A**. It follows that the under-perfused regions deny access for GA, and thus are free of fixation effects as shown by region **a** of Fig 6.6 **A**. The

total section area and unperfused area were measured using Image-Pro-Plus software and the fraction of unperfused tissue was calculated. An average of 10 and 15 sections were analysed for each experiment for study 1 and 2 respectively. For Study 3, 7μm frozen sections were mounted in aqueous mounting medium and subjected to fluorescence microscopic examination. Approximately 2-4 micrographs (400X) were captured to cover each area having fluorescent capillaries within each section. The number of fluorescent capillaries was counted and expressed as perfused capillaries per section. An average of 8 sections was analysed for each experiment. The exposure times were adjusted to optimize the image intensity from the fluorescent Rhodamine-dextran containing vessels.

To analyse results generated from the section examination, a mean value was calculated from a number of sections for each experiment and the coefficient of variance was also determined to indicate the variation among sections. The mean values from each experiment were used to compute the mean and SE for each treatment group.

6.2.7 Statistical Analysis

Statistical difference between groups was assessed by one-way measure analysis of variance (ANOVA). When a significant difference ($P<0.05$) was found, the Student-Newman-Keuls test was used to determine which two groups had the significant difference. Paired *t*-test was used to assess whether a treatment has a significant effect on the same experimental animals. These tests were performed using the SigmaStat statistical program (Jandel Software). All data are presented as means ± SE with significant difference recognized at $P<0.05$ level.

6.3 RESULTS

6.3.1 Perfusion Pressure and Hindlimb Oxygen Consumption (VO_2) Measurements

In this series of experiments, the mean perfusate arterial oxygen levels were 673.56 ± 7.25, 666.76 ± 7.62 and 676.31 ± 9.17 mmHg for vehicle (n=13), AII (n=13) and 5-

HT (n=14) groups, respectively (NS among groups). The basal venous PO_2 values for the rat hindlimb obtained at 0 time point after the initial 40min equilibration period were 326.16 ± 12.31, 333.66 ± 6.59, 317.86 ± 5.9mmHg for vehicle, AII and 5-HT groups, respectively (NS among groups). Consequently, the basal VO_2 by the hindlimb calculated as previously described (section 2.3.4) was similar among the three groups (Fig 6.2B). Furthermore, all treatment groups had similar basal perfusion pressure (Fig 6.2A). Vehicle infusion had no effect on either VO_2 or perfusion pressure (Fig 6.2). AII at 15nM and 5-HT at 1μM each caused vasoconstriction, giving rise to a steady-state perfusion pressure significantly higher than their corresponding basal values (Fig 6.2). In contrast, these two vasoconstrictors had opposite effects on VO_2 as the steady-state VO_2 was 35% higher in AII group and 45% lower in 5-HT group than their corresponding basal values (Fig6.2). It is relevant to note that the infusion of Rhodamin-dextran70 in Study 3 had no effect on VO_2 or perfusion pressure (data not shown) and thus the steady-state measurements of these two parameters were obtained at the end of Rhodamine-dextran70 infusion as indicated in Fig 6.1 and included in the data shown (Fig 6.2).

6.3.2 GA Perfusion Fixation Measurements

In study 1, the change in perfusion pressure seen between the value before the commencement of GA fixation and during GA perfusion was not significantly different among the treatment groups, although there was a trend of increase in pressure in the 5-HT group (Fig 6.3). This indicates that the perfusion pressure was successfully controlled during GA fixation by varying perfusion flow rate. The final flow rates for vehicle and 5-HT groups were similar but significantly lower than that of the AII group (Table 6.1). It is relevant to note that during equilibration of the pump-perfused hindlimb there is extensive washout of RBC. Once the hindlimb has equilibrated there is almost no further appearance of cells in the venous effluent. If they do appear, it is usually indicative of flow extending into previously poorly, or unperfused, nutritive regions (227) and this is invariably associated with a pressure rise. In this set of experiments, there was essentially no RBC washout during the 3min of GA perfusion as the perfusion pressure was deliberately kept constantly.

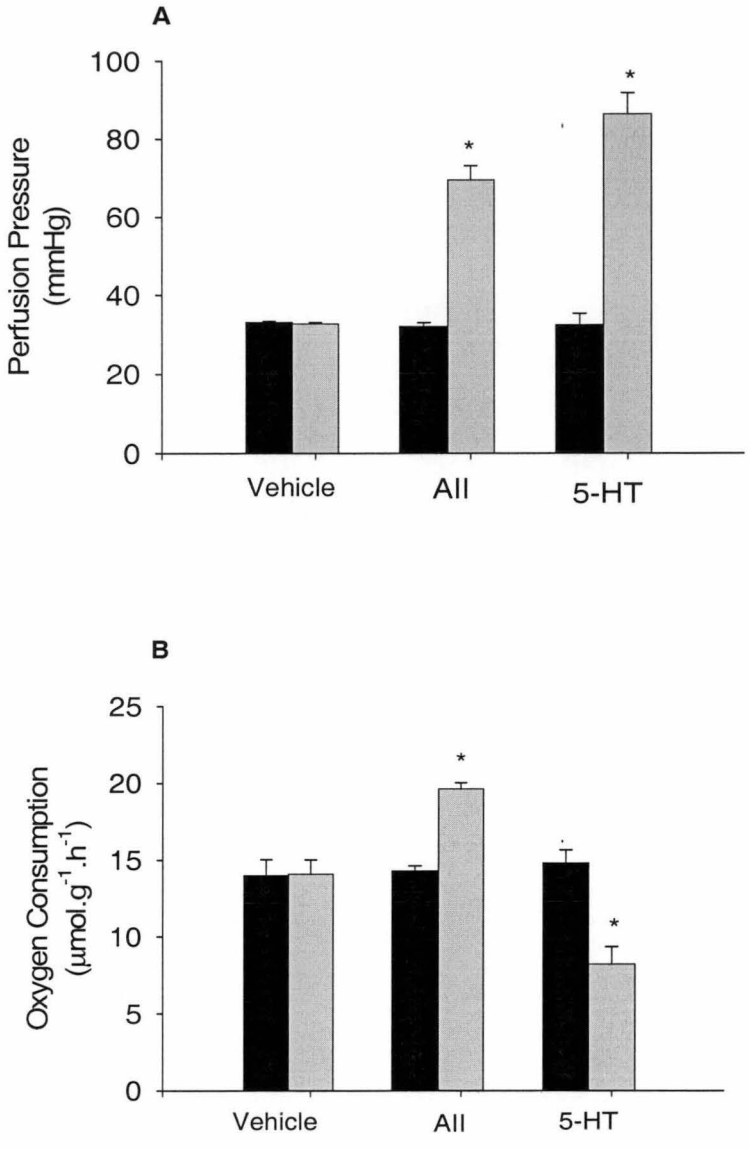

Fig 6.2 Perfusion pressure (A) and oxygen consumption (B) for vehicle group (n=13), AII group (n=13) and 5-HT group (n=14) at basal condition (■) and post-treatment steady state (□). Samples were taken at time points indicated by ↓ in Fig 6.1. For each treatment, values from 3 studies obtained at the same time point were combined together. Values are means ± SE. *Significantly (P<0.05) different from the basal value.

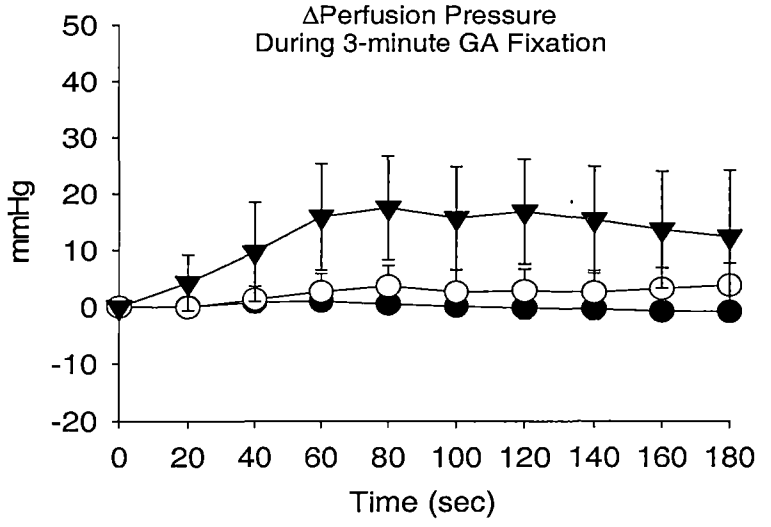

Fig 6.3 Change in perfusion pressure during the 3min GA perfusion in Study 1 in comparison to the value before the commencement of GA fixation for vehicle group (●, n=6), AII group (○, n=6) and 5-HT group (▼, n=7). Values are means ± SE.

Table 6.1 Perfusion flow rate at the end of the 3min GA perfusion. Experimental details are as for Study 1 of Fig 6.1.

	Vehicle (n=2)	AII (n=2)	5-HT (n=3)
GA perfusion final flow rate ($ml.min^{-1}$)	6.9 ± 0.1	7.75 ± 0.05 *	7.03 ± 0.15

Values are means ± SE. *Significantly different (P<0.05) from vehicle group.

Table 6.2 Effects of AII and 5-HT on steady state perfusion pressure in the constant-flow pump-perfused rat hindlimb and resultant pressure following perfusion with a fixed volume (40ml) of GA-containing medium. Experimental details are as for Study 2 of Fig 6.1.

	Vehicle (n=4)	AII (n=4)	5-HT (n=4)
Steady-state perfusion pressure (mmHg)	32.69 ± 0.34	69.48 ± 3.62*	86.42 ± 5.39*
Perfusion pressure after GA fixation (mmHg)	30.28 ± 0.24	66.27 ± 2.85*	113.1 ± 33.27*
Duration of GA fixation (min)	6.42 ± 0.21	5.82 ± 0.05	10.22 ± 1.43*

Values are means ± SE. *Significantly different (P<0.05) from vehicle group.

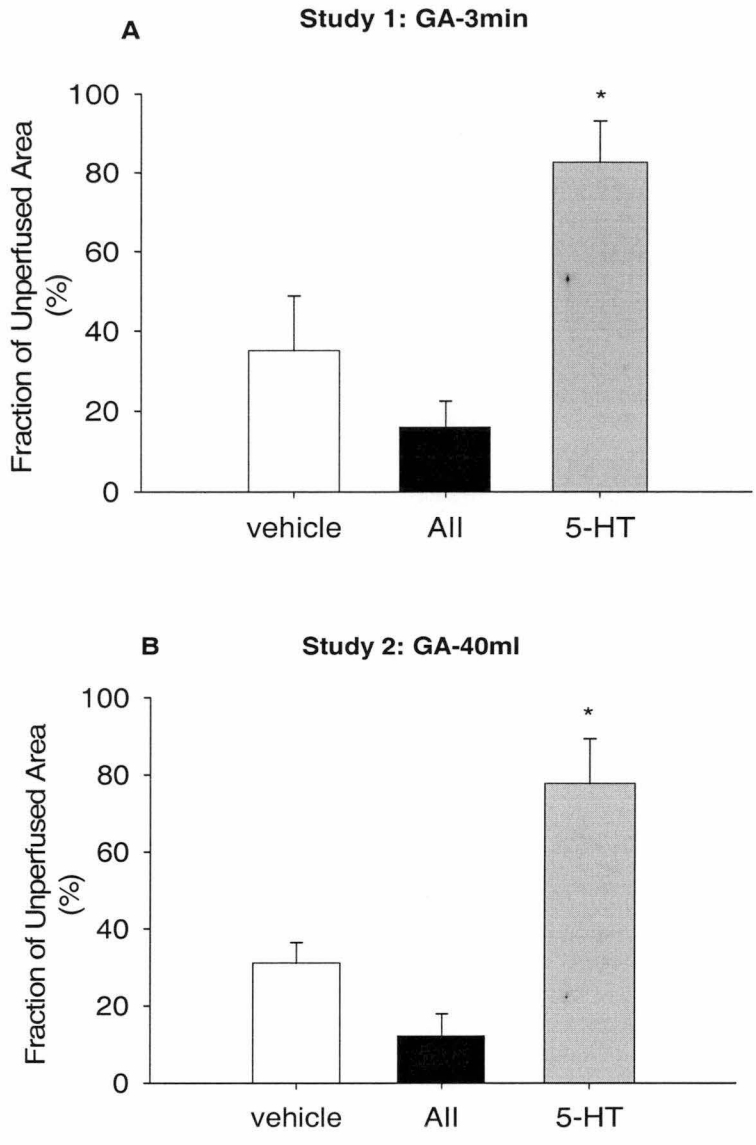

Fig 6.4 Fraction of unperfused area measured from sections of Study 1 (A) and Study 2 (B) for vehicle group (□, n=6 in A, n=4 in B), AII group (■, n=5 in A, n=4 in B) and 5-HT group (▨, n=7 in A, n=4 in B). An unperfused area is defined as a region having closed capillaries surrounded by muscle fibers darkly stained from GSL-1 binding. Total section area and unperfused area were measured using Image-Pro-Plus software. The ratio of unperfused to total area was calculated and presented as means ± SE. An average of 10 and 15 sections were analysed for each experiment in Study 1 and Study 2 respectively. *Significantly different ($P<0.05$) from vehicle group.

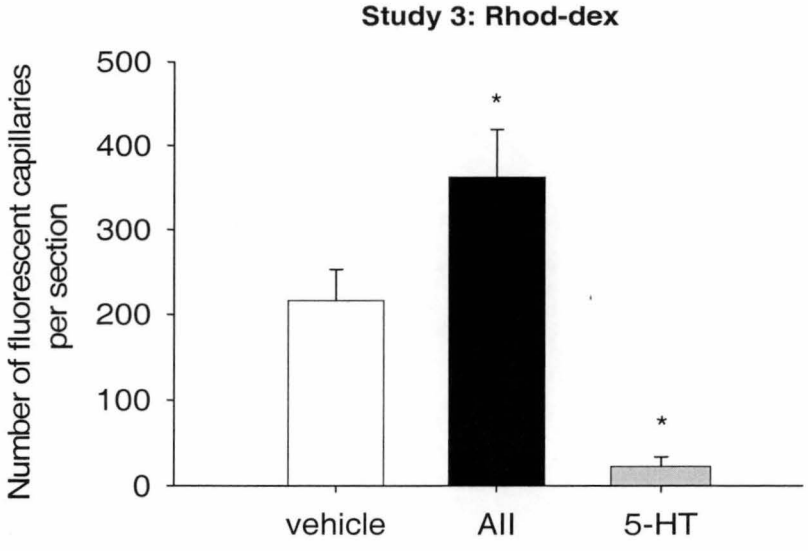

Fig 6.5 Number of fluorescent capillaries per section for vehicle group (□), AII group (■) and 5-HT group (▨). N=3 for all groups. Rhodamine-dextran70 was infused during experiments and fixed in vascular bed to mark perfused vessels. Capillaries visible under fluorescent microscope were counted for each section. An average of 6 sections were analysed for each experiment. Values are means ± SE. *Significantly different ($P<0.05$) from vehicle group.

In Study 2, the perfusion pressure after the 40ml GA perfusion was not significantly different from that seen during the steady state due to the treatment for all groups (Table 6.2). In these experiments some washout of RBC was observed after 3-5min GA perfusion in the vehicle and 5-HT groups but this was reduced when the perfusion flow rate was reduced to maintain constant pressure consistent with the steady state pre-GA value. For the AII group, 3 out of 4 experiments showed no RBC washout and one showed a slight washout only in the last 30s of GA perfusion. Since the flow rate was varied to keep a relatively constant perfusion pressure and minimize the RBC appearance in venous flow, the duration required to perfuse 40ml GA through the hindlimb was different for each experiment. The mean duration for the 5-HT group was significantly higher than either the vehicle or AII groups (Table 6.2).

6.3.3 Tissue Perfusion Measurements

Fig 6.6, 6.7 and 6.8 show the representative images of sections for vehicle, AII and 5-HT groups respectively in Study 1 where all hindlimbs were exposed to GA for the same time. The perfused and unperfused regions were in close proximity and normally well defined in either the vehicle or AII groups. In some sections, the boundary between perfused and unperfused region was less distinct and this region may not be perfused by itself but benefit from the adjacent perfused region, thus regarded as an unperfused area during image analysis. The fraction of unperfused area was less in the AII group (16.0 ± 7%) than the vehicle group (35.1 ± 14%), although this difference was not statistically significant (Fig 6.4A). The mean value for each group was calculated from the means of individual experiments within that group and the coefficient of variance ranged from 2.72% to 68.87% and from 21.66% to 115.45% for the vehicle and AII group, respectively. As shown in Fig 6.8, the 5-HT group showed a distinct perfusion pattern as most of the regions were unperfused and the connective tissues surrounding bigger vessels appeared to be the areas receiving perfusion. The fraction of unperfused tissue (82.6 ± 10.5%) was significantly higher than either the vehicle or AII group and the coefficient of variance ranged from 0 to 30.313%.

In study 2 where all hindlimbs received the same amount of GA, the image results (Fig 6.9) were similar to Study 1. When the proportion of unperfused / total tissue

perfused was determined, the 5-HT group (77.8 ± 11.5%) had a significantly higher unperfused tissue ratio than either the vehicle (31.1 ± 5.4%) or AII group (12.2 ± 5.7%) (Fig 6.4 B). The AII group had fewer regions that were unperfused than the vehicle group, although this difference did not reach statistical significance. The coefficient of variance ranged from 36.95 to 54.67%, 33.65 to 300% and 1.52 to 51.20% for vehicle, AII and 5-HT, respectively.

In Study 3, perfusate containing the fluorescent Rhodamine-dextran70 was fixed *in situ* at steady state with vehicle, AII or 5-HT as background. Thus vessels receiving flow during perfusion are fluorescent in the sections. The representative section images for the vehicle, AII and 5-HT groups are shown in Fig 6.10, 6.11 and 6.12 respectively. For vehicle and AII group, there were bundles of fluorescent capillaries and possibly arterioles and venules unevenly distributed across the sections. However, these bundles in the AII group sections were located closer to each other and thus the sections appeared more homogenous than the vehicle group. Furthermore, the fluorescence was generally stronger in the AII group section and can be clearly viewed under lower magnification (200X, Fig 6.11 **A**). 5-HT sections overall were less fluorescent and with far fewer regions containing fluorescent capillaries. Some 5-HT sections had a cloudy appearance presumably resulting from the mild oedema due to 5-HT-induced vasoconstriction. There was also some evidence of fluorescent material in vessels larger than capillaries (Fig 6.12 **A**). The average number of perfused capillaries per section was highest in the AII group and lowest in the 5-HT group and both were significantly different from the value of the vehicle group (Fig 6.5). The coefficient of variance ranged from 19.98 to 35.51%, 9.6 to 56.38% and 65.21 to 173.21 % for the vehicle, AII and 5-HT groups, respectively.

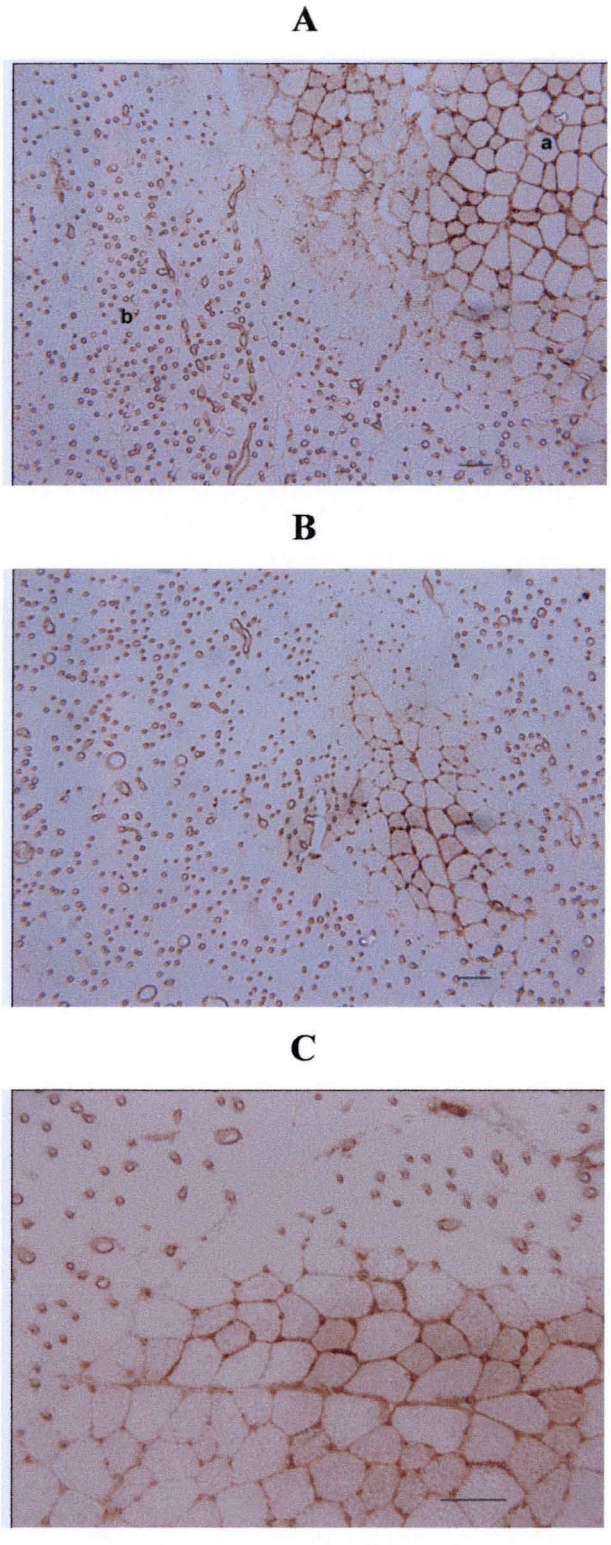

Fig 6.6 Representative transverse frozen sections of EDL muscle obtained from Study 1 vehicle group. Capillaries, endothelial cells and edges of muscle fibers were identified by immunostaining of bound *Griffonia (Bandeirae) Simplicifolia* lectin. In micrograph **A**, region **a** represents the "unperfused region"; region **b** represents the "perfused region". Scale bar=50μm

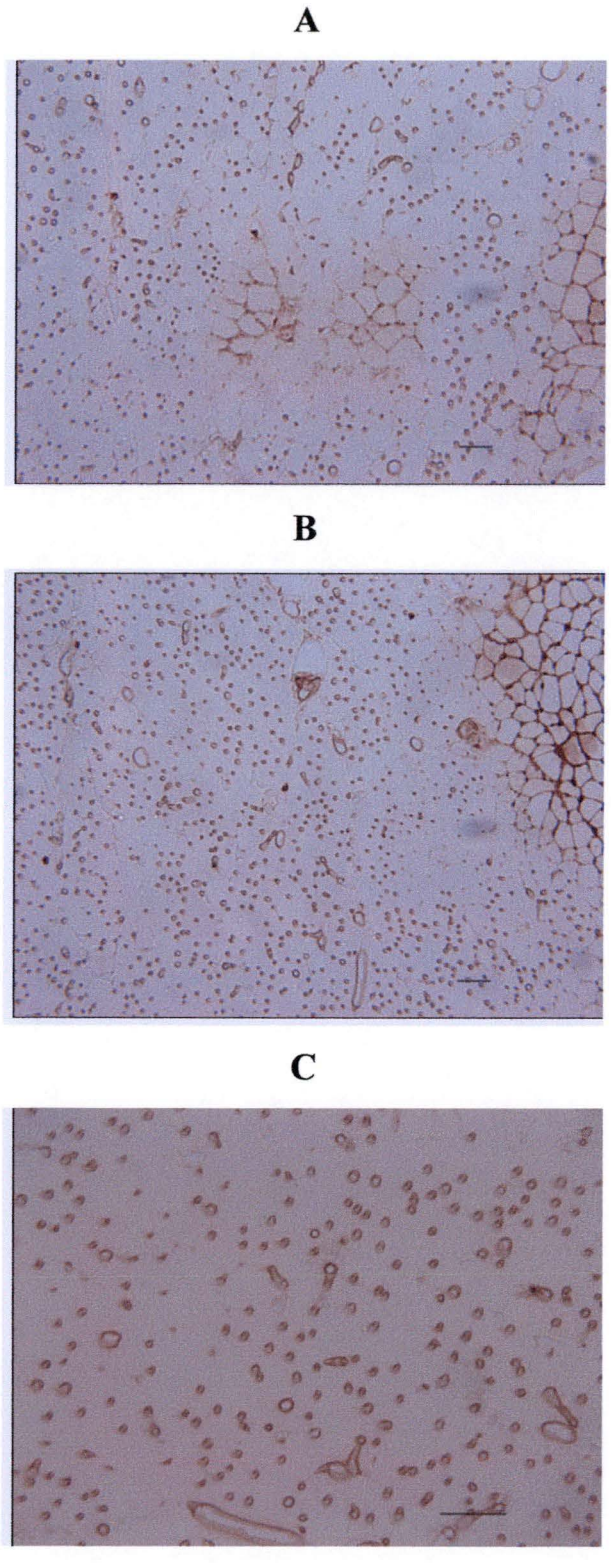

Fig 6.7 Representative transverse frozen sections of EDL muscle obtained from Study 1, AII group. Capillaries, endothelial cells and edges of muscle fibers were identified by immunostaining of bound *Griffonia (Bandeirae) Simplicifolia* lectin. Scale bar=50μm.

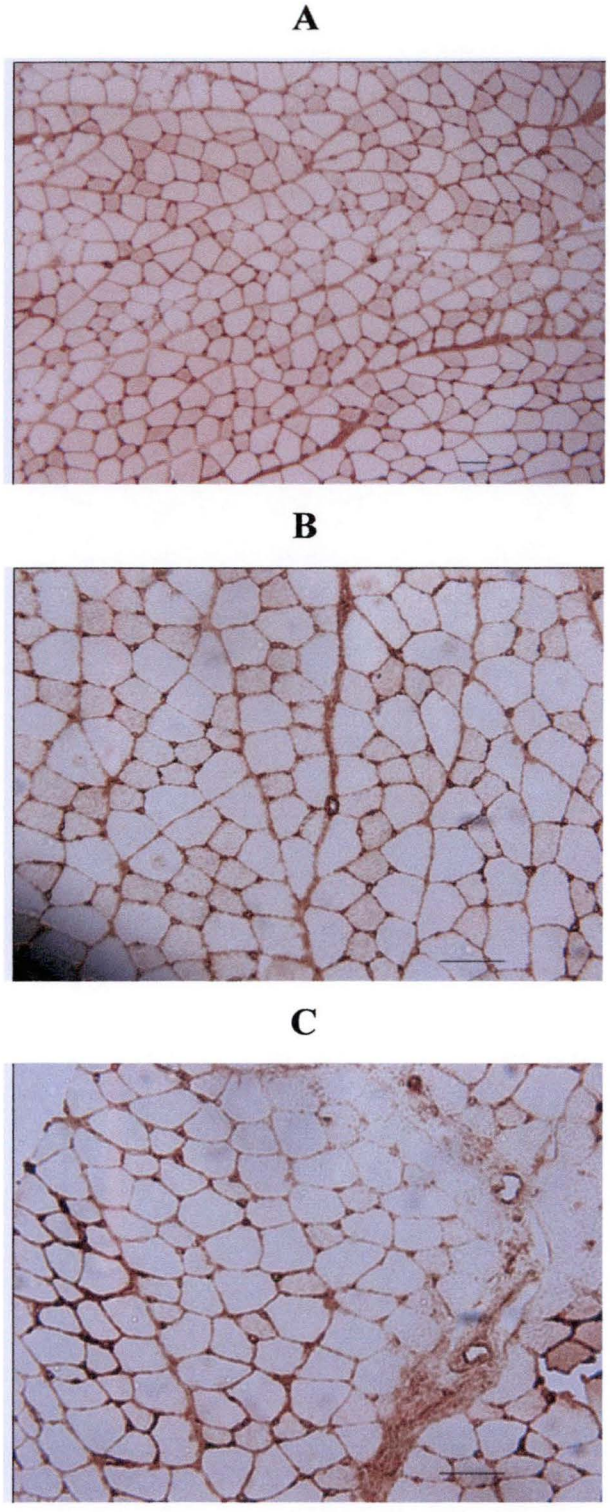

Fig 6.8 Representative transverse frozen sections of EDL muscle obtained from Study 1, 5-HT group. Capillaries, endothelial cells and edges of muscle fibers were identified by immunostaining of bound *Griffonia (Bandeirae) Simplicifolia* lectin. Scale bar=50μm.

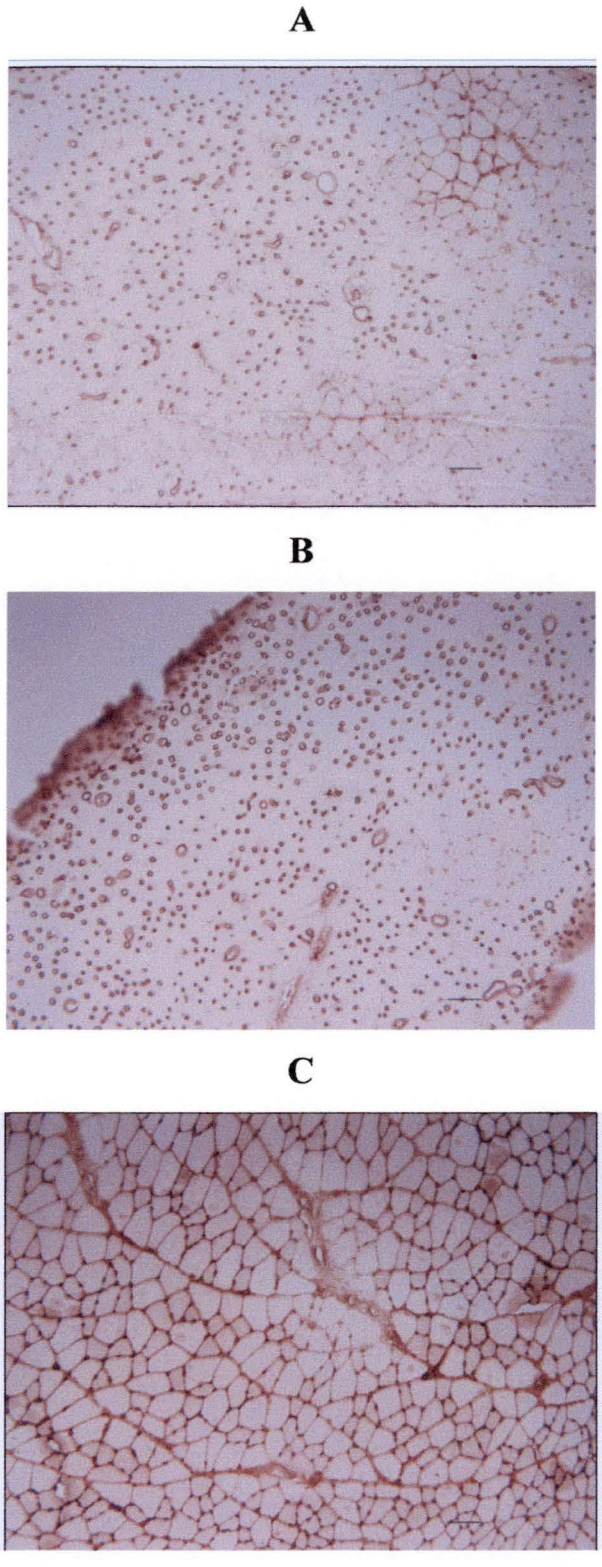

Fig 6.9 Representative transverse frozen sections of EDL muscle obtained from Study 2 of the vehicle (**A**), AII (**B**) and 5-HT (**C**) groups. Capillaries, endothelial cells and edges of muscle fibers were identified by immunostaining of bound *Griffonia (Bandeirae) Simplicifolia* lectin. Scale bar=50μm

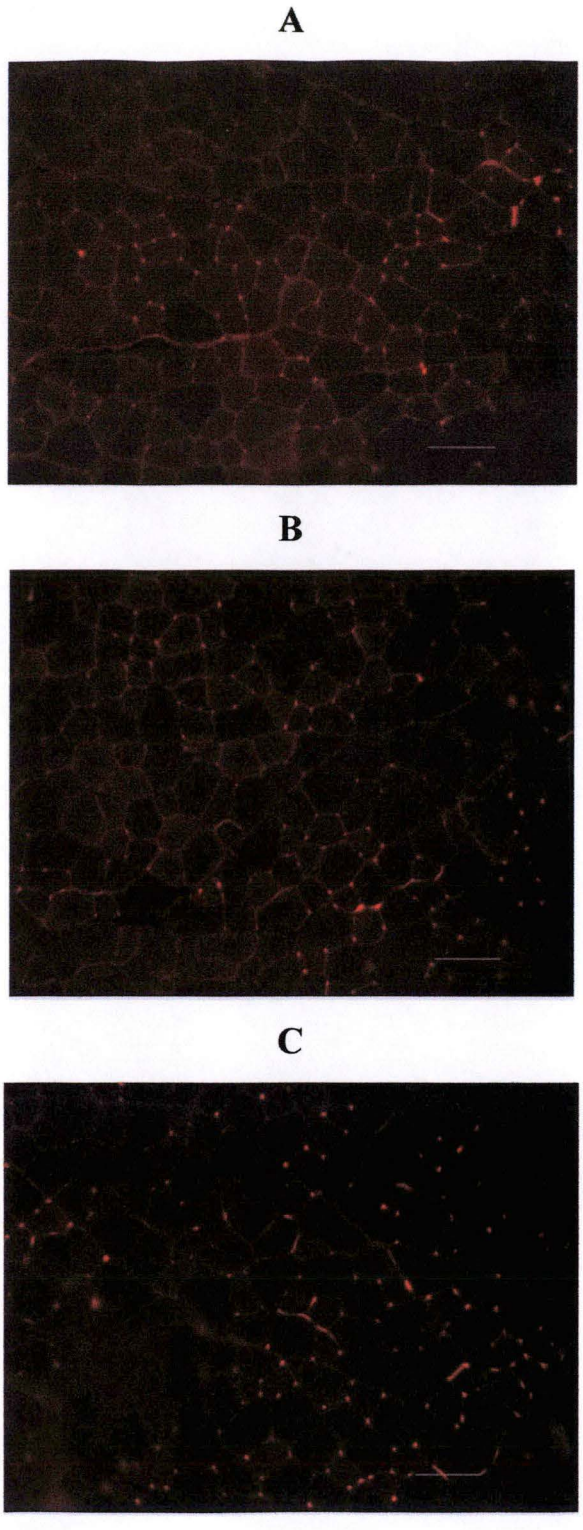

Fig 6.10 Representative transverse frozen sections of EDL muscle obtained from Study 3, vehicle group. Vessels having fluorescence (Rhodamine-dextran70) represent those that were perfused during hindlimb perfusion. Exposure time is 1/4, 1/3 and 1/4 sec for **A**, **B** and **C** respectively. Scale bar=50μm.

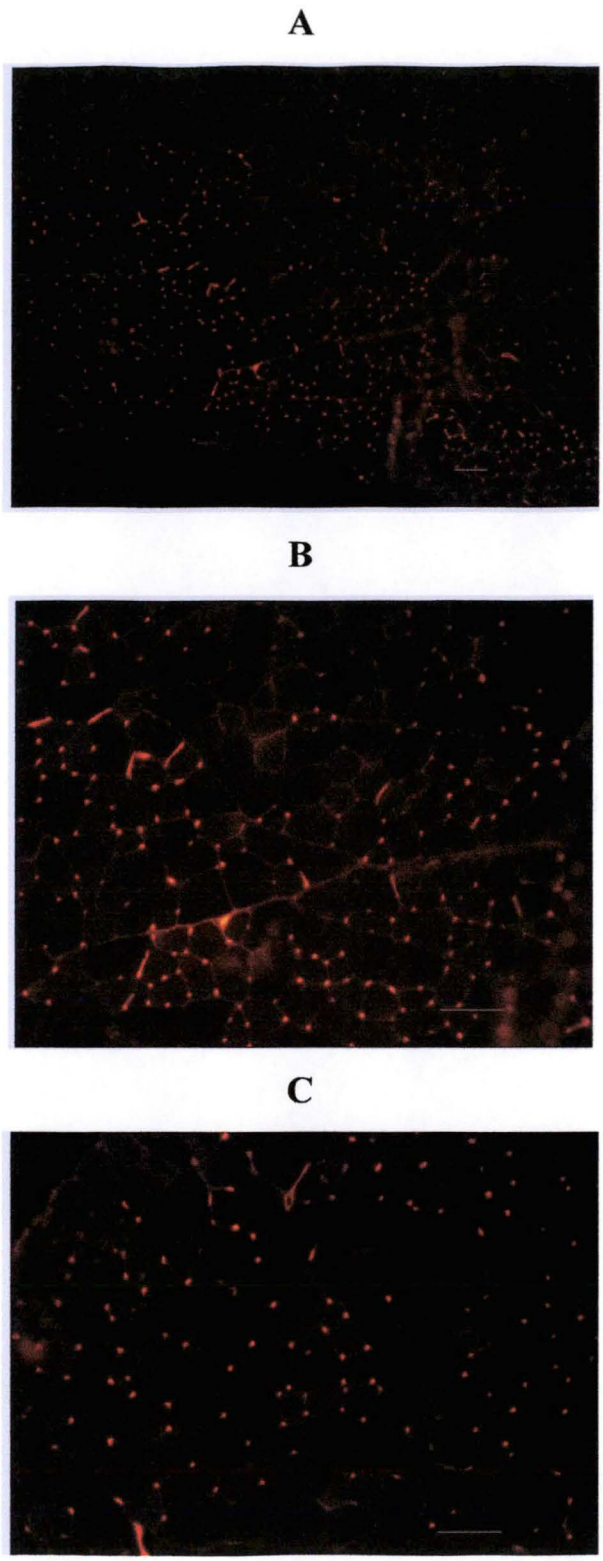

Fig 6.11 Representative transverse frozen sections of EDL muscle obtained from Study 3, AII group. Vessels having fluorescence (Rhodamine-dextran70) represent those that were perfused during hindlimb perfusion. Micrograph **A** was taken by 200X magnification. The exposure time is 1/3, 1 /2 and 1/3 sec for **A**, **B** and **C** respectively. Scale bar=50μm.

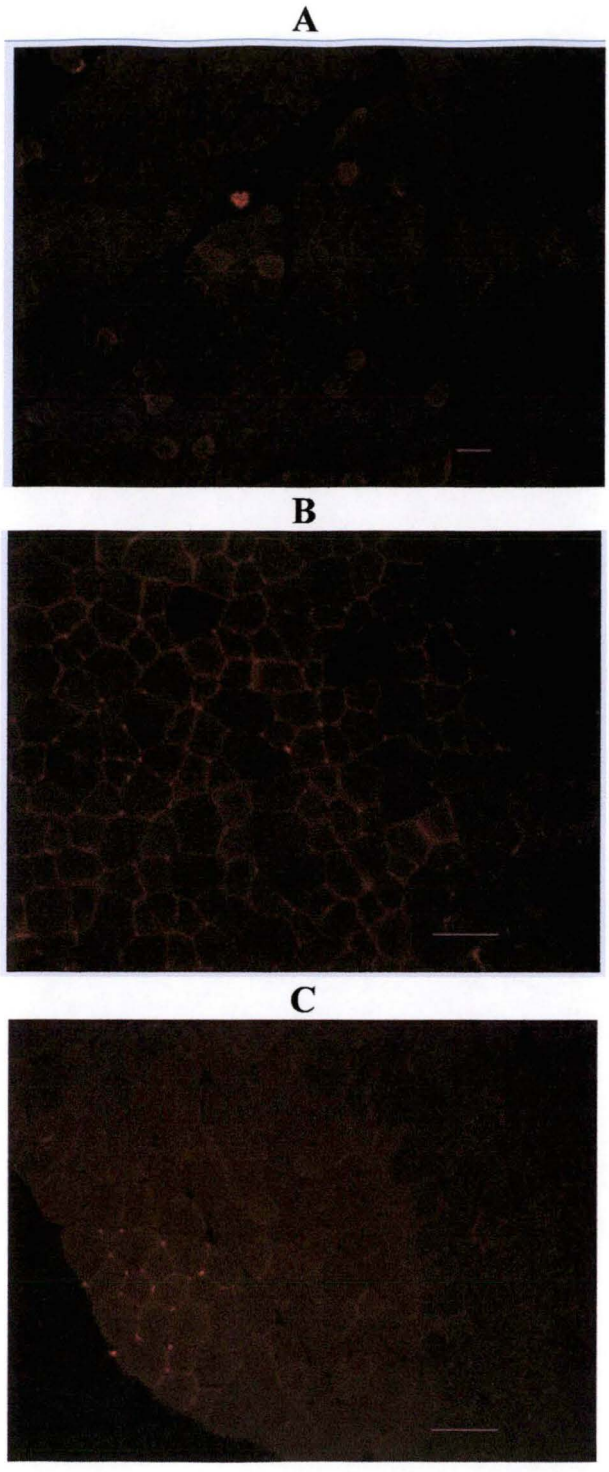

Fig 6.12 Representative transverse frozen sections of EDL muscle obtained from Study 3, 5-HT group. Vessels having fluorescence (Rhodamine-dextran70) represent those that were perfused during hindlimb perfusion. Micrograph **A** was taken by 200X magnification. The exposure time is 1/3, 1 /2.3 and 1 /2.8 sec for **A, B** and **C** respectively. Scale bar =50μm.

6.4 DISCUSSION

The present study lends support to the notion that blood flow redistribution within muscle accounts for the differing metabolic effects of the vasoconstrictors, AII and 5-HT, when added to the constant flow perfused rat hindlimb. Thus AII, which increases metabolism, increases the number of perfused capillaries (nutritive) by vasoconstricting entry to an alternate route, presumed to be non-nutritive. In contrast, 5-HT markedly diminishes the number of perfused capillaries by vasoconstricting entry to the nutritive capillaries and diverting flow to the non-nutritive route. As such, the findings are consistent with proposals by others (17, 115, 242) and by our group [*e.g.* see review (51)]. In addition, the findings provide some information as to the anatomical identity of the non-nutritive flow route. Thus during 5-HT infusion although very few of the capillaries are perfused in the transverse sections examined, flow can be seen occasionally to be carried by somewhat larger, more heavily sheathed vessels (*e.g.* Fig 6.8, Fig 6.9 C).

Our research group has previously proposed that the so-called 'non-nutritive' vessels of muscle are connective tissue vessels that are closely associated with each muscle and which can be viewed as separate entities on relatively exposed thin tendons such as the tibial tendon of the rat biceps femoris (17, 115) but do not behave as shunts (125). Our proposal was based on a study where we measured flow to connective tissue in the constant-flow perfused rat hindlimb (228). Exposed tibial tendon vessels of the biceps femoris muscle of the perfused leg were positioned either under a surface fluorometer probe to monitor signal strength when pulses of fluorescein isothiocyanate dextran were infused or over the objective lens of an inverted microscope for photography when pulses of India ink were infused. Measurements were conducted under steady state with vehicle, noradrenaline (a Type A vasoconstrictor like AII) or serotonin (a Type B vasoconstrictor) infusion. Noradrenaline increased perfusion pressure and oxygen uptake, but decreased fluorescence signal from the tendon vessels. Photomicroscopy of the India ink-filled vessels confirmed that the tendon vessels had generally decreased in diameter. Serotonin, although increasing perfusion pressure like noradrenaline had quite the opposite effect on the other parameters. Oxygen uptake was decreased and fluorescence signal from the tendon vessels increased. For serotonin, the tendon

vessels had clearly increased in diameter. Analysis of data for a range of concentrations of norepinephrine as well as serotonin showed that a reciprocal relationship existed between resting muscle metabolism (reflected by oxygen uptake) as controlled by vasoconstrictors and flow through muscle tendon vessels. Overall such findings heighten the possibility that vessels supplying septa and tendons are the functional shunts, or the non-nutritive flow route, for muscle as proposed by others (17, 115) several years ago. In addition, the data indicated that flow through the tendon vessels does not cease even when nutritive flow is high. This is consistent with an earlier study from our laboratory where Type A vasoconstriction recruited a new space without closing off a vascular space (227).

In addition to being present in superficial connective tissue, we have speculated that these vessels may be interspersed between fibre bundles and constitute loci where fat accretion can take place to possibly give rise to the "marbling" of meat. This was based on a series of perfusions aimed at assessing the effect of low nutritive flow (and hence high non-nutritive flow in a constant total flow hindlimb) on clearance of triglyceride as chylomicron emulsion. Quite unexpectedly we found that clearance was increased under conditions of predominantly non-nutritive flow (59), indicating that lipoprotein lipase was likely to be more concentrated in the non-nutritive than the nutritive route. Since lipoprotein lipase is synthesized in fat and muscle cells and secreted into neighbouring capillaries and adipose tissue contains more activity of lipoprotein than muscle, the higher clearance of triglyceride during non-nutritive flow would suggest an active presence of adipocytes on this route. Indeed, adipocytes have been reported on connective tissue vessels in muscle, particularly on the vessels that pass through the perimysium and epimysium (220).

Data from the use of fluorescent microspheres (52), where there was no major redistribution of flow between different muscles or between muscle and non-muscle tissue as a result of vasoconstrictor action might suggest that vessels representing the non-nutritive route would have been more numerous in muscle sections. In addition, since we have described increased flow in superficial connective tissue vessels following 5-HT infusion (228), flow-carrying vessels might have been expected to be found on or near the surface of the muscle as viewed in transverse sections of frozen muscle in this study, but this was not the case (not shown). The relative paucity of the

non-nutritive vessels may reflect a considerable difference in diameter and therefore flow capacity. Potter and Groom (263) showed that the distribution of capillary diameters in the gastrocnemius and gracilis muscles was bimodal in nature with 12% of capillaries having a diameter between 7.5 and 9.5 μm. These larger diameter capillaries could, therefore account for approximately 46% of the flow, since according to Poiseuille's Law, the flow through a tube is proportional to the diameter raised to the fourth power. In addition, if the larger vessels are originally closed and 5-HT infusion opened them, then approximately 85% of the flow could in principle be redistributed from the smaller diameter capillaries without requiring any pressure increase. If the larger diameter capillaries are also half the length, then the number of capillaries during 5-HT infusion required to take all the flow would be below 10% as suggested by Fig 6.5. Similar calculations can be made based on a normal distribution of capillary diameters. Kano *et al.* (161) for example determined the diameter of capillaries in the white gastrocnemius muscle of the rat to be 5.07 ± 1.82 μm (mean ± SD). In this case, assuming all capillaries are within 2 SD's of the mean and the 10% of capillaries with the largest diameters (>7.2μm) are half the length, then the entire flow can be redistributed to them without requiring a pressure change. In any event, there are sufficient available data to suggest that the non-nutritive vessels would need to be of high capacitance and low resistance and therefore capable of carrying high flow when muscle is at rest. However, although they may be larger than the nutritive capillaries nourishing muscle cells, these connective tissue adipocyte vessels do not allow the passage of 15 μm microspheres [*i.e.* when non-nutritive flow is high (227)]. Clearly further studies are needed to map the complete architecture of these larger putative non-nutritive vessels seen occasionally in muscle transverse sections with the expectation that they will be found to branch to capillaries nourishing adipocytes in connective tissue.

Other attempts to characterize non-nutritive flow routes in muscle have been more concerned with the holistic picture. Indeed, Friedman attempted to measure non-nutritive flow in muscle and assessed its contribution to total flow (103-105). Differing blood volumes were determined by indicator dilution patterns of infused marker substances. Total blood volume was derived from radioactively labelled albumin and non-nutritional blood volume from ^{86}Rb. A key assumption was that the

inability of rubidium to exchange with tissue was solely the result of it passing through a well-perfused channel which exhibited low extraction. It was also assumed that capillary permeability to rubidium was not limited. With this approach, Friedman estimated non-nutritive blood volume in the whole leg of a dog to be 75% of the total volume (105). Even though flow in the skin was not taken into account, the correction would be small, and the value agrees surprisingly well with values estimated by others using quite different methods (130).

Since total muscle blood flow comprises two components, one nutritive and the other non-nutritive, other approaches have attempted to determine nutritive flow in the first instance. A common method has involved measuring removal of intramuscularly injected radioactive markers, and then based on a joint measure of total flow deduced the amount that must be non-nutritive. A summary of estimated proportions and the methods used to assess them appears in Hudlicka (144).

In summary, I have used two methods and three protocols in an attempt to examine differences in muscle microvascular perfusion that might be occurring as a consequence of vasoconstrictor action in the pump-perfused constant flow rat hindlimb. The first method involved a combination of perfusion fixation with glutaraldehyde and post-perfusion GSL-1; the second, perfusion with rhodamine-dextran 70 (lysine fixable) and post-fixation with formaldehyde. By using three markedly differing experimental situations where the level of resultant metabolism differed from low (5-HT) through medium (vehicle) to high (AII), I have succeeded in finding clear evidence of tissue perfusion differences. Most notable, microscopic examination of muscle sections following AII showed an increase in perfused capillaries with fewer areas of under-perfusion, relative to control. In contrast, 5-HT caused a marked decrease in perfused capillaries relative to control and evidence that flow was carried by connective tissue vessels that on average were of greater diameter than capillaries and more sparsely distributed than capillaries. It is concluded that vasoconstrictors that alter hindlimb metabolism do so by intra-muscle redistribution between capillaries (nutritive) and connective tissue vessels (non-nutritive) within each muscle.

CHAPTER 7
DISCUSSION

7.1 KEY FINDINGS

The work described in this thesis investigated the regulatory and anatomical aspects of insulin-mediated capillary recruitment. In response to serial doses of insulin (1, 1.5, 3, 10 and 30mU.min^{-1}.kg^{-1}), capillary recruitment assessed in anesthetized rats showed the highest sensitivity to plasma insulin reflected by being activated at the two lowest insulin doses of 1 and 1.5mU.min^{-1}.kg^{-1} which stimulated neither femoral blood flow nor muscle glucose uptake. Femoral blood flow and muscle glucose disposal were activated by insulin at 3mU.min^{-1}.kg^{-1} when full stimulation of capillary recruitment was already induced. Maximal glucose uptake with insulin was observed at 10mU.min^{-1}.kg^{-1} whereas total blood flow increased further with increasing insulin dose from 10 to 30mU.min^{-1}.kg^{-1}. In response to the removal of physiologic insulin (3mU.min^{-1}.kg^{-1}) from the circulation, insulin-activated capillary recruitment reversed slower than activated glucose metabolism but at a similar rate to bulk blood flow. Furthermore, when TNFα (0.5μg.kg^{-1}.h^{-1}) was added against serial doses of insulin (3, 10 and 30mU.min^{-1}.kg^{-1}), the response of capillary recruitment was closely coupled to that of muscle glucose uptake. Thus, both were opposed at the two lower insulin doses (3 and 10mU.min^{-1}.kg^{-1}) but unaffected at the highest dose (30mU.min^{-1}.kg^{-1}), whereas changes in total blood flow due to highest dose insulin was still half inhibited by TNFα. As insulin may recruit capillaries by redirecting flow from non-nutritive vessels to nutritive routes, the anatomical evidence of the two vascular routes was sought by using the constant-flow pump-perfused rat hindlimb preparation. Perfusion patterns revealed in muscle sections were distinctly different under predominantly nutritive (by AII) or non-nutritive (by 5-HT) flow conditions. Vessels in connective tissue interspersed between muscle bundles and on average of greater diameter than muscle capillaries appear to serve as the non-nutritive route. Collectively, these results lend support to the notion that insulin-mediated capillary recruitment has a physiological contribution to insulin-stimulated glucose disposal and involves

redirecting flow from the non-nutritive route to the nutritive network in skeletal muscle, particularly at physiologic insulin when bulk flow does not change.

7.2 INSULIN-MEDIATED CAPILLARY RECRUITMENT AND INCREASE IN TOTAL BLOOD FLOW

In conjunction with our collaborators, we have developed three independent techniques to assess muscle microvascular perfusion. The studies presented herein used two of three methods, namely 1-MX metabolism and CEU, to examine insulin's action on muscle microvasculature. Although equally indicative of the status of muscle capillary perfusion, these two techniques are based on distinctly different principles. On the one hand, 1-MX metabolism method relies on the conversion of exogenously infused 1-MX to a single product 1-MU by the enzyme XO, present primarily in endothelial cells of the capillaries and small arterioles of muscle tissue (132, 156). Thus, it gives measure of perfused capillary surface area. CEU on the other hand, involves the continuous infusion of microbubbles as an intravascular tracer and the destruction of these microbubbles to produce measurable signals. The signals arising from larger vessels in which flow is rapid are removed by background subtraction. Thus, CEU provides measure of microvascular vascular blood volume. It is relevant to note that positron emission tomography by which Raitakari *et al* (267) reported insulin increased blood volume in human muscle measures blood within both the larger vessels and the microvasculature. Furthermore, CEU measurement is made in one area of the hindquarter which is in contrast to 1-MX metabolism that is made across the whole hindlimb. Despite the different working principles, in previous studies CEU and 1-MX metabolism each have demonstrated the ability of insulin (62, 273) and exercise (66, 353) to enhance muscle microvascular perfusion and results obtained using the two techniques were strikingly similar (50).

The sensitivity of insulin-mediated capillary recruitment to plasma insulin was assessed in studies described herein. No matter whether it was measured by 1-MX metabolism or CEU, capillary recruitment at the end of 2h insulin clamp in anaesthetized rats was activated by very low dose insulin (1mU.min^{-1}.kg^{-1}, 356pM) and fully stimulated at physiological hyperinsulinemia (3mU.min^{-1}.kg^{-1}, 638pM). This high insulin sensitivity of capillary recruitment is in contrast to the response of total

blood flow. Low dose insulin infusion (1mU.min^{-1}.kg^{-1}) had no effect on total limb blood flow. With increasing insulin doses, total blood flow increased progressively and did not reach maximal activation even at the highest dose (30mU.min^{-1}.kg^{-1}, 9666pM). This insulin dose-related difference between capillary recruitment and bulk blood appears to also hold in human muscle. Thus in human forearm, modest physiologic increases in plasma insulin concentration (53mU.L^{-1}, 318pM), which did not augment forearm or brachial artery flow, increased microvascular volume (62).

The activation time-course of the two hemodynamic actions of insulin also appears to be different. During physiological insulin infusion (3mU.min^{-1}.kg^{-1}), capillary recruitment was stimulated within 5-10min and reached steady state at 30min whereas total blood flow began to rise during the second hour of insulin exposure (332, 333). This result is reminiscent of another observation in anesthetized animals using pharmacological doses of insulin (10mU.min^{-1}.kg^{-1}) and LDF to assess microvascular perfusion (48). In that study, insulin infusion caused an increase in laser Doppler signal in muscle within 20min that reached the maximum by 50min. Femoral blood flow was not increased until at least the 60min time point (48). The time course response of insulin-mediated capillary recruitment has not been examined in human skeletal muscle. However, in human skin there is similar report on the quick action of insulin on microvasculature. Locally administrated insulin increased skin microcirculatory blood flow measured by laser Doppler fluxmetry within 13.5min (291). An earlier stimulation of total blood flow seems possible but would require much higher insulin concentrations. Inasmuch as significant increase in limb blood flow in the anaesthetized rat was observed 1h and 30min after insulin infusion at 10 and 30mU.min^{-1}.kg^{-1} respectively (Chapter 3). In conscious animals, there are similar reports (110, 259). For example, four-fold increases in insulin concentration to the supra-physiologic level (4554pM) shortened the time duration to significantly activate hindquarter blood flow from 30min to 15min (259). However, it is clear that even if very high doses of insulin are used to accelerate the activation of total blood flow, it still wouldn't achieve the time frame of 5-10min that is adequate to activate capillary recruitment at a physiologic insulin dose. Interestingly, after the termination of insulin infusion, capillary recruitment and limb blood flow each remained fully activated for another 15min beyond the reversal of glucose uptake and required a further 45min to return to basal, suggesting the signal reversal of these two vascular responses has

similarly relatively slow kinetics. A previous study in humans under conditions of systemic insulin infusion showed that increased forearm blood flow was maintained after insulin concentrations returned to the baseline value (6), consistent with the findings described in the current work. However, there was no concomitant measures of capillary recruitment in that study (6).

Taken together, it appears that insulin's action to recruit capillaries occurs at low insulin concentration and at a very early stage when physiologic insulin is administered. At higher insulin doses and prolonged insulin exposure, there is a further action of insulin to increase bulk blood flow. However, these two hemodynamic responses have similar slow reversal time-courses following the rapid fall in plasma insulin concentration when administration of physiologic insulin is halted.

7.3 MECHANISMS OF INSULIN-MEDIATED CAPILLARY RECRUITMENT

The differential dose- and time-related characteristics of insulin's action on capillary flow and bulk blood flow suggest mechanisms for these two vascular effects may also differ. Generally, the regulation of total flow to muscle resides at resistant vessels (1^{st} -3^{rd} order arterioles), whereas distribution of flow or capillary recruitment is regulated by terminal arterioles (3^{rd} – 5^{th} order) (219). Isolated 1^{st} order arterioles from rat cremaster muscle (44) and calf muscle (289) relax in response to insulin in a dose-dependent manner (60pM – 60nM), indicating increase in total blood flow may result from a direct action of insulin on these resistant vessels. Smaller vessels, although they can not be isolated due to their inaccessibility, certainly respond to insulin either systemically or topically applied to the muscle. Renaudin *et al.* (278) observed dilation of arterioles (<20μm diameter), viewed by intravital microscopy of rat spinotrapezius muscle in response to subcutaneous insulin injection resulting a serum insulin of 915pM. This arteriolar dilation occurred within 12min after insulin injection when blood glucose had not changed (278); consistent with the quick activation of capillary recruitment *in vivo* (332, 333). In rat cremaster microvasculature, Iwashita *et al.* (150) reported that dilation of 4^{th}-order arterioles (10μm diameter) persisted after serum insulin concentration had returned to basal which would be in line with the slow deactivation of capillary recruitment *in vivo*. However, effects from counter-

regulatory hormone release due to the fall in blood glucose (from 7.1mM to 5.5mM) may confound insulin's actions in this study (150). There is evidence that sensitivity to insulin-mediated vasodilation increases with decreasing vessel size (205, 238, 262). For example, 3rd order arterioles (20μm diameter) of rat cremaster muscle dilated *in situ* at insulin concentration of 4800pM within 15min, whereas larger vessels (1st-2nd order arterioles) were unresponsive ever after 30min treatment of insulin at a level of 480nM (262). Overall, it appears likely that insulin's effects on 3rd - 4th order arterioles result in capillary recruitment. However, due to the difficulty of isolation, these small arterioles have only been studied *in situ* with intravital microscopy. Thus, it is unknown whether insulin's effects on these microvessels are direct.

Many studies suggest a NO-dependent mechanism by which insulin induces vasodilation. The insulin resistance exhibited in skeletal muscle of eNOS knockout mouse appears to be consistent with this view (85). For insulin-mediated increase in total blood flow, it appears that NO production mainly results from a local effect of insulin. During a systemic hyperinsulinemic clamp, local inhibition of NO release by L-NMMA abolished augmentation of forearm blood flow in human forearm (288, 308). Consistently, isolated 1st-order arterioles (77μm diameter) from gastrocnemius muscle dilated to insulin and this dilation was inhibited by the NOS blocker, L-NNA (289). Furthermore, cell culture studies have demonstrated that vascular endothelial cells (212, 349, 350), VSMCs (318, 319) and skeletal muscle cells (160) each respond to insulin with the release of NO. Thus, the insulin-mediated increase in total blood flow may be the result of effects on either of these cell types, or a combination of the three. However, in the cell culture systems, supra-physiological doses of insulin are often required to elicit detectable responses and cells are often obtained from large vessels. Therefore results obtained from these studies may not be able to readily assist in the interpretation of insulin-mediated recruitment of capillary flow that is highly sensitive to insulin and controlled by small arterioles. In fact, Oltman *et al.* (238) reported that the NOS pathway is involved in insulin's action to dilate canine coronary conduit arteries but not microvessels. In accordance with this, Hester *et al.* (135) reported a longitudinal gradient in the tonic release of NO in muscle microcirculation and dilation of 3rd-5th – order arterioles appear to have much less dependency on NO production (249, 250). With regards to skeletal muscle-induced

NO production, it seems unlikely to be playing a role in capillary recruitment as insulin-mediated capillary recruitment occurs rapidly (332, 333) and transcapillary transport of insulin to reach myocytes is rate-limiting (264, 344). Nevertheless, there is *in vivo* evidence suggesting a NO-dependent mechanism for insulin-mediated capillary recruitment although this NO dependency only manifested at the systemic level. Thus, systemic (331) but not local (196) NOS inhibition by L-NAME abolished insulin-mediated capillary recruitment in rat hindlimb muscle. These observations suggest that a central control on NO release may contribute to insulin's action to enhance microvascular perfusion which would be in line with observations that intracerebroventricular administration of L-NMMA induced hypertension-associated insulin resistance without producing detectable presence of L-NMMA in the circulation (293). Furthermore, local administration of Mch potentiated insulin-mediated capillary recruitment, indicating a regulatory role of a local NO-dependent mechanism in insulin's microvascular action (197). Nevertheless, within the context of NO-related vascular regulation, the tightly related reversal kinetics of the two vascular actions of insulin observed *in vivo* (Chapter 4) suggest that insulin-stimulated NO-induced vascular responses in different tissues may have a similar deactivation rate. In addition, both hemodynamic actions reversed slower than insulin-stimulated muscle glucose uptake. This is unexpected as there is striking parallel between signalling pathway in metabolic targets with respect to glucose transport (43, 65) and signalling pathways in vascular endothelium regulating the production of NO by insulin (212, 351, 352). A lower phosphatase activity at one or more steps in the insulin signalling cascade resulting in NO production in insulin-sensitive tissues may contribute to the slow reversal of the total flow increase and capillary recruitment. Further studies are needed to test this hypothesis.

Recently Oltman *et al.* (238) reported that in isolated coronary microvessels, relaxation in response to insulin was mediated through K^+-dependent mechanisms rather than NOS pathways. It is possible that the K^+-dependent mechanisms are also involved in playing a role in insulin-mediated capillary recruitment in terminal arterioles of skeletal muscle. In deed, Mahajan *et al.* (196) have recently found that local infusion of tetraethylammonium chloride (TEA), an inhibitor of Ca^{2+} dependent K^+ (K_{Ca}) channels, blocked systemic insulin-mediated capillary recruitment and glucose uptake in rat leg muscle *in vivo*. This K_{Ca} channel-dependent mechanism

seems specific for capillary recruitment as blockage of this channel by TEA had no effect on the increase in forearm blood flow during the hyperinsulinemic clamp in humans (1). The ATP-dependent K^+ (K_{ATP}) channel was reported to play no role in insulin-meditated increase in total blood flow in human forearm. However, McKay and Hester (205) observed an inhibition of 4^{th}-order arteriolar dilation induced by topically applied insulin in hamster cremaster muscle when K_{ATP} channel was blocked by glibenclamide, indicating a control of K_{ATP} channel on insulin-induced response in small arterioles. Therefore, it is possible the K_{ATP} channel may play a role in insulin-mediated capillary recruitment. An *in vivo* study using the combination of systemic hyperinsulinemia and a local K_{ATP} channel blockage may prove useful to test this hypothesis.

Studies presented in the thesis as well as previous studies (333) have provided more than circumstantial evidence that the two hemodynamic effects of insulin are independent of each other. For capillary recruitment to occur in the absence of changes in total blood flow, flow might redistribute to support the increase in capillary number with a decrease in blood flow velocity throughout the microvasculature. Flow might also be recruited from the non-nutritive route by vasoconstriction at sites that control entry to this route. Recent *in vivo* studies using CEU to investigate changes in microvascular volume and cell velocity found no slowing down in cell velocity during capillary recruitment process induced by physiologic insulin (66, 333), favouring the latter explanation. In fact, studies in our laboratory have yielded substantial evidence for the existence of two vascular circuits within muscle, namely nutritive and non-nutritive routes (51). Our studies indicate that the nutritive network contains a greater capillary surface area, allowing more extensive perfusion of the muscle (51); the non-nutritive route, on the other hand, is associated with septa and tendon (228) and very likely nourishes associated adipocytes (59). Work from the present studies suggests that the non-nutritive route supplies connective tissue wrapping muscle bundles and the non-nutritive vessels are on average of greater diameter than muscle capillaries. This greater diameter may allow these vessels to be rapidly filled and thus blood in these vessels is eliminated from microvascular volume measurement when using CEU.

To redistribute flow from non-nutritive to nutritive route, insulin may in fact exert a dual action to constrict vessels preceding the non-nutritive route and vasodilate into nutritive capillaries so that the net result is no change in overall vascular resistance. One possible candidate to fulfil the vasoconstriction role is endothelin- 1 (ET-1), a potent and enduring vasoconstrictor (260, 341). ET-1 is released upon insulin stimulation from cultured human endothelial cells and VSMCs (8, 97). During insulin infusion elevated circulating ET-1 levels were observed in most (8, 97, 207, 254, 339) although not all (207) whole body studies. In the constant-flow pump-perfused rat hindlimb, low dose ET-1-induced vasoconstriction enhanced nutritive flow evidenced by an increase in hindlimb oxygen consumption which was abolished when SNP was added to block ET-1-induced vascular effects (168). Therefore, ET-1 at low dose may be able to constrict at entry points to the non-nutritive vessels to recruit capillaries leading to increased nutrient delivery and thus potentially assist insulin action. To test this hypothesis, it may be useful to conduct euglycemic hyperinsulinemic clamp with superimposed infusion of ET-1 receptor blocker to see whether abolished ET-1 action inhibits insulin's ability to recruit capillaries *in vivo*. Since ET-1 takes part in the maintenance of basal vascular tone (42, 204), it may be necessary to administer an ET-1 receptor blocker locally to avoid undesirable systemic effects. ET-1 at high dose leads to a net inhibition of oxygen uptake in the constant-flow pump-perfused rat hindlimb preparation (168), indicating a restricted muscle perfusion by ET-1 at the high dose. This observation raises the possibility that an excessive level of ET-1 may become potentially antagonistic of insulin action rather than potentiating it. Indeed, elevated ET-1 was reported in a number of clinical disorders associated with insulin resistance including type 2 diabetes (41, 96), obesity (95, 202) and hypertension (42, 184). Insulin-mediated capillary recruitment is likely to be impaired in these insulin resistant situations and the elevated ET-1 may conceivably play a role. In this regard, it would be interesting to see whether insulin-stimulated capillary recruitment and muscle glucose uptake in these patients could be improved by lowering ET-1 levels.

Insulin-mediated MSNA may provide another possible vasoconstrictor mechanism by which insulin enhances microvascular perfusion at the expense of non-nutritive flow. Support for this hypothesis may draw from the remarkable similarity in the time-course and dose responses to insulin between MSNA and capillary recruitment. MSNA appears to be a quick action of insulin (6, 31, 304). In particular, Spraul *et al.*

reported that MSNA increased 15min after the onset of insulin infusion (80mU.m^{-2}.min^{-1}) in human subjects and the time required to reach the half maximal effect was approximately 25min while calf blood flow showed a significant rise only after 45min of insulin infusion (304). This time frame of MSNA is comparable to the 5-10min required to activate capillary recruitment in rats using 3mU.min^{-1}.kg^{-1} dose of insulin (332, 333). Moreover, there are reports on persistent MSNA 1h after the termination of insulin infusion (6) or 90min after carbohydrate ingestion (30). This slow reversal of MSNA would match the slow deactivation of capillary recruitment in rats following the cessation of 3mU.min^{-1}.kg^{-1} insulin clamp (Chapter 4). Furthermore, there is evidence that MSNA is activated and saturated by insulin at low dose which is inadequate to stimulate total blood flow (131). This high insulin sensitivity of MSNA is also consistent with studies in rats showing the high insulin sensitivity of capillary recruitment (Chapter 3). Thus, the possible MSNA involvement in insulin's action to recruit capillaries may be worth further exploration.

7.4 ROLE OF INSULIN-MEDIATED CAPILLARY RECRUITMENT IN INSULIN-MEDIATED GLUCOSE UPTAKE IN SKELETAL MUSCLE

The finding that insulin has hemodynamic actions leads to the hypothesis that insulin's stimulatory effects on muscle glucose uptake have two components: one is the activation of cellular glucose metabolism; the other is an increase in the delivery of glucose and insulin itself to myocytes. Some researchers tested this hypothesis by examining the effects of altering bulk blood flow using vasoactive agents on limb glucose utilization and results from these studies were inconsistent. Whereas each similarly augmented total blood flow, Mch (25, 27, 197, 285) but not SNP (224, 258, 285), adenosine (223) or bradykinin (174, 233) enhanced insulin-mediated glucose uptake. These differential effects of vasoactive agents on glucose disposal seem unrelated to the possible confounding effects of NO on muscle glucose metabolism or differences in insulin-induced glucose gradient across the vascular bed. Rather, they appear to be associated with modulating actions of these drugs on insulin-stimulated capillary recruitment (197, 258). Therefore, these observations favour a prominent role of the microvascular action of insulin in facilitating glucose disposal in muscle. In support of this view is the demonstration that exercise training resulted in enhanced microvascular response in association with enhanced glucose uptake (277). Thus, it is

conceivable that in some insulin resistant states, the defect in insulin action may result not only from some intrinsic defect in the cellular metabolic steps involved in glucose metabolism but also from a defect in insulin's action to improve microvascular perfusion. Consistent with this view, previous work from our group has shown a close association of impaired insulin-mediated capillary recruitment with impaired insulin-mediated glucose uptake in a number of animal models of insulin resistance. For example, the obese insulin resistant Zucker rat is markedly unresponsive to insulin-mediated capillary recruitment and shows almost no response to maximum insulin in terms of muscle glucose uptake (336). In addition, each of the following: α-met5-HT (272), TNFα (350), or Intralipid + heparin (58) infusions acutely blocked insulin's microvascular action of capillary recruitment and impaired insulin-mediated glucose disposal in each case by approximately 50%. It is of added interest that TNFα-induced inhibition of insulin-mediated capillary recruitment was overcome by high level insulin which was associated with a fully restored insulin action on muscle glucose uptake (Chapter 5). In contrast, total blood flow induced by this high dose insulin was still partly inhibited by TNFα.

The dose and time characteristics of insulin-mediated increase in limb bulk blood flow in relation to insulin-stimulated muscle glucose metabolism have been extensively studied in humans. At physiological insulin concentrations, insulin increases glucose extraction maximally within 30-60min (325) during which time the response of limb flow is highly variable, with significant increases (20-60%) (6, 308, 335), no or marginal increases (34, 233, 325, 348) in blood flow. During prolonged or high-dose insulin infusions, blood flow increases markedly up to 80-110% above basal whereas glucose extraction remains constant (171, 325). Thus it was concluded from these studies that an increase in total flow may play a role in facilitating muscle glucose uptake when the insulin concentration is supra-physiological and exposure to this hormone is prolonged, yet under physiologic conditions and insulin concentrations the role of total flow is questionable. We characterized the time-course and dose-curve responses of insulin-mediated capillary recruitment using hyperinsulinemic clamp in anesthetized rats and obtained results in contrast to those relating to total blood flow. Thus insulin recruited muscle capillaries at concentrations lower than those required to stimulate glucose disposal (Chapter 3). When insulin

was infused at a physiologic concentration and then halted, capillary recruitment was activated earlier (332) and reversed slower (Chapter 4) than muscle glucose uptake. To have capillary recruitment activated earlier and at lower insulin concentrations may be essential to ensure optimal muscle glucose storage after meal where insulin is secreted in phasic manner and its level rises and falls rapidly. Thus, a possible situation after a meal in insulin resistant subjects may be that equilibration of interstitial insulin may not be reached before plasma insulin level falls due to the defective insulin action to facilitate capillary delivery. If this is the case, the diminished muscle glucose uptake in insulin resistant individuals observed using a constant hyperinsulinemic clamp would be more prominent when experiments were conducted using oral glucose load or food ingestion. Moreover, the reason for the slow reversal of insulin-mediated capillary recruitment is not clear. It is possible that the slow reversal allows washout of insulin from muscle for clearance by liver and kidney following the decline of the peak of plasma insulin at the end of the absorptive state. In this manner, anabolic processes stimulated by insulin in the myocytes would be more readily reversed. This might limit late hypoglycemia which wouldn't occur under a clamp condition since it has been prevented by infusing variable rates of glucose. To further explore the physiologic aspects of insulin-mediated capillary recruitment and the contribution of defects in this insulin action to muscle insulin resistance, it may be useful to examine the response of capillary recruitment and muscle glucose disposal following intravenous glucose infusion, oral glucose load or mixed meal ingestion in both insulin sensitive and resistant models. In this respect, CEU is providing an ideal tool to conduct continuous measurement of capillary recruitment.

7.5 CONCLUSION

To summarize, the work present herein extends our previous findings that insulin's microvascular action and macrovascular action are disassociated and lends support to the notion that insulin-mediated capillary recruitment has a physiological contribution to insulin's stimulatory effects on muscle glucose uptake. The findings also shed an insight into the anatomic vascular process by which insulin may act to recruit capillaries without changing total blood flow. The TNFα studies show that when used

against serial doses of insulin, there was a constant association between capillary recruitment and muscle glucose uptake whereas the association between total blood flow and glucose disposal was only apparent at two lower insulin doses. Furthermore, capillary recruitment was found to be more sensitive to plasma insulin concentrations than either muscle glucose uptake or total blood flow. In conjunction with previous findings that capillary recruitment is an early event of insulin action that precedes insulin-mediated increase in total blood flow and muscle glucose uptake, the microvascular action of insulin may confer an advantage for insulin and glucose delivery to muscle by ensuring that optimal muscle glucose storage occurs after meals. The time and insulin dose-related differences between capillary recruitment and total blood flow suggest these two hemodynamic actions of insulin are differentially regulated. However, the similar reversal kinetics of insulin-mediated capillary recruitment and increase in total flow following the removal of physiological dose insulin indicate that the two vascular actions of insulin have similar deactivation mechanisms. Nevertheless, to have new capillaries recruited without altering bulk blood flow, insulin may redistribute flow from the non-nutritive route to the nutritive capillary network. Anatomical proof of the non-nutritive route was sought and it appears likely that the non-nutritive vessels supply connective tissue and have slightly greater diameters than muscle capillaries. Collectively, these results highlight the physiologic importance of insulin's action to enhance nutritive capillary flow likely at the expense of non-nutritive connective tissue flow in the determination of skeletal muscle glucose uptake.

REFERENCE LIST

1. **Abbink EJ, Walker AJ, Van Der Sluijs HA, Tack CJ, and Smits P.** No role of calcium- and ATP-dependent potassium channels in insulin-induced vasodilation in humans in vivo. *Diabetes Metab Res Rev* 18: 143-148, 2002.

2. **Abdullah MS, Wild G, Jacob V, Milford-Ward A, Ryad R, Zanaty M, Ali MH, and el Nahas AM.** Cytokines and the malnutrition of chronic renal failure. *Miner Electrolyte Metab* 23: 237-242, 1997.

3. **Abramson DI, Schkloven N, Margolis MN, and Mirsky IA.** Influence of massive doses of insulin on peripheral blood flow in man. *Am J Physiol* 128: 124-132, 1939.

4. **Allwood MJ, Birchall I, and Staffurth JS.** Circulatory changes in the forearm during insulin hypoglycaemia studied by regional 24Na clearance and by plethysmography. *J Physiol* 143: 332-342, 1958.

5. **Allwood MJ, Hensel H, and Papenberg J.** Muscle and skin blood flow in the human forearm during insulin hypoglycaemia. *J Physiol (Lond)* 147: 269-273, 1959.

6. **Anderson EA, Hoffman RP, Balon TW, Sinkey CA, and Mark AL.** Hyperinsulinemia produces both sympathetic neural activation and vasodilation in normal humans. *J Clin Invest* 87: 2246-2252, 1991.

7. **Andreasson K, Galuska D, Thorne A, Sonnenfeld T, and Wallberg-Henriksson H.** Decreased insulin-stimulated 3-O-methylglucose transport in in vitro incubated muscle strips from type II diabetic subjects. *Acta Physiol Scand* 142: 255-260, 1991.

8. **Anfossi G, Cavalot F, Massucco P, Mattiello L, Mularoni EM, Burzacca S, Hahn A, and Trovati M.** Insulin increases endothelin-1 production by vascular smooth muscle cells derived from human microvessels. *FrontDiabetes* 12: 272-274, 1993.

9. **Armstrong RB and Laughlin MH.** Blood flows within and among rat muscles as a function of time during high speed treadmill exercise. *J Physiol (Lond)* 344: 189-208, 1983.

10. **Armstrong RB and Phelps RO.** Muscle fiber type composition of the rat hindlimb. *Am J Anat* 171: 259-272, 1984.

11. **Avogaro A, Piarulli F, Valerio A, Miola M, Calveri M, Pavan P, Vicini P, Cobelli C, Tiengo A, Calo L, and DelPrato S.** Forearm nitric oxide balance, vascular relaxation and glucose metabolism in NIDDM patients. *Diabetes* 46: 1040-1046, 1997.

12. **Bagby GJ, Lang CH, Hargrove DM, Thompson JJ, Wilson LA, and Spitzer JJ.** Glucose kinetics in rats infused with endotoxin-induced monokines or tumor necrosis factor. *Circ Shock* 24: 111-121, 1988.

13. **Balon TW and Nadler JL.** Evidence that nitric oxide increases glucose transport in skeletal muscle. *J Appl Physiol* 82: 359-363, 1997.

14. **Bar RS, Boes M, and Sandra A.** Vascular transport of insulin to rat cardiac muscle. Central role of the capillary endothelium. *J Clin Invest* 81: 1225-1233, 1988.

15. **Barlow TE.** Vascular patterns in the alimentary canal. In: Visceral Circulation, Ciba Foundation Symposium, edited by Wolstenholme GEW. *London: Churchill,* 1952, p. 21-31.

16. **Barlow TE and Haigh AL.** Dual circulation in skeletal muscle. *J Physiol (Lond)* 149: 18P-19P, 1959.

17. **Barlow TE, Haigh AL, and Walder DN.** Evidence for two vascular pathways in skeletal muscle. *Clin Sci (Colch)* 20: 367-385, 1961.

18. **Baron AD.** Hemodynamic actions of insulin. *Am J Physiol* 267: E187-E202, 1994.

19. **Baron AD and Brechtel G.** Insulin differentially regulates systemic and skeletal muscle vascular resistance. *Am J Physiol* 265: E61-E67, 1993.

20. **Baron AD, Brechtel G, Wallace P, and Edelman SV.** Rates and tissue sites of non-insulin- and insulin-mediated glucose uptake in humans. *Am J Physiol* 255: E769-E774, 1988.

21. **Baron AD, Brechtel-Hook G, Johnson A, Cronin J, Leaming R, and Steinberg HO.** Effect of perfusion rate on the time course of insulin-mediated skeletal muscle glucose uptake. *Am J Physiol* 271: E1067-E1072, 1996.

22. **Baron AD, Brechtel-Hook G, Johnson A, and Hardin D.** Skeletal muscle blood flow. A possible link between insulin resistance and blood pressure. *Hypertension* 21: 129-135, 1993.

23. **Baron AD, Laakso M, Brechtel G, and Edelman SV.** Mechanism of insulin resistance in insulin-dependent diabetes mellitus: a major role for reduced skeletal muscle blood flow. *J Clin Endocrinol Metab* 73: 637-643, 1991.

24. **Baron AD, Laakso M, Brechtel G, Hoit B, Watt C, and Edelman SV.** Reduced postprandial skeletal muscle blood flow contributes to glucose intolerance in human obesity. *J Clin Endocrinol Metab* 70: 1525-1533, 1990.

25. **Baron AD, Steinberg H, Brechtel G, and Johnson A.** Skeletal muscle blood flow independently modulates insulin-mediated glucose uptake. *Am J Physiol* 266: E248-E253, 1994.

26. **Baron AD, Steinberg HO, Chaker H, Leaming R, Johnson A, and Brechtel G.** Insulin-mediated skeletal muscle vasodilation contributes to both insulin sensitivity and responsiveness in lean humans. *J Clin Invest* 96: 786-792, 1995.

27. **Baron AD, Tarshoby M, Hook G, Lazaridis EN, Cronin J, Johnson A, and Steinberg HO.** Interaction between insulin sensitivity and muscle perfusion on glucose uptake in human skeletal muscle: evidence for capillary recruitment. *Diabetes* 49: 768-774, 2000.

28. **Begum N and Ragolia L.** Effect of tumor necrosis factor-alpha on insulin action in cultured rat skeletal muscle cells. *Endocrinology* 137: 2441-2446, 1996.

29. **Bergeron R, Previs SF, Cline GW, Perret P, Russell RR, III, Young LH, and Shulman GI.** Effect of 5-aminoimidazole-4-carboxamide-1-beta-D-ribofuranoside infusion on in vivo glucose and lipid metabolism in lean and obese Zucker rats. *Diabetes* 50: 1076-1082, 2001.

30. **Berne C, Fagius J, and Niklasson F.** Sympathetic response to oral carbohydrate administration. *J Clin Invest* 84: 1403-1409, 1989.

31. **Berne C, Fagius J, Pollare T, and Hjemdahl P.** The sympathetic response to euglycaemic hyperinsulinaemia. Evidence from microelectrode nerve recordings in healthy subjects. *Diabetologia* 35: 873-879, 1992.

32. **Beutler B and Cerami A.** The biology of cachectin/TNF--a primary mediator of the host response. *Annu Rev Immunol* 7:625-55.: 625-655, 1989.

33. **Biolo G, Toigo G, Ciocchi B, Situlin R, and Guarnieri G.** Slower activation of insulin action in hypertension associated with obesity. *J Hypertens* 16: 1783-1788, 1998.

34. **Bonadonna RC, Del Prato S, Saccomani MP, Bonora E, Gulli G, Bier D, Cobelli C, and Defronzo RA.** Transmembrane glucose transport in skeletal muscle of patients with non-insulin-dependent diabetes. *J Clin Invest* 92: 486-494, 1993.

35. **Bonadonna RC, Saccomani MP, Del Prato S, Bonora E, Defronzo RA, and Cobelli C.** Role of tissue-specific blood flow and tissue recruitment in insulin- mediated glucose uptake of human skeletal muscle. *Circulation* 98: 234-241, 1998.

36. **Bonen A, Clark MG, and Henriksen EJ.** Experimental approaches in muscle metabolism: hindlimb perfusion and isolated muscle incubations. *Am J Physiol* 266: E1-16, 1994.

37. **Borgstrom P, Lindbom L, Arfors KE, and Intaglietta M.** Beta-adrenergic control of resistance in individual vessels in rabbit tenuissimus muscle. *Am J Physiol* 254: H631-H635, 1988.

38. **Borst SE and Bagby GJ.** Neutralization of tumor necrosis factor reverses age-induced impairment of insulin responsiveness in skeletal muscle of Sprague-Dawley rats. *Metabolism* 51: 1061-1064, 2002.

39. **Buchanan TA, Thawani H, Kades W, Modrall JG, Weaver FA, Laurel C, Poppiti R, Xiang A, and Hsueh W.** Angiotensin II increases glucose utilization during acute hyperinsulinemia via a hemodynamic mechanism. *J Clin Invest* 92: 720-726, 1993.

40. **Capaldo B, Lembo G, Napoli R, Rendina V, Albano G, Sacca L, and Trimarco B.** Skeletal muscle is a primary site of insulin resistance in essential hypertension. *Metabolism* 40: 1320-1322, 1991.

41. **Cardillo C, Campia U, Bryant MB, and Panza JA.** Increased activity of endogenous endothelin in patients with Type II diabetes mellitus. *Circulation* 106: 1783-1787, 2002.

42. **Cardillo C, Kilcoyne CM, Waclawiw M, Cannon RO, III, and Panza JA.** Role of endothelin in the increased vascular tone of patients with essential hypertension. *Hypertension* 33: 753-758, 1999.

43. **Cheatham B and Kahn CR.** Insulin action and the insulin signaling network. *Endocr Rev* 16: 117-142, 1995.

44. **Chen YL and Messina EJ.** Dilation of isolated skeletal muscle arterioles by insulin is endothelium dependent and nitric oxide mediated. *Am J Physiol* 270: H2120-H2124, 1996.

45. **Chou YC, Perng JC, Juan CC, Jang SY, Kwok CF, Chen WL, Fong JC, and Ho LT.** Endothelin-1 inhibits insulin-stimulated glucose uptake in isolated rat adipocytes. *Biochem Biophys Res Commun* 202: 688-693, 1994.

46. **Chowienczyk PJ, Cockcroft JR, and Ritter JM.** Inhibition of acetylcholinesterase selectively potentiates NG-monomethyl-L-arginine-resistant actions of acetylcholine in human forearm vasculature. *Clin Sci (Lond)* 88: 111-117, 1995.

47. **Christoforides C, Laasberg LH, and Hedley-Whyte J.** Effect of temperature on solubility of O2 in human plasma. *J Appl Physiol* 26: 56-60, 1969.

48. **Clark ADH, Barrett EJ, Rattigan S, Wallis MG, and Clark MG.** Insulin stimulates laser Doppler signal by rat muscle in vivo consistent with nutritive flow recruitment. *Clin Sci (Colch)* 100: 283-290, 2001.

49. **Clark ADH, Youd JM, Rattigan S, Barrett EJ, and Clark MG.** Heterogeneity of laser Doppler flowmetry in perfused muscle indicative of nutritive and nonnutritive flow. *Am J Physiol* 280: H1324-H1333, 200.

50. **Clark MG, Barrett EJ, Wallis MG, Vincent MA, and Rattigan S.** The microvasculature in insulin resistance and Type 2 diabetes. *Semin Vasc Med* 2: 21-31, 2002.

51. **Clark MG, Colquhoun EQ, Rattigan S, Dora KA, Eldershaw TP, Hall JL, and Ye J.** Vascular and endocrine control of muscle metabolism. *Am J Physiol* 268: E797-E812, 1995.

52. **Clark MG, Rattigan S, Clerk LH, Vincent MA, Clark AD, Youd JM, and Newman JM.** Nutritive and non-nutritive blood flow: rest and exercise. *Acta Physiol Scand* 168: 519-530, 2000.

53. **Clark MG, Rattigan S, Dora KA, Newman JMB, Steen JT, Miller KA, and Vincent MA.** Vascular and metabolic regulation of muscle. In: Physiology, Stress, and Malnutrition: Functional Correlates, Nutritional Intervention, edited by Kinney JM and Tucker HN. *New York: Lippincott-Raven,* 1997, p. 325-346.

54. **Clark MG, Wallis MG, Barrett EJ, Vincent MA, Richards SM, Clerk LH, and Rattigan S.** Blood flow and muscle metabolism: a focus on insulin action. *Am J Physiol Endocrinol Metab* 284: E241-E258, 2003.

55. **Clark PW, Jenkins AB, and Kraegen EW.** Pentobarbital reduces basal liver glucose output and its insulin suppression in rats. *Am J Physiol* 258: E701-707, 1990.

56. **Cleland SJ, Petrie JR, Small M, Elliott HL, and Connell JM.** Insulin action is associated with endothelial function in hypertension and type 2 diabetes. *Hypertension* 35: 507-511, 2000.

57. **Cleland SJ, Petrie JR, Ueda S, Elliott HL, and Connell JM.** Insulin-mediated vasodilation and glucose uptake are functionally linked in humans. *Hypertension* 33: 554-558, 1999.

58. **Clerk LH, Rattigan S, and Clark MG.** Lipid infusion impairs physiologic insulin-mediated capillary recruitment and muscle glucose uptake in vivo. *Diabetes* 51: 1138-1145, 2002.

59. **Clerk LH, Smith ME, Rattigan S, and Clark MG.** Increased chylomicron triglyceride hydrolysis by connective tissue flow in perfused rat hindlimb. Implications for lipid storage. *J Lipid Res* 41: 329-335, 2000.

60. **Clerk LH, Vincent MA, Lindner JR, Clark MG, Rattigan S, and Barrett EJ.** The vasodilatory actions of insulin on resistance and terminal arterioles and their impact on muscle glucose uptake. *Diabetes Metab Res Rev* 20: 3-12, 2004.

61. **Clumeck N, De Troyer A, Naeije R, Somers G, Smekens L, and Balasse EO.** Treatment of diabetic coma with small intravenous insulin boluses. *Br Med J* 2: 394-396, 1976.

62. **Coggins M, Lindner J, Rattigan S, Jahn L, Fasy E, Kaul S, and Barrett E.** Physiologic hyperinsulinemia enhances human skeletal muscle perfusion by capillary recruitment. *Diabetes* 50: 2682-2690, 2001.

63. **Colquhoun EQ, Hettiarachchi M, Ye JM, Rattigan S, and Clark MG.** Inhibition by vasodilators of noradrenaline and vasoconstrictor-mediated, but not skeletal muscle contraction-induced oxygen uptake in the perfused rat hindlimb; implications for non-shivering thermogenesis in muscle tissue. *Gen Pharmacol* 21: 141-148, 1990.

64. **Colquhoun EQ, Hettiarachchi M, Ye JM, Richter EA, Hniat AJ, Rattigan S, and Clark MG.** Vasopressin and angiotensin II stimulate oxygen uptake in the perfused rat hindlimb. *Life Sci* 43: 1747-1754, 1988.

65. **Czech MP and Corvera S.** Signaling mechanisms that regulate glucose transport. *J Biol Chem* 274: 1865-1868, 1999.

66. **Dawson D, Vincent MA, Barrett EJ, Kaul S, Clark A, Leong-Poi H, and Lindner JR.** Vascular recruitment in skeletal muscle during exercise and hyperinsulinemia assessed by contrast ultrasound. *Am J Physiol Endocrinol Metab* 282: E714-E720, 2002.

67. **Day RO, Miners J, Birkett DJ, Graham GG, and Whitehead A.** Relationship between plasma oxipurinol concentrations and xanthine oxidase activity in volunteers dosed with allopurinol. *Br J Clin Pharmacol* 26: 429-434, 1988.

68. **de Jongh RT, Clark AD, IJzerman RG, Serne EH, De Vries G, and Stehouwer CD.** Physiological hyperinsulinaemia increases intramuscular microvascular reactive hyperaemia and vasomotion in healthy volunteers. *Diabetologia* 47: 978-986, 2004.

69. **de Jongh RT, Serne EH, IJzerman RG, De Vries G, and Stehouwer CD.** Free fatty acid levels modulate microvascular function: relevance for obesity-associated insulin resistance, hypertension, and microangiopathy. *Diabetes* 53: 2873-2882, 2004.

70. **de Jongh RT, Serne EH, IJzerman RG, De Vries G, and Stehouwer CD.** Impaired microvascular function in obesity: implications for obesity-associated microangiopathy, hypertension, and insulin resistance. *Circulation* 109: 2529-2535, 2004.

71. **Defronzo RA, Gunnarsson R, Bjorkman O, Olsson M, and Wahren J.** Effects of insulin on peripheral and splanchnic glucose metabolism in noninsulin-dependent (type II) diabetes mellitus. *J Clin Invest* 76: 149-155, 1985.

72. **Defronzo RA, Hendler R, and Simonson D.** Insulin resistance is a prominent feature of insulin-dependent diabetes. *Diabetes* 31: 795-801, 1982.

73. **Defronzo RA, Jacot E, Jequier E, Maeder E, Wahren J, and Felber JP.** The effect of insulin on the disposal of intravenous glucose. Results from indirect calorimetry and hepatic and femoral venous catheterization. *Diabetes* 30: 1000-1007, 1981.

74. **del Aguila LF, Claffey KP, and Kirwan JP.** TNF-alpha impairs insulin signaling and insulin stimulation of glucose uptake in C2C12 muscle cells. *Am J Physiol* 276: E849-E855, 1999.

75. **Del Prato S, Nosadini R, Tessari P, Tiengo A, Avogaro A, Trevisan R, Valerio A, Muggeo M, Cobelli C, and Toffolo G.** Insulin-mediated glucose disposal in type I diabetes: Evidence for insulin resistance. *J Clin Endocrinol Metab* 57: 904-910, 1983.

76. **Dela F, Larssen JJ, Mikines KJ, and Galbo H.** Normal effect of insulin to stimulate leg blood flow in NIDDM. *Diabetes* 44: 221-226, 1995.

77. **DeMeyts P, Bainco AR, and Roth J.** Site-site interactions among insulin receptors. Characterization of the negative cooperativity. *J Biol Chem* 251: 1877-1888, 1976.

78. **Dernovsek KD, Bar RS, Ginsberg BH, and Lioubin MN.** Rapid transport of biologically intact insulin through cultured endothelial cells. *J Clin Endocrinol Metab* 58: 761-763, 1984.

79. **Diehl KH, Hull R, Morton D, Pfister R, Rabemampianina Y, Smith D, Vidal JM, van de Vorstenbosch C**; European Federation of Pharmaceutical Industries Association and European Centre for the Validation of Alternative Methods. A good practice guide to the administration of substances and removal of blood, including routes and volumes. *J Appl Toxicol* 21: 15-23, 2001.

80. **Dohm GL, Tapscott EB, Pories WJ, Dabbs DJ, Flickinger EG, Meelheim D, Fushiki T, Atkinson SM, Elton CW, and Caro JF.** An in vitro human muscle preparation suitable for metabolic studies: Decreased insulin stimulation of glucose transport in muscle from morbidly obese and diabetic subjects. *J Clin Invest* 82: 486-494, 1988.

81. **Dora KA, Rattigan S, Colquhoun EQ, and Clark MG.** Aerobic muscle contraction impaired by serotonin-mediated vasoconstriction. *J Appl Physiol* 77: 277-284, 1994.

82. **Dora KA, Richards SM, Rattigan S, Colquhoun EQ, and Clark MG.** Serotonin and norepinephrine vasoconstriction in rat hindlimb have different oxygen requirements. *Am J Physiol* 262: H698-H703, 1992.

83. **Dosekun FO.** The measurement of metabolic and vascular responses in the human skeletal muscle with observations on its response to insulin and glucose. *Clin Sci (Colch)* 22:287-94.: 287-294, 1962.

84. **Dosekun FO, Grayson J, and Mendel D.** The measurement of metabolic and vascular responses in liver and muscle with observations on their responses to insulin and glucose. *J Physiol (Lond)* 150: 581-606, 1960.

85. **Duplain H, Burcelin R, Sartori C, Cook S, Egli M, Lepori M, Vollenweider P, Pedrazzini T, Nicod P, Thorens B, and Scherrer U.** Insulin resistance, hyperlipidemia, and hypertension in mice lacking endothelial nitric oxide synthase. *Circulation* 104: 342-345, 2001.

86. **Ebeling P, Bourey R, Koranyi L, Tuominen JA, Groop LC, Henriksson J, Mueckler M, Sovijarvi A, and Koivisto VA.** Mechanism of enhanced insulin sensitivity in athletes.

Increased blood flow, muscle glucose transport protein (GLUT-4) concentration, and glycogen synthase activity. *J Clin Invest* 92: 1623-1631, 1993.

87. **Elder GC, Bradbury K, and Roberts R.** Variability of fiber type distributions within human muscles. *J Appl Physiol* 53: 1473-1480, 1982.

88. **Emmerson BT, Gordon RB, Cross M, and Thomson DB.** Plasma oxipurinol concentrations during allopurinol therapy. *Br J Rheumatol* 26: 445-449, 1987.

89. **Etgen GJ, Jr, Fryburg DA, and Gibbs EM.** Nitric oxide stimulates skeletal muscle glucose transport through a calcium/contraction- and phosphatidylinositol-3-kinase-independent pathway. *Diabetes* 46: 1915-1919, 1997.

90. **Evans DA, Jacobs DO, and Wilmore DW.** Tumor necrosis factor enhances glucose uptake by peripheral tissues. *Am J Physiol* 257: R1182-R1189, 1989.

91. **Faber JE, Harris PD, and Wiegman DL.** Anesthetic depression of microcirculation, central hemodynamics, and respiration in decerebrate rats. *Am J Physiol* 243: H837-H843, 1982.

92. **Felber JP, Ferrannini E, Golay A, Meyer HU, Theibaud D, Curchod B, Maeder E, Jequier E, and Defronzo RA.** Role of lipid oxidation in pathogenesis of insulin resistance of obesity and type II diabetes. *Diabetes* 36: 1341-1350, 1987.

93. **Ferrannini E, Barrett EJ, and Bevilacqua S.** Effect of fatty acids on glucose production and utilization in man. *J Clin Invest* 72: 1737-1747, 1983.

94. **Ferrannini E, Buzzigoli G, Bonadonna R, Giorico MA, Oleggini M, Graziadei L, Pedrinelli R, Brandi L, and Bevilacqua S.** Insulin resistance in essential hypertension. *N Engl J Med* 317: 350-357, 1987.

95. **Ferri C, Bellini C, Desideri G, Di Francesco L, Baldoncini R, Santucci A, and De Mattia G.** Plasma endothelin-1 levels in obese hypertensive and normotensive men. *Diabetes* 44: 431-436, 1995.

96. **Ferri C, Carlomagno A, Coassin S, Baldoncini R, Faldetta MRC, Laurenti O, Properzi G, Santucci A, and De Mattia G.** Circulating endothelin-1 levels increase

during euglycemic hyperinsulinemic clamp in lean NIDDM men. *Diabetes Care* 18: 226-233, 1995.

97. **Ferri C, Pittoni V, Piccoli A, Laurenti O, Cassone MR, Bellini C, Properzi G, Valesini G, De Mattia G, and Santucci A.** Insulin stimulates endothelin-1 secretion from human endothelial cells and modulates its circulating levels in vivo. *J Clin Endocrinol Metab* 80: 829-835, 1995.

98. **Fingar DC and Birnbaum MJ.** Characterization of the mitogen-activated protein kinase/90-kilodalton ribosomal protein S6 kinase signaling pathway in 3T3-L1 adipocytes and its role in insulin-stimulated glucose transport. *Endocrinology* 134: 728-735, 1994.

99. **Fliser D, Dikow R, Demukaj S, and Ritz E.** Opposing effects of angiotensin II on muscle and renal blood flow under euglycemic conditions. *J Am Soc Nephrol* 11: 2001-2006, 2000.

100. **Flores EA, Bistrian BR, Pomposelli JJ, Dinarello CA, Blackburn GL, and Istfan NW.** Infusion of tumor necrosis factor/cachectin promotes muscle catabolism in the rat. A synergistic effect with interleukin 1. *J Clin Invest* 83: 1614-1622, 1989.

101. **Freidenberg GR, Suter S, Henry RR, Nolan J, Reichart D, and Olefsky JM.** Delayed onset of insulin activation of the insulin receptor kinase in vivo in human skeletal muscle. *Diabetes* 43: 118-126, 1994.

102. **Friedman JE, Caro JF, Pories WJ, Azevedo JL, and Dohm GL.** Glucose metabolism in incubated human muscle: effect of obesity and non- insulin-dependent diabetes mellitus. *Metabolism* 43: 1047-1054, 1994.

103. **Friedman JJ.** 86Rb extraction as an indicator of capillary flow. *Circ Res* 28: I15-I20, 1971.

104. **Friedman JJ.** Single-passage extraction of 86Rb from the circulation of skeletal muscle. *Am J Physiol* 216: 460-466, 1968.

105. **Friedman JJ.** Total, non-nutritional, and nutritional blood volume in isolated dog hindlimb. *Am J Physiol* 210: 151-156, 1966.

106. **Fronek K and Zweifach BW.** Microvascular pressure distribution in skeletal muscle and the effect of vasodilation. *Am J Physiol* 228: 791-796, 1975.

107. **Fueger PT, Bracy DP, Malabanan CM, Pencek RR, Granner DK, and Wasserman DH.** Hexokinase II overexpression improves exercise-stimulated but not insulin-stimulated muscle glucose uptake in high-fat-fed C57BL/6J mice. *Diabetes* 53: 306-314, 2004.

108. **Fugmann A, Lind L, Andersson PE, Millgard J, Hanni A, Berne C, and Lithell H.** The effect of euglucaemic hyperinsulinaemia on forearm blood flow and glucose uptake in the human forearm. *Acta Diabetol* 35: 203-206, 1998.

109. **Furnsinn C, Neschen S, Wagner O, Roden M, Bisschop M, and Waldhausl W.** Acute and chronic exposure to tumor necrosis factor-alpha fails to affect insulin-stimulated glucose metabolism of isolated rat soleus muscle. *Endocrinology* 138: 2674-2679, 1997.

110. **Gaudreault N, Santure M, Pitre M, Nadeau A, Marette A, and Bachelard H.** Effects of insulin on regional blood flow and glucose uptake in Wistar and Sprague-Dawley rats. *Metabolism* 50: 65-73, 2001.

111. **Gelfand RA and Barrett EJ.** Effects of physiologic hyperinsulinemia on skeletal muscle protein synthesis and breakdown in man. *J Clin Invest* 80: 1-6, 1987.

112. **Goetz KL, Wang BC, Madwed JB, Zhu JL, and Leadley RJ, Jr.** Cardiovascular, renal, and endocrine responses to intravenous endothelin in conscious dogs. *Am J Physiol* 255: R1064-R1068, 1988.

113. **Goetze S, Kintscher U, Kawano H, Kawano Y, Wakino S, Fleck E, Hsueh WA, and Law RE.** Tumor necrosis factor alpha inhibits insulin-induced mitogenic signaling in vascular smooth muscle cells. *J Biol Chem* 275: 18279-18283, 2000.

114. **Gorczynski RJ, Klitzman B, and Duling BR.** Interrelations between contracting striated muscle and precapillary microvessels. *Am J Physiol* 235: H494-H504, 1978.

115. **Grant RT and Wright HP.** Anatomical basis for non-nutritive circulation in skeletal muscle exemplified by blood vessels of rat biceps femoris tendon. *J Anat* 106: 125-133, 1970.

116. **Gray RS, Scarlett JA, Griffin J, Olefsky JM, and Kolterman OG.** In vivo deactivation of peripheral, hepatic, and pancreatic insulin action in man. *Diabetes* 31: 929-936, 1982.

117. **Greene EC.** Anatomy of the rat. *New York: Hafner Publishing Co.* 1968.

118. **Grunfeld C and Feingold KR.** The metabolic effects of tumor necrosis factor and other cytokines. *Cytokines Biotherapy* 3: 143-158, 1991.

119. **Gudbjornsdottir S, Sjostrand M, Strindberg L, and Lonnroth P.** Decreased muscle capillary permeability surface area in type 2 diabetic subjects. *J Clin Endocrinol Metab* 90: 1078-1082, 2005.

120. **Guo D and Donner DB.** Tumor necrosis factor promotes phosphorylation and binding of insulin receptor substrate 1 to phosphatidylinositol 3-kinase in 3T3-L1 adipocytes. *J Biol Chem* 271: 615-618, 1996.

121. **Halseth AE, Bracy DP, and Wasserman DH.** Functional limitations to glucose uptake in muscles comprised of different fiber types. *Am J Physiol Endocrinol Metab* 280: E994-E999, 2001.

122. **Halseth AE, Bracy DP, and Wasserman DH.** Limitations to basal and insulin-stimulated skeletal muscle glucose uptake in the high-fat-fed rat. *Am J Physiol Endocrinol Metab* 279: E1064-E1071, 2000.

123. **Halseth AE, Bracy DP, and Wasserman DH.** Limitations to exercise- and maximal insulin-stimulated muscle glucose uptake. *J Appl Physiol* 85: 2305-2313, 1998.

124. **Hamilton-Wessler M, Ader M, Dea MK, Moore D, Loftager M, Markussen J, and Bergman RN.** Mode of transcapillary transport of insulin and insulin analog NN304 in dog hindlimb: evidence for passive diffusion. *Diabetes* 51: 574-582, 2002.

125. **Hammersen F.** The terminal vascular bed in skeletal muscle with special regard to the problem of shunts. In: Capillary Permeability. The Transfer of Molecules and Ions Between Capillary Blood and Tissue", edited by Crone C and Lassen NA: *Munksgaard Copenhagen*, 1970, p. 351-371.

126. **Handoko K, Yang K, Strutt B, Khalil W, and Killinger D.** Insulin attenuates the stimulatory effects of tumor necrosis factor alpha on 11beta-hydroxysteroid dehydrogenase 1 in human adipose stromal cells. *J Steroid Biochem Mol Biol* 72: 163-168, 2000.

127. **Hansen-Smith FM, Watson L, Lu DY, and Goldstein I.** Griffonia simplicifolia I: fluorescent tracer for microcirculatory vessels in nonperfused thin muscles and sectioned muscle. *Microvasc Res* 36: 199-215, 1988.

128. **Haraldsson B and Johansson BR.** Changes in transcapillary exchange induced by perfusion fixation with glutaraldehyde, followed by measurements of capillary filtration coefficient, diffusion capacity and albumin clearance. *Acta Physiol Scand* 124: 99-106, 1985.

129. **Haring HU, Biermann E, and Kemmler W.** Relation of insulin receptor occupancy and deactivation of glucose transport. *Am J Physiol* 242: E234-E240, 1982.

130. **Harrison DK, Birkenhake S, Knauf SK, and Kessler M.** Local oxygen supply and blood flow regulation in contracting muscle in dogs and rabbits. *J Physiol (Lond)* 422: 227-243, 1990.

131. **Hausberg M, Mark AL, Hoffman RP, Sinkey CA, and Anderson EA.** Dissociation of sympathoexcitatory and vasodilator actions of modestly elevated plasma insulin levels. *J Hypertens* 13: 1015-1021, 1995.

132. **Hellsten Y, Frandsen U, Orthenblad N, Sjodin B, and Richter EA.** Xanthine oxidase in human skeletal muscle following eccentric exercise: a role in inflammation. *J Physiol (Lond)* 498: 239-248, 1997.

133. **Herkner H, Klein N, Joukhadar C, Lackner E, Langenberger H, Frossard M, Bieglmayer C, Wagner O, Roden M, and Muller M.** Transcapillary insulin transfer in human skeletal muscle. *Eur J Clin Invest* 33: 141-146, 2003.

134. **Hermann TS, Rask-Madsen C, Ihlemann N, Dominguez H, Jensen CB, Storgaard H, Vaag AA, Kober L, and Torp-Pedersen C.** Normal insulin-stimulated endothelial function and impaired insulin-stimulated muscle glucose uptake in young adults with low birth weight. *J Clin Endocrinol Metab* 88: 1252-1257, 2003.

135. **Hester RL, Eraslan A, and Saito Y.** Differences in EDNO contribution to arteriolar diameters at rest and during functional dilation in striated muscle. *Am J Physiol* 265: H146-H151, 1993.

136. **Hettiarachchi M, Parsons KM, Richards SM, Dora KM, Rattigan S, Colquhoun EQ, and Clark MG.** Vasoconstrictor-mediated release of lactate from the perfused rat hindlimb. *J Appl Physiol* 73: 2544-2551, 1992.

137. **Holmang A, Mimura K, Bjorntorp P, and Lonnroth P.** Interstitial muscle insulin and glucose levels in normal and insulin- resistant Zucker rats. *Diabetes* 46: 1799-1804, 1997.

138. **Holmang A, Muller M, Andersson OK, and Lonnroth P.** Minimal influence of blood flow on interstitial glucose and lactate-normal and insulin-resistant muscle. *Am J Physiol* 274: E446-E452, 1998.

139. **Honig CR, Odoroff CL, and Frierson JL.** Active and passive capillary control in red muscle at rest and in exercise. *Am J Physiol* 243: H196-H206, 1982.

140. **Hotamisligil GS.** Mechanisms of TNF-alpha-induced insulin resistance. Exp Clin Endocrinol *Diabetes* 107: 119-125, 1999.

141. **Hotamisligil GS.** Molecular mechanisms of insulin resistance and the role of the adipocyte. *Int J Obes Relat Metab Disord* 24 Suppl 4:S23-7.: S23-S27, 2000.

142. **Hotamisligil GS, Shargill NS, and Spiegelman BM.** Adipose expression of tumor necrosis factor-alpha: Direct role in obesity- linked insulin resistance. *Science* 259: 87-91, 1993.

143. **Hotamisligil GS and Spiegelman BM.** Tumor necrosis factor alpha: a key component of the obesity-diabetes link. *Diabetes* 43: 1271-1278, 1994.

144. **Hudlicka O.** Basic mechanisms regulating muscle blood flow. In: Muscle blood flow: Its relation to muscle metabolism and function. Amersterdam: *Swets & Zeitlinger,* 1973, p. 29-54.

145. **Hulthen UL, Endre T, Mattiasson I, and Berglund G.** Insulin and forearm vasodilation in hypertension-prone men. *Hypertension* 25: 214-218, 1995.

146. **Hundal HS, Marette A, Mitsumoto Y, Ramlal T, Blostein R, and Klip A.** Insulin induces translocation of the alpha 2 and beta 1 subunits of the Na+/K(+)-ATPase from intracellular compartments to the plasma membrane in mammalian skeletal muscle. *J Biol Chem* 267: 5040-5043, 1992.

147. **Hunter SJ, Harper R, Ennis CN, Sheridan B, Atkinson AB, and Bell PM.** Skeletal muscle blood flow is not a determinant of insulin resistance in essential hypertension. *J Hypertens* 15: 73-77, 1997.

148. **Idris I, Patiag D, Gray S, and Donnelly R.** Tissue- and time-dependent effects of endothelin-1 on insulin-stimulated glucose uptake. *Biochem Pharmacol* 62: 1705-1708, 2001.

149. **Iversen PO and Nicolaysen G.** High correlation of fractals for regional blood flows among resting and exercising skeletal muscles. *Am J Physiol* 269: H7-H13, 1995.

150. **Iwashita S, Yanagi K, Ohshima N, and Suzuki M.** Insulin increases blood flow rate in the microvasculature of cremaster muscle of the anesthetized rats. *In Vivo* 15: 11-15, 2001.

151. **Jackson RA, Hamling JB, Blix PM, Sim BM, Hawa MI, Jaspan JB, Belin, J, and Nabarro JD.** The influence of graded hyperglycemia with and without physiological hyperinsulinemia on forearm glucose uptake and other metabolic responses in man. *J Clin Endocrinol Metab* 63: 594-604, 1986.

152. **James DE, Burleigh KM, and Kraegen EW.** Time dependence of insulin action in muscle and adipose tissue in the rat in vivo. An increasing response in adipose tissue with time. *Diabetes* 34: 1049-1054, 1985.

153. **James DE, Burleigh KM, Storlien LH, Bennett SP, and Kraegen EW.** Heterogeneity of insulin action in muscle: influence of blood flow. *Am J Physiol* 251: E422-E430, 1986.

154. **James DE, Jenkins AB, and Kraegen EW.** Heterogeneity of insulin action in individual muscles in vivo: euglycemic clamp studies in rats. *Am J Physiol* 248: E567-E574, 1985.

155. **Jansson PA, Fowelin JP, von Schenck HP, Smith UP, and Lonnroth PN.** Measurement by microdialysis of the insulin concentration in subcutaneous interstitial fluid. Importance of the endothelial barrier for insulin. *Diabetes* 42: 1469-1473, 1993.

156. **Jarasch ED, Bruder G, and Heid HW.** Significance of xanthine oxidase in capillary endothelial cells. *Acta Physiol Scand Suppl.*548: 39-46, 1986.

157. **Jayaweera AR, Edwards N, Glasheen WP, Villanueva FS, Abbott RD, and Kaul S.** In vivo myocardial kinetics of air-filled albumin microbubbles during myocardial contrast echocardiography. Comparison with radiolabeled red blood cells. *Circ Res* 74: 1157-1165, 1994.

158. **Johnson JM, Pergola PE, Liao FK, Kellogg DL, Jr., and Crandall CG.** Skin of the dorsal aspect of human hands and fingers possesses an active vasodilator system. *J Appl Physiol* 78: 948-954, 1995.

159. **Juan CC, Fang VS, Huang YJ, Kwok CF, Hsu YP, and Ho LT.** Endothelin-1 induces insulin resistance in conscious rats. *Biochem Biophys Res Commun* 227: 694-699, 1996.

160. **Kahn NN, Acharya K, Bhattacharya S, Acharya R, Mazumder S, Bauman WA, and Sinha AK.** Nitric oxide: the "second messenger" of insulin. *IUBMB Life* 49: 441-450, 2000.

161. **Kano Y, Sampei K, and Matsudo H.** Time course of capillary structure changes in rat skeletal muscle following strenuous eccentric exercise. *Acta Physiol Scand* 180: 291-299, 2004.

162. **Kapur S, Bedard S, Marcotte B, Cote CH, and Marette A.** Expression of nitric oxide synthase in skeletal muscle: a novel role for nitric oxide as a modulator of insulin action. *Diabetes* 46: 1691-1700, 1997.

163. **Kasuga M, Zick Y, Blith DL, Karlsson FA, Haring HU, and Kahn CR.** Insulin stimulation of phosphorylation of the beta subunit of the insulin receptor. Formation of both phosphoserine and phosphotyrosine. *J Biol Chem* 257: 9891-9894, 1982.

164. **Kelley DE, Reilly JP, Veneman T, and Mandarino LJ.** Effects of insulin on skeletal muscle glucose storage, oxidation, and glycolysis in humans. *Am J Physiol* 258: E923-E929, 1990.

165. **Kim F, Gallis B, and Corson MA.** TNF-alpha inhibits flow and insulin signaling leading to NO production in aortic endothelial cells. *Am J Physiol Cell Physiol* 280: C1057-C1065, 2000.

166. **King GL and Johnson SM.** Receptor-mediated transport of insulin across endothelial cells. *Science* 227: 1583-1586, 1985.

167. **Kobzik L, Reid MB, Bredt DS, and Stamler JS.** Nitric oxide in skeletal muscle. *Nature* 372: 546-548, 1994.

168. **Kolka CM, Rattigan S, Rachards SM, and Clark MG.** Endothelin-1 as a messenger for insulin has both stimulatory and inhibitory effects on perfused muscle metabolism via its vascular actions. *Diabetes* 53: A368, 2004.

169. **Kraegen EW, James DE, Jenkins AB, and Chisholm DJ.** Dose-response curves for in vivo insulin sensitivity in individual tissues in rats. *Am J Physiol* 248: E353-E362, 1985.

170. **Kuznetsova LV, Tomasek N, Sigurdsson GH, Banic A, Erni D, and Wheatley AM.** Dissociation between volume blood flow and laser-Doppler signal from rat muscle during changes in vascular tone. *Am J Physiol* 274: H1248-H1254, 1998.

171. **Laakso M, Edelman SV, Brechtel G, and Baron AD.** Decreased effect of insulin to stimulate skeletal muscle blood flow in obese man. *J Clin Invest* 85: 1844-1852, 1990.

172. **Laakso M, Edelman SV, Brechtel G, and Baron AD.** Impaired insulin-mediated skeletal muscle blood flow in patients with NIDDM. *Diabetes* 41: 1076-1083, 1992.

173. **Laine H, Knuuti MJ, Ruotsalainen U, Raitakari M, Iida H, Kapanen J, Kirvela O, Haaparanta M, Yki-Jarvinen H, and Nuutila P.** Insulin resistance in essential hypertension is characterized by impaired insulin stimulation of blood flow in skeletal muscle. *J Hypertens* 16: 211-219, 1998.

174. **Laine H, Yki-Jarvinen H, Kirvela O, Tolvanen T, Raitakari M, Solin O, Haaparanta M, Knuuti J, and Nuutila P.** Insulin resistance of glucose uptake in skeletal muscle cannot be ameliorated by enhancing endothelium-dependent blood flow in obesity. *J Clin Invest* 101: 1156-1162, 1998.

175. **Laitinen L.** Griffonia simplicifolia lectins bind specifically to endothelial cells and some epithelial cells in mouse tissues. *Histochem J* 19: 225-234, 1987.

176. **Lang CH.** IGF-I stimulates muscle glucose uptake during sepsis. *Shock* 5: 22-27, 1996.

177. **Lang CH,** Dobrescu C, and Bagby GJ. Tumor necrosis factor impairs insulin action on peripheral glucose disposal and hepatic glucose output. *Endocrinology* 130: 43-52, 1992.

178. **Lassen NA and Perl W.** Tracer kinetic methods in medical physiology. *New York: NY; Raven Press,* 1979.

179. **Lechleitner M, Koch T, Herold M, Dzien A, and Hoppichler F.** Tumour necrosis factor-alpha plasma level in patients with type 1 diabetes mellitus and its association with glycaemic control and cardiovascular risk factors. *J Intern Med* 248: 67-76, 2000.

180. **Lee YC, Juan CC, Fang VS, Hsu YP, Lin SH, Kwok CF, and Ho LT.** Evidence that endothelin-1 (ET-1) inhibits insulin-stimulated glucose uptake in rat adipocytes mainly through ETA receptors. *Metabolism* 47: 1468-1471, 1998.

181. **Lembo G, Napoli R, Capaldo B, Rendina V, Iaccarino G, Volpe M, and Sacca L.** Abnormal sympathetic overactivity evoked by insulin in the skeletal muscle of patients with essential hypertension. *J Clin Invest* 90: 24-29, 1992.

182. **LeRoith D.** Insulin-like growth factor I receptor signaling--overlapping or redundant pathways? *Endocrinology* 141: 1287-1288, 2000.

183. **LeRoith D, Werner H, Beitner-Johnson D, and Roberts CT, Jr.** Molecular and cellular aspects of the insulin-like growth factor I receptor. *Endocr Rev* 16: 143-163, 1995.

184. **Levin ER.** Endothelins. *N Engl J Med* 333: 356-363, 1995.

185. **Lewis SB, Schultz TA, Daniels EL, Bliziotes MM, and Montague W.** Prolonged effect of insulin on glucose uptake by rat skeletal muscle. *Biochem J* 186: 733-738, 1980.

186. **Liang C, Doherty JU, Faillace R, Maekawa K, Arnold S, Gavras H, and Hood WB, Jr.** Insulin infusion in conscious dogs. Effects on systemic and coronary hemodynamics, regional blood flows, and plasma catecholamines. *J Clin Invest* 69: 1321-1336, 1982.

187. **Lind L, Fugmann A, Branth S, Vessby B, Millgard J, Berne C, and Lithell H.** The impairment in endothelial function induced by non-esterified fatty acids can be reversed by insulin. *Clin Sci (Colch)* 99: 169-174, 2000.

188. **Lindbom L and Arfors KE.** Mechanism and site of control for variation in the number of perfused capillaries in skeletal muscle. *Int J Microcirc Clin Exp* 4: 19-30, 1985.

189. **Lindbom L and Arfors KE.** Non-homogeneous blood flow distribution in the rabbit tenuissimus muscle Differential control of total blood flow and capillary perfusion. *Acta Physiol Scand* 122: 225-233, 1984.

190. **Lindbom L, Tuma RF, and Arfors KE.** Influence of oxygen on perfused capillary density and capillary red cell velocity in rabbit skeletal muscle. *Microvasc Res* 19: 197-208, 1980.

191. **Lindner JR, Villanueva FS, Dent JM, Wei K, Sklenar J, and Kaul S.** Assessment of resting perfusion with myocardial contrast echocardiography: theoretical and practical considerations. *Am Heart J* 139: 231-240, 2000.

192. **Ling PR, Bistrian BR, Mendez B, and Istfan NW.** Effects of systemic infusions of endotoxin, tumor necrosis factor, and interleukin-1 on glucose metabolism in the rat: relationship to endogenous glucose production and peripheral tissue glucose uptake. *Metabolism* 43: 279-284, 1994.

193. **Ling PR, Sierra P, Qu Z, and Bistrian BR.** Insulin-like growth factor-I improves glucose utilization in tumor necrosis factor-treated rats under hyperinsulinemic-euglycemic conditions. *Metabolism* 46: 1052-1058, 1997.

194. **Lombard JH and Roman RJ.** Assessment of muscle blood flow by laser-Doppler flowmetry during hemorrhage in SHR. *Am J Physiol* 259: H860-H865, 1990.

195. **Lundgren F, Eden E, Arfvidsson B, and Lundholm K.** Insulin time-dependent effects on the leg exchange of glucose and amino acids in man. *Eur J Clin Invest* 21: 421-429, 1991.

196. **Mahajan H, Rachards SM, Rattigan S, and Clark MG.** Local infusion of an inhibitor of Ca2+ dependent K+ channels (TEA), but not L-NAME blocks insulin-mediated capillary recruitment and glucose uptake in muscle in vivo. *Diabetes* 54, 2005 [Abstract] (in press).

197. **Mahajan H, Richards SM, Rattigan S, and Clark MG.** Local methacholine but not bradykinin potentiates insulin-mediated glucose uptake in muscle in vivo by augmenting capillary recruitment. *Diabetologia* 47: 2226-2234, 2004.

198. **Mak RH.** Insulin resistance but IGF-I sensitivity in chronic renal failure. *Am J Physiol* 271: F114-F119, 1996.

199. **Makimattila S, Virkamaki A, Groop PH, Cockcroft J, Utriainen T, Fagerudd J, and Yki-Jarvinen H.** Chronic hyperglycemia impairs endothelial function and insulin sensitivity via different mechanisms in insulin-dependent diabetes mellitus. *Circulation* 94: 1276-1282, 1996.

200. **Margolis RU and Altszuler N.** Insulin in the cerebrospinal fluid. *Nature* 215: 1375-1376, 1967.

201. **Mather K, Laakso M, Edelman S, Hook G, and Baron A.** Evidence for physiological coupling of insulin-mediated glucose metabolism and limb blood flow. *Am J Physiol Endocrinol Metab* 279: E1264-E1270, 2000.

202. **Mather KJ, Mirzamohammadi B, Lteif A, Steinberg HO, and Baron AD.** Endothelin contributes to basal vascular tone and endothelial dysfunction in human obesity and type 2 diabetes. *Diabetes* 51: 3517-3523, 2002.

203. **Mathias CJ, da Costa DF, Fosbraey P, Christensen NJ, and Bannister R.** Hypotensive and sedative effects of insulin in autonomic failure. *Br Med J (Clin Res Ed)* 295: 161-163, 1987.

204. **McEniery CM, Wilkinson IB, Jenkins DG, and Webb DJ.** Endogenous endothelin-1 limits exercise-induced vasodilation in hypertensive humans. *Hypertension* 40: 202-206, 2002.

205. **McKay MK and Hester RL.** Role of nitric oxide, adenosine, and ATP-sensitive potassium channels in insulin-induced vasodilation. *Hypertension* 28: 202-208, 1996.

206. **McVeigh GE, Brennan GM, Johnston GD, McDermott BJ, McGrath LT, HenryWR., Andrews JW, and Hayes JR.** Impaired endothelium-dependent and independent vasodilation in patients with type 2 (non-insulin-dependent) diabetes mellitus. *Diabetologia* 35: 771-776, 1992.

207. **Metsarinne K, Saijonmaa O, Yki-Jarvinen H, and Fyhrquist F.** Insulin increases the release of endothelin in endothelial cell cultures in vitro but not in vivo. *Metabolism* 43: 878-882, 1994.

208. **Miles PD, Li S, Hart M, Romeo O, Cheng J, Cohen A, Raafat K, Moossa AR, and Olefsky JM.** Mechanisms of insulin resistance in experimental hyperinsulinemic dogs. *J Clin Invest* 101: 202-211, 1998.

209. **Miles PDG, Levisetti M, Reichart D, Khoursheed M, Moossa AR, and Olefsky JM.** Kinetics of insulin action in vivo - Identification of rate-limiting steps. *Diabetes* 44: 947-953, 1995.

210. **Milton SG and Knutson VP.** Insulin receptor characterization and function in bovine aorta endothelial cells: insulin degradation by a plasma membrane, protease-resistant insulin receptor. *J Cell Physiol* 157: 333-343, 1993.

211. **Mishima Y, Kuyama A, Tada A, Takahashi K, Ishioka T, and Kibata M.** Relationship between serum tumor necrosis factor-alpha and insulin resistance in obese men with Type 2 diabetes mellitus. *Diabetes Res Clin Pract* 52: 119-123, 2001.

212. **Montagnani M, Ravichandran LV, Chen H, Esposito DL, and Quon MJ.** Insulin receptor substrate-1 and phosphoinositide-dependent kinase-1 are required for insulin-stimulated production of nitric oxide in endothelial cells. *Mol Endocrinol* 16: 1931-1942, 2002.

213. **Morgan DA, Balon TW, Ginsberg BH, and Mark AL.** Nonuniform regional sympathetic nerve responses to hyperinsulinemia in rats. *Am J Physiol* 264: R423-R427, 1993.

214. **Mossberg KA and Taegtmeyer H.** Time course of skeletal muscle glucose uptake during euglycemic hyperinsulinemia in the anesthetized rabbit: a fluorine-18-2-deoxy-2-fluoro-D-glucose study. *J Nucl Med* 33: 1523-1529, 1992.

215. **Muller M, Holmang A, Andersson OK, Eichler HG, and Lonnroth P.** Measurement of interstitial muscle glucose and lactate concentrations during an oral glucose tolerance test. *Am J Physiol* 271: E1003-E1007, 1996.

216. **Muntzel MS, Anderson EA, Johnson AK, and Mark AL.** Mechanisms of insulin action on sympathetic nerve activity. *Clin Exp Hypertens* 17: 39-50, 1995.

217. **Muntzel MS, Morgan DA, Mark AL, and Johnson AK.** Intracerebroventricular insulin produces nonuniform regional increases in sympathetic nerve activity. *Am J Physiol* 267: R1350-R1355, 1994.

218. **Murphy LA and Goldstein IJ.** Five alpha-D-galactopyranosyl-binding isolectins from Bandeiraea simplicifolia seeds. *J Biol Chem* 252: 4739-4742, 1977.

219. **Murrant CL and Sarelius IH.** Coupling of muscle metabolism and muscle blood flow in capillary units during contraction. *Acta Physiol Scand* 168: 531-541, 2000.

220. **Myrhage R and Eriksson E.** Vascular arrangements in hindlimb muscles of the cat. *J Anat* 131: 1-17, 1980.

221. **Natali A.** Skeletal muscle blood flow and insulin action. *Nutr Metab Cardiovasc Dis* 7: 105-109, 1997.

222. **Natali A, Baldeweg S, Toschi E, Capaldo B, Barbaro D, Gastaldelli A, Yudkin JS, and Ferrannini E.** Vascular effects of improving metabolic control with metformin or rosiglitazone in type 2 diabetes. *Diabetes Care* 27: 1349-1357, 2004.

223. **Natali A, Bonadonna R, Santoro D, Galvan AQ, Baldi S, Frascerra S, Palombo C, Ghione S, and Ferrannini E.** Insulin resistance and vasodilation in essential hypertension. Studies with adenosine. *J Clin Invest* 94: 1570-1576, 1994.

224. **Natali A, Quinones GA, Pecori N, Sanna G, Toschi E, and Ferrannini E.** Vasodilation with sodium nitroprusside does not improve insulin action in essential hypertension. *Hypertension* 31: 632-636, 1998.

225. **Natali A, Santoro D, Palombo C, Cerri M, Ghione S, and Ferrannini E.** Impaired insulin action on skeletal muscle metabolism in essential hypertension. *Hypertension* 17: 170-178, 1991.

226. **Natali A, Taddei S, Galvan AQ, Camastra S, Baldi S, Frascerra S, Virdis, Sudano I, Salvetti A, and Ferrannini E.** Insulin sensitivity, vascular reactivity, and clamp-induced vasodilatation in essential hypertension. *Circulation* 96: 849-855, 1997.

227. **Newman JM, Dora KA, Rattigan S, Edwards SJ, Colquhoun EQ, and Clark MG.** Norepinephrine and serotonin vasoconstriction in rat hindlimb control different vascular flow routes. *Am J Physiol* 270: E689-E699, 1996.

228. **Newman JM, Steen JT, and Clark MG.** Vessels supplying septa and tendons as functional shunts in perfused rat hindlimb. *Microvasc Res* 54: 49-57, 1997.

229. **Nilsson J, Jovinge S, Niemann A, Reneland R, and Lithell H.** Relation between plasma tumor necrosis factor-alpha and insulin sensitivity in elderly men with non-insulin-dependent diabetes mellitus. *Arterioscler Thromb Vasc Biol* 18: 1199-1202, 1998.

230. **Nolan JJ, Ludvik B, Baloga J, Reichart D, and Olefsky JM.** Mechanisms of the kinetic defect in insulin action in obesity and NIDDM. *Diabetes* 46: 994-1000, 1997.

231. **Nolte LA, Hansen PA, Chen MM, Schluter JM, Gulve EA, and Holloszy JO.** Short-term exposure to tumor necrosis factor-alpha does not affect insulin-stimulated glucose uptake in skeletal muscle. *Diabetes* 47: 721-726, 1998.

232. **Nuutila P, Knuuti MJ, Heinonen OJ, Ruotsalainen U, Teras M, Bergman J, Solin O, Yki-Jarvinen H, Voipio-Pulkki LM and Wegelius U.** Different alterations in the

insulin-stimulated glucose uptake in the athlete's heart and skeletal muscle. *J Clin Invest* 93: 2267-2274, 1994.

233. **Nuutila P, Raitakari M, Laine H, Kirvela O, Takala T, Utriainen T, Makimattila S, Pitkanen OP, Ruotsalainen U, Iida H, Knuuti J, and Yki-Jarvinen H.** Role of blood flow in regulating insulin-stimulated glucose uptake in humans. Studies using bradykinin, [15O]water, and [18F]fluoro-deoxy- glucose and positron emission tomography. *J Clin Invest* 97: 1741-1747, 1996.

234. **O'Doherty RM, Halseth AE, Granner DK, Bracy DP, and Wasserman DH.** Analysis of insulin-stimulated skeletal muscle glucose uptake in conscious rat using isotopic glucose analogs. *Am J Physiol* 274: E287-E296, 1998.

235. **Offner F, Philippe J, Vogelaers D, Colardyn F, Baele G, Baudrihaye M, Vermeulen A, and Leroux-Roels G.** Serum tumor necrosis factor levels in patients with infectious disease and septic shock. *J Lab Clin Med* 116: 100-105, 1990.

236. **Okamoto H, Hudetz AG, Roman RJ, Bosnjak ZJ, and Kampine JP.** Neuronal NOS-derived NO plays permissive role in cerebral blood flow response to hypercapnia. *Am J Physiol* 272: H559-H566, 1997.

237. **Oliver FJ, de la RG, Feener EP, Lee ME, Loeken MR, Shiba T, Quertermous T, and King GL.** Stimulation of endothelin-1 gene expression by insulin in endothelial cells. *J Biol Chem* 266: 23251-23256, 1991.

238. **Oltman CL, Kane NL, Gutterman DD, Bar RS, and Dellsperger KC.** Mechanism of coronary vasodilation to insulin and insulin-like growth factor I is dependent on vessel size. *Am J Physiol Endocrinol Metab* 279: E176-E181, 2000.

239. **Omatsu-Kanbe M and Kitasato H.** Insulin stimulates the translocation of Na+/K(+)-dependent ATPase molecules from intracellular stores to the plasma membrane in frog skeletal muscle. *Biochem* J 272: 727-733, 1990.

240. **O'Shaughnessy IM, Myers TJ, Stepniakowski K, Nazzaro P, Kelly TM, Hoffmann RG, Egan BM, and Kissebah AH.** Glucose metabolism in abdominally obese hypertensive and normotensive subjects. *Hypertension* 26: 186-192, 1995.

241. **Ottosson-Seeberger A, Lundberg JM, Alvestrand A, and Ahlborg G.** Exogenous endothelin-1 causes peripheral insulin resistance in healthy humans. *Acta Physiol Scand* 161: 211-220, 1997.

242. **Pappenheimer JR.** Vasoconstrictor nerves and oxygen consumption in the isolated perfused hindlimb muscles of the dog. J Physiol (Lond) 99: 182-200, 1941.

243. **Pedersen O and Beck-Nielsen H.** Insulin resistance and insulin-dependent diabetes mellitus. *Diabetes Care* 10: 516-523, 1987.

244. **Pelberg RA, Wei K, Kamiyama N, Sklenar J, Bin J, and Kaul S.** Potential advantage of flash echocardiography for digital subtraction of B-mode images acquired during myocardial contrast echocardiography. *J Am Soc Echocardiogr* 12: 85-93, 1999.

245. **Pendergast DR, Krasney JA, Ellis A, McDonald B, Marconi C, and Cerretelli P.** Cardiac output and muscle blood flow in exercising dogs. *Respir Physiol* 61: 317-326, 1985.

246. **Penschow JD, Giles ME, Coghlan JP, and Fernley RT.** Redistribution of carbonic anhydrase VI expression from ducts to acini during development of ovine parotid and submandibular glands. *HistochemCell Biol* 107: 417-422, 1997.

247. **Peraldi P, Hotamisligil GS, Buurman WA, White MF, and Spiegelman BM.** Tumor necrosis factor (TNF)-alpha inhibits insulin signaling through stimulation of the p55 TNF receptor and activation of sphingomyelinase. *J Biol Chem* 271: 13018-13022, 1996.

248. **Pereda SA, Eckstein JW, and Abboud FM.** Cardiovascular responses to insulin in the absence of hypoglycemia. *Am J Physiol* 202: 249-252, 1962.

249. **Persson MG, Gustafsson LE, Wiklund NP, Hedqvist P, and Moncada S.** Endogenous nitric oxide as a modulator of rabbit skeletal muscle micro- circulation in vivo. *Br J Pharmacol* 100: 463-466, 1990.

250. **Persson MG, Wiklund NP, and Gustafsson LE.** Nitric oxide requirement for vasomotor nerve-induced vasodilatation and modulation of resting blood flow in muscle microcirculation. *Acta Physiol Scand* 141: 49-56, 1991.

251. **Peters BP and Goldstein IJ.** The use of fluorescein-conjugated Bandeiraea simplicifolia B4-isolectin as a histochemical reagent for the detection of alpha-D-galactopyranosyl groups. Their occurrence in basement membranes. *Exp Cell Res* 120: 321-334, 1979.

252. **Petrie JR, Ueda S, Webb DJ, Elliott HL, and Connell JM.** Endothelial nitric oxide production and insulin sensitivity. A physiological link with implications for pathogenesis of cardiovascular disease. *Circulation* 93: 1331-1333, 1996.

253. **Philippe J, Halban PA, Gjinovci A, Duckworth WC, Estreicher J, and Renold AE.** Increased clearance and degradation of [3H]insulin in streptozotocin diabetic rats. *J Clin Invest* 67: 673-680, 1981.

254. **Piatti PM, Monti LD, Conti M, Baruffaldi L, Galli L, Phan CV, Guazzini B, Pontiroli AE, and Pozza G.** Hypertriglyceridemia and hyperinsulinemia are potent inducers of endothelin-1 release in humans. *Diabetes* 45: 316-321, 1996.

255. **Piiper J, Marconi C, Heisler N, Meyer M, Weitz H, Pendergast DR, and Cerretelli P.** Spatial and temporal variability of blood flow in stimulated dog gastrocnemius muscle. *Adv Exp Med Biol* 248: 719-743, 1989.

256. **Piiper J, Pendergast DR, Marconi C, Meyer M, Heisler N, and Cerretelli P.** Blood flow distribution in dog gastrocnemius muscle at rest and during stimulation. *J Appl Physiol* 58: 2068-2074, 1985.

257. **Piiper J and Rosell S.** Attempt to demonstrate large arteriovenous shunts in skeletal muscle during stimulation of sympathetic vasodilator nerves. *Acta Physiol Scand* 53: 214-217, 1961.

258. **Pitkanen OP, Laine H, Kemppainen J, Eronen E, Alanen A, Raitakari M, Kirvela O, Ruotsalainen U, Knuuti J, Koivisto VA, and Nuutila P.** Sodium nitroprusside increases human skeletal muscle blood flow, but does not change flow distribution or glucose uptake. *J Physiol (Lond)* 521: 729-737, 1999.

259. **Pitre M, Nadeau A, and Bachelard H.** Insulin sensitivity and hemodynamic responses to insulin in Wistar-Kyoto and spontaneously hypertensive rats. *Am J Physiol* 271: E658-668, 1996.

260. **Plusczyk T, Bersal B, Menger MD, and Feifel G.** Differential effects of ET-1, ET-2, and ET-3 on pancreatic microcirculation, tissue integrity, and inflammation. *Dig Dis Sci* 46: 1343-1351, 2001.

261. **Pollare T, Lithell H, and Berne C.** Insulin resistance is a characteristic feature of primary hypertension independent of obesity. *Metabolism* 39: 167-174, 1990.

262. **Porter JP, Joshua IG, Kabithe D, and Bokil HS.** Vasodilator effect of insulin on the microcirculation of the rat cremaster muscle. *Life Sci* 61: 673-684, 1997.

263. **Potter RF and Groom AC.** Capillary diameter and geometry in cardiac and skeletal muscle studied by means of corrosion casts. *Microvasc Res* 25: 68-84, 1983.

264. **Poulin RA, Steil GM, Moore DM, Ader M, and Bergman RN.** Dynamics of glucose production and uptake are more closely related to insulin in hindlimb lymph than in thoracic duct lymph. *Diabetes* 43: 180-190, 1994.

265. **Prager R, Wallace P, and Olefsky JM.** In vivo kinetics of insulin action on peripheral glucose disposal and hepatic glucose output in normal and obese subjects. *J Clin Invest* 78: 472-481, 1986.

266. **Rabinowitz D and Zierler KL.** Forearm metabolism in obesity and its response to intra-arterial insulin. Characterization of insulin resistance and evidence for adaptive hyperinsulinism. *J Clin Invest* 41:2173-81.: 2173-2181, 1962.

267. **Raitakari M, Knuuti MJ, Ruotsalainen U, Laine H, Makela P, Teras M, Sipila H, Niskanen T, and Raitakari OT.** Insulin increases blood volume in human skeletal muscle: studies using [15O]CO and positron emission tomography. *Am J Physiol* 269: E1000-E1005, 1995.

268. **Raitakari M, Nuutila P, Knuuti J, Raitakari OT, Laine H, Ruotsalainen U, Kirvela O, Takala TO, Iida H, and Yki-Jarvinen H.** Effects of insulin on blood flow and volume in skeletal muscle of patients with IDDM: studies using [15O]H2O, [15O]CO, and positron emission tomography. *Diabetes* 46: 2017-2021, 1997.

269. **Raitakari M, Nuutila P, Ruotsalainen U, Laine H, Teras M, Iida H, Makimattila S, Utriainen T, Oikonen V, and Sipila H.** Evidence for dissociation of insulin stimulation

of blood flow and glucose uptake in human skeletal muscle - Studies using [15O]H2O, [18F]fluoro-2-deoxy-D-glucose, and positron emission tomography. *Diabetes* 45: 1471-1477, 1996.

270. **Rask-Madsen C, Dominguez H, Ihlemann N, Hermann T, Kober L, and Torp-Pedersen C.** Tumor necrosis factor-alpha inhibits insulin's stimulating effect on glucose uptake and endothelium-dependent vasodilation in humans. *Circulation* 108: 1815-1821, 2003.

271. **Rattigan S, Appleby GJ, Miller KA, Steen JT, Dora KA, Colquhoun EQ, and Clark MG.** Serotonin inhibition of 1-methylxanthine metabolism parallels its vasoconstrictor activity and inhibition of oxygen uptake in perfused rat hindlimb. *Acta Physiol Scand* 161: 161-169, 1997.

272. **Rattigan S, Clark MG, and Barrett EJ.** Acute vasoconstriction-induced insulin resistance in rat muscle in vivo. *Diabetes* 48: 564-569, 1999.

273. **Rattigan S, Clark MG, and Barrett EJ.** Hemodynamic actions of insulin in rat skeletal muscle: evidence for capillary recruitment. *Diabetes* 46: 1381-1388, 1997.

274. **Rattigan S, Dora KA, Colquhoun EQ, and Clark MG.** Inhibition of insulin-mediated glucose uptake in rat hindlimb by an alpha-adrenergic vascular effect. *Am J Physiol* 268: E305-E311, 1995.

275. **Rattigan S, Dora KA, Colquhoun EQ, and Clark MG.** Serotonin-mediated acute insulin resistance in the perfused rat hindlimb but not in incubated muscle: a role for the vascular system. *Life Sci* 53: 1545-1555, 1993.

276. **Rattigan S, Dora KA, Tong ACY, and Clark MG.** Perfused skeletal muscle contraction and metabolism improved by angiotensin II-mediated vasoconstriction. *Am J Physiol* 271: E96-103, 1996.

277. **Rattigan S, Wallis MG, Youd JM, and Clark MG.** Exercise training improves insulin-mediated capillary recruitment in association with glucose uptake in rat hindlimb. *Diabetes* 50: 2659-2665, 2001.

278. **Renaudin C, Michoud E, Rapin JR, Lagarde M, and Wiernsperger N.** Hyperglycaemia modifies the reaction of microvessels to insulin in rat skeletal muscle. *Diabetologia* 41: 26-33, 1998.

279. **Renkin EM.** Control of microcirculation and blood-tissue exchange. In: Handbook of Physiology - The Cardiovascular System IV, edited by Renkin EM, Michel CC and Geiger SR: *American Physiological Society Bethesda*, 1984, p. 627-687.

280. **Rich S and McLaughlin VV.** Endothelin receptor blockers in cardiovascular disease. *Circulation* 108: 2184-2190, 2003.

281. **Richter EA, Ruderman NB, Gavras H, Belur ER, and Galbo H.** Muscle glycogenolysis during exercise: dual control by epinephrine and contractions. *Am J Physiol* 242: E25-E32, 1982.

282. **Rizza RA, Mandarino LJ, and Gerich JE.** Dose-response characteristics for effects of insulin on production and utilization of glucose in man. *Am J Physiol* 240: E630-E639, 1981.

283. **Rowe JW, Young JB, Minaker KL, Stevens AL, Pallotta J, and Landsberg L.** Effect of insulin and glucose infusions on sympathetic nervous system activity in normal man. *Diabetes* 30: 219-225, 1981.

284. **Ruderman NB, Houghton CR, and Hems R.** Evaluation of the isolated perfused rat hindquarter for the study of muscle metabolism. *Biochem J* 124: 639-651, 1971.

285. **Sarabi M, Lind L, Millgard J, Hanni A, Hagg A, Berne C, and Lithell H.** Local vasodilatation with metacholine, but not with nitroprusside, increases forearm glucose uptake. *Physiol Res* 48: 291-295, 1999.

286. **Sartori C, Trueb L, Nicod P, and Scherrer U.** Effects of sympathectomy and nitric oxide synthase inhibition on vascular actions of insulin in humans. *Hypertension* 34: 586-589, 1999.

287. **Sauter A, Goldstein M, Engel J, and Ueta K.** Effect of insulin on central catecholamines. *Brain Res* 260: 330-333, 1983.

288. **Scherrer U, Randin D, Vollenweider P, Vollenweider L, and Nicod P.** Nitric oxide release accounts for insulin's vascular effects in humans. *J Clin Invest* 94: 2511-2515, 1994.

289. **Schroeder CA, Jr, Chen YL, and Messina EJ.** Inhibition of NO synthesis or endothelium removal reveals a vasoconstrictor effect of insulin on isolated arterioles. *Am J Physiol* 276: H815-H820, 1999.

290. **Serne EH, Gans RO, ter Maaten JC, ter Wee PM, Donker AJ, and Stehouwer CD.** Capillary recruitment is impaired in essential hypertension and relates to insulin's metabolic and vascular actions. *Cardiovasc Res* 49: 161-168, 2001.

291. **Serne EH, IJzerman RG, Gans RO, Nijveldt R, De Vries G, Evertz R, Donker AJ, and Stehouwer CD.** Direct evidence for insulin-induced capillary recruitment in skin of healthy subjects during physiological hyperinsulinemia. *Diabetes* 51: 1515-1522, 2002.

292. **Serne EH, Stehouwer CD, ter Maaten JC, ter Wee PM, Rauwerda JA, Donker AJ, and Gans RO.** Microvascular Function Relates to Insulin Sensitivity and Blood Pressure in Normal Subjects. *Circulation* 99: 896-902, 1999.

293. **Shankar R, Zhu JS, Ladd B, Henry D, Shen HQ, and Baron AD.** Central nervous system nitric oxide synthase activity regulates insulin secretion and insulin action. *J Clin Invest* 102: 1403-1412, 1998.

294. **Shen HQ, Zhu JS, and Baron AD.** Dose-response relationship of insulin to glucose fluxes in the awake and unrestrained mouse. *Metabolism* 48: 965-970, 1999.

295. **Shulman GI.** Unraveling the cellular mechanism of insulin resistance in humans: new insights from magnetic resonance spectroscopy. *Physiology (Bethesda)* 19:183-90.: 183-190, 2004.

296. **Silvagno F, Xia HH, and Bredt DS.** Neuronal nitric-oxide synthase-æ, an alternatively spliced isoform expressed in differentiated skeletal muscle. *J Biol Chem* 271: 11204-11208, 1996.

297. **Sjostrand M, Gudbjornsdottir S, Holmang A, Lonn L, Strindberg L, and Lonnroth P.** Delayed transcapillary transport of insulin to muscle interstitial fluid in obese subjects. *Diabetes* 51: 2742-2748, 2002.

298. **Sjostrand M, Gudbjornsdottir S, Strindberg L, and Lonnroth P.** Delayed transcapillary delivery of insulin to muscle interstitial fluid after oral glucose load in obese subjects. *Diabetes* 54: 152-157, 2005.

299. **Sjostrand M, Holmang A, and Lonnroth P.** Measurement of interstitial insulin in human muscle. *Am J Physiol* 276: E151-E154, 1999.

300. **Sjostrand M, Holmang A, Strindberg L, and Lonnroth P.** Estimations of muscle interstitial insulin, glucose, and lactate in type 2 diabetic subjects. *Am J Physiol* 279: E1097-E1103, 2000.

301. **Smith D, Rossetti L, Ferrannini E, Johnson CM, Cobelli C, Toffolo G, Katz LD, and Defronzo RA.** In vivo glucose metabolism in the awake rat: tracer and insulin clamp studies. *Metabolism* 36: 1167-1174, 1987.

302. **Sodoyez JC, Sodoyez-Goffaux FR, and Moris YM.** 125I-insulin: kinetics of interaction with its receptors and rate of degradation in vivo. *Am J Physiol* 239: E3-E8, 1980.

303. **Spokes RA, Ghatei MA, and Bloom SR.** Studies with endothelin-3 and endothelin-1 on rat blood pressure and isolated tissues: evidence for multiple endothelin receptor subtypes. *J Cardiovasc Pharmacol* 13 Suppl 5:S191-2.: S191-S192, 1989.

304. **Spraul M, Ravussin E, and Baron AD.** Lack of relationship between muscle sympathetic nerve activity and skeletal muscle vasodilation in response to insulin infusion. *Diabetologia* 39: 91-96, 1996.

305. **Stadtmauer LA and Rosen OM.** Phosphorylation of exogenous substrates by the insulin receptor-associated protein kinase. *J Biol Chem* 258: 6682-6685, 1983.

306. **Stapleton DD, Moffett TC, Baskin DG, and Bassingthwaighte JB.** Autoradiographic assessment of blood flow heterogeneity in the hamster heart. *Microcirculation* 2: 277-282, 1995.

307. **Steil GM, Ader M, Moore DM, Rebrin K, and Bergman RN.** Transendothelial insulin transport is not saturable in vivo - No evidence for a receptor-mediated process. *J Clin Invest* 97: 1497-1503, 1996.

308. **Steinberg HO, Brechtel G, Johnson A, Fineberg N, and Baron AD.** Insulin-mediated skeletal muscle vasodilation is nitric oxide dependent. A novel action of insulin to increase nitric oxide release. *J Clin Invest* 94: 1172-1179, 1994.

309. **Steinberg HO, Chaker H, Leaming R, Johnson A, Brechtel G, and Baron AD.** Obesity/insulin resistance is associated with endothelial dysfunction. Implications for the syndrome of insulin resistance. *J Clin Invest* 97: 2601-2610, 1996.

310. **Steinberg HO, Paradisi G, Hook G, Crowder K, Cronin J, and Baron AD.** Free fatty acid elevation impairs insulin-mediated vasodilation and nitric oxide production. *Diabetes* 49: 1231-1238, 2000.

311. **Stephens JM, Lee J, and Pilch PF.** Tumor necrosis factor-alpha-induced insulin resistance in 3T3-L1 adipocytes is accompanied by a loss of insulin receptor substrate-1 and GLUT4 expression without a loss of insulin receptor-mediated signal transduction. *J Biol Chem* 272: 971-976, 1997.

312. **Stephens JM and Pekala PH.** Transcriptional repression of the GLUT4 and C/EBP genes in 3T3-L1 adipocytes by tumor necrosis factor-alpha. *J Biol Chem* 266: 21839-21845, 1991.

313. **Tack CJ, Lenders JW, Goldstein DS, Lutterman JA, Smits P, and Thien T.** Haemodynamic actions of insulin. *Curr Opin Nephrol Hypertens* 7: 99-106, 1998.

314. **Tack CJ, Lutterman JA, Vervoort G, Thien T, and Smits P.** Activation of the sodium-potassium pump contributes to insulin-induced vasodilation in humans. *Hypertension* 28: 426-432, 1996.

315. **Tack CJ, Ong MK, Lutterman JA, and Smits P.** Insulin-induced vasodilatation and endothelial function in obesity/insulin resistance. Effects of troglitazone. *Diabetologia* 41: 569-576, 1998.

316. **Taddei S, Virdis A, Mattei P, Natali A, Ferrannini E, and Salvetti A.** Effect of insulin on acetylcholine-induced vasodilation in normotensive subjects and patients with essential hypertension. *Circulation* 92: 2911-2918, 1995.

317. **Townsend RR and DiPette DJ.** Pressor doses of angiotensin II increase insulin-mediated glucose uptake in normotensive men. *Am J Physiol* 265: E362-E366, 1993.

318. **Trovati M, Massucco P, Mattiello L, Cavalot F, Mularoni E, Hahn A, and Anfossi G.** Insulin increases cyclic nucleotide content in human vascular smooth muscle cells: a mechanism potentially involved in insulin-induced modulation of vascular tone. *Diabetologia* 38: 936-941, 1995.

319. **Trovati M, Massucco P, Mattiello L, Costamagna C, Aldieri E, Cavalot F, Anfossi G, Bosia A, and Ghigo D.** Human vascular smooth muscle cells express a constitutive nitric oxide synthase that insulin rapidly activates, thus increasing guanosine 3':5'-cyclic monophosphate and adenosine 3':5'-cyclic monophosphate concentrations. *Diabetologia* 42: 831-839, 1999.

320. 319.**Turk D, Alzaid A, Dinneen S, Nair KS, and Rizza R.** The effects of non-insulin-dependent diabetes mellitus on the kinetics of onset of insulin action in hepatic and extrahepatic tissues. *J Clin Invest* 95: 755-762, 1995.

321. **Ueda S, Petrie JR, Cleland SJ, Elliott HL, and Connell JM.** The vasodilating effect of insulin is dependent on local glucose uptake: a double blind, placebo-controlled study. *J Clin Endocrinol Metab* 83: 2126-2131, 1998.

322. **Ullrich A, Gray A, Tam AW, Yang-Feng T, Tsubokawa M, Collins C, Henzel W, Le Bon T, Kathuria S, Chen E.** Insulin-like growth factor I receptor primary structure: comparison with insulin receptor suggests structural determinants that define functional specificity. *EMBO J* 5: 2503-2512, 1986.

323. **Utriainen T, Makimattila S, Virkamaki A, Bergholm R, and Yki-Jarvinen H.** Dissociation between insulin sensitivity of glucose uptake and endothelial function in normal subjects. *Diabetologia* 39: 1477-1482, 1996.

324. **Utriainen T, Makimattila S, Virkamaki A, Lindholm H, Sovijarvi A, and Yki-Jarvinen H.** Physical fitness and endothelial function (nitric oxide synthesis) are

independent determinants of insulin-stimulated blood flow in normal subjects. *J Clin Endocrinol Metab* 81: 4258-4263, 1996.

325. **Utriainen T, Malmstrom R, Makimattila S, and Yki-Jarvinen H.** Methodological aspects, dose-response characteristics and causes of interindividual variation in insulin stimulation of limb blood flow in normal subjects. *Diabetologia* 38: 555-564, 1995.

326. **Utriainen T, Nuutila P, Takala T, Vicini P, Ruotsalainen U, Ronnemaa T, Tolvanen T, Raitakari M, Haaparanta M, Kirvela O, Cobelli C, and Yki-Jarvinen H.** Intact insulin stimulation of skeletal muscle blood flow, its heterogeneity and redistribution, but not of glucose uptake in non-insulin-dependent diabetes mellitus. *J Clin Invest* 100: 777-785, 1997.

327. **Valensi P, Behar A, Cohen-Boulakia F, Valensi J, Wiernsperger N, and Attali JR.** In vivo kinetics of 123 iodine-labelled insulin in skeletal muscle of patients with type 2 diabetes. Effect of metformin. *Diabetes Metab* 28: 95-103, 2002.

328. **Vicent D, Ilany J, Kondo T, Naruse K, Fisher SJ, Kisanuki YY, Bursell S, Yanagisawa M, King GL, and Kahn CR.** The role of endothelial insulin signaling in the regulation of vascular tone and insulin resistance. *J Clin Invest* 111: 1373-1380, 2003.

329. **Vicini P, Bonadonna RC, Lehtovirta M, Groop LC, and Cobelli C.** Estimation of blood flow heterogeneity in human skeletal muscle using intravascular tracer data: importance for modeling transcapillary exchange. *Ann Biomed Eng* 26: 764-774, 1998.

330. **Vicini P, Bonadonna RC, Utriainen T, Nuutila P, Raitakari M, Yki-Jarvinen H, and Cobelli C.** Estimation of blood flow heterogeneity distribution in human skeletal muscle from positron emission tomography data. *Ann Biomed Eng* 25: 906-910, 1997.

331. **Vincent MA, Barrett EJ, Lindner JR, Clark MG, and Rattigan S.** Inhibiting NOS blocks microvascular recruitment and blunts muscle glucose uptake in response to insulin. *Am J Physiol Endocrinol Metab* 285: E123-E129, 2003.

332. **Vincent MA, Clerk LH, Lindner JR, Klibanov AL, Clark MG, Rattigan S, and Barrett EJ.** Microvascular recruitment is an early insulin effect that regulates skeletal muscle glucose uptake in vivo. *Diabetes* 53: 1418-1423, 2004.

333. **Vincent MA, Dawson D, Clark AD, Lindner JR, Rattigan S, Clark MG, and Barrett EJ.** Skeletal muscle microvascular recruitment by physiological hyperinsulinemia precedes increases in total blood flow. *Diabetes* 51: 42-48, 2002.

334. **Vollenweider P, Randin D, Tappy L, Jequier E, Nicod P, and Scherrer U.** Impaired insulin-induced sympathetic neural activation and vasodilation in skeletal muscle in obese humans. *J Clin Invest* 93: 2365-2371, 1994.

335. **Vollenweider P, Tappy L, Randin D, Schneiter P, Jequier E, Nicod P, and Scherrer U.** Differential effects of hyperinsulinemia and carbohydrate metabolism on sympathetic nerve activity and muscle blood flow in humans. *J Clin Invest* 92: 147-154, 1993.

336. **Wallis MG, Wheatley CM, Rattigan S, Barrett EJ, Clark AD, and Clark MG.** Insulin-mediated hemodynamic changes are impaired in muscle of zucker obese rats. *Diabetes* 51: 3492-3498, 2002.

337. **Wei K, Jayaweera AR, Firoozan S, Linka A, Skyba DM, and Kaul S.** Quantification of myocardial blood flow with ultrasound-induced destruction of microbubbles administered as a constant venous infusion. *Circulation* 97: 473-483, 1998.

338. **White MF and Kahn CR.** The insulin signaling system. *J Biol Chem* 269: 1-4, 1994.

339. **Wolpert HA, Steen SN, Istfan NW, and Simonson DC.** Insulin modulates circulating endothelin-1 levels in humans. *Metabolism* 42: 1027-1030, 1993.

340. **Wu-Wong JR, Berg CE, Wang J, Chiou WJ, and Fissel B.** Endothelin stimulates glucose uptake and GLUT4 translocation via activation of endothelin ETA receptor in 3T3-L1 adipocytes. *J Biol Chem* 19;274: 8103-8110, 1999.

341. **Yanagisawa M, Kurihara H, Kimura S, Tomobe Y, Kobayashi M, Mitsui Y, Yazaki Y, Goto K, and Masaki T.** A novel potent vasoconstrictor peptide produced by vascular endothelial cells. *Nature* 332: 411-415, 1988.

342. **Yanagisawa M and Masaki T.** Molecular biology and biochemistry of the endothelins. *Trends Pharmacol Sci* 10: 374-378, 1989.

343. **Yang YJ, Hope I, Ader M, Poulin RA, and Bergman RN.** Dose-response relationship between lymph insulin and glucose uptake reveals enhanced insulin sensitivity of peripheral tissues. *Diabetes* 41: 241-253, 1992.

344. **Yang YJ, Hope ID, Ader M, and Bergman RN.** Insulin transport across capillaries is rate limiting for insulin action in dogs. *J Clin Invest* 84: 1620-1628, 1989.

345. **Ye JM, Clark MG, and Colquhoun EQ.** Constant-pressure perfusion of rat hindlimb shows alpha- and beta- adrenergic stimulation of oxygen consumption. *Am J Physiol* 269: E960-E968, 1995.

346. **Yki-Jarvinen H, Sahlin K, Ren JM, and Koivisto VA.** Localization of rate-limiting defect for glucose disposal in skeletal muscle of insulin-resistant type I diabetic patients. *Diabetes* 39: 157-167, 1990.

347. **Yki-Jarvinen H and Utriainen T.** Insulin-induced vasodilatation: physiology or pharmacology? *Diabetologia* 41: 369-379, 1998.

348. **Yki-Jarvinen H, Young AA, Lamkin C, and Foley JE.** Kinetics of glucose disposal in whole body and across the forearm in man. *J Clin Invest* 79: 1713-1719, 1987.

349. **Youd JM, Newman JM, Clark MG, Appleby GJ, Rattigan S, Tong AC, and Vincent MA.** Increased metabolism of infused 1-methylxanthine by working muscle. *Acta Physiol Scand* 166: 301-308, 1999.

350. **Youd JM, Rattigan S, and Clark MG.** Acute impairment of insulin-mediated capillary recruitment and glucose uptake in rat skeletal muscle in vivo by TNFa. *Diabetes* 49: 1904-1909, 2000.

351. **Zeng G, Nystrom FH, Ravichandran LV, Cong LN, Kirby M, Mostowski H, and Quon MJ.** Roles for insulin receptor, PI3-kinase, and Akt in insulin-signaling pathways related to production of nitric oxide in human vascular endothelial cells. *Circulation* 101: 1539-1545, 2000.

352. **Zeng GY and Quon MJ.** Insulin-stimulated production of nitric oxide is inhibited by wortmannin - Direct measurement in vascular endothelial cells. *J Clin Invest* 98: 894-898, 1996.

353. **Zhang L, Wheatley CM, Richards SM, Barrett EJ, Clark MG, and Rattigan S.** TNF-alpha acutely inhibits vascular effects of physiological but not high insulin or contraction. *Am J Physiol Endocrinol Metab* 285: E654-E660, 2003.